ISSN 0003-2670

ANALYTICA CHIMICA ACTA

International monthly devoted to all branches of analytical chemistry
Revue mensuelle internationale consacrée à tous les domaines de la chimie analytique
Internationale Monatsschrift für alle Gebiete der analytischen Chemie

ELSEVIER SCIENTIFIC PUBLISHING COMPANY

AMSTERDAM

Anal. Chim. Acta, Vol. 92, 1–232, August 1977

Published monthly

ANALYTICA CHIMICA ACTA

Publication Schedule for 1977

Vol. 88, No. 1	January 1977	
Vol. 88, No. 2	February 1977	(completing Vol. 88)
Vol. 89, No. 1	March 1977	
Vol. 89, No. 2	April 1977	(completing Vol. 89)
Vol. 90	May 1977	(complete in one issue)
Vol. 91, No. 1	June 1977	
Vol. 91, No. 2	July 1977	(completing Vol. 91)
Vol. 92, No. 1	August 1977	
Vol. 92, No. 2	September 1977	(completing Vol. 92)
Vol. 93	October 1977	(complete in one issue)
Vol. 94, No. 1	November 1977	
Vol. 94, No. 2	December 1977	(completing Vol. 94)

Subscription price for 1977 (Vols. 88–95): Dfl. 920.00 plus Dfl. 112.00 postage (approx. U.S.$421.22 inclusive of postage). Claims for issues not received should be made within three months of publication of the issues; if not, they cannot be honoured free of charge. Subscribers in the U.S.A. and Canada receive their copies by airmail. Additional charges for airmail to other countries are available on request. For advertising rates apply to the publishers.

Subscriptions should be sent to:
Elsevier Scientific Publishing Company, P.O. Box 211, Amsterdam, The Netherlands.

GENERAL INFORMATION

Languages

Papers will be published in English, French or German.

Detailed information

Authors should consult Vol. 73, p. 435 for detailed instructions. Reprints of this information are obtainable from Dr. Macdonald or from: Elsevier Editorial Services Ltd., Mayfield House, 256 Banbury Road, Oxford (Great Britain).

Submission of papers

Papers should be sent to:

Prof. Philip W. West,
Chemistry Department,
College of Chemistry and Physics,
Louisiana State University,
Baton Rouge,
La. 70803 (U.S.A.)

or to:

Dr. A. M. G. Macdonald,
Department of Chemistry,
The University,
P.O. Box 363
Birmingham B15 2TT (Great Britain)

Reprints

Fifty reprints will be supplied free of charge. Additional reprints (minimum 100) can be ordered at quoted prices. They must be ordered on order forms which are sent together with the proofs.

Gas Chromatography of Polymers

by **V.G. BEREZKIN, V.R. ALISHOYEV** and **I.B. NEMIROVSKAYA,** Institute of Petrochemical Synthesis, Academy of Sciences of the U.S.S.R., Moscow.

JOURNAL OF CHROMATOGRAPHY LIBRARY, Vol. 10

1977. xiii+225 pages. US $41.25/Dfl. 103.00. ISBN 0-444-41514-9

This book is devoted to the strategy of application of GC in polymer chemistry and discusses, in detail, the use of GC in research work and the polymeric compounds industry. It is the second, revised and enlarged edition of the original version published in the U.S.S.R. in 1972.

The following principal applications are covered: analysis of monomers and solvents, determination of the contents of volatile substances in polymers, study of polymer formation processes, investigation into types of disintegration of high-molecular-weight compounds, polymer analysis by reaction and pyrolytic chromatography, and study of polymers and their reactivity with the aid of inverse chromatography.

This work will be of value to research institutions, industrial enterprises and senior students engaged in the fields of polymer or analytical chemistry and GC.

CONTENTS: Basic principles of gas chromatography. GC methods for the analysis of monomers and solvents. The study of polymer formation reactions. Determination of volatile compounds in polymer systems. Study of the kinetics and mechanisms of chemical transformations of polymers at elevated temperatures. Reaction GC of polymers. Pyrolysis GC. Inverse GC. Conclusion.

ELSEVIER SCIENTIFIC PUBLISHING COMPANY
P.O. Box 211, Amsterdam,
The Netherlands

Distributor in the U.S.A. and Canada:
ELSEVIER NORTH-HOLLAND, INC.,
52 Vanderbilt Ave., New York., N.Y. 10017

Dutch guilder price is definitive.
$ prices are subject to exchange rate fluctuations.

CHROMATOGRAPHY '77

INTERNATIONAL SYMPOSIUM ON ADVANCES IN CHROMATOGRAPHY

The 12th International Symposium on Advances in Chromatography will be held in November 7-10, 1977 at the International Congress Centre RAI in Amsterdam, The Netherlands.

The scope of the meeting will cover papers and informal discussion groups by outstanding researchers from throughout the world in all fields of chromatography. In particular, new developments in gas, liquid and high performance thin-layer chromatography will be included.

A total of 84 papers will be presented at the Symposium representing contributions from 20 countries. A special feature of the meeting will be an exposition of the latest instrumentation and books.

Registration should be made in advance. The programs, registration forms and hotel reservation cards can be obtained from:

Organisatie Bureau Amsterdam b.v.
International Congress Centre RAI
P.O. Box 7205
Europaplein 14
Amsterdam, The Netherlands

or

Prof. A. Zlatkis
Chemistry Department
University of Houston
Houston, Texas 77004
U.S.A.

ANALYTICA CHIMICA ACTA
Vol. 92 (1977)

ANALYTICA CHIMICA ACTA

International monthly devoted to all branches of analytical chemistry
Revue mensuelle internationale consacrée à tous les domaines de la chimie analytique
Internationale Monatsschrift für alle Gebiete der analytischen Chemie

ELSEVIER SCIENTIFIC PUBLISHING COMPANY

AMSTERDAM

PRINTED IN THE NETHERLANDS

Analytica Chimica Acta, 92 (1977) 1—11

AMERICAN BICENTENARY, 1776—1976

Two-Hundred Years of Anglo-American Analytical Chemistry: Applied Aspects*†

HAROLD EGAN

Laboratory of the Government Chemist, London (England)

(Received 6th January 1977)

Chemistry is an ancient art-turned-science; although the origins of analytical chemistry can be recognized in ancient times, it is basically a modern science. In looking at analytical chemistry and its applied aspects, it is difficult to offer a better introduction than that written recently by Irving [1] "As Society has become more organized and standards of living have changed and improved, analytical chemistry has become increasingly important and its influence extends over every aspect of our life. It is an essential feature of all manufacturing operations, from the examination of the raw materials to the finished products, and it dominates all problems involving the control of environmental pollution. It plays an ever increasing rôle in controlling the content and quality of the food we eat; it influences the vessels we cook with, the plates we eat off, the houses we live in, the clothes we wear, and even our modes of transport, education and entertainment — although the connexions may not be immediately obvious. The medicines we use in ever increasing numbers could not be designed, tested, manufactured or distributed without the aid of analytical chemistry. The constant battle against fraud and crime ... — all call on the skill of the analyst". This illustrates well the kinds of areas which come to mind when considering the applied aspects of the subject.

Applied aspects of analytical chemistry developed mainly within the last two hundred years, mostly during the past century. The subject of "200 years of Anglo-American applied analytical chemistry" is not one which, from the literature, appears to have been deeply explored; and the evidence afforded by reading, for example, Farber's wide-ranging 1964 Dexter Award paper on published histories of chemistry [2], does not throw any immediate light on the matter. Nor does the approach used by van Klooster [3], who examined the first (1906) edition of "American Men of Science" for the

*For "200 Years of Anglo-American Analytical Chemistry: Academic Aspects" see R. Belcher, Anal. Chim. Acta, 86 (1976) 1.

†Plenary lecture delivered at the 27th Pittsburgh Conference, March, 1976.

names of those who had been associated earlier with Liebig (by comparison with the authors in Liebig's Annalen 1834—73), offer much help.

Joseph Priestley, the English scientist and theologian, spent the last ten years of his life in the United States, settling finally in Northumberland, Pennsylvania. Two years ago bicentennial celebrations were held for his discovery, in England in August 1774, of "dephlogisticated air" (subsequently recognized by Antoine Lavoisier in France as his own "vital air" and renamed by him oxygen). Priestley developed semi-quantitative procedures for gas analysis, but he was a politician as well as a scientist, and it might be said on this bicentennial occasion that his biggest contribution to Anglo—American relationships was not in chemistry at all. The modern concept of democracy is distinguished in Abraham Lincoln's famous phrase (1863) "government of the people, by the people, for the people" from the ancient classical idea of democracy as being government by the dominant, largely poorer, masses in the interest of their own class. Joseph Priestley was one of those who used Francis Hutcheson's phrase (1726) "the greatest happiness of the greatest number", and he was one of the first to associate this with the principle of democracy. Indeed, Priestley was serving in the office of Librarian to Lord Shelburne at Calne in Wiltshire, England, when he discovered oxygen. Lord Shelburne himself had been Secretary of State in the William Pitt administration of 1766, but had been dismissed in 1768 on account of his conciliatory policy towards America.

Joseph Priestley's arrival in America in 1794 perhaps marks the beginning of significant Anglo-American interaction in science, although this was academic rather than applied. By the 1830's a notable number of American college graduates were coming to Europe, principally to Giessen in Germany, for further study. One important effect of this was on the approach to individual student instruction, as pioneered by von Liebig, a matter of substantial practical (and hence applied) significance. However, Liebig was not the only, or even the first, pioneer in this field. Nor is this to say that applied chemistry was not previously taught in America. According to Rosen [4], Boston High School for Girls was advertising "as much chemistry as would be useful in domestic economy" in its prospectus in 1826. Thereafter "laboratory chemistry" developed and flourished in American teaching to the extent that, by the turn of the century, there had been complaints of what Rosen calls "an irresistible wave of laboratory madness". This was in contrast to the European scene, where teaching by textbook excelled and individual laboratory work by students was not emphasized. The successors of these textbooks, a century later, were accompanied by a new kind of textbook with a strong applied bias, perhaps reflecting to some degree the applied analytical methods books which had begun to appear in Britain half a century earlier [5].

In the early days of the period concerned, say 1776—1850, a number of American chemists visited Europe and a few chemists from various European countries visited the United States. Analytical chemistry itself

was, at the beginning of the period, still in its formative years; the distinction between pure and applied analytical chemistry, as it would be seen now, hardly existed. The initial emphasis was, understandably, on qualitative rather than quantitative aspects, as illustrated by the work of Kirwan in 1784 [6]: this provided the foundation for the basic qualitative group analysis separations which were to be highly systematized later and which undoubtedly form one of the cornerstones of applied analytical chemistry. It would be difficult to say in which direction the influence was dominant, but it appears that chemists in France, Germany and Britain led the thinking, though there was certainly independence of thought in the United States, particularly from the close of the eighteenth century onwards. If one chemist who at the time had the greatest influence on applied analytical chemistry in the United States had to be selected, there would be no difficulty in choosing Fredrick Accum (1769—1838), born Friedrich Christian Accum in Germany, but resident in London from 1793 until 1823, when, at the age of 52, he returned to Germany in some disgrace [7].

Accum was a versatile and accomplished, if controversial, figure; he was a pioneer in a number of fields of applied chemistry, including gas illumination, the recognition of the gross adulteration of food, and mineralogical analysis. His published works in these and some more popular fields of chemistry were widely read and well respected; many were also published in America as well as being translated into French, German and Italian. The second (1807) edition of his "System of Theoretical and Practical Chemistry" for example, first published privately in London, in 1803, was reprinted in Philadelphia in 1808. Thomas Elwell of Virginia gave special credit to Accum in the preface of his book "Plain Discoveries on the Laws or Properties of Matter" (New York, 1806).

Fredrick Accum worked for many years at the Royal Institution in London; from 1800, he also ran his own laboratory businesss which included commercial analysis and the supply of chemicals and equipment. Accum also gave popular series of chemical lectures. His establishment in Old Compton Street was the first European school in which students from the United States could, and did, receive practical laboratory instruction. It pre-dated, by some twenty years, Liebig's famous Institute at Giessen. Several of the first college laboratories in the United States were fitted up by Accum, whose customers included Harvard and Yale. Accum's personality and analytical skills were undoubtedly an influence on William Peck (Harvard), James Freeman Dana (Dartmouth) and Benjamin Silliman Sr., (Yale), all of whom were among his early students. Silliman, whom Accum introduced to Sir Humphry Davy, studied with Accum in the summer of 1805, and described him as "well acquainted with practical chemistry and much more resorted to make chemical analyses and examination of many things". Accum gave Silliman private instruction on various subjects, including the analysis of ores. William Peck was similarly impressed three years later, and both placed considerable orders for reagents and equipment for laboratories in the United States.

Silliman, with his son Benjamin, Jr., and James Dana, founded the American Journal of Science in July 1818. For more than 70 years afterwards, "Silliman's Journal" was the outstanding scientific periodical in America, with an international circulation. Its papers ranged widely and included many practical papers on analysis. As Greenaway [8] has pointed out, the industrial development of the western world in the 18th and 19th centuries depended for its profitability on the optimum use of raw materials and on the maintenance of regular production. Chemical analysis was essential for both these purposes. The early story of the chemical industry in America has been well documented by Haynes [9], who suggests that it was the initial ability to analyse natural raw materials, and the exact knowledge of their composition gained thereby, which indicated the routes to the manufacture of their active principles and thus put chemical manufacturing on a firm footing. Until the middle of the 1820's, the United States relied on importation for all of its basic chemical raw materials. The development of domestic resources was encouraged by the imposition of protective tariffs; in 1824 and 1831 the "friends of domestic industry" were able to report [10] that nearly all the materials used in chemical establishments, including ammonia, hydrochloric, nitric and sulfuric acids, calomel, calcium hypochlorite and potassium dichromate, were produced in the United States. These products were all cheaper than the imported materials; in some cases they were also purer, but the rôle that analysis may have played in this is not clear. Indeed, an export trade developed in some areas, but the British were not slow to retaliate with their own protective tariffs.

The original basis of much of the qualitative and quantitative analytical chemistry of today was laid in the decades around the year 1800. Mellon [11] in his 1952 Fisher Award Lecture has given a brief comparative historical account of the development of gravimetry (which began to take shape in Europe under Lavoisier in the middle of the 18th century, and was more fully developed by Berzelius in Sweden in the first part of the 19th century), titrimetry (perfected by Mohr in Germany in the middle part of the 19th century) and colorimetry (absorptiometry) which became fully established towards the end of the 19th century. Until about 1810, much of the analytical equipment was ad hoc in character, being made in individual laboratories for the purpose in hand and with a specificity or exactness of a different order from that now regarded as proper to quantitative (and qualitative) analysis [12]. By about 1850 such basic processes as precipitation, filtration, titration, and volumetric gas analysis were well established, and a deeper understanding of the potential application of analysis to everyday matters had developed.

Gas analysis was, in a sense, a precursor of gas chromatography, although techniques in the nineteenth century were concerned mainly with carbon dioxide and permanent gases such as oxygen and nitrogen; separations were based on combustion or on the use of chemical absorbent solutions.

Another important separation technique in both trace and compositional analysis is solvent extraction. The means for achieving this in 1875 were relatively imprecise, depending on removal of the upper phase by mouth-pipette. Specially designed glass separators were developed in the later years of the century; the separating funnel in its present form was introduced in the 1890's.

The basic laws of optical absorption had already been established by Beer and Lambert earlier in the century, and there had been an important contribution to the improvement of techniques for trace analysis in the Duboscq colorimeter [1]. This was developed further during the latter half of the century and improved the means for the colorimetric estimation of trace metals, such as lead and iron. Similar instruments also provided the basis for the development in the 1930's of photoelectric spectrometers, the precursors of a whole range of infra-red, visible, and ultra-violet spectrophotometers, and their counterparts in the fields of nuclear magnetic and electron spin resonance spectrometry that are still developing today. Mellon has also briefly reviewed the part which American scientists played, during the first half of the present century, in the measurement and comparison of colours in terms of tristimulus values, dominant hue, colour purity and luminance [11]. To take just one British example with an optical flavour, Lyle and Lyle, at the ACS Symposium on The History of Equipment and Instrumentation in 1963 [12], indicated the rôle of William Nicol [13] in the development of the polarimeter by the introduction of his specially designed Iceland spar polarizer and analyzer prism in the first half of the nineteenth century. The polarimeter has contributed notably to the development of theoretical organic chemistry, and is widely used in the analysis of sugar solutions.

One of the earliest laws which set standards and relied on analysis for their enforcement was the 1863 Alkali Act in Britain, in relation to air quality. By the turn of the century, analytical chemistry was also well established as the basis for the statutory control of problems concerning the quality of water, food, and similar aspects of concern in relation to the health and well-being of the people. Today, the applied analytical method, soundly based on fundamental theoretical aspects and duly validated by collaborative, cooperative practical study, is one of the most important end-products of analytical chemistry. It was these environmental and health aspects which served in the past 200 years, and particularly in the past 100 years, as the basis and motivation for this development. Perhaps this can best be illustrated by looking in a little more detail at food quality, and how analysis has come to be one of the basic means for its assessment and, where necessary, control.

It was just about a century ago that analysis, for the first time, became involved in the laws controlling the composition and purity of food effectively. The essential knowledge of the chemical composition of the substances (or of their individual constituents) to be analyzed was developed through studies which continued well into the nineteenth century. The

search for such knowledge continues in various forms today. The compositional aspects, upon which food analysis is still broadly based, were recognized by von Liebig in 1846. Foods are composed largely of carbohydrates, fats, and proteins; these, together with water and smaller amounts of other substances recognized more recently, e.g. mineral salts, vitamins, colours, and flavours, still form the essential foundation for food analysis. Chirnside and Hamence [14] have surveyed the state of analytical chemistry as applied to the work of the Public Analysts appointed to enforce the food laws in Britain 100 years ago. By 1874, the main classes of the organic components of food were recognized as acids, albuminous matter (proteins), colouring matter, fats and oils, fibrous matter, gums, starches, sugars, and tannins, but there were no reliable methods for estimating the proportions of these various components and no general textbooks of food analysis at that time. There was, in consequence, no full understanding of the variation in proportions which occurred naturally in foods, nor of the limits of composition which can be regarded as characterizing genuine products. As regards basic quantitative analytical processes, titrimetry had already gained considerable benefit by 1874 from the development by Mohr in 1853 [15] of the precursor of the modern burette. Mohr's apparatus was substantially more precise and controllable in everyday use than the earlier designs such as the fragile Gay-Lussac tube with a long narrow side-arm. Gravimetric analysis was also improved and its application extended in 1878 by the introduction of the Gooch asbestos crucible.

Few general textbooks of food analysis were available before this period, but the precursors of the present-day compendia were just beginning to appear as slim, pocket-sized volumes devoted to individual foods. Among the first of these were Wanklyn's "Milk Analysis" [16], Wanklyn's "Tea, Coffee and Cocoa Analysis" [17], and Hehner and Angell's "Butter" [18], all published in 1874, and Wanklyn and Cooper's "Bread Analysis" [19]. Many went through subsequent editions. They were joined at a later stage by contributions from authors in industry [20] such as Droop Richmond's "Laboratory Book of Dairy Analysis" [21]. The Laboratory of the Government Chemist in London (then the Inland Revenue Laboratory) was brought into the story about this time. After it had been in existence for some 43 years, it was given a statutory analytical referee function under the Food and Drugs Act in 1875 [5]. As a consequence of this involvement in food analysis, the director of the Laboratory initiated a full study of analytical methods for food; volumes describing such methods were published in 1881 [22] and 1883 [23].

Much of the development of food analysis during the first half of the twentieth century involved consolidating the techniques of the previous decades. The principles of gravimetry, titrimetry, and colorimetry were already well established. Commercial laboratory equipment became available more easily, designs were improved and standards were developed for calibrated glassware and the purity of reagent chemicals. Until the first

world war, the United Kingdom had come to rely upon the European continent (particularly Germany) for the reagent-quality chemicals essential for reliable food analysis. As a result of a joint initiative of the Society of Public Analysts and the Institute of Chemistry (now the Royal Institute of Chemistry) in 1915, the range of AnalaR chemicals (still used today) was launched in Britain. Improved reagents and apparatus then made it possible, through collaborative study, to standardize the analytical methods themselves, so facilitating agreement between analysts and between laboratories. This in turn led to the acceptance of quality criteria, based on direct analytical evidence, for such aspects as nutritional value. The Analytical Methods Committee of the Society of Public Analysts (the predecessor of the present-day Analytical Division of the Chemical Society) was set up in 1935; there had been earlier studies of the standardization of methods, dating back to 1882 [14]. Similar developments in the central standardization of analytical methods followed in the U.S.A. in the early years of the present century [24]: although these centred on methods of food analysis, as in Britain, the organization in this case took place at federal government level and the Association of Official Agricultural Chemists (now the Association of Official Analytical Chemists) was founded in 1886. This body has had a strong influence on the philosophy and development, by collaborative study, of standard methods of food analysis; although the problems of food adulteration were not its concern initially, the strong analytical interest in this area that began in 1896 [25, 26] is still sustained today. Similarly, the American Society for Testing and Materials, founded in 1898, developed standard methods of analysis for many materials and products of commerce.

U.S. Food and Drugs Commissioner Alexander Schmidt, commenting in London in 1976 on the early colonial food laws in America [27], said that although from the beginning these were quite diverse, largely indigenous and responding principally to the needs of producers and consumers in the thirteen separate colonies, they nevertheless reflected a heritage from English law. The first U.S. national food and drug law was not passed until 1906; but the first really effective and comprehensive pure food law was not enacted in England until 1875, and it was analytical aspects as much as any other which enabled it to take effect. In fact, it was an Englishman, Wigner, who won in 1880 the U.S. National Board of Trade's competition for the best food Act, accompanied by an essay. The Wigner Bill was introduced in Congress and became one of the early ancestors of the U.S. Food and Drugs Act of 1906. The development of applied analysis in Britain during the nineteenth century and the role which it played in the establishment of the first effective laws for the control of the purity and composition of food [7, 24] is an important part of the story of the history of applied analytical chemistry. The subject has also been reviewed by Ihde [24], who comments that the somewhat later, but parallel development which took place in the United States, differed from the pattern in Britain in that the stimulus arose very largely out of agricultural problems, although the results ultimately also

figured heavily in the field of food regulations. Ihde [24] describes how, by 1870, the depleted soil fertility in the southern and north eastern states led to the development of the use of fertilizers and to the agricultural experimental station movement, which followed in the 1870's and 1880's in response to the need for the protection of farmers who found themselves purchasing commercial fertilizers of indifferent quality. Harvey W. Wiley, who had studied earlier in Europe, was a pioneer in this field of analysis; he was appointed chief of the U.S. Department of Agriculture's Division of Chemistry in 1883. Wiley was, in effect, the father of the Association of Official Analytical Chemists in North America today, the development of which largely parallels that of the Society for Analytical Chemistry in Britain. The Methods Book of the AOAC is but one notable example of analytical chemistry successfully applied and widely accepted on an international basis in the important areas of food, drugs, and animal feeds. There are many other examples, on both a national and an international scale, not least the very comprehensive work of the American Society for Testing and Materials, now claimed as the world's largest source of voluntary concensus standards [28].

Among the many Americans to have impressed their mark on the applied analytical literature on both sides of the Atlantic are Wolcott Gibbs (1822—1908), perhaps the first great personality in American chemistry and the discoverer of electrogravimetry; Otto Folin (1867—1934), born in Sweden, Professor of Analytical Chemistry at the University of Virginia and later Professor of Biochemistry at Harvard, is still well remembered in clinical biochemistry, a very important area of applied analytical chemistry; George Frederick Smith [29] who, among other things, pioneered the use of perchloric acid for sample digestion; G. E. F. Lundell [30], who once described the analytical chemist's idea of heaven as a room with shelves for 92 reagent solutions, each one specific for a different element; the Snells, Foster D. and Cornelia T., [31, 32] whose volumes on colorimetric analysis bridged the gap between the pioneering days of instrumentation and the commercial world of instrumentation today; and among those happily still with us is Izaac Kolthoff, Professor of Analytical Chemistry at the University of Minnesota [33, 34]. All of these, and many others, have shared in the strong two-way transatlantic exchange in the field of applied analytical chemistry; there are others on the British side such as Arthur Vogel [35, 36] and the Wilson brothers [37] who, through their industry and publications, have helped to shape the present international scene. And there is perhaps no better example of Anglo-American co-operation in analytical chemistry than that of Kolthoff and Belcher [38].

Applied analytical chemistry today still has its pioneers in university departments and other institutions; the latter now frequently include the large industrial corporations, departments of state, and other public institutions. However, the emphasis has changed in the past 30—40 years and the importance of analytical chemistry in everyday life mentioned at

the beginning of this review is now more widely and more fully understood and recognized.

Today, analytical chemistry, both compositional analysis and trace analysis, is a fully integral part of everyday life. In an ironic way the trace analyst has come to fulfil the classical definition of an expert — one who knows more and more about less and less. One notable feature which the law has introduced into applied analysis in North America in recent years is the concept of zero tolerance, e.g. for residues of pesticides in food. This arose from the 1958 so-called Delaney amendment to the Federal Food, Drug and Cosmetic Act of 1938 which said that no (food) additive shall be deemed safe if it is found to induce cancer when ingested by man or animal. The Act was amended in 1962 to allow the use of carcinogenic substances in livestock feed provided that no drug residue could be detected by analysis in the edible tissues; the usage of such materials was therefore dependent on the sensitivity of the analytical method used to detect the residues and is liable to change as the analytical ability improves. Earlier this year, however, the situation again changed when the Food and Drug Administration proposed the revocation of the official analytical method for residues of diethylstilbestrol, when (for want of a better official method) residues could not be detected. At the same time, the alternative procedure of banning the veterinary use of diethylstilbestrol came under consideration. The difficulty was avoided in Britain, not by having zero tolerances, but by having no tolerances at all; but that is another story. The difficulty is illustrated by the story of the lawyer who, impressed by an analytical report full of zeros for cadmium, lead, mercury, and so on, said "If you can make the pH zero as well, we really have something" [26].

Looking back rapidly over the past 200 years, America and Britain, in common with a number of other European countries, developed the application of analytical chemistry to matters of everyday life from a largely common pool of academic wisdom and enterprise. During the intervening years, a number of distinct and well-defined areas developed, and were largely perfected, on each side of the Atlantic — with some interchange, perhaps largely at the fundamental, theoretical level, as much as in the field of fully developed, applied analysis. "Chemical" analytical chemistry, as we know it today, became recognizable; the applied aspects were developed largely during the first half of the bicentennial period, from about 1750 to 1850. Then came the conscious adaptation in applied chemical analysis of discoveries in physics, mainly electrical and optical. These in turn made possible a further notable change, dating roughly from the start of the 20th century, in the reduction in scale from milligrams to micrograms; this continues today in trace analysis into picograms and femtograms. Some of the wide-reaching implications of automation and the application of computers to applied analytical chemistry are beginning to be seen, and the need for, and value of, standardized methods based on the systematic evaluation of practical procedures in collaborative, cooperative, or similar studies is now more clearly

realized. The need for some harmonization of the philosophy of this process so that different standardized procedures can be compared, and where appropriate equated, not only between America and Britain but between other national and international levels has also been realized. Perfection is not an instantaneous matter; Rome was not built in a day. Or, as Ben Johnson put it 366 years ago in The Alchemist:

> "..... for 'twere absurd
> To think that nature
> In the earth bred gold
> Perfect in the instant.
> Something went before."

REFERENCES

1 The Techniques of Analytical Chemistry, H. M. N. H. Irving, HM Stationery Office, London, 1974.
2 E. Farber, J. Chem. Educ., 42 (1965) 120.
3 H. S. van Klooster, J. Chem. Educ., 33 (1956) 493.
4 S. Rosen, J. Chem. Educ., 33 (1956) 627.
5 H. Egan, Proc. Symp. Pure Food and Drug Centenary, HM Stationery Office, London, 1976, p. 105.
6 R. Kirwan, Elements of Mineralogy, London, 1784.
7 C. A. Browne, The Life and Chemical Services of Frederick Accum, US Department of Agriculture, Washington, 1925.
8 F. Greenaway, Anal. Chem., 48(1976) 148.
9 W. Haynes, American Chemical Industry: A History, Vol. 1, van Nostrand, 1954.
10 I. Tyson, Report on Chemistry, Friends of Domestic Industry, Baltimore, 1831.
11 M. G. Mellon, Anal. Chem., 24 (1952) 924.
12 M. Daumas, Scientific Instruments of the 17th and 18th Centuries and Their Makers, Batsford, London, 1972.
13 W. Nicol, New Phil. J. Edinburgh, 6 (1828) 83.
14 R. C. Chirnside and J. H. Hamence, The "Practising Chemists", The Society for Analytical Chemistry, London, 1974.
15 F. Szabadvary, History of Analytical Chemistry, Pergamon Press, Oxford, 1966, p. 243.
16 J. A. Wanklyn, Milk Analysis, Trübner, London, 1874.
17 J. A. Wanklyn, Tea, Coffee and Cocoa Analysis, Trübner, London, 1874.
18 O. Hehner and A. Angell, Butter, its Analysis and Adulteration, Churchill, London, 1874.
19 J. A. Wanklyn and W. J. Cooper, Bread Analysis, Trübner, London, 1881.
20 E. B. Hughes, in A. J. Amos (Ed.), Pure Food and Pure Food Legislation, Butterworths, London, 1960, p. 24.
21 H. Droop Richmond, The Laboratory Book of Dairy Analysis, Chas. Griffin, London, 1905.
22 J. Bell, The Analysis and Adulteration of Foods, Part I, Tea, Coffee, Cocoa, Sugar, Chapman and Hall, London, 1881.
23 J. Bell, The Analysis and Adulteration of Foods, Part II, Milk, Butter, Cheese, Cereal Foods, Prepared Starches, Chapman and Hall, London, 1883.
24 A. J. Ihde, J. Chem. Educ., 51 (1974) 295.
25 W. Horwitz and H. L. Reynolds, J. Assoc. Off. Anal. Chem., 56 (1967) 1024.
26 W. Horwitz, J. Assoc. Off. Anal. Chem., 65 (1976) 238.

27 A. M. Schmidt, Proc. Symp. Pure Food and Drug Centenary, HM Stationery Office, London, 1976, p. 151.
28 Annual Book of ASTM Standards, (48 vol.) American Society for Testing and Materials, Philadelphia, 1976.
29 G. F. Smith, Analyst, 80 (1955) 16; (see also 84 (1959) 214).
30 G. E. F. Lundell, Ind. Eng. Chem. Anal. Ed., 5 (1933) 221.
31 F. D. Snell and C. T. Snell, Colorimetric Methods of Analysis, 3rd edn., Van Nostrand, New York, 1962.
32 F. D. Snell and C. L. Hilton (Eds.), Encyclopedia of Industrial Chemical Analysis, Wiley, New York, 1966 ff.
33 I. M. Kolthoff and E. B. Sandell, Textbook of Quantitative Inorganic Analysis, Macmillan, London, 1950.
34 I. M. Kolthoff and P. J. Elving (Eds.), Treatise on Analytical Chemistry, Interscience, New York, 1959.
35 A. I. Vogel, Textbook of Quantitative Inorganic Analysis, 3rd edn., Longmans, London, 1961.
36 A. I. Vogel, Textbook of Macro and Semimicro Qualitative Inorganic Analysis, 4th edn., Longmans, London, 1954.
37 C. L. Wilson and D. W. Wilson (Eds.), Comprehensive Analytical Chemistry, Elsevier, London, 1959.
38 I. M. Kolthoff and R. Belcher, Volumetric Analysis, Vol. III, Oxidation—Reduction Reactions, Interscience, New York, 1957.

Analytica Chimica Acta, 92 (1977) 13—21

REAL-TIME OBSERVATION OF LASER-INDUCED IR FLUORESCENCE OF ORGANIC POLLUTANTS IN THE AMBIENT ATMOSPHERE: SUGGESTED MECHANISM OF LASER-INDUCED IR FLUORESCENCE

J. W. ROBINSON*, D. NETTLES and P. L. H. JOWETT

Department of Chemistry, Louisiana State University, Baton Rouge, Louisiana 70803 (U.S.A.)

(Received 12th January 1977)

SUMMARY

A modified optical system has been developed for the continuous monitoring of hydrocarbons in the atmosphere by laser-induced i.r. fluorescence. The system includes a large gathering mirror, a modulated laser source to eliminate interferences from thermal emission, and phase-shifting equipment to eliminate interferences from back-scatter, particularly at the resonance wavelengths. The mechanism of excitation is discussed and a proposal put forward to explain how several photons may be simultaneously absorbed, causing fluorescence at wavelengths shorter than that of the excitation beam. Some data on the variation of the fluorescence intensity from ambient pollutants with time of day are presented for a TGS detector and a cryogenic detector.

For the remote sensing of molecular pollutants, several techniques are available, e.g., Mie scattering [1], laser Raman scattering [2—5], electronic fluorescence [2, 6—8], and i.r. fluorescence [9—12]. Of these, i.r. fluorescence holds the promise of optimum sensitivity, selectivity, and ease of operation.

In prior work in this laboratory, fluorescence spectra and other analytical data have been obtained for a large number of compounds [13—20]. With a hypothetical monitoring system it was calculated that the fluorescence of ethylene, which exhibits strong resonant fluorescence, was strong enough to be measured under ideal conditions with a resolution of 100 m at a range of 100 km at a concentration of 100 p.p.m. [21].

In later studies, attempts were made to measure atmospheric pollutants experimentally with a cassegrainian optical system. Significant but unreproducible results were obtained [21]. On the basis of these data, a different design of optical system was developed. The laser beam was aimed out of the laboratory window with the use of a single flat surface reflecting mirror. A concave collecting mirror was placed beside the flat mirror and coaxially with the laser beam so that the collecting mirror viewed several meters of the light path outside the laboratory, but not that between the laser itself and the flat mirror. The i.r. signals obtained were inaccurate because they did not

eliminate radiation scattered from the laser beam, although scattered radiation did not greatly affect the size of the "fluorescence" signals [22]. Under the conditions tested, it could conceivably be a serious source of error in smoggy atmospheres.

In an attempt to improve sensitivity and monitor resonance emission, discriminating laser back-scatter, a different optical system was employed (Fig. 1). The laser beam was aligned so that it would shine directly outside the laboratory window without using a system of mirrors. This prevented loss of laser power normally encountered at each reflecting surface. A concave collecting mirror was placed coaxially with the beam of light at the laser itself so that most of the points on the beam path could be focused on the concave mirror, especially the path closest to the source. The signals obtained showed an increase in sensitivity; even better results can be achieved.

EXPERIMENTAL

Equipment

A Perkin-Elmer model 6200 (quasi-continuous CO_2) laser was used at an operating power of 7—9 W cm^{-2} (principal lasing wavelength, 10.6 μm). A Princeton Applied Research (PAR) model 125 mechanical chopper and a coherent radiation model 201 power meter were also used. A 16-in. diameter concave mirror was coated with liquid bright gold—ethyl acetate mixture using an air brush, and then baked at ca. 600°C for several hours. The mirror had a focusing volume, rather than a point, ca. 10 cm long and 2 cm in

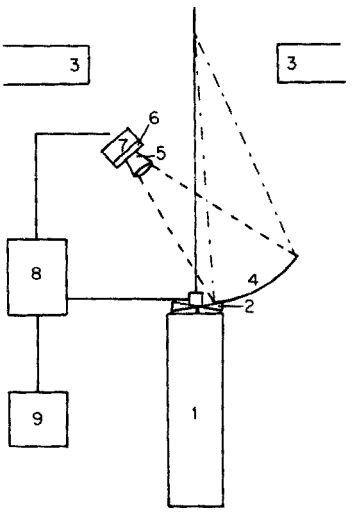

Fig. 1. Schematic diagram of laser system for remote, continuous analysis of ambient air. 1, Laser. 2, Chopper. 3, Window frame. 4, Collecting mirror. 5, Cone. 6, Filter. 7, Detector. 8, Pre-amp lock-in amplifier. 9, Recorder.

TABLE 1

Transmission range of filters on filter wheel

Filter	Transmission range[a]
1	Open (no filter)
2	1.7—5.0
3	3.0—9.5
4	7.0—15

[a]Ranges (in μm) are the total bandwidth and not necessarily the optimum transmission ranges.

diameter. The filter system was a McPherson model filter wheel; Table 1 shows the transmission range of each filter.

The detectors were a Barnes model 662 TGS pyroelectric detector with FET Amplifier (area, $4 \cdot 10^{-2}$ cm^2; detectivity, $8.1 \cdot 10^8$), and an Opto-electronic model cryogenic detector model OE-4M. (Hg—Cd—telluride; area, $4.9 \cdot 10^{-7}$ cm^2; detectivity, $2.3 \cdot 10^9$). A PAR model 124 lock-in amplifier with a PAR model 116 differential preamplifier, and a Beckman 10-in. single pen recorder were employed.

The advantages over the cassegrainian optical system were: (1) it monitored a section of the atmosphere close (1—2 m) to the laser generator; (2) loss of laser intensity caused by laser dispersion was at a minimum in this section; (3) fluorescence close to the detector was monitored. This radiation may be reabsorbed by pollutants in the air. Also, the signal intensity decreased with distance (ca. $1/d^2$). Reabsorption and dispersion were at a minimum in this section.

The optical system was aligned by placing a heating lamp emitting i.r. radiation in the laser beam path. The lamp was aligned with a He—Ne laser which passed through the CO_2 laser cavity without impinging on the sides. The radiation was attenuated by placing a box with a centered pin hole over the lamp and making sure that the collecting mirror was totally covered by this radiation. The detector was then placed where a maximum signal was obtained with filter 2 (1.7—5.0 μm).

This i.r. source was placed about 2 m from the laser and about 70 cm outside the laboratory window.

Operating conditions

Figure 1 depicts the experimental apparatus. As previously indicated, a quasi-continuous CO_2 laser was placed so that the beam of light was not reflected by any mirror to exit the laboratory. A He—Ne meteorological laser, shining through the CO_2 laser cavity, was used to ensure that there was no permanent obstruction in the path of the beam. (It was aimed to clear the top of a nearby building.) The beam shone over a university parking lot which was a source of organic emissions. To collect the emitted radiation,

the 16-in. gold coated concave mirror was placed coaxially with the laser beam so that it viewed a large portion of the beam path, especially that which was near to the source.

The lock-in amplifier received signals from the detector and the output signals from it were recorded on a Beckman recorder.

RESULTS

Signals were monitored for several months; Fig. 2 shows a typical response with the TGS detector and Fig. 3 shows the signal response with the cryogenic detector.

To attenuate the a.c. output of the PSD resulting from asynchronous signals, a capacitor is placed across the output so as to leave a d.c. output arising from an in-phase signal. The time constant is then given by the capacitor and the output resistance of the PSD (T=RC).

Measurement of fluorescence intensity

A laser power of 7—9 W cm^{-2} was used to induce fluorescence. The fluorescence intensity was measured by comparing the signals when the laser was shining (on) to those when the laser beam was physically blocked with a

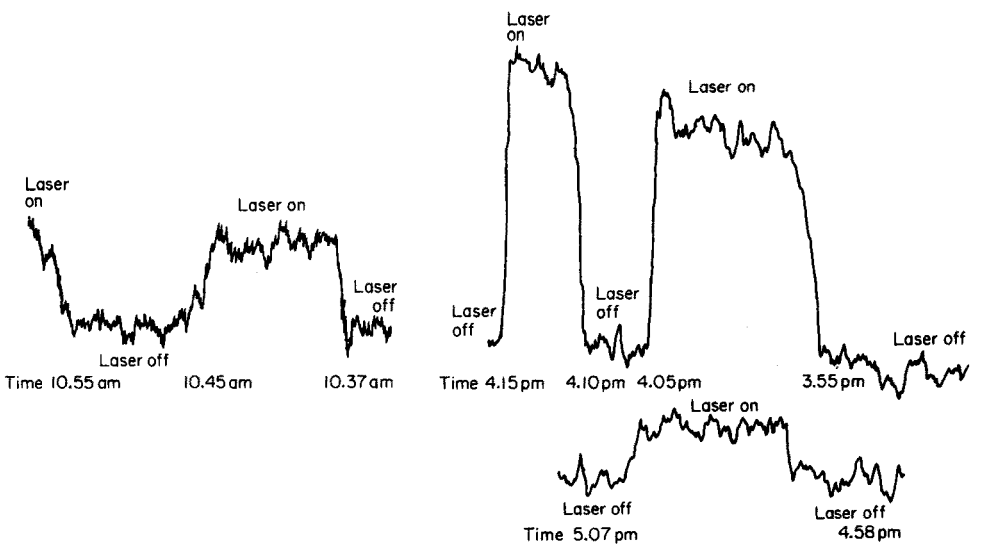

Fig. 2. Tracing of fluorescence signal vs. background with the TGS detector. Laser power, 7 W. Time constant, 30 s. Phase shift, 105°. Sensitivity, 2 μV. Filter no. 3, 3.0—9.5 μm.

Fig. 3. Tracing of fluorescence signals taken at different times of the day with the cryogenic detector. Laser power, 7 W. Time constants, 10 s. Phase shift 71°. Sensitivity, 200 nV. No filter.

piece of transite (off). The laser beam was blocked to avoid any fluctuation in laser power as a result of stopping the lasing action. Turning off the laser caused the geometry of the system to change as the laser cavity cooled down, resulting in the laser power becoming unstable.

Figure 4 shows diurnal variations of fluorescence intensity. Considerable variations were noticed from day to day; on some occasions, interpretation of the data was very difficult because of the changes in meteorological conditions. This is understandable as the fluorescence being measured (of the order of 5 μV) was a few orders of magnitude smaller than background radiation (of the order of 500 μV).

Phase-shifting

Radiation scattering is virtually an instantaneous phenomenon. It can be observed readily when the detector and the laser beam are in phase, i.e., there is zero phase shift. However, there is a finite delay between excitation and emission in i.r. fluorescence. This can be detected and distinguished from scattered radiation by phase-shifting the detector. In previous studies it was observed that in the case of ethylene the maximum signals were obtained with a 90° phase shift.

All signals observed were fluorescence rather than scattered light at 10.6 μm since not only was this radiation transmitted through filter 3 (3—9.5 μm) but all signals were monitored at 71° or 106° out of phase with respect to the reference signal. High signal intensity was observed using these phase shifts (Fig. 5). Studies with the cryogenic detector were carried out with no filter to obtain a maximum signal.

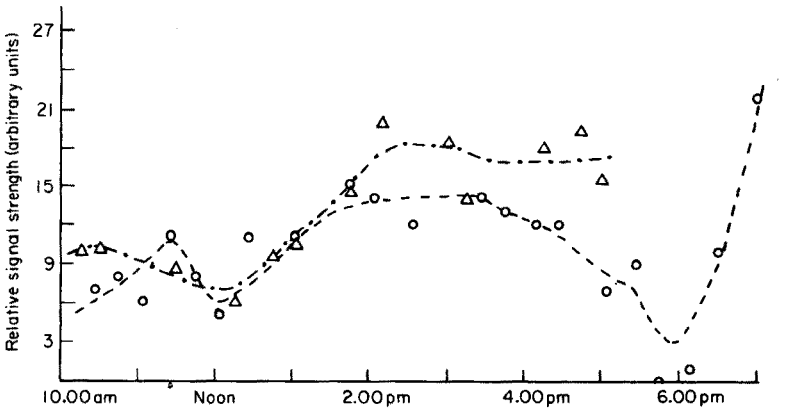

Fig. 4. Diurnal pattern of fluorescence intensity on two separate days. Note the broad maximum observed during the middle of the day. TGS; filter no. 3; 2 μV; Z = 30 s. ○ June 2, 1976, clear, sunny. △ June 30, 1976, clear, overcast.

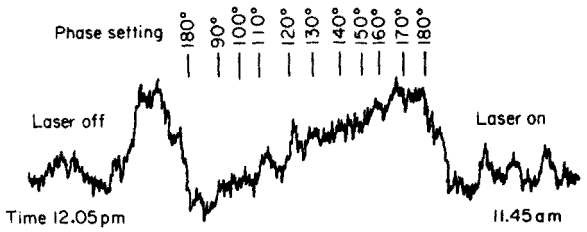

Fig. 5. Variation in fluorescence intensity vs. phase shift. Note maximum was observed at a setting of 160—180°, equivalent to a phase shift of 76—96°. Laser power, 7 W. Time constant, 30 s. Sensitivity, 2 μV. Filter no. 3. June 30, 1976 (Clear day). Phase shift is the difference between readings given above and reference phase (86°).

DISCUSSION

The sensitivities achieved with this system are greater than those reported previously [22]. It is felt that these can be improved further with increased laser power, as has been shown to occur [22].

Because of the size of the TGS detector (2 × 2 mm), focusing the collected radiation is very critical. The mirror used unfortunately had a "focusing volume" 10 cm long and ca. 2 cm in diameter. Consequently a large part of the collected signal was not focused on the detector, with the loss of several orders of magnitude of sensitivity. Sensitivity was also lost because the surface of the collecting mirror had an uneven surface.

The signals observed varied considerably, as would be expected, because of change in pollution levels. Figure 2 is a typical monitoring signal showing the change in intensity when the laser is switched on. The response times were relatively high because of the damping effect on signals caused by the long time constants used.

The data were sometimes difficult to interpret because of changes in background noise. This occurred even when a truncated cone, made of aluminium foil, was placed on the face of the detector housing looking at the collecting mirror. The cone was placed so that stray radiation around the mirror would not be seen by the detector.

Attempts to characterize pollutants were not made and resolution of pollutant distance from the detector was not attempted. However, such studies should be achieved with an improvement in the optical system.

Fluorescence intensities were measured and diurnal variations were recorded. There appears to be an increase of species as the day progresses. A nocturnal variation was not performed.

Activation and deactivation processes

Various mechanisms have been proposed whereby a laser beam of 10.6 μm wavelength is able to induce fluorescence at considerably shorter wavelengths such as 5.8 μm ($c \Rightarrow 0$) and 3.3 μm ($c \rightarrow H$). These studies do not seem to give any new insight into the true nature of this phenomenon, but a very interesting observation was made during these studies. The method used to distinguish

between fluorescence and scatter was by phase shifting. The chopping frequency of the laser was 26.3 cycles s^{-1} and the phase shifting was 71 or 106°. The delay was therefore [1/26.3] × [71(or 106)/360] = 7.5 (or 11.2) ms. Consequently, radiation emitted 7.5 (or 11.2) ms after excitation had taken place was monitored.

Collision deactivation in ambient air

At ambient temperatures and pressures, nitrogen molecules undergo $2 \cdot 10^{10}$ collisions per second [23]. During the period of phase shifting (7.5 ms) the number of collisions would be $2 \cdot 10^{10} \cdot 7.5 \cdot 10^{-3}$ or $1.4 \cdot 10^{8}$. The extent of the phase shift was selected because maximum fluorescence signals were experienced under these conditions and it was felt that this was related to the lifetime of the vibrationally excited molecule.

The number of collisions taking place during the lifetime of the excited molecule depends on that lifetime and is clearly a very large number. Deactivation would be expected to take place during this time, and no fluorescence observed. However, this was clearly not the case. There are at least two explanations; the first is that the number of collisions per unit time is very much less, but a simple calculation shows that this cannot be true. The second is that although many collisions take place, deactivation nevertheless does not occur. This may be explained as follows. The energy released in deactivation of an organic molecule is equivalent to its vibrational energy. If the molecule is in air, the energy would be transferred to an oxygen or nitrogen molecule which would become vibrationally excited only if vibrational levels of similar energy are available. If they are not available, excitation may not be possible and energy transfer may be forbidden. The data obtained in these studies indicate that such energy transfers are uncommon and the excited organic molecule remains excited in spite of many collisions with the oxygen or nitrogen in the atmosphere.

Other organic pollutant molecules have many more degrees of vibrational freedom than N_2 or O_2 and would not find difficulty in deactivating the excited organic molecules. However, the concentration of all the organic molecules present in the atmosphere is very low. Concentrations of the order of 1 $\mu g\ m^{-3}$ of air are typical; for many compounds the concentration would be significantly lower than this. Consequently, collisions between excited organic molecules and other pollutant organic molecules in the atmosphere are uncommon and this is an unlikely process for deactivation based purely on the kinetics of the frequency of collision between the various organic molecules present in the atmosphere.

Multi-photon absorption

In this study fluorescence at wavelengths as short as 3.3 μm (CH stretch) were observed, although the excitation wavelength was 10.6 μm. The absorption of 4 or more photons is necessary for such excitations. The mechanism of this excitation is not understood; several proposals have been put forward

but none is entirely satisfactory. Multi-photon absorption seems to be likely, although this phenomenon is not observed with normal non-coherent radiation. For multi-photon absorption, suitable energy levels must be available before the photons can be absorbed. Successive photons can be absorbed and the molecule excited to a very high vibrational state if the excited molecules are relatively stable and enjoy a long lifetime. This would permit the higher states to become populated and further absorption to take place, even with non-coherent light. However, this does not happen and the molecules are presumably deactivated before becoming further excited.

However, when coherent radiation is absorbed, it is possible that several photons may be absorbed simultaneously if the available upper vibrational levels meet the energy requirements. The laser photons form a wave train and are already correctly oriented relative to the molecule for absorption. After absorbing the first photon, a second photon would reach the molecule after a period of 10.6 $\mu s/c$ (in μs), i.e. $10.6 \cdot 10^{-10} \cdot 10^{-4}/3$ s or $3 \cdot 10^{-14}$ s. If the molecule has not undergone transition to an excited state during this time, the second photon may be absorbed, causing a transition to a higher state.

Because of the wavetrain nature of the laser, several photons would interact with the molecule in less than 10^{-13} s, causing excitation to very high vibrational levels. The absorbed energy may then be re-distributed through the molecule resulting in excitation of modes requiring high energy. These modes may then fluoresce, resulting in the observed phenomenon.

There are two requirements for this process to exist. First, a small amount of energy must be lost to maintain the balance between energy absorbed (10.6 μm) and energy emitted (3.3 μm). Secondly it must be possible to go from V_0 to V_3 in a single step. This may seem unlikely but bearing in mind the coherence of the radiation, the possibility cannot be ignored.

The short time period ($3 \cdot 10^{-14}$ s) between the arrival of successive photons in a wave train appears to preclude the possibility of populating successive excitation steps. For the latter to take place, the molecule would be vibrationally excited by the first photon from V_0 to V_1. The second photon would arrive after $3 \cdot 10^{-14}$ s and further excitation would take place if the transition V_0 to V_1 was completed before the arrival of the second photon. Similar excitation steps would be necessary to reach V_4 (for the absorption of four photons). This process is highly unlikely since the transition time is greater than this period ($3 \cdot 10^{-14}$ s).

Conclusions

The results show that it is feasible to monitor organic pollutants in the atmosphere with laser-induced i.r. fluorescence. The equipment used could be greatly improved; significant increases in sensitivity (several orders of magnitude) could be achieved with a more intense laser beam, better collecting mirrors, and a detector with a broader cross-sectional area than those used in this work.

Quantitative studies were not undertaken although it should not be difficult to obtain quantitative results based on the fluorescence intensity

emanating from systems in an enclosure wherein the concentration, temperature, etc. are carefully controlled.

The salient conclusion of this work is that laser-induced i.r. fluorescence can be used to monitor pollution levels in real time. No sample collection is necessary, thus avoiding many of the errors involved in this step. There is no time delay necessary for collecting and transferring the sample to the laboratory. This procedure should permit the development of real-time analyses of atmospheric pollutants and of warning systems based on the data.

Selectivity should be achievable with several lasers at different wavelengths, selectively exciting different molecular species.

Another real advantage is that this method is single ended. A laser beam and mirror detector system can be located at one point; by rotating the system, an atmosphere can be monitored in any direction. It is not necessary to use a reflecting mirror to reflect the beam, as in infrared absorption techniques, nor to locate the detector at the end of the laser beam, as is necessary in some other i.r. absorption procedures. This greatly facilitates monitoring since reasonably large areas should be monitorable from the tops of buildings and other suitable platforms in the ambient air.

REFERENCES

1 R. T. H. Collis and M. G. H. Ligda, Nature, 203, (1964) 508.
2 H. Kildal and R. L. Byer, Proc. IEEE, 59 (1971) 1644.
3 H. Inaba and T. Kobayasi, Nature, 224 (1969) 170.
4 T. Kobayasi and H. Inaba, Appl. Phys. Let., 17 (1970) 139.
5 E. R. Schildkraut, Am. Lab., Dec. (1972) 23.
6 R. N. Measures, A Comparative Study of Laser Methods of Air Pollution Mapping, Utias Report No. 174 (1971).
7 S. A. Ahmed, Appl. Opt., 12 (1973) 901.
8 M. R. Bowman, A. J. Gibson and M. C. W. Sanford, Nature, 221 (1969) 456.
9 J. W. Robinson, H. M. Barnes, D. Truitt, D. M. Hailey, H. P. Loftim, C. Woodward and J. D. Rosamond, Research on New Techniques on Absorption and Emission spectroscopy, Final Comprehensive Report, Dept. of the Army, Contract DA-18-035-AMC-378(A) (1969).
10 R. T. Menzies, Appl. Opt., 10 (1971) 1532.
11 I. Melngailis, Trans. IEEE, GE-10, (1972) 7.
12 R. T. Menzies, Appl. Phys. Lett., 22 (1973) 592.
13 J. W. Robinson, H. M. Barnes and C. Woodward, Spectrosc. Lett., 1 (1968) 109.
14 J. W. Robinson, H. M. Barnes and C. Woodward, Anal. Chim. Acta, 43 (1968) 119.
15 J. W. Robinson, D. M. Hailey and H. M. Barnes, Talanta, 16 (1969) 1109.
16 D. M. Hailey, H. M. Barnes, C. W. Woodward and J. W. Robinson, Anal. Chim. Acta, 56 (1971) 161.
17 D. M. Hailey, H. M. Barnes and J. W. Robinson, Anal. Chim. Acta, 56 (1971) 175.
18 C. M. Christian and J. W. Robinson, Spectrosc. Lett., 4 (1971) 255.
19 J. W. Robinson and J. L. Guagliardo, Spec. Lett., 6 (1973) 271.
20 N. Katayama, A Study of the Applications of Laser Induced Fluorescence in Analytical Chemistry, Dissertation, LSU (1974).
21 J. Dake, Analytical Parameters in the Remote Sensing in Air Pollutants using Laser-Induced IR Fluorescence, Dissertation, LSU (1973).
22 J. W. Robinson and J. L. Guagliardo, Spectrosc. Lett., 7 (1974) 121.
23 F. Danniels, R. A. Alberty, J. Wiley, Physical Chemistry, 3rd edn., 1966.

Analytica Chimica Acta, 92 (1977) 23—32

APPLICATION OF THE MÖSSBAUER EFFECT TO MICROGRAM SAMPLES WITH RESONANCE SAMPLE SCINTILLATORS

Ts. BONCHEV* and B. MANOUCHEV
Faculty of Physics, University of Sofia, Sofia 1126 (Bulgaria)
M. VUCHKOV
Niproruda Institute, Sofia (Bulgaria)
(Received 5th September 1976)

SUMMARY

The possibilities of the Mössbauer effect for qualitative and quantitative measurements of microgram amounts of resonance absorbing matter are considered. The sample is placed in a plastic scintillator and the conversion electrons emitted are measured. The preparation of the resonance sample scintillators (RSS) and the methods of measurement are described in detail. Mössbauer spectra of different samples containing SnO_2 are given as an example. The sensitivity of the method is around 10^{-7} g (even less in some cases). A concentration of $4 \cdot 10^{-6}$% $SnCl_2$ in aqueous solution can be measured. The methods can be used for surface studies of small particles.

The parameters of the Mössbauer spectrum permit the identification and determination of chemical compounds containing resonance absorbing atoms. The usual Mössbauer methods require samples of the order of several milligrams. In the present paper, a new method of analysis is proposed, which can be applied to samples smaller by several orders of magnitude; the samples are introduced into a plastic scintillator.

Levy et al. [1] were the first to suggest the measurement of conversion electrons with a scintillator; they proposed SnO_2 for the detection of tin with a plastic scintillator. Increasing the concentration of the resonant matter affects the properties of such detectors adversely. Only 10—20% of the total number of γ-quanta are measured because of fogging of the scintillator. With minute quantities of matter, there are no such limitations. A scintillation detector with the sample placed in the detector itself is called a resonant sample scintillator (RSS).

Some earlier results obtained in the studies described here have already been reported [2, 3].

Preparation of resonant sample scintillators (RSS)

The substance introduced into the scintillator must be chemically inert and must not affect adversely the properties of the scintillator. Organic scintillators are suitable, as they are very effective for conversion electron measurement but show low sensitivity for γ-quanta. The probability of photon or Compton effects in such scintillators is low. The optimum thickness of the scintillator is such that emitted conversion electrons are stopped, while measurement of γ-quanta is not significant.

Plastic scintillator of the NE-102 type (English) was used. Enough of this is dissolved in scintillation-pure toluene to form a film of the required thickness after drying. The sample is ground in an agate mortar and then mixed with the scintillator solution. It is assumed that the ratio between the initial weights of the substance and the scintillator do not change after preparation of the detector. After homogenization the mixture is poured over a clean glass plate which is kept strictly horizontal until drying is complete. The prepared RSS is removed carefully from the glass, and stuck to the surface of a light conductor with transparent silicone grease. The other side of the scintillator can be covered with aluminized mylar as a light reflector. The light conductor is used to avoid any considerable increase in the background if γ-quanta reach the photocathode directly, as the pulses formed from the γ-quanta and those from the scintillations have comparable amplitude. A Plexiglas block with the front portion cut at an angle of 45° was used as the light conductor (Fig. 1). Plexiglas also gives scintillations but the number of pulses is two orders of magnitude less than the background pulses obtained without a light conductor.

With dark or black substances it is better to apply the scintillator on top of a fixed powder sample. The scintillator thus remains transparent and the light conditions are improved. Only conversion electrons from the upper

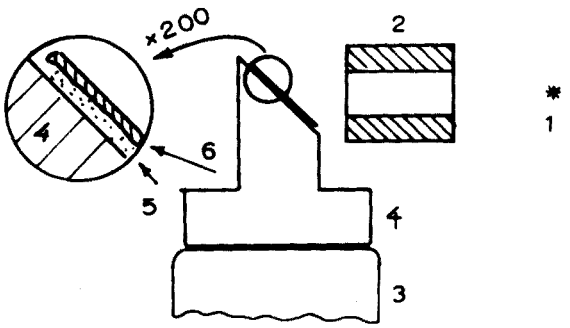

Fig. 1. Design of a resonant sample scintillation detector. (1) Source; (2) collimator; (3) photomultiplier; (4) light conductor; (5) transparent grease; (6) resonant sample scintillator.

portion of the sample are investigated. This method can be used to study surfaces of massive samples as well.

Amplitude spectrum of the pulses recorded

The background pulses consist of: (1) scintillation from absorption of resonant and non-resonant γ-quanta in the plastic scintillator; (2) scintillation from photon effects in the sample; (3) scintillation from interactions of the γ-rays and the Plexiglas; and (4) electronic noise in the photomultiplier. Sources (1) and (2) are the most important. These effects can be minimized by correct selection of the resonant substance/scintillator ratio, by using a suitable particle size and by working with substances enriched with Mössbauer isotopes (see later).

The photomultiplier noise can be reduced by cooling. If photomultipliers of the EMI 6097S type are used, the number of noise pulses is sufficiently low even at room temperature. With ^{119}Sn, cooling is not necessary. Iron requires lower temperatures (—10°C to 0°C), as the Mössbauer transitions are of lower energy.

Figure 2 shows the amplitude spectra of RSS made with $^{119}SnO_2$; the source was $Ba^{119}SnO_2$. Figure 2(b) shows the same spectra normalized to the number of pulses in an initial channel. The four spectra were obtained as follows: (1) at zero velocity (maximum resonance absorption); (2) at infinite velocity (disturbed resonance); (3) without the RSS (scintillation in the light conductor only); and (4) without a γ-source (photomultiplier noise only). Curves 1 and 2 in Fig. 2(b) are similar, which indicates the identical origin of the pulses measured. Curve 1 shows the conversion electron spectrum, and curve 2 the spectrum of photoelectrons with the same energy. Curve 3 is

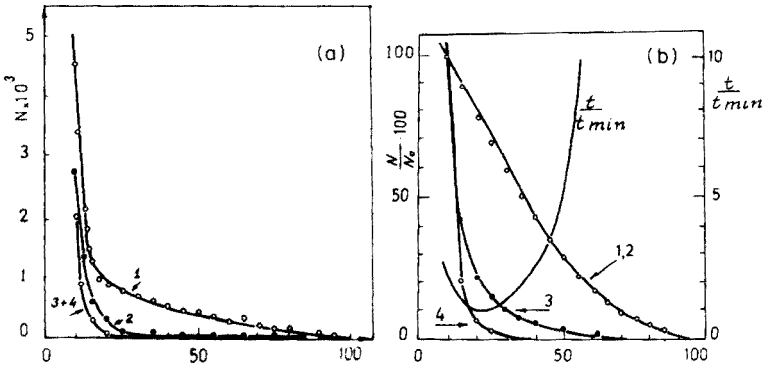

Fig. 2(a) RSS pulse amplitude spectra. (1) At zero velocity; (2) at infinite velocity; (3) scintillation of the light conductor; (4) photomultiplier noise. (b) These amplitude spectra normalized to the number of pulses in an initial channel and the relative measuring time change necessary to achieve a preset accuracy, t/t_{min}, depending on the discriminator threshold.

close to the curve of one-electron noise pulses of the photomultiplier (curve 4), thus showing that the background pulses are far fewer than the useful pulses presented by curve 1.

The time required to obtain a preset accuracy of measurement depending on the threshold of the integrating discriminator is also plotted in relative units in Fig. 2(b); t is the time required for measuring the effect with the preset accuracy when the discriminator threshold is placed in a specified position. Its minimum value is t_{min}. The background increases at low threshold values, whereas at high threshold values some of the "useful" pulses are lost. Both types of operation result in an increase of the measuring time.

QUANTITATIVE EVALUATION

The number of recorded photons N (γ-quanta) of the resonance line for time t (s) when there is no Mössbauer effect can be determined by

$$N = J_0 \, t \, e_1 \tag{1}$$

where J_0 is the intensity of radiation falling on the detector (γ-quanta/s), and e_1 is the efficiency of the γ-quanta recording. For simplicity, it is assumed that the radioactive source emits only the γ-quanta resonance line; non-resonance absorption processes are neglected. J_0 is obtained from

$$J_0 = 3.7 \cdot 10^7 \, A_0 \rho \, \omega/(1 + \alpha) \tag{2}$$

where A_0 is the activity of the source (mCi); ρ is the relative portion of the resonance transitions in the general decay scheme; ω is the solid angle relative to 4π units; $1/(1 + \alpha)$ is the probability of γ-quanta radiation from a resonance level; and α is the total internal conversion coefficient.

The theoretical value of the Mössbauer absorption in a sample at the resonance absorption maximum is

$$\Delta N = J_0 f \, [1 - e^{-\frac{x}{2}} I_0 \, (x/2)] t \tag{3}$$

where f is the probability of recoilless γ-quanta radiation; x is the effective thickness of the absorber; $I_0 \, (x/2)$ is the zero-order Bessel function; and t is the measuring time (s).

ΔN can also be expressed as $\Delta N = J_0 \, \epsilon_t \, t$, where ϵ_t is the theoretical value of the Mössbauer effect measured in ordinary transition geometry: $\epsilon_t = (N_\infty - N_0)/N_\infty$, N_0 and N_∞ being the count rates in the resonance and non-resonance positions, respectively. The experimental value of the Mössbauer effect is $\epsilon_e = (N_\infty - N_0)/(N_\infty + N_b)$, where N_b is the count rate of the background.

The effective thickness of the absorber, X, is

$$X = \mu f' d \tag{4}$$

where μ is the mass absorption coefficient ($cm^2 \, g^{-1}$) for the resonant radiation;

f' is the recoilless absorption probability; d is the amount of absorber (g cm^{-2}). μ is determined from $\mu = \sigma_0 L a/A$, where σ_0 is the maximum effective cross-section for absorption from the Mössbauer isotope (cm^2/atom); L is the Loschmid—Avogadro number ($6.02 \cdot 10^{23}$ atoms mol^{-1}); A is the atomic weight of the element; and a is the relative content of the Mössbauer isotope in the sample.

In the present case, $X \ll 1$, and the number of resonance absorptions measured with an ordinary detector is $\Delta N = \frac{1}{2} J_0 f X t e_1$. With an RSS the number of pulses measured is

$$\Delta N^* = \tfrac{1}{2} J_0 f X e^* t^* \alpha/(1 + \alpha) \tag{5}$$

where $\alpha/(1 + \alpha)$ is the probability of conversion electron emission from a particular resonance absorption; e^* is the efficiency of measurement for a conversion electron by the photomultiplier; and t^* is the measuring time with an RSS.

Combination of eqns. (2) and (4) with eqn. (5) yields the final expression for ΔN^*:

$$\Delta N^* = \tfrac{1}{2} \cdot 3.7 \cdot 10^7 A_0 \rho f f' \mu d\omega e^* t^* \alpha/(1 + \alpha)^2 = \text{const} \times A_0 f f' d\omega e^* t^* \tag{6}$$

Some of the parameters in expression (6) concerning iron and tin are given in Table 1.

The advantages of RSS can be illustrated by comparing the times needed to obtain the same relative statistical error by working with an ordinary detector and with an RSS.

The relative statistical error, η, in measuring ΔN with an ordinary detector is

$$\eta = 2^{\frac{1}{2}}(1 + \beta)^{\frac{1}{2}}/\epsilon_t N^{\frac{1}{2}} \tag{7}$$

where $\beta = N_b/N$, N_b being the background radiation measured.

The relative statistical error η^* in measuring ΔN^* with an RSS is

$$\eta^* = (1 + \epsilon^*)^{\frac{1}{2}}(\epsilon^* + 2)^{\frac{1}{2}}/\epsilon^* N^{\frac{1}{2}} = (\epsilon^* + 2)^{\frac{1}{2}}/\epsilon^* N_b{}^{*\frac{1}{2}} = (\epsilon^* + 2)^{\frac{1}{2}}/(\epsilon^* \Delta N^*)^{\frac{1}{2}} \tag{8}$$

η^* is determined by N^*, $N_b{}^*$ or ΔN^*, where N^* is the number of pulses

TABLE 1

Data of some Mössbauer parameters for iron and tin
(E_γ — energy of the resonance line: a_n — relative content of the Mössbauer isotope in the element as it is found in nature. Values for a_n, E_γ, α and σ_0 are taken from Spinel [4].)

Isotope	a_n	E_γ (keV)	α	σ_0 (cm^2 mg^{-1})	μ (cm^2 mg^{-1})		Const. eqn. (6) ($\cdot 10^{-7}$)	
					$a = 1$	a_n	$a = 1$	a_n
^{57}Fe	0.0217	14.39	9.0	23.63	25.4	0.558	4.24	0.092
^{119}Sn	0.0858	23.8	5.5	13.26	6.7	0.573	1.62	0.139

measured in the resonance absorption peak, and N_b^* is the background radiation measured; $N^* = \Delta N^* + N_b^*$.

$\epsilon^* = \Delta N^*/N_b^*$ is the magnitude of the experimental Mössbauer effect for the given sample. The ratio between the time t necessary for measurement with an ordinary detector and the time t^* necessary for measurement with the RSS when the relative statistical errors are the same ($\eta = \eta^*$) is

$$t/t^* = \left[2(1 + \beta)\frac{\alpha}{1 + \alpha}e^*\right] / [e_1\,\epsilon_t(1 + 2/\epsilon^*)] \tag{9}$$

This equation can be approximated as

$$t/t^* \approx \epsilon^*/\epsilon_t = \Delta N^*/N_b^*\epsilon_t$$

for small values of the measured effect ($\epsilon^* \ll 1$).

The resonance sample detectors have definite advantages over any conventional detector when small quantities of substances are studied, because t/t^* is increased by decreasing the amount of sample. In such cases the term $\Delta N^*/\epsilon_t$ remains constant but N_b^* decreases. N_b^* is determined by

$$N_b^* = [(J_b^{(1)} + J_b^{(2)}) + \sum_{i,j}\sigma(Z_i,E_j)J_j d_i e^*] \tag{10}$$

where $J_b^{(1)}$ is the photomultiplier noise (pulses/s); $J_b^{(2)}$ is the scintillation intensity in the light conductor (pulses/s); $\sigma(Z_i, E_j)$ [cm^2 g^{-1}] is the effective cross-section for an element in the sample with atomic number Z_i and γ-quantum energy E_j; J_j is the intensity of γ-radiation of energy E_j; and d_i is the amount (g cm^{-2}) of element Z_i in the sample.

The background is lower for lower values of $\sigma_{i,j}$. Values of σ_{ij} can be obtained by extrapolating the data given by Storm and Israel [5]. The values of some elements for iron and tin resonance radiation are presented in Table 2. It is interesting to compare these values with the real mass absorption coefficient of the Mössbauer radiation, $\mu_r = ff'\mu/2$. If we assume that $f = f' = 0.5$, as is the case with SnO_2 as source and absorber, the values of μ_r (cm^2 g^{-1}) are as follows:

— for iron of natural isotope composition (a_n),	69
— for enriched iron (a = 1),	3185
— for tin of natural isotope composition (a_n),	72
— for enriched tin (a = 1)	841

For natural iron and tin, with $f = f' = 0.5$, the ratios μ_r/σ_{ij} for the corresponding resonance radiation are 1 and 1.56, respectively. The value 1.56 for tin is very close to the experimentally obtained value $\epsilon^* = \Delta N^*/N_b^* = \mu_r/\sigma_{ij} = 1.6$ (Table 3). The content of unenriched SnO_2 in the sample was 1.1 mg cm^{-2}.

RESULTS AND DISCUSSION

The possibilities of RSS for measuring small quantities of resonance-absorbing matter were tested with four series of samples containing SnO_2.

TABLE 2

μ_{ij} values for some elements ($cm^2\ g^{-1}$)

Source	E_γ (keV)	Fe $Z = 26$	Sn 50	W 74	Pb 82
^{57}Co	14.39	68	55	150	125
^{119}Sn	23.8	16	46	62	67

Measurements were done only at zero and infinite velocities, because the maximum of the Mössbauer spectrum for SnO_2 with a $Ba^{119}SnO_3$ source is at zero velocity.

Four series of samples were analyzed. Unenriched SnO_2 was measured alone, in mixtures with Ce_2O_3, and in mixtures with Mn_2O_3—NiO—PbO (which were black). The results are given in Table 3. Samples were also prepared by adsorption of $SnCl_2$ (containing 85% ^{119}Sn), on freshly prepared β-stannic acid (containing 85% of the Mössbauer inactive isotope ^{118}Sn). The absorption conditions and results are shown in Table 4; heating the samples at 300°C converted the adsorbed substance to SnO_2.

TABLE 3

Results of Mössbauer effect measurements of micro amounts of SnO_2 with the RSS

Sample	(%)	Thickness of Scintillator (mg cm^{-2})	Thickness of Sample (mg cm^{-2})	SnO_2 (mg cm^{-2})	$\Delta N^*/d$ (c.p.m.)	ϵ^* (×100)	ϵ (×100)	t/t^*	Total time of measurement (min)
I-1[a]	100	2.7	1.1	1.1	10.2 ± 0.3	161 ± 5	6.0	13	8
I-2	100	1.3	0.06	0.06	13.7 ± 1.2	27 ± 3	0.34	55	40
I-3	100	0.8	0.0035	0.0035	21 ± 9.4	2.7 ± 1	0.02	113	200
II-1[b]	25	2.0	0.33	0.083	3.2 ± 0.6	6.5 ± 1	0.47	11	64
II-2	25	3.5	0.20	0.050	6.3 ± 1	6.8 ± 1.5	0.28	26	64
II-3	25	4.2	0.19	0.047	7.3 ± 2	8.7 ± 1.4	0.25	28	80
II-4	25	5.2	0.17	0.043	9.0 ± 1.5	8.6 ± 1.6	0.23	30	64
II-5	25	6.9	0.20	0.043	7.8 ± 1.3	8.5 ± 1.5	0.28	25	64
II-6	25	7.9	0.20	0.047	9.4 ± 1.4	8.3 ± 1.2	0.25	27	80
II-7	25	9.5	0.18	0.045	10.6 ± 1.5	8.6 ± 1.2	0.27	27	80
II-8	50	1.5	0.14	0.070	9.3 ± 1	11.2 ± 1.5	0.40	28	64
II-9	10	7.1	0.43	0.043	6.1 ± 1	5.3 ± 1.3	0.25	18	80
III-1[c]	50	1.6	0.15	0.075	6.3 ± 0.6	1.6 ± 1	0.42	22	64
III-2	25	3.9	0.66	0.17	2.2 ± 1	2.9 ± 1.4	0.93	3	80
III-3	25	5.2	0.69	0.17	3.9 ± 1.1	5.6 ± 1.5	0.25	5	64
III-4	25	5.5	0.18	0.046	6.1 ± 1.1	10.0 ± 2	0.25	32	64
III-5	25	5.8	0.58	0.15	5.2 ± 1.3	5.8 ± 1.5	0.82	6	64
III-6	25	8.0	0.69	0.18	5.6 ± 1.1	5.8 ± 1.2	0.98	5	80
III-7	25	9.1	0.51	0.13	4.2 ± 1.6	3.2 ± 1.2	0.72	4	80
III-8	25	10.7	0.75	0.19	3.0 ± 1	4.1 ± 1.4	1.1	3	64
III-9	25	12.1	0.74	0.18	2.9 ± 1.2	3.1 ± 1.3	0.97	3	64
III-10	10	6.0	0.4	0.04	3.3 ± 1.5	5.2 ± 2.4	0.22	20	56
III-11	10	7.8	0.3	0.03	5.1 ± 1.2	5.7 ± 2.0	0.18	26	56

[a]Pure unenriched SnO_2. [b]Mixtures of Ce_2O_3 with unenriched SnO_2 (10—50%, as indicated). [c]Unenriched SnO_2 added as indicated to a mixture containing 15% Mn_2O_3, 15% NiO and 70% PbO.

TABLE 4

Results of Mössbauer effect measurements of $^{119}SnO_2$ adsorbed on β-stannic acid prepared with ^{118}Sn
(The amount of ^{119}Sn was determined by assuming that all the ^{119}Sn in solution had been adsorbed.)

	Total Sn in soln.	Sn concn. ($g\ g^{-1}$)	pH	Drying temp. (°C)	Weight of Scintillator (mg cm^{-2})	Weight of Sample (mg cm^{-2})	ΔN^* (c.p.m.)	ϵ^* (×100)	Time of measurement (min)	^{119}Sn (mg)
IV-1	10^{-1}	$6.7 \cdot 10^{-7}$	4.5	20	1.3	0.37	13.4 ± 3.2	6.6 ± 1.6	80	$7.4 \cdot 10^{-4}$
IV-2	10^{-2}	$6.7 \cdot 10^{-7}$	4.5	300	1.0	0.16	7.9 ± 2.8	4.3 ± 1.5	96	$2.7 \cdot 10^{-4}$
IV-3	10^{-2}	$4.0 \cdot 10^{-8}$	6.5	300	2.1	0.62	14.2 ± 3.5	4.9 ± 1.2	96	$3.1 \cdot 10^{-4}$
IV-4	10^{-2}	$4.0 \cdot 10^{-8}$	8.0	300	1.6	0.55	2.4 ± 3.3	0	96	0
IV-5	10^{-3}	$1.7 \cdot 10^{-7}$	5.0	300	1.8	0.45	8.4 ± 3.2	4.1 ± 1.6	80	$0.9 \cdot 10^{-4}$
IV-6	0	0	7.0	300	1.1	0.27	2.3 ± 2.2	0	160	0

The following conclusions can be made from Table 3. RSS prepared with pure unenriched SnO_2 suspended in the scintillator (samples I-1 and I-3) give very good results; the measuring time is reduced by several orders of magnitude. The conversion electron yield per unit resonant substance, $\Delta N^*/d$, is higher for more transparent scintillators, i.e. for smaller amounts of sample (column 6); 3.5 μg of ordinary SnO_2, corresponding to 0.4 μg of $^{119}SnO_2$ (sample I-3) were counted for about 200 min. This is the total time for measuring N^* and N_b^*.

The number of conversion electrons and the value of the Mössbauer effect ϵ^* per 1 μg of SnO_2 (columns 6 and 7, respectively) for series II and III are lower than the corresponding values for series I. This is to be expected because series II and III contained inert and Mössbauer inactive ingredients. Moreover, series II was yellow and series III was black. In both cases, the number of conversion electrons per 1 μg of SnO_2 is higher for lower concentrations of the test substance in the scintillator (Fig. 3); the number is lowest for the opaque series III. The value t/t^* for this series calculated from eqn. (9) is also the lowest. In this case, t/t^* is low not only because of the opacity of the sample but also because the background is increased by the high number of photoelectrons for heavy atoms. The results from series III illustrate the difficulties of quantitative measurements with the RSS. In such cases, the "internal standard" method might be used. A known quantity of substance with a high isomeric shift of its Mössbauer line compared to the Mössbauer line of the test substance can be added. For SnO_2 a suitable compound would be $SnSO_4$ with two lines displaced towards the SnO_2 line at +3.42 and 4.47 mm s^{-1}, respectively.

The results of the sample series IV (Table 4) are interesting. They show that adsorption of $SnCl_2$ on β-stannic acid from aqueous solution occurs below pH 7. The quantities of ^{119}Sn given in the final column were calculated on the assumption of total adsorption of the $SnCl_2$, which may not be true. Despite this uncertainty, it is clearly possible to measure amounts of ^{119}Sn less than 10^{-6} g.

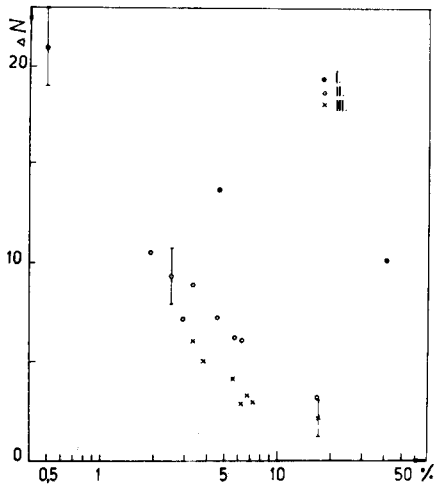

Fig. 3. Yield of conversion electrons per unit quantity of the resonant substance as a function of the percentage of resonant substance in the RSS. •, I; ○, II; ×, III.

It is necessary to establish the optimum quantity of the test substance in working with the RSS. Small quantities are required with dark coloured substances, so that the RSS will be sufficiently transparent for the scintillations. A good spectrum of SnO prepared with unenriched tin, for example, was obtained with about 0.01 mg cm^{-2} (Fig. 4, curve b). Curve (a) was obtained for the same substance by the ordinary Mössbauer absorption method for a sample of thickness 15 mg cm^{-2}. Both spectra show the SnO_2 line. Most probably, partial oxidation of the SnO occurred. The relative intensity of the SnO_2 line in curve (b) is considerably higher than that in curve (a). A likely explanation is that oxidation mainly affects the surface particles, thus increasing the proportion of conversion electrons coming from the SnO_2 surface rather than from the bulk material. This suggests the possibility of investigating surfaces of small particles, e.g. in studies of adsorption, catalysis, etc.

Figure 5 shows spectra of whiskers containing unenriched tin, and illustrates the possibilities of investigating the composition of very small samples. About 20 whiskers (10—20 μm diameter; 1—2 mm long) were incorporated in an RSS; spectra were recorded at room temperature where the probability of recording the $SnCl_2$ line is very low. Its observation was possible because the concentration of $SnCl_2$ on the sample surface was high.

In conclusion, the results described above suggest new possibilities for the application of Mössbauer spectroscopy. With the resonance sample scintillators, it is possible to investigate the chemical structure and the composition of samples in the microgram range. The sensitivity approaches that of conventional chemical and physical analytical methods. With RSS it is possible to investigate changes of chemical structure on the surfaces of small particles.

TABLE 5

Comparison of the sensitivity of some methods for tin

Method	Max. Sensitivity		Reference
	Relative Amount %	Absolute amount (g)	
Emission spectrometry:			
arc	$5 \cdot 10^{-4}$		[6]
Flame	$1 \cdot 10^{-4}$		[6]
Flame photometry		10^{-9}	[7]
Proposed method		10^{-7}	

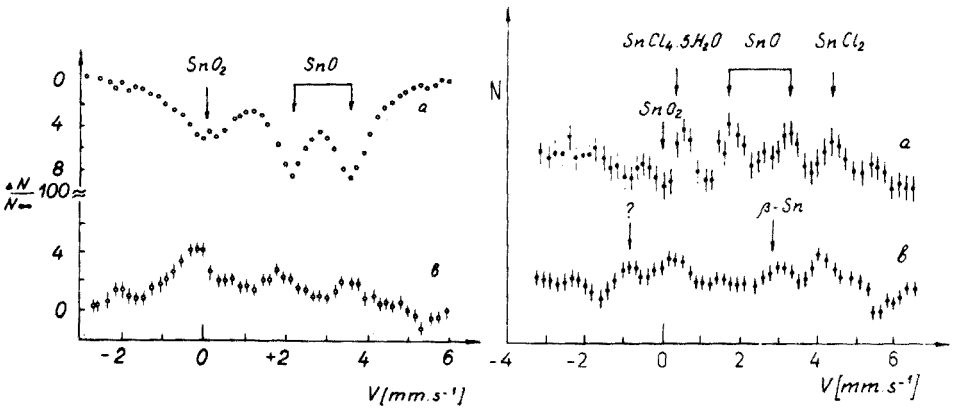

Fig. 4. Mössbauer spectrum of SnO, partially oxidized to SnO_2. (a) Measured with an ordinary detector. (b) Measured with an RSS.

Fig. 5. Mössbauer spectra of whiskers, grown from $SnCl_2$ during heating: (a) in air; (b) in a hydrogen atmosphere.

This work was performed under IAEA (Vienna) contract 1141. The authors are grateful for this financial and moral support. The authors thank P. Mihailova and P. Petrova for technical assistance.

REFERENCES

1 L. Levy, L. Mitrami and S. Ormandjiev, Nucl. Instrum. Methods, 41 (1964) 233.
2 Research Contract No. 1141, Technical Reports Series No. 154, IAEA, Viene (1974).
3 Proc. 5th Int. Conf. Mössbauer Spectrosc., Bratislava, part 3, (1973) 687.
4 V. S. Spinel, Resonance of Gamma-Rays in Crystals (Resonans gamma — lutchei v kristallah), Moskwa, 1969.
5 E. Storm and H. Israel, Photon Cross-Sections from 0.001 to 100 MeV, Los Alamos Scientific Laboratory, New Mexico, 1967.
6 W. Schorön and L. Rost, Atom-Spectralanalyse, Leipzig, 1969.
7 I. Yudelevich, XVII Coll. Spectroscopium Intern. Firenze, Vol. I., 1973, p. 388.

Analytica Chimica Acta, 92 (1977) 33—41

MOLECULAR EMISSION CAVITY ANALYSIS
Part X. The Separation and Simultaneous Determination of Arsenic and Antimony by Hydride Generation

R. BELCHER, S. L. BOGDANSKI, E. HENDEN† and ALAN TOWNSHEND*

Chemistry Department, University of Birmingham, P.O. Box 363, Birmingham B15 2TT, (England)

(Received 14th March 1977)

SUMMARY

Arsenic and antimony (both 0—50 p.p.m.) are determined simultaneously by conversion to their hydrides with sodium borohydride, followed by gas chromatographic separation, and measurement of the eluted gases by molecular emission cavity analysis at 400 nm. Tin can also be determined simultaneously. All interferences are masked by EDTA. A more sensitive procedure for arsenic (0—2 p.p.m.) or antimony (0—4 p.p.m.) is also described, based on a cold trap collection technique.

The determination of arsenic and antimony has been achieved by the production of their volatile hydrides which are then converted to their atomic species and detected spectrophotometrically. The conversion to arsine and stibine has been found to be a convenient means of separating these elements from interfering matrices as well as offering enhanced sensitivities.

Reductants which have been used to generate the hydrides include zinc [1—3], magnesium [4, 5], titanium(III) chloride [4, 5], and sodium borohydride [6—14]. The analyte vapours formed in a reaction vessel have been swept directly into a flame for analysis [14, 15], or collected in a liquid nitrogen cold trap [1, 8, 10] or a balloon reservoir [2, 3, 9, 12] before measurement.

Atomic absorption is the method most widely used for the final measurement, although atomic emission in a d.c. discharge [7] and atomic fluorescence in an argon—hydrogen—entrained air flame [11] have also been employed. An automated system for determination of arsenic and antimony via sodium borohydride reduction followed by atomic absorption is described by Schmidt et al. [13].

---

†Present address: Department of Analytical Chemistry, Faculty of Science, University of Ege, Bornova, Izmir, Turkey.

Detection limits

Generally, nanogram amounts of arsine and stibine can be detected in 1 ml of sample initially injected into the reaction chamber. Using a sodium borohydride reduction and a balloon reservoir collection with atomic absorption, Fernandez [12] found detection limits of 10 ng for As and 5 ng for Sb at 194 nm and 218 nm, respectively. The detection limit for arsenic was reduced to 3 ng by using an electrodeless-discharge lamp in place of the hollow-cathode lamp. Thompson and Thomerson [14] achieved detection limits of 0.8 ng for As and 0.5 ng for Sb by atomic absorption, employing a 17-cm long silica tube mounted in an air—acetylene flame into which the hydrides were introduced directly from the reaction chamber. Using an atomic fluorescence measurement, Thompson [11] found that for determinations of less than 1 ng, the purity of the ingredients used in generating the hydrides, particularly sodium borohydride, is a limiting factor.

Interferences

Although numerous papers have been published on the hydride generation technique for the determination of elements which yield volatile hydrides, few have investigated interferences. These occur mainly during the vaporization step. Smith [16] reported that hydride generation by sodium borohydride is severely depressed by the presence of many cations. Belcher et al. [17] eliminated the suppression of arsenic and antimony emission caused by Co^{2+}, Ni^{2+}, Zn^{2+}, Fe^{3+}, Bi^{3+}, Cd^{2+}, Cu^{2+} and Ag^{+} by making the sodium borohydride reaction solution 0.01 M in EDTA. The use of EDTA to suppress interferences was later applied by Drinkwater [18] for the determination of bismuth in nickel-based alloys by a hydride generation—atomic absorption procedure.

Molecular emission cavity analysis

Belcher et al. [19] applied the sodium borohydride reduction system for the determination of arsenic and antimony by molecular emission cavity analysis (MECA) with a hydrogen—nitrogen flame. Molecular emissions believed to be derived from AsO and SbO were formed within the MECA cavity by supplying a small flow of oxygen along with the vaporized hydrides into the cavity; 0.5—5 μg of As and 1—10 μg of Sb were determined in ca. 1 ml of sample.

The molecular emissions obtained for As and Sb had broad spectra over the range 330—550 nm, with maxima at 400 nm and 355 nm, respectively. Most cationic interferences can be eliminated by the addition of EDTA, but arsenic and antimony mutually interfere because of the almost complete spectral overlap. The present paper describes the simultaneous determination of arsenic and antimony based on a gas chromatographic separation of arsine and stibine followed by a MECA measurement of both oxide emissions at a single wavelength. In addition, a more sensitive procedure for arsenic or antimony, by collection in a cold trap, is described.

EXPERIMENTAL

Instrumentation

Molecular emissions were measured by an Evans Electroselenium EEL 240 flame spectrophotometer operating in the emission mode and modified to accommodate a MECA cavity holding assembly [20]. A maximal slit of 12, corresponding to 0.91 mm (spectral bandpass 3 nm), were used throughout. A Servoscribe 1S chart recorder, having a response time of 0.5 s was connected to the 10 mV output of the instrument.

The cavity cross-section is illustrated in Fig. 1. It is a stainless steel water-cooled cavity, 8 mm in diameter and 5 mm deep. Cooling the cavity prevents incandescence of the cavity material as well as enhancing the emissions from As and Sb. Oxygen and carrier gas were introduced into the cavity via stainless steel capillary tubing entering tangentially through two holes (0.8 mm diameter) in the side wall of the cavity. The cavity was positioned at 6° below the horizontal and cooled with water flowing at 40 ml min^{-1}.

The complete volatilization system for the generation of arsine and stibine is shown in Fig. 2. The generation tube consists of a glass reaction vessel, 13 cm long and 2 cm in diameter, with a side arm. A glass syringe with a Teflon needle was used for injection of the sample into the reaction vessel. The needle was fixed in the hole of a rubber stopper which was then attached to the side arm. The top of the reaction vessel was closed with a rubber bung with two holes for carrier gas inlet and outlet. Both bungs were covered with Teflon tape. The reaction products were dried by passing through a 10-cm long, U-shaped, PVC drying tube packed with Drierite between two cotton wool plugs, before proceeding to the gas chromatographic column.

The gas chromatographic column [21] was a 25-cm length of 3-mm bore

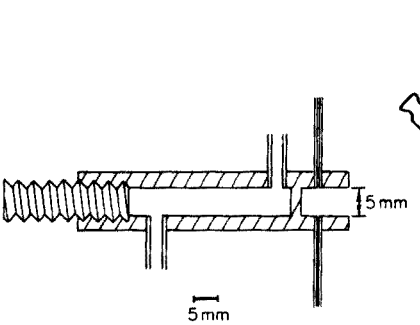

Fig. 1. Cross-section of cavity.

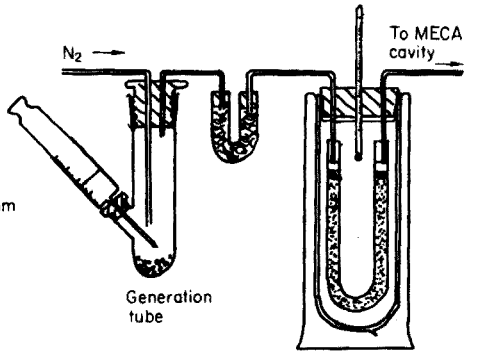

Fig. 2. Complete volatilization and gas chromatographic system for determination of arsenic and antimony (components described in text).

Teflon tubing packed with 10% Silicone Gum Rubber E-301 on a Porapak Q support (50—80 mesh). The column was conditioned at 105°C in an oven for 24 h in a nitrogen purge of 30 ml min^{-1}. The column was connected to the volatilization system as shown in Fig. 2 and its temperature controlled to 16 ± 0.5°C by immersing it in water contained in a Dewar flask.

The components of the system were connected with Teflon tubing. To avoid any possibility of decomposition or retention of hydrides, no grease or metallic parts were used, except for a 4-cm long piece of 0.8-mm i.d. stainless steel tubing for introducing the reaction products into the cavity.

REAGENTS

Arsenic stock solution (1000 p.p.m.). Arsenic(III) oxide (0.66 g; A.R.) was dissolved in about 15 ml of water containing 0.5 g of A.R. sodium hydroxide. The solution was diluted to 500 ml with water and A.R. hydrochloric acid to give a final acidity of 2 M.

Antimony stock solution (1000 p.p.m.). Antimony potassium tartrate (1.34 g; reagent grade) was dissolved in 500 ml of distilled water.

Tin stock solution (1000 p.p.m.). Tin metal (0.25 g; reagent grade) was dissolved in A.R. hydrochloric acid and diluted to 500 ml with distilled water to give a final acidity of 2 M.

Sodium borohydride powder (British Drug Houses; reagent grade) was used as the reducing agent.

Determination of arsenic and antimony (both 0—50 μg) with the g.c. system

The oxygen flow to the cavity and the nitrogen carrier gas were kept on throughout a series of experiments. About 30 mg of sodium borohydride powder was placed in the reaction vessel with a glass spatula. The syringe containing 1 ml of a sample solution was then connected to the reaction vessel and the volatilization system was closed. The chart recorder was turned on and the hydrogen—nitrogen diffusion flame was ignited. After the system had been deaerated for 30 s with the nitrogen carrier gas, the test solution was injected and the resulting emissions from oxide-containing species of arsenic and antimony were recorded at 400 nm as the hydrides were eluted from the gas chromatographic column.

Peak height and peak area measurements for arsenic and peak area measurements for antimony were made. Peak areas were measured by triangulation.

Determination of arsenic (0—2 μg) or antimony (0—4 μg) with the cold trap system

The volatilization system described above was applied to the separate determinations of arsenic or antimony without gas chromatographic separation. The gas chromatographic column was replaced by a 75-cm length of 3-mm bore Teflon tubing which was formed into a coil and used as a hydride trap by cooling it with liquid nitrogen in the Dewar flask. The optimized conditions described above were used, except for a nitrogen carrier gas flow rate of 50 ml min^{-1}.

The syringe containing 1 ml of an arsenic or antimony test solution was connected to the reaction vessel containing about 30 mg of sodium borohydride powder. The system was degassed for 30—35 s with the nitrogen carrier gas and the trap was placed in the liquid nitrogen. The trap was cooled for 15 s before the solution was injected. The flame was ignited and the oxygen flow to the cavity turned on. The hydride generated was collected for 1.5 min in the cold trap, which was then taken out of the liquid nitrogen and quickly immersed in a water bath at 40°C. The hydride was swept into the cavity and the emission from arsenic or antimony recorded at 400 nm.

Optimization of conditions

The best position of the cavity was found to be 27 mm above the burner head in the centre of the flame. The optimal gas flows were found to be: hydrogen, 2.8 l min^{-1}; nitrogen, 4.4 l min^{-1}; oxygen into cavity, 85 ml min^{-1}; nitrogen carrier gas, 86 ml min^{-1}.

To introduce arsine and stibine into the column in a reasonably short time it is essential to prepare the solutions of arsenic and antimony in acidic media to speed up the reduction. The acid concentration was optimized by preparing a series of solutions each 10 p.p.m. in arsenic and 50 p.p.m. in antimony in various concentrations of hydrochloric acid and injecting 1 ml of each solution onto an excess of sodium borohydride powder. The emissions were measured as above.

As would be expected, a change in the acid concentration affects the volume of hydrogen generated by the reaction, which also acts as a carrier gas. It thus changes the rate of formation and degassing of the hydrides from the solutions, and thus changes the retention time and the resulting emission intensities. This is shown in Table 1. The retention time for arsenic and antimony slightly decreased with increasing acid concentration. Also the height of an earlier, small peak (retention time 15 s), arising from an increase in the flame background by the hydrogen generated in the reaction, increased with acid concentration. An acid concentration of 0.1 M hydrochloric acid was found to be optimal.

TABLE 1

Effect of hydrochloric acid concentration on the separation and emission of arsenic and antimony

HCl Concn. (M)	Arsine		Stibine	
	Peak height (arbitrary units)	Retention time (s)	Peak area (arbitrary units)	Retention time (s)
0.05	42	66	58	245
0.10	51	61	62	245
0.20	54	60	57	241
0.30	47	60	52	235

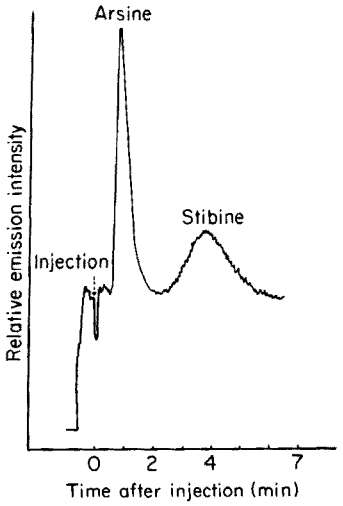

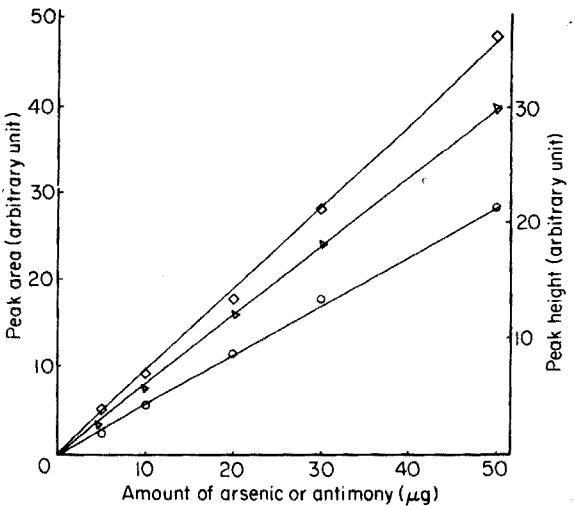

Fig. 3. Separation of arsine and stibine (10 μg of As and 50 μg of Sb).

Fig. 4. Calibration graphs for arsenic (△, by peak ht., ○ by peak area) and antimony (□) by the gas chromatographic procedure.

The separation of arsine and stibine under the above optimal conditions is shown in Fig. 3. The retention times were 61 s for arsine and 245 s for stibine. All the stibine had eluted 360 s after injection of the solution.

RESULTS

The gas chromatographic system

Calibration graphs (Fig. 4) obtained by injection of 1 ml of the arsenic or antimony solutions were rectilinear up to 50 μg of arsenic and antimony. The effects of arsenic on the emission of antimony and vice versa were studied; the results are shown in Tables 2 and 3. They show that 5 and 50 μg of antimony do not interfere with the emission from 1—10 μg of arsenic, and 50 μg of arsenic does not interfere with the emission from 5—50 μg of antimony.

The standard deviations for the determination of arsenic and antimony depended on how closely the column temperature was controlled. When the column temperature was controlled to within ± 0.5°C the relative standard deviations (for 8 replicate determinations of a mixture) for the determination of 5 μg of arsenic, by peak height and peak area measurements, were 4.0 and 3.5%, respectively. For the determination of 25 μg of antimony, with peak area measurements, the relative standard deviation was 2.7%. When the column temperature was controlled to within ± 0.2°C, the above standard deviations were decreased to 2.5, 2.9 and 1.8%, respectively. However, because of the difficulty of controlling the column temperature to within ± 0.2°C with the present system, the tolerance used was normally ± 0.5°C.

TABLE 2

Effect of antimony on arsenic response

Amount of As (μg)	Emission intensity (peak ht.)			Peak area for 50 μg Sb
	As alone	As+ 5 μg Sb	As+ 50 μg Sb	
0	0	0	0	4.2
1	5	5	4	4.4
3	11	12	12	4.4
5	19	19	20	4.3
7	28	28	29	4.2
10	42	41	43	3.9

TABLE 3

Effect of arsenic on antimony response

Amount of Sb (μg)	Emission intensity (peak ht.)		Peak area for 50 μg As
	Sb alone	Sb+ 50 μg As	
0	0	0	30
5	0.50	0.50	31
10	1.00	1.05	30
20	2.05	2.1	30
30	2.9	2.9	29
50	5.3	5.2	29

The limits of detection (signal = twice background noise) for arsenic and antimony were 0.2 μg (4 ng s^{-1}) and 1 μg (6 ng s^{-1}), respectively. The detection limits could be greatly improved by measuring larger portions of the broad spectra and by using a purpose-built instrument.

Further improvement could probably be achieved by replacing the nitrogen carrier and burner gases with argon or helium, to eliminate the quenching effect [20] of nitrogen on the emissions. Also, collection of arsine and stibine in a liquid nitrogen trap before their introduction into the g.c. column, would allow the hydrides to be introduced into the column in a shorter time, which would result in sharper peaks and allow a shorter column and a slower carrier gas flow to be used.

Interferences. The effect was studied of some cations and anions in the determination of arsenic-antimony mixtures. The effect of tin is described below. An interference was defined as significant if a change of more than two standard deviations (i.e. changes of 8% for arsenic and 5% for antimony) was observed in the measurement of 10 μg of arsenic and 25 μg of antimony. Al^{3+}, Mn^{2+}, Hg^{2+}, Ba^{2+}, Cr^{3+}, SeO_3^{2-}, TeO_3^{2-}, Ge(IV), SiO_4^{4-}, Pb^{2+}, SO_4^{2-}, oxalate,

phosphate and acetate ions (50 μg) did not interfere. Cobalt, Ni^{2+}, Zn^{2+}, Fe^{3+}, Bi^{3+}, Cd^{2+}, Cu^{2+} and Ag^{+} suppressed the arsenic and antimony emission peaks, but the interference was removed by making the test solution 0.01 M in EDTA (disodium salt) [17].

Separation of arsenic, antimony and tin

Tin gives a blue emission, probably arising from SnO species [22], in the cavity. Stannane (SnH_4) is generated under the conditions described above, and is eluted from the column between arsine and stibine with a retention time of 108 s under the above column conditions. The presence of 50 μg of tin did not interfere with the determination of antimony, but because the tin peak overlapped the arsenic peak, tin interfered with the determination of arsenic when peak area measurements were used. However, it had no effect when peak height measurements were used.

The separation of arsine, stannane and stibine was achieved, as shown in Fig. 5, by a 47-cm Teflon column (3-mm bore), packed as before. The column was operated at 9°C, and the nitrogen carrier gas flow rate was 75 ml min^{-1}. Under these conditions the retention times for arsine, stannane and stibine were 132 s, 251 s and 639 s, respectively.

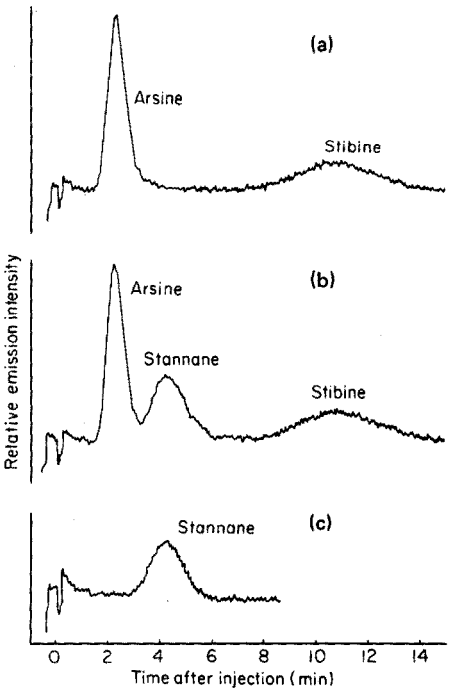

Fig. 5. Separation of arsenic (10 μg), antimony (25 μg) and tin (25 μg) hydrides by gas chromatography. (a) As and Sb only; (b) As, Sn and Sb; (c) Sn alone; all under the same conditions.

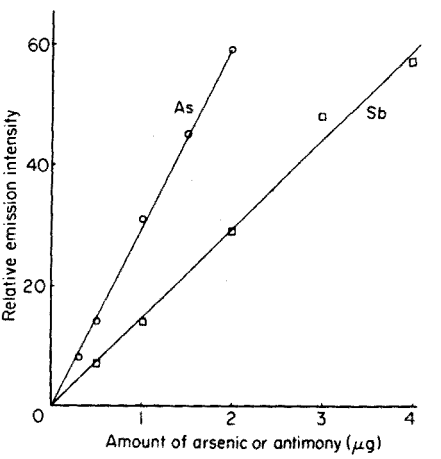

Fig. 6. Calibration graphs for arsenic (○) and antimony (□) by the cold trap procedure.

The liquid nitrogen trap system

Linear calibration graphs (Fig. 6) were obtained over the ranges 0—2.0 μg of arsenic and 0—4.0 μg of antimony, with relative standard deviations (8 experiments) of 4.9 and 3.0%, respectively, for 1 μg of arsenic and 2 μg of antimony. These represent a marked improvement in sensitivity over the previous MECA procedure [19] for these elements.

Conclusion

MECA, when coupled with a sodium borohydride reduction technique and a gas chromatographic separation, is a very simple and sensitive technique for the simultaneous determination of arsenic and antimony. It is also possible to determine arsenic, antimony and tin simultaneously at a single wavelength, a distinct advantage over atomic absorption measurements. MECA also offers a much wider linear calibration range than atomic absorption measurement. Although sensitivities are not as good as reported for atomic absorption, there are many major improvements yet to be made which will give rise to better MECA sensitivities.

E. H. thanks the Turkish Ministry of Education for a research scholarship. The authors thank Mr. S. Greenfield and Mr. I. L. Jones for advice concerning the gas chromatographic aspects of this study.

REFERENCES

1 W. Holak, Anal. Chem., 41 (1969) 1712.
2 Y. Yamamoto, T. Kumamaru, Y. Hayashi and R. Tsujino, Anal. Lett., 5 (1972) 419.
3 R. C. Chu, G. P. Barron and P. A. W. Baumgarner, Anal. Chem., 44 (1972) 1476.
4 E. N. Pollock and S. J. West, At. Absorpt. Newsl., 11 (1972) 104.
5 E. N. Pollock and S. J. West, At. Absorpt. Newsl., 12 (1973) 6.
6 F. J. Schmidt and J. L. Royer, Anal. Lett., 6 (1973) 17.
7 R. S. Braman, L. L. Justen and C. C. Foreback, Anal. Chem., 44 (1972) 2195.
8 E. J. Knudson and G. D. Christian, Anal. Lett., 6 (1973) 1039.
9 H. C. Freeman and J. F. Uthe, At. Absorpt. Newsl., 13 (1974) 75.
10 H. R. Griffin, M. B. Hocking and D. G. Lowery, Anal. Chem., 47 (1975) 229.
11 K. C. Thompson, Analyst, 100 (1975) 307.
12 F. J. Fernandez, At. Absorpt. Newsl., 12 (1973) 93.
13 F. J. Schmidt, J. L. Royer and S. M. Muir, Anal. Lett., 8 (1975) 123.
14 K. C. Thompson and D. R. Thomerson, Analyst, 99 (1974) 595.
15 F. E. Lichte and R. K. Skogerboe, Anal. Chem., 44 (1972) 1480.
16 A. E. Smith, Analyst, 100 (1975) 300.
17 R. Belcher, S. L. Bogdanski, E. Henden and A. Townshend, Analyst, 100 (1975) 522.
18 J. E. Drinkwater, Analyst, 101 (1976) 672.
19 R. Belcher, S. L. Bogdanski, S. A. Ghonaim and A. Townshend, Anal. Chim. Acta, 72 (1974) 183.
20 R. Belcher, S. L. Bogdanski and A. Townshend, Anal. Chim. Acta, 67 (1973) 1.
21 I. L. Jones and S. Greenfield, private communication.
22 R. M. Dagnall, K. C. Thompson and T. S. West, Analyst, 93 (1968) 518.

Analytica Chimica Acta, 92 (1977) 43—48

THE DETERMINATION OF TRACES OF AMMONIUM-NITROGEN IN AQUEOUS SOLUTION BY OPTICAL EMISSION SPECTROMETRY WITH A HIGH-FREQUENCY INDUCTIVELY COUPLED ARGON PLASMA SOURCE

J. F. ALDER, A. M. GUNN and G. F. KIRKBRIGHT

Chemistry Department, Imperial College, London SW7 2AY (England)

(Received 28th January 1977)

SUMMARY

A method for the determination of low levels of ammonium ion in solution by optical emission spectrometry with an inductively coupled argon plasma source operated at 27 MHz is presented. The ammonium ion is oxidized with sodium hypobromite in alkaline medium, the evolved nitrogen is passed into the argon plasma, and the NH emission intensity produced in the plasma at 336.0 nm is monitored. A practical detection limit of 0.1 μg N ml^{-1} for 5-ml aqueous sample solutions has been obtained. The method has been applied to the determination of the exchangeable ammonium content of soil samples.

Ammonium salts are oxidized by sodium hypobromite in alkaline medium with the evolution of nitrogen: $2NH_3 + 3NaOBr \rightarrow 3NaBr + 3H_2O + N_2$. Stehle [1] and Van Slyke and Kugel [2, 3] used this reaction analytically as an alternative to the ammonia distillation in the micro-Kjeldahl determination of nitrogen in clinical samples. These early methods relied on manometric estimation of the evolved nitrogen. More recently, micro- and submicro-Kjeldahl techniques [4—6] involving reaction of ammonium ion with hypobromite, followed by titration of the excess of reagent, have been reported. In this paper we describe a rapid and convenient method in which the nitrogen evolved in the hypobromite oxidation reaction is determined by optical emission spectrometry with an inductively coupled plasma source (i.c.p.).

EXPERIMENTAL

Plasma instrumentation

The instrumental system employed utilized a 2-kW crystal-controlled radiofrequency generator operating at 27 MHz (International Plasma Corporation, model 120-27) and a 1-m plane grating scanning monochromator. (Monospek 1000, Rank Hilger Ltd., Margate, Kent). Details of the instrumental system are given in Table 1. A demountable plasma torch with tangential argon inlets and sample introduction from a central injector

TABLE 1

Instrumentation

Plasma power supply	IPC model 120-27. Operating frequency 27.12 MHz; power output 0—2 kW continuously variable. Work coil 1½ turns 6-mm o.d. copper tubing.
Spectrometer	Hilger Monospek 1000. Czerny—Turner scanning monochromator with grating (1200 lines mm^{-1}) blazed at 300 nm; reciprocal linear dispersion 0.8 nm mm^{-1}.
Optics	Plasma imaged in 1:1 ratio onto entrance slit with two 7.5-cm focal length × 5 cm diameter fused silica lenses.
Readout	Signal from EMI 6256B photomultiplier tube displayed on Servoscribe chart recorder.
Plasma torch	Demountable fused silica torch with brass base. Coolant gas tubing, 21 mm o.d. Plasma gas tubing, 17 mm o.d. Injector tube, 6 mm o.d.

tube was used. The outer quartz tubing was extended to a height of 40 mm above the work coil to prevent entrainment of atmospheric nitrogen into the discharge.

Nitrogen generation apparatus

The nitrogen generation apparatus is shown in Fig. 1. A three-way tap allowed the system to be flushed free of air before the injector gas was introduced to the plasma. Addition of hypobromite reagent solution to the sample was achieved by rotation of the glass bulb in the sidearm through 180°.

Reagents

Ammonium ion stock solution (100 $\mu g\ ml^{-1}$) was prepared by dissolving ammonium sulphate in distilled water. The sodium hypochlorite solution

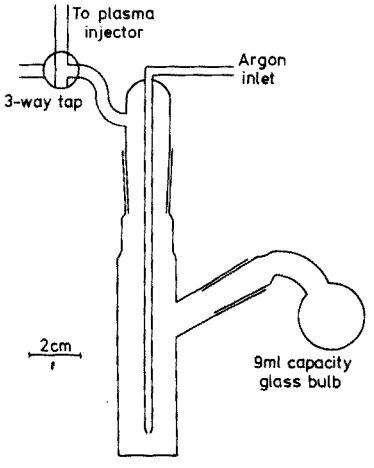

Fig. 1. Apparatus employed for generation of nitrogen from aqueous samples.

used contained 1 part commercial hypochlorite solution (10—15% available chlorine) and 5 parts distilled water. The mixed hypobromite reagent for analysis was prepared by mixing 1 ml of 10% (w/v) KBr solution with 10 ml of hypochlorite solution. The reagent was degassed with argon before use to remove any dissolved nitrogen.

Procedure

A 5-ml sample containing ammonium ion was placed in the nitrogen generation flask. The 9-ml glass bulb was filled with the degassed hypobromite solution and inserted in the sidearm of the apparatus. After flushing the system free of air, argon was passed through the flask to the plasma injector inlet at 2300 cm^3 min^{-1}. The hypobromite solution was then added to the sample by inverting the glass bulb; the NH 336.0-nm emission intensity was measured in the plasma at a height of 30 mm above the work coil.

RESULTS AND DISCUSSION

Development of the method

An attempt was first made to determine the ammonium content of solutions by direct nebulization of aqueous solutions containing ammonium salts into the plasma. The plasma emission spectrum in the region 200—650 nm was recorded during nebulization of an aqueous 2.5% solution of NH_4Cl. A small increase in the intensity of the emission from the NH species at 336.0 nm was observed in the presence of NH_4Cl but the sensitivity was too low to be of any practical value. No atomic nitrogen emission was observed.

A study of the feasibility of determining ammonium ion in aqueous solutions by measuring the u.v. absorbance of ammonia vapour displaced from alkaline medium has been reported by Cresser [7, 8]. It was decided to investigate the possibility of modifying this technique by determining the displaced ammonia by optical emission spectrometry with the i.c.p. source. Promising results were obtained by measurement of the NH emission intensity at 336.0 nm; the sensitivity, however, was limited by the slow rate of displacement of ammonia at the argon flow-rates used for the injector gas stream.

To overcome this problem, the hypobromite oxidation method was utilized for the generation of nitrogen. This has the advantage that the nitrogen produced is liberated much more rapidly, because its solubility in aqueous solutions is lower than that of ammonia.

The emission from the nitrogen-containing species in the plasma was investigated in order to establish the most favourable species and wavelength for the determination. The N_2 "second positive" system bandhead at 337.13 nm, the N_2^+ "main" system bandhead at 391.44 nm, the NH "A" system maximum at 336.0 nm and the nitrogen atom line at 410.99 nm

were each examined. The emission from the NH species at 336.0 nm was found to give the greatest signal to background intensity ratios and lowest limit of detection and was therefore selected for further work.

The plasma operating parameters employed in the study are shown in Table 2. These were chosen to optimize the signal-to-background intensity ratio at the NH band head at 336.0 nm. Further improvement could have been achieved by decreasing the operating power to 600 W but at this level the plasma was extinguished when ammonium ion samples of high concentration were analysed.

Typical analytical signals obtained for ammonium ion solutions containing 2,4 and 10 μg N ml^{-1} are shown in Fig. 2. The total signal duration under the conditions employed was approximately 30 s.

A calibration graph, obtained by plotting the peak emission intensity at 336.0 nm vs. concentration, was found to be linear over the range 1—2000 μg N ml^{-1} with a slope of 0.75 when plotted on logarithmic axes. At concentrations of 3000 μg ml^{-1} or greater, the evolved nitrogen extinguished the plasma, and at concentrations below 1 μg ml^{-1} the use of the peak emission intensity as the analytical signal became unreliable. The integrated emission intensity for the whole signal at 336.0 nm gave a linear response with concentration over the range 0.1—2 μg N ml^{-1} and so this method of calibration was employed at these levels.

The precision of the method was estimated by repetitive determination of the N_2 liberated from sample solutions containing 100 μg N ml^{-1}. A

TABLE 2

Plasma operating conditions

Net forward r.f. power	1000 W
Spectrometer slits	20 μ entrance and exit slits
Argon coolant gas flow rate	12700 cm^3 min^{-1}
Argon plasma gas flow rate	1000 cm^3 min^{-1}
Argon sample transport flow rate	2300 cm^3 min^{-1}
Viewing height	30 mm above work coil

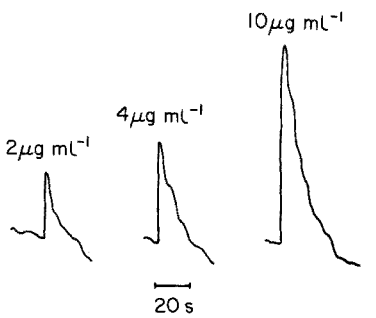

Fig. 2. Typical analytical signals obtained at 336.0 nm at different concentrations of ammonium ion (expressed as μg N ml^{-1}).

relative standard deviation of 0.02 was obtained for the determination of nitrogen in pure aqueous solutions.

The limit of detection of the method depended not on the background noise level but on the reproducibility of the blank determination. The concentration required to produce a signal equal to three times the standard deviation on the blank above the mean blank was found to be 0.1 μg N ml^{-1} for a 5-ml sample.

Analysis of soil samples

As an application of the method the exchangeable ammonium-nitrogen content of six soil samples was determined. The soil samples, supplied by the Macaulay Institute for Soil Research (Aberdeen), were first air-dried at 25°C and sieved to 2 mm.

The ammonium ion was extracted by the method described by Bremner [9]. A 10-g sample of each of the soils was shaken with 40 ml of neutral 2 M potassium chloride solution for 1 h. After the extracts had settled, 5-ml aliquots were removed from the clear supernatant liquid and analysed for ammonium nitrogen.

The results of the analyses are shown in the first column of Table 3. The values obtained are all within the expected range for exchangeable ammonium in soils.

Recovery experiments

To test the method, a set of recovery experiments was carried out. In each case 200 μg N (as ammonium sulphate) was added to a 10-g soil sample before extraction with 2 M KCl as described above. Table 3 shows the recovery of ammonium-nitrogen obtained on analysis of the extracts. The relative standard deviation obtained on repetitive analysis of a single soil extract was found to be 0.06; thus the spread in the results obtained for the recovery experiments is not significant, and essentially quantitative recoveries appear to be obtained in the procedure employed.

TABLE 3

Recovery experiments on potassium chloride soil extracts

Soil sample	NH_4-N in soil ($\mu g\ g^{-1}$)	NH_4-N added ($\mu g\ g^{-1}$)	NH_4-N found ($\mu g\ g^{-1}$)	Recovery (%)
Shaggart	10.0	20.0	32.1	107
Drumforber	10.1	20.0	30.2	100
Ardconnon	11.6	20.0	30.7	97
Smiddyhowe Wartie	13.6	20.0	33.8	101
Waulkmill Strachan	15.2	20.0	38.2	108
Logie Newton	16.2	20.0	34.1	94

Interference studies

The effect of various possible interferences in soil extracts was investigated. This was achieved by analyzing samples containing 20 μg N ml^{-1} in the presence of 1000 μg ml^{-1} of the possible interfering ion. No interference was observed in the case of Na^+, K^+, Ca^{2+}, Mg^{2+}, Cl^-, NO_3^- and SO_4^{2-}. With Al^{3+} and Mn^{2+}, however, where a precipitate was formed on addition of the hypobromite reagent, the rate of evolution of nitrogen was found to be reduced, resulting in a reduction in the emission peak height. Such samples could still be analyzed if the peak area was used as the analytical signal since this was unaffected by precipitate formation.

The effect of the 2 M potassium chloride solutions used for the soil extractions was also studied. As the signal obtained for nitrogen generation from this medium was identical to that obtained from pure aqueous solutions it was possible to use aqueous standards for the construction of the calibration curve for ammonium ion.

Conclusion

The technique provides a rapid and sensitive method for the determination of ammonium-nitrogen in solution. The attained sensitivity is sufficient for the analysis of exchangeable ammonium ion at the levels commonly found in soil samples. Results of the recovery experiments indicate that the soil extract analyses were free from interference from those ions likely to be present in such samples.

The technique should be applicable to the determination of ammonium-nitrogen in a wide variety of samples and could also prove useful as an alternative to the time-consuming ammonia distillation step in the determination of total nitrogen by the Kjeldahl method.

We are grateful to Dr. A. M. Ure of the Macaulay Institute for Soil Research, Aberdeen for provision of the soil samples examined.

REFERENCES

1 R. L. Stehle, J. Biol. Chem., 45 (1920—21) 223.
2 D. D. Van Slyke, J. Biol. Chem., 71 (1927) 235.
3 D. D. Van Slyke and V. H. Kugel, J. Biol. Chem., 102 (1933) 489.
4 J. P. Dixon, Anal. Chim. Acta, 13 (1955) 12.
5 R. Belcher and M. K. Bhatty, Mikrochim. Acta, 7—8 (1956) 1183.
6 R. Belcher, T. S. West and M. Williams, J. Chem. Soc., (1957) 4323.
7 M. S. Cresser, Anal. Chim. Acta, 85 (1976) 253.
8 M. S. Cresser, Lab. Pract., 26 (1977) 19.
9 J. M. Bremner, Monogr. Am. Soc. Argon., 9 (1965).

Analytica Chimica Acta, 92 (1977) 49—53

AN INDIRECT METHOD FOR THE SEQUENTIAL DETERMINATION OF SILICON AND PHOSPHORUS IN ROCK ANALYSIS BY ATOMIC ABSORPTION SPECTROMETRY

CHRIS RIDDLE and ANDREW TUREK

Department of Geology, University of Windsor, Windsor, Ontario N9B 3P4 (Canada)

(Received 4th January 1977)

SUMMARY

An indirect method is described for the determination of silicon and phosphorus in rocks. Ammonium molybdate is added to a solution of the rock powder and the molybdophosphoric and molybdosilicic acids formed are extracted sequentially. Indirect analyses for phosphorus and silicon are obtained by subsequent decomposition of the heteropoly acids and determination by a.a.s. of the molybdenum released. Most rock samples contain a large excess of silicon over phosphorus; correction can be made for the interference that results, and the procedure is recommended for rock powders with a silicon:phosphorus ratio of ca. 400:1 or less.

The determination of phosphorus and silicon in rock samples is usually achieved by x-ray fluorescence analysis or by a colorimetric method based on the formation of a phospho- or silico-molybdate which is reduced to "molybdenum blue" [1]. Heteropolymolybdates form with P, Si, As, Ge, Ti and Zr. In rock analysis it is usually safe to assume that As, Ge and Zr are present at such low levels, compared with P, Si and Ti, that they may be ignored. Wet chemical techniques, based on heteropolymolybdate formation, require the separation of P, Si and Ti from each other.

Several authors have discussed the formation and separation of heteropolymolybdates from an analytical viewpoint. A common procedure has been to determine the molybdenum in the complex extracted into an organic phase [2—5]. However, atomic absorption determinations on organic solutions suffer from several disadvantages. Although the signal intensity may be enhanced, its stability is usually poor, and results become irreproducible [4]. Several organic extractant media are obnoxious.

Some workers have continued to use the colorimetric method [6], in one case incorporating it into a kinetic analysis [7].

The organic extraction procedure has been improved [8] by decomposing the heteropolymolybdate extracts after separation, thereby returning them to an aqueous phase. Determination of the molybdenum could then involve u.v. or a.a. [8] spectrometry or even a further indirect determination of lead [9]. The extraction of either molybdophosphoric or molybdosilicic acid

is selective, being dependent on the pH of the sample solution [10]. These studies [8—10] have been exhaustive; the method of Hurford and Boltz for the decomposition of the extracted heteropolymolybdate has been adopted.

In rock analysis, silicon is usually present in at least fifty-fold excess over phosphorus; separations which appear quite selective may not be so when the relative concentrations are so disparate.

There are conflicting statements regarding the interference of titanium on phosphorus. Kirkbright et al. [2] found no interference; Ramakrishna et al. [5] did. The effect may be dependent upon the organic extractant used. There is no evidence that the ether—pentanol medium [8] gives rise to any titanium interference, and this extractant has been used here.

EXPERIMENTAL

Reagents

Sample solutions are prepared from a flux-fused rock-powder bead. The oven-dried (110°C) rock powder (0.2500 g) is mixed with a flux (ca. 2.5 g) of 1 part lithium metaborate: 2 parts lithium tetraborate, placed in a graphite crucible, and held at 1050°C for 0.5 h. On cooling, the fused bead is dissolved in 150 ml of 2 M nitric acid and made up to 500 ml with triple-distilled water.

The stock solutions required in the extraction procedure are: 4 M hydrochloric acid; 10% ammonium molybdate solution; diethyl ether:pentan-1-ol (5:1) extractant (prepared fresh daily); 1.1 M hydrochloric acid; buffer, pH 9.3, prepared by adding 70 ml of ammonia liquor to a solution containing 53.5 g of ammonium chloride in 500 ml of distilled water, and making up to 1 l. These stock solutions are stored in Nalgene bottles.

Standard solutions of 1, 2, 3, 4, 6, 8 and 10 μg ml^{-1} molybdenum are prepared from 1000 μg ml^{-1} ionic standard (Fisher Scientific), buffered with stock solution to the same extent as the samples (50 ml of buffer solution per 100 ml of solution).

A non-silicone grease, e.g. Vaseline, is used on all stop-cocks.

Procedure

Nalgene vessels are used, where possible, in preference to glass. When glassware is used it should be cleaned, stood overnight in a mixture (1 + 1) of concentrated nitric and sulfuric acids, rinsed thoroughly with triple-distilled water, and kept wet until use.

Formation of the heteropoly acids. Pipet 10 ml of the sample solution (prepared as above) into a 125-ml separatory funnel. By syringe, add 1 ml of 4 M hydrochloric acid and make up to 40 ml with distilled water. Add 10 ml of 10% ammonium molybdate solution and wait 10 min. The solution should have pH 1.0.

Extraction of phosphomolybdate. Add 20 ml of the ether—pentanol extractant and shake for 3 min. Rinse the separatory funnel stopper with

4 ml of ether and drain the lower (aqueous) phase into a 200-ml volumetric flask. Wash the upper (organic) phase with a 25-ml aliquot of 1.1 M hydrochloric acid, shake for 15 s, and drain the lower phase into the 200-ml volumetric flask. Repeat twice. Add 30 ml of the buffer solution to the washed organic phase and shake for 30 s. Rinse the stem of the separatory funnel with distilled water and drain the lower (aqueous) phase from the funnel into a 100-ml volumetric flask. Add 15 ml of the buffer solution to the organic phase, shake for 30 s, and drain into the 100-ml volumetric flask. Dilute the contents of the 100-ml volumetric flask to the mark. This solution contains the decomposed phosphomolybdate and its determination by a.a.s. for molybdenum leads to a result for phosphorus.

Extraction of silicomolybdate. Dilute the 200-ml volumetric flask contents (see above) to the mark and pipet 10 ml of this solution into a second separatory funnel. Add 2 ml of the 10% ammonium molybdate solution; let stand for 10 min. Add 25 ml of 4 M hydrochloric acid and let stand for 5 min. The solution should have an acidity equivalent to 2.5—3.5 M hydrochloric acid.

Add 35 ml of the ether—pentanol extractant and shake for 3 min. Rinse the separatory funnel stopper with 4 ml of ether and drain and discard the lower (aqueous) layer. Wash the upper (organic) layer with a 25-ml aliquot of 1.1 M hydrochloric acid, shake for 15 s, and discard the aqueous phase. Repeat twice. Add 40 ml of the buffer solution to the washed organic phase and shake for 30 s. Rinse the stem of the separatory funnel with distilled water and drain the lower (aqueous) phase from the funnel into a 100-ml volumetric flask. Add 15 ml of the buffer solution to the organic phase, shake for 30 s, and drain into the 100-ml volumetric flask. Dilute the 100-ml volumetric flask contents to the mark. This solution contains the decomposed silicomolybdate and its determination by a.a.s. for molybdenum leads to a result for silicon.

Calculation

The above procedure is performed with each rock sample solution, with a fusion blank, and with a pure silica "blank". The fusion blank allows the correction of constant errors, e.g. those introduced by any residual silicon or phosphorus in the reagents. The silica "blank" allows for the correction of silicon interference with the phosphorus determination.

The quantity determined for each solution is the molybdenum content in $\mu g\ ml^{-1}$. All values are first corrected for the fusion blank value. From the silica "blank" it is possible to obtain a value of "μg of Mo per % of SiO_2", extracted and determined as if it were molybdophosphoric acid. The silica blank also yields an analysis for silicon that acts as a calibration check on the method. (Since some silicon has been extracted as if it were molybdophosphoric acid, a correction equal to 5% of the Mo ascribed to molybdophosphoric acid should be applied to the silica result. The factor arises because the sample solution is diluted from 10 ml to 200 ml between the molybdophosphoric acid extraction and the molybdosilicic acid extraction.)

From these analyses, it is possible (i) to calculate the approximate % SiO_2 from the decomposed molybdosilicic acid; (ii) to calculate the % P_2O_5, correcting for the blank and silicon interference with the value of "μg Mo per % SiO_2" already calculated; (iii) to recalculate the final % SiO_2 by adding the correction factor for Si determined as P.

The weight (μg) of Mo determined in the 100-ml sample solution is converted to the % oxide knowing (i) the weight of rock powder sample taken; (ii) the dilution factors (50 for phosphorus, 1000 for silicon); (iii) the conversion factors for the P_2O_5 and SiO_2 molybdenum equivalents (1 g Mo $\equiv$ 0.06164 g P_2O_5 and 0.05219 g SiO_2).

Instrumentation

Molybdenum was determined with a Varian Techtron AA-5 atomic absorption instrument. All determinations were made in sequence with the buffered ionic standards described. Conditions were: hollow-cathode lamp current, 5 mA; slit-width, 0.1 nm; wavelength, 313.3 nm; strongly reducing acetylene—nitrous oxide flame (2—3-cm red cone).

RESULTS AND DISCUSSION

This procedure for the sequential determination of silicon and phosphorus is an extension of work previously described by Kirkbright et al. [2] and by Simon and Boltz [10]; their extraction schemes have been modified to apply to solutions of rock powder. Most igneous rocks contain silicon in at least 100-fold excess over phosphorus and at this level there is serious interference under most extraction conditions. For example at pH 1, the optimum condition for phosphomolybdate extraction, the distribution ratio [10] for silicomolybdate is ca. 0.04:1 whilst that for phosphomolybdate is 410:1 between organic and aqueous phases. Thus, although the phosphomolybdate is essentially quantitatively extracted, the small fraction of available silicomolybdate that accompanies it is significant when the total silicomolybdate is present in such excess. The interference is comparable in magnitude to the level of phosphomolybdate for rock samples with a silicon:phosphorus ratio of ca. 200:1. Obviously the lower the ratio, the more confidence there will be in a phosphorus determination. The method is not recommended for phosphorus at ratios greater than ca. 400:1, and the observation that a consistent and significant blank is obtained for silicon [2] is confirmed.

When these two effects are corrected, the method gives good analytical data for silicon and phosphorus. A slight further correction involves the addition of the silicon determined as phosphorus to the silicon determination. To demonstrate the reproducibility of the method, ten replicate determinations were made on a rock sample (used as a benchmark standard by the Manitoba Mines Branch and identified as "Manitoba no. 8") which is an intermediate metaintrusive. The analytical data are presented in Table 1. The standard deviation for the phosphorus determination is 0.14%; this

TABLE 1

Silicon and phosphorus in the rock sample, Manitoba no. 8

	Silicon as SiO_2 (%)[a]	Phosphorus as P_2O_5 (%)[a]
Range (10 samples)	53.7—65.9	0.11—0.49
Mean	60.5	0.25
Standard deviation	3.3	0.14
Literature value [11]	60.7	0.27

[a]Values corrected for interference and blank as described in text. The fusion blanks in the sample solution were 2.27 μg Si 100 ml^{-1} and 9.90 μg P 100 ml^{-1}. The silica "blank" gave an interference equivalent to 0.17 μg P in 100 ml per % SiO_2.

reflects the difficulty of obtaining good separations when silicon is present in great excess.

Conclusion

The convenient method described allows the sequential determination of silicon and phosphorus in rock powder samples; a standard rock dissolution procedure and a conventional atomic absorption determination are used. The separation procedures are straightforward. An average of 30 min per sample solution, for a series of samples, is required; this is not an unusual work-up time for the determination of two elements. Possible interferences are arsenic (with phosphorus) and germanium (with silicon); neither of these elements is abundant in most rock samples. Titanium does not interfere with phosphorus when an ether—pentanol extraction is used. When the silicon:phosphorus ratio exceeds ca. 400:1 the phosphorus determination suffers from interference and is unreliable but the method still gives good results for silicon.

The discussion of experimental results by members of the late D. F. Boltz's research group is gratefully acknowledged.

REFERENCES

1 P. G. Jeffery, Chemical Methods of Rock Analysis, Pergamon Press, Oxford, 1970, p. 389.
2 G. F. Kirkbright, A. M. Smith and T. S. West, Analyst, 92 (1967) 411.
3 T. Kumamaru, Y. Otani and Y. Yamamoto, Bull. Chem. Soc. Jpn., 40 (1967) 429.
4 W. S. Zaugg and R. J. Knox, Anal. Chem., 38 (1966) 1759.
5 T. V. Ramakrishna, J. W. Robinson and P. W. West, Anal. Chim. Acta, 45 (1969) 43.
6 M. J. Pedrosa and J. Paul, Mikrochem. J., 19 (1974) 314.
7 W. D. Bostick, C. A. Burtis and C. D. Scott, Anal. Lett., 9 (1976) 65.
8 T. R. Hurford and D. F. Boltz, Anal. Chem., 40 (1968) 379.
9 L. A. Trudell and D. F. Boltz, Mikrochim. Acta, (1970) 1220.
10 S. J. Simon and D. F. Boltz, Anal. Chem., 47 (1975) 1758.
11 A. M. MacKay, personal communication, Manitoba Mines Branch Analytical Laboratory.

Analytica Chimica Acta, 92 (1977) 55—60

THE PREPARATION OF STANDARD SOLUTIONS OF MERCURY AT THE p.p.b. LEVEL

MITSUKO AMBE and KIWAKO SUWABE

Sagami Chemical Research Center, Nishi-Ohnuma, Sagamihara, 229 (Japan)

(Received 15th November 1976)

SUMMARY

The preparation of standard solutions containing mercury at the p.p.b. level has been investigated. Addition of sodium chloride to dilute mercury solutions below pH 1 improves the stability of the solutions greatly. Standard solutions containing 1—1000 p.p.b. Hg sealed in Pyrex glass ampoules are stable and usable for 18 months.

For the determination of trace constituents in natural waters, common standard solutions of accurately known concentration are required to ensure comparability of the data obtained in different laboratories. Series of standard solutions of nutrient elements were prepared in this laboratory [1—3] and distributed tc many scientists for the determination of nutrient elements in sea water. Attempts were also made to prepare standard solutions of mercury satisfying the following requirements: (1) with the highest accuracy attainable, (2) stability for at least one year after preparation, and (3) with a concentration as near as possible the content of mercury in natural waters.

The determination of mercury has received much attention recently, especially the cold-vapor atomic absorption method, which can be used to determine mercury in sea and terrestrial water at levels below 0.01 p.p.b. The handling of samples containing mercury involves difficult problems because of the chemical and physical characteristics of mercury and mercury compounds. Several workers have noted the decrease in concentration of mercury in natural and distilled water during storage [4—12]; the loss of mercury has been ascribed to adsorption on the walls of storage vessels, and to volatilization from solution. Losses could be prevented by keeping solutions at pH 0.5—1.0, or by adding perchromate and acid [6—9], but the solutions were stable for only about 10 days.

A procedure for the preparation of standard solutions with addition of sodium chloride is reported in this paper. Standard solutions with mercury concentrations of 1—1000 p.p.b. are stable for more than one year.

EXPERIMENTAL

Instrumentation

A Nippon Jarrell-Ash type AA-1 atomic absorption spectrometer equipped with a quartz absorption cell of 18 mm diameter and 250 mm length, was used.

Chemicals

Stock standard solution of mercury (1000 p.p.m.). Mercury(II) chloride (guaranteed reagent; Kishida Chemical Co.) was recrystallized and dried under reduced pressure; 1.3535 g was dissolved in 1 l of water. This solution was stored in a dark bottle and was stable for several months.

Tin(II) chloride solution. Tin(II) chloride (10 g) was wetted with 1 ml of 18 M sulphuric acid, and diluted with water to 100 ml.

Sulphuric acid. A super special grade of sulphuric acid containing less than 0.2 ng Hg ml^{-1} was used.

Sodium chloride solution. Sodium chloride (guaranteed reagent) was heated at 110°C for several hours, and then at 650°C for 1 h. The product contained no trace of mercury.

All solutions were prepared with deionized water made by passing distilled water through a mixed-bed, ion-exchange resin column.

Procedures

For samples containing mercury in the range 0.1—15 p.p.b., 3 ml of 18 M (v/v) sulphuric acid and 2 ml of tin(II) chloride solution were added to 50 ml of the sample in a suitable reaction vessel. Air was passed at a rate of 2.4 l min^{-1} to sweep the released mercury vapor to the cell of the spectrometer. The peak height at 253.7 nm was recorded.

For samples containing less than 0.1 p.p.b. mercury, 10 ml of 18 M (v/v) sulphuric acid and 2 ml of tin(II) chloride solution were added to 200 ml of sample, and mixed well. Then air was passed at a rate of 2.4 l min^{-1} for 4 min through the reaction vessel, a spiral trap cooled at 0°C and a gold collector to gather the released mercury vapor. (The collector was constructed from quartz tubing (4 mm diameter, 150 mm long); a 10-mm packing of gold chips was supported by quartz wool plugs. Gold chips were prepared by cutting pure gold wire of 0.2 mm diameter into 2 mm lengths). The gold amalgam was then heated for 2 min in an electric furnace at 700°C, while the mercury vapor was swept into the cell of the spectrometer with nitrogen passing through the collector and the cooled spiral trap, at a constant flow rate of 1.2 l min^{-1}. The cooled spiral trap is very efficient in improving the reproducibility of the determination.

Examination of stability of the standard solutions

Mercury standard solutions were prepared under different conditions as described below, and 50 ml of each was immediately sealed in a storage

vessel. The mercury concentration of the sealed samples was inspected at regular intervals at a concentration of 1 or 10 p.p.b. prepared by adding purified water and sulphuric acid (10 ml l^{-1}). The results were compared with freshly prepared standard solutions.

RESULTS AND DISCUSSION

Reproducibility of the cold-vapor method for standard solutions

The reproducibility of the analysis for standard solutions containing 0—15 p.p.b. of mercury is given in Table 1. The absorption—concentration curves gave a linear correlation in this range of mercury concentration for the same volume of sample.

Material of storage vessel

Three kinds of vessel were examined for suitability for storing the standard solutions: (1) Pyrex glass ampoules, (2) glass bottles with Teflon sheet covering the internal wall and sealed with polycarbonate caps, and (3) high-density polyethylene bottles. Glass ampoules and bottles were cleaned by soaking in 3 M sodium hydroxide solution for 1 h, rinsing with water, and soaking in chromic acid mixture solution for 1 h. After washing, they were steamed for 3 h and dried in an electric oven at 110°C.

Mercury standard solutions (500 and 1000 p.p.b.) with pH adjusted to 2—3, were sealed in each type of vessel. As shown in Fig. 1, in the Pyrex glass ampoules, the mercury content remained constant during 13 months; in the polyethylene bottles, loss of mercury was observed after one month.

Effect of pH on the stability of standard solutions

Mercury standard solutions (500 and 1000 p.p.b.) with the pH adjusted to about 1, 2, 3 and 5, were sealed in Pyrex glass ampoules. At pH 1 and 3, losses of mercury were not observed for 12 months, but at pH 5 the concentration decreased gradually by 15% after 8 months (Fig. 2). The mercury content of the solutions at pH 1 sealed in polyethylene bottles decreased after one month.

TABLE 1

Reproducibility of the determination of mercury by cold-vapor atomic absorption spectrometry

Hg (p.p.b.)	0.000	0.005	0.010	0.020	0.030	1.0	5.0	10.0	15.0
Sample (ml)	200	200	200	200	200	50	50	50	50
Scale expansion	10	10	10	10	10	10	1	1	1
Absorption (%)	4.7	10.4	16.8	30.9	42.7	29.2	15.3	31.7	37.9
s	0.3	0.7	1.0	0.8	0.7	0.5	0.3	0.4	0.3
s_r (%)	6.4	7.0	5.8	2.1	1.6	1.7	1.9	1.2	0.8

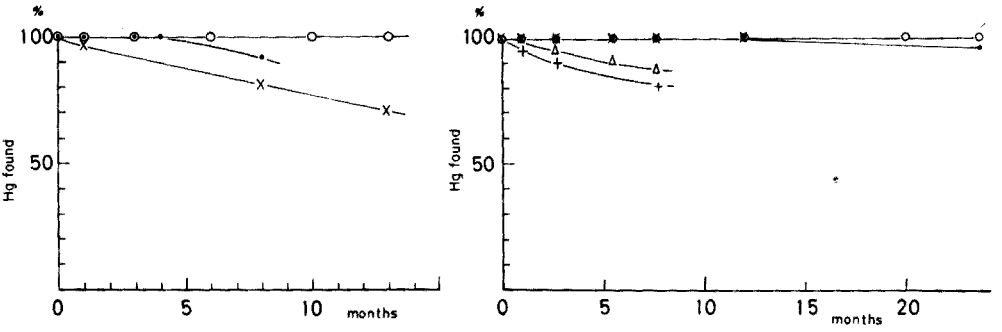

Fig. 1. Stability of mercury solution in various storage vessels. ○ Glass ampoule. • Glass bottle. × Polyethylene bottle.

Fig. 2. Effect of pH of the mercury solutions on stability. Glass ampoules: pH 1 (○), pH 2 (•), pH 3 (×), pH 5 (△). Polyethylene bottle: pH 1 (+).

These tests were also done with standard solutions of lower mercury concentration at pH 1 and 3. At pH 1 a solution containing 20 p.p.b. mercury was stable for 21 months, but at pH 3 it decreased in concentration by 80% one month after preparation. A 1 p.p.b. solution at pH 1 showed a slight decrease after 2 months. (Fig. 3).

Effect of sodium chloride on stability

To improve the stability of the standard 1-p.p.b. solutions, mercury solutions containing sodium chloride were tested. The 1 p.p.b.-solutions containing 3% sodium chloride and adjusted to below pH 1 with sulphuric acid, were sealed in glass ampoules or glass bottles. As shown in Fig. 4, the concentration remained constant during the 35 days of the test, whereas the

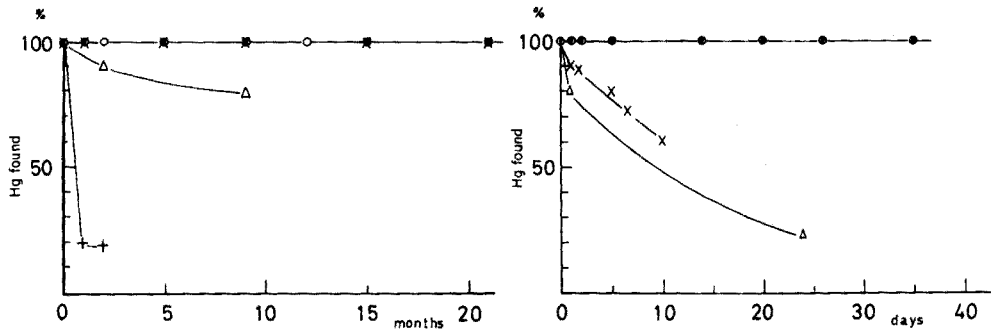

Fig. 3. Stability of mercury solutions of various concentrations at pH 1 and 3 sealed in Pyrex glass ampoules. At pH 1, 1000 p.p.b. (○), 500 p.p.b. (•), 20 p.p.b. (×), 1 p.p.b. (△). At pH 3, 20 p.p.b. (+).

Fig. 4. Stability of mercury solutions (1 p.p.b.) containing 3.0% sodium chloride solution. 3% NaCl solution: glass ampoule (○), glass bottle (•). Aqueous solution: glass ampoule (×), glass bottle (△).

mercury concentration decreased rapidly in the solutions without sodium chloride which were prepared as a reference.

Tests made with solutions containing 0.1—3.0% sodium chloride showed that at least 2% sodium chloride should be added (Fig. 5). The determination of mercury in sodium chloride solution gave the same values as in aqueous solution of the same concentration when fresh solutions were used.

As a result of the above experiments, mercury standard solutions (1.0, 10.0, 100 and 1000 p.p.b.) were prepared containing 3.0% sodium chloride and adjusted to pH 0.5—1.0 with sulphuric acid; these solutions were sealed in Pyrex glass ampoules. The concentrations of the samples did not change during at least 18 months (Table 2).

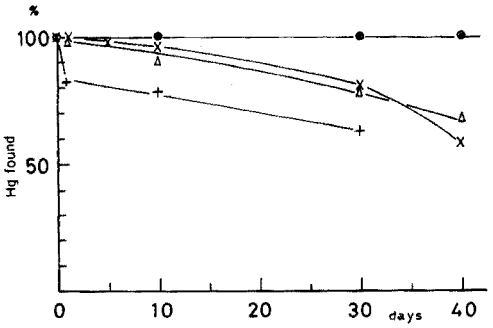

Fig. 5. Effect of the concentration of sodium chloride on the stability of 1 p.p.b. Hg solutions adjusted to pH 0.5 in Pyrex glass ampoules. NaCl: 3.0% (○), 2.0% (●), 1.0% (×), 0.5% (△), 0.1% (+).

TABLE 2

Stability of the ampouled mercury standard solutions during storage
(The values given are absorbances.)

Months	Hg (p.p.b.)			
	1.0	10.0	100	1000
0	0.150 ± 0.002[a]	0.169 ± 0.010[a]	0.173 ± 0.006[a]	0.171 ± 0.008[b]
6	0.150 ± 0.001[b]	0.172 ± 0.001[c]	0.174 ± 0.004[b]	0.169 ± 0.003[c]
18	0.149 ± 0.000[a]	0.169 ± 0.002[a]	0.171 ± 0.002[a]	0.172 ± 0.005[a]

[a] Average of 5 results with range.
[b] Average of 3 results with range.
[c] Average of 4 results with range.

These results indicate that the recommended procedure can be applied not only for preparation of standard solutions in routine analytical work, but for preserving samples of natural waters.

The authors are indebted to Prof. Dr. Ken Sugawara for his kind guidance and criticism. They are also grateful to H. Matsumoto for her help.

REFERENCES

1 SCOR (ICSU), IOC (UNESCO) and Chemistry W. G., Subcommittee for CSK, National Committee on Oceanic Research, Science Council of Japan, On the Preparation of CSK Standards for Marine Nutrient Analysis, 1969.
2 M. Ambe, J. Kajiwara, T. Yoshihara and K. Sugawara, J. Oceanogr. Soc. Jpn., 31 (1975) 85.
3 M. Ambe, IOC (UNESCO) Report, Accuracy of the determination of nutrient elements in sea water by using CSK standard solutions, in press.
4 S. Shimomura, Y. Nishihara and Y. Tanase, Jpn. Anal., 17 (1968) 1148.
5 S. Shimomura, Y. Nishihara and Y. Tanase, Jpn. Anal., 18 (1969) 1072.
6 R. V. Coyne and J. A. Collins, Anal. Chem., 44 (1972) 1093.
7 R. M. Rosain and C. M. Wai, Anal. Chim. Acta, 65 (1973) 279.
8 R. A. Carr and P. E. Wilknics, Environ. Sci. Technol., 7 (1973) 62.
9 C. Feldman, Anal. Chem., 46 (1974) 99.
10 Y. Dokiya, S. Yamazaki and K. Fuwa, Environ. Lett., 7 (1974) 67.
11 Y. Umezaki and K. Iwamoto, Jpn. Anal., 20 (1971) 173.
12 D. R. Christmann and J. D. Ingle, Jr., Anal. Chim. Acta, 86 (1976) 53.

Analytica Chimica Acta, 92 (1977) 61—70

PRESERVATION OF SUB-p.p.b. LEVELS OF MERCURY IN DISTILLED AND NATURAL FRESH WATERS

JOHN CARRON and HAIG AGEMIAN

Canada Centre For Inland Waters, Water Quality Laboratory, Special Services Section, 867 Lakeshore Rd., P.O. Box 5050, Burlington, Ontario (Canada)

(Received 6th December 1976)

SUMMARY

Several preservatives, containers, etc. have been suggested in relation to the preservation of mercury samples. This paper reports a comparison of sample containers and of preservatives for synthetic and natural low-level (sub-p.p.b.) mercury samples. It is shown that 1% H_2SO_4 + 0.05% $K_2Cr_2O_7$ is most advantageous with respect to accuracy, precision and practical aspects such as low detection limits and adaptability to the automated cold-vapor atomic absorption technique. Glass is the best container, and is best washed with concentrated nitric acid or chromic acid. Data from a national interlaboratory quality control study on the determination of mercury show that this preservative is satisfactory for the long-term storage of sub-p.p.b. mercury solutions. The presence of mercury as CH_3Hg^+ improves preservation efficiency. The method of total errors is used in comparing the methods.

The problems of preserving mercury in solution are well known. Although controversy still exists over which preservative is the best, agreement on several of the factors which affect the stability of mercury solutions seems to have been reached. For example, it is agreed that low pH values, high ionic strengths and oxidizing environments help in keeping mercury in solution. Acids such as H_2SO_4 [1], HNO_3 [2—8], and HCl [7, 9] have been widely used in different amounts. Oxidants such as permanganate [10—14] and dichromate [15—18] have been shown to prevent volatilization of mercury. Sodium chloride [9] and gold(III) [16, 18] have also been used as preservatives.

The preservation of sub-p.p.b. levels of mercury in natural fresh waters is of interest. These waters rarely contain mercury at levels over 0.5 p.p.b. and in most cases contain less than 0.2 p.p.b. Hg. Unfortunately, most investigators have performed their tests at high levels, although it is agreed that the stability of mercury solutions decreases with decreasing concentration.

A simple preservation method for mercury in water has been addition of 1% sulfuric acid [1]. This method is adequate for a variety of natural waters, but for some fairly pure waters which approach synthetic samples, as well as those containing reductants and organics, it was found to be unsatisfactory.

The sulfuric acid provides a low pH, but does not provide the strong oxidizing environment required to prevent volatilization losses of mercury. In this study, preservation methods which provide both low pH values as well as oxidizing environments were tested on both synthetic and natural samples in a variety of containers, in order to obtain a practical method which would be adaptable to routine analysis for mercury in natural waters at sub-p.p.b. levels by the automated cold-vapor atomic absorption technique. The essential requirement is that the preservation method should maintain mercury in waters of low salt content (low conductivity such as distilled water) and of high salt content (high conductivity).

Most investigators have compared preservation methods by using only the recovery of mercury from solution as a measure of preservation; little attention has been given to the relative statistical reproducibility of the methods. However, recovery and precision are equally important in comparing any analytical methods. Thus, the method of total errors [19] is used here as a criterion for comparing the preservatives studied.

Different species of mercury may interact differently with container walls. Thus, in addition to the Hg^{2+} preservation studies, some results on the preservation of CH_3Hg^+ solutions are also presented. The recommended preservative was tested in a national quality control study and was shown to be satisfactory for different levels of mercury in distilled and natural freshwaters

EXPERIMENTAL

Apparatus

The equipment used consisted of a proportionating pump (Carlo Erba, model 08-59-10202), Technicon AutoAnalyzer tubing of specified dimensions [1, 18], a gas separator as used by Goulden and Afghan [1], a mercury monitor (Pharmacia Fine Chemicals), and a strip-chart recorder (Hewlett-Packard 17051A).

The system [20] used is a modification of that used by Goulden and Afghan [1] and gives a detection limit of 0.01 μg Hg l^{-1}.

Reagents

Certified reagent-grade chemicals were used for all analyses. The sulfuric acid had a mercury content of 10^{-7}%.

A mercury(II) chloride stock solution (1000 mg Hg l^{-1}) was used for all standards. The same stock solution was used for spiking over the time period of the preservation study.

Procedure

Dilute mercury standards were prepared to cover the range 0.01—1.00 μg Hg l^{-1} (as $HgCl_2$). All standards were made to contain the reagents added to the samples.

Samples were analyzed periodically with a new set of standards. Samples

were spiked with either Hg^{2+} or CH_3Hg^+ (as their chlorides). All preservation studies and analyses were performed at room temperature. All solutions were stored in 250-ml bottles throughout the study.

DISCUSSION

Several factors may affect the stability of mercury in solutions [21]. These include: (a) the level of mercury, (b) the type of container, (c) the method of cleaning containers, and (d) the type of preservative (i.e., acid, oxidizing agents or complexing agent).

The level of mercury has a great effect on the efficiency of preservation [10, 22]. The natural fresh water levels of mercury are in the range 0.01—0.7 $\mu g\ l^{-1}$, and this range was covered in the present study. Table 1 provides a summary of some preservation methods in use. The most popular types of container are glass and polyethylene.

Cleaning of containers

Before actual preservation methods were studied, it was necessary to establish the effect of containers on possible contamination of test solutions, the efficiency of the bottle washing technique, and the ease of washing different types of containers. This test involved intentionally contaminating a variety of containers by soaking them in a 100 μg Hg l^{-1} solution for several days. Three bottle-cleaning methods were then used: (a) concentrated nitric acid (b) concentrated chromic acid, and (c) 10% HNO_3 followed by rinsing with 0.1 M HCl—1 M NaCl solution [9]. After the wash, the containers were filled with 1% H_2SO_4 and left to stand overnight before the solutions were analyzed. The levels of mercury leached from the container by the 1% H_2SO_4 are shown in Table 2. Obviously, glass containers are the most easily cleaned by all methods. Of the plastic bottles, high-density polypropylene and high-density linear polyethylene are easiest to clean, followed by soft polyethylene. Of the washing solutions, concentrated nitric acid and chromic acid seem to be best. The bottle-washing technique is clearly critical, especially for plastic bottles. Weiss et al. [23] stress the need for proper bottle treatment.

Choice of preservatives

Although organic complexing agents are promising as preservatives, they are not compatible with the system in use, because their high stability affects the chemical equilibrium of the automated detection system. For example, if cysteine [23] is used, an extra step of liberating the mercury by coprecipitation with copper sulfide is required. This is not desirable for routine monitoring of a large number of samples. Similarly, EDTA [24] is undesirable.

Initially, an attempt was made to replace the 1% H_2SO_4 method [1] with one using nitric acid [2—8]. A concentration of 5% HNO_3 was tested on distilled and ground water. The distilled water spiked at a level of 0.25 $\mu g\ l^{-1}$ stored in high-density linear polyethylene showed a loss of 80% mercury in 8 days. Ground water at a level of 0.10 $\mu g\ l^{-1}$ under the same conditions did

TABLE 1

Summary of some preservation methods for mercury in water

Type of sample	Hg level ($\mu g\ ml^{-1}$)	Preservative	Containers	Ref.
Natural water	—	H_2SO_4 (pH < 1) 1%	—	1
Distilled and creek water	25	HNO_3 (pH 0.5)	Polyethylene, PVC, glass	2
Distilled and creek water	50	HNO_3 (pH 1) 1%	Polyethylene	6
Distilled and Ohio river water	0.2—5	HNO_3 (pH < 2)	Glass	5
Distilled water	1000	HNO_3 (1.6 N)	Polyethylene	8
Bay water and melted glacial ice	1—100	HNO_3 (pH 1)	Polyethylene	3
Contaminated water	12	NaCl and/or HCl	Polyethylene, glass	9
Dilute solutions	2	$KMnO_4$ and/or strong oxidizing acid	Polyethylene, polypropylene, glass	10
Distilled water	0.1—10	5% HNO_3 + 0.05% $K_2Cr_2O_7$	Polyethylene, glass	15
Distilled water, surface water	0.5—1	HNO_3 (pH 1) or excess $KMnO_4$	Polyethylene, flint glass	4
Distilled and sea water	0.34—6.3	HNO_3 (pH 0.5) HCl (pH 1.5)	Polyethylene, Pyrex	7
Demineralized water	5	5% HNO_3 + 0.05% $K_2Cr_2O_7$	Polyethylene	16
	0.52—1.65	0.05% $KMnO_4$	Polyethylene	14
	2—3	0.5% HNO_3 + 0.05% $K_2Cr_2O_7$	Polyethylene, glass	17

TABLE 2

Mercury levels ($\mu g\ l^{-1}$) from different types of containers after washing with different types of solutions

Container	Wash solution		
	HNO_3	Chromic acid	10% HNO_3 + rinse of 0.1 M HCl—1 M NaCl
Glass	< 0.01	< 0.01	< 0.01
	< 0.01	< 0.01	< 0.01
	< 0.01	< 0.01	< 0.01
High-density linear polyethylene	0.02	0.03	0.03
	0.01	0.02	0.02
	0.02	0.02	0.01
High-density polypropylene	0.01	0.02	0.02
	0.02	0	0.02
	0.02	0.02	0.04
Soft polyethylene	0.02	0.05	0.07
	0.02	0.09	0.02
	0.02	0.03	0.03

not show appreciable loss of mercury after 48 days. This confirms previous findings that mercury solutions of different matrices have different stabilities [10]. Rosain and Wai [2] noted that loss of mercury in creek water (conductivity 836 μmhos cm^{-1}) was slower than that in distilled water. The present results show that 5% HNO_3, like 1% H_2SO_4, is not suitable for all types of samples. Although it has been stated [18] that HNO_3 alone is a better preservative than H_2SO_4 alone, it is now well established that both are inadequate.

The above acid mixtures coupled with high salt content were then considered. $NaNO_3$, KCl and NaCl were used. With 5% $NaNO_3$ solutions together with each of the above acids, a 50% loss of mercury was observed at the 0.30 $\mu g\ l^{-1}$ level after 48 days for distilled water. This mixture was, however, satisfactory in preserving 0.15 μg Hg l^{-1} in ground water. Both KCl and NaCl showed promise as preservatives for mercury in distilled and natural waters at similar levels in polyethylene bottles. However, these salts are not compatible with the mercury manifold used, because chlorine [7] is produced by the oxidation of the resulting saline water, and because these salts reduce the $KMnO_4$ used in the system for oxidation of organo-mercurials.

The use of acids coupled with strong oxidants such as $KMnO_4$ and $K_2Cr_2O_7$ has been widely recommended. Permanganate is not desirable for routine monitoring of waters by the cold-vapor atomic absorption method, because the precipitation of MnO_2 necessitates an additional step in the automated analysis; the precipitate must be removed by addition of a weak reducing agent. Agemian and Chau [25] have studied different methods of dissolving the precipitate for the determination of mercury in sediments. This type of pretreatment is suitable for sediment analysis since samples have to be predigested anyway, but for routine water analysis, this oxidant necessitates an extra step, increases the blank, and consumes the whole sample. An additional disadvantage is that $KMnO_4$ produces chlorine in high chloride samples, and the additional $KMnO_4$ required to counter this effect increases the blank.

The use of $K_2Cr_2O_7$ avoids these problems. Most investigators have used 0.05% $K_2Cr_2O_7$. In this study, concentrations of 0.005—0.5% $K_2Cr_2O_7$ were found to be compatible with the chemistry of the system used [1, 21]. Table 3 shows the preservation of a synthetic water (deionized) and a natural sample (specific conductance = 500 μmhos cm^{-1}) stored under the following conditions. Each sample was split into three identical portions, and the second and third portions of each were spiked with 0.20 and 0.60 $\mu g\ l^{-1}$, respectively. Six different preservatives were used for each resulting sample. The final solutions were then split and stored in two different containers, high density polyethylene and glass. The preservation study was extended to 120 days. Table 3 shows that $K_2Cr_2O_7$ definitely improves preservation. The solutions were analyzed several times during the experiment to provide a large enough population to allow statistical calculations on the data.

TABLE 3

Final concentration of mercury in solution after 120 days of preservation

Preservation Method	Synthetic sample (Distilled water)				Natural sample (Hamilton Harbour, Ontario)			
	0.2 $\mu g\ l^{-1}$		0.6 $\mu g\ l^{-1}$		0.2 $\mu g\ l^{-1}$		0.6 $\mu g\ l^{-1}$	
	P[a]	G[a]	P	G	P	G	P	G
1 5% HNO_3	0.08	0.05	0.27	0.42	0.20	0.21	0.63	0.63
2 1% H_2SO_4	0.03	0.04	0.34	0.64	0.08	0.28	0.60	0.70
3 5% HNO_3 + 0.005% $K_2Cr_2O_7$	0.09	0.20	0.42	0.64	0.24	0.22	0.65	0.61
4 1% H_2SO_4 + 0.005% $K_2Cr_2O_7$	0.24	0.21	0.64	0.67	0.24	0.24	0.66	0.68
5 1% H_2SO_4 + 1% HNO_3 + 0.005% $K_2Cr_2O_7$	0.23	0.22	0.63	0.69	0.23	0.24	0.66	0.66
6 2% HCl + 0.005% $K_2Cr_2O_7$	0.24	0.26	0.70	0.72	0.27	0.26	0.73	0.72

[a]P = High density polyethylene. G = Glass.

Comparisons by the method of total errors

McFarren et al. [19] have shown that the total error concept is an effective means of judging the acceptability of analytical methods. The total error is defined [19]

% Total error = [Absolute value of mean error + 2 (s.d.) × 100] /True value

McFarren et al. [19] have suggested that total errors of less than 25% represent excellent results, less than 50% represent acceptable results, and those over 50% represent unacceptable results.

The method of total errors [19] is used here to show rigidly the lack of preservation for a given set of conditions, and to indicate the precision of the method for those samples that are adequately preserved. The determined value for the spiked samples is known, so that the total error of each group can be computed. Table 4 shows the overall total error for each sample with the different preservatives. The expression for total error takes into account both precision and accuracy and thus is the only valid way of comparing analytical methods. The overall conclusion from Table 4 is that preservatives 3, 4 and 5 are far superior to the other three methods. The results show a few trends. The total errors are higher in most cases at 0.2 μg Hg l^{-1} than at

TABLE 4

% Total error for the different preservation methods (Hg as $HgCl_2$)

Preservation Method[a]	Synthetic sample (Distilled water)				Natural sample (Hamilton Harbour, Ont.)			
	0.2 $\mu g\ l^{-1}$		0.6 $\mu g\ l^{-1}$		0.2 $\mu g\ l^{-1}$		0.6 $\mu g\ l^{-1}$	
	P[a]	G[a]	P	G	P	G	P	G
1	84	125	87	50	7	23	11	7
2	107	104	53	107	136	56	35	33
3	74	18	37	10	30	17	24	5
4	24	12	15	16	49	24	15	19
5	20	18	9	16	48	25	13	13
6	123	112	43	42	84	47	43	28

[a]See Table 3.

0.6 $\mu g\ Hg\ l^{-1}$. Glass bottles show lower errors than plastic. The synthetic water shows higher errors than the natural water. Of the better methods (3, 4 and 5) the type or concentration of acid makes little difference as long as pH < 1. The preferred method is 1% H_2SO_4 + 0.005% $K_2Cr_2O_7$. Nitric acid is more volatile and less stable than H_2SO_4, it is more difficult to handle, and it contains higher mercury blanks. High-purity nitric acid is expensive. The use of 1% H_2SO_4 + 0.005% $K_2Cr_2O_7$ was found to be compatible with the automated cold vapor atomic absorption method and introduced a blank of less than 0.01 $\mu g\ Hg\ l^{-1}$. Thus low-level mercury solutions could be adequately preserved without any interference from the blank.

The effect of the concentration of $K_2Cr_2O_7$ on the preservation was studied further. It was found that 1% H_2SO_4 + 0.05% $K_2Cr_2O_7$ gave lower error values than 1%H_2SO_4 + 0.005% $K_2Cr_2O_7$, i.e. the precision and accuracy were considerably improved. No further advantage was found when more $K_2Cr_2O_7$ was used.

Effect of container material

Six different container types were investigated, and the concentrations of 0.005% and 0.05% $K_2Cr_2O_7$ with 1% H_2SO_4 were tested on 0.5 p.p.b. mercury solutions for 60 days. The containers tested were Teflon, polypropylene, linear polyethylene, common polyethylene, Pyrex and soft glass. In all cases, the 0.05% $K_2Cr_2O_7$ solutions were either as good as, or better than, the 0.005% $K_2Cr_2O_7$ solutions. Teflon, polypropylene, linear polyethylene, Pyrex and soft glass gave excellent total error expressions with the increased $K_2Cr_2O_7$ (i.e. less than 25% [19]). Common polyethylene was the only type which gave an unsatisfactory total error (i.e. greater than 50%).

For the five satisfactory container materials, the order of increasing total error was: Pyrex = soft glass < teflon = polypropylene = linear polyethylene <

common polyethylene. Further precision and accuracy studies confirmed this trend. Therefore the recommended container is glass, with the 1% H_2SO_4 + 0.05% $K_2Cr_2O_7$ preservative.

Preservation of methylmercury

A brief study was performed to see if the form of mercury affects preservation. Methylmercury(I) is the commonest form of organomercurial [26] in aquatic systems. Therefore experiments similar to the above were performed with CH_3HgCl as the spiking solution. Table 5 provides total error data for the 1% H_2SO_4 + 0.05% $K_2Cr_2O_7$ method. The total error expressions are in most cases excellent (i.e. less than 25%). The dependence on container type is somewhat lessened compared with that for inorganic mercury. The reduced charge on the CH_3Hg^+ compared with Hg^{2+} and its larger size probably change the mechanism of adsorption on the containers.

Interlaboratory study

The preservative properties of the 1% H_2SO_4 + 0.05% $K_2Cr_2O_7$ technique were tested in a national quality control study in which 27 participating laboratories were involved. Full details are given by Aspila and Carron [27]. Samples, including synthetic and spiked natural waters, were sent ready to analyze to participants. The study lasted for 4 months, during which preservation was critical. The precision and accuracy data are summarized in Table 6, together with comparable data from an Environmental Protection Agency (EPA) study [28]. The EPA study did not involve the preservative as a variable; concentrated solutions were sent and participants were asked to dilute the solutions before analysis. Thus, if our recommended preservative did not function properly, the quality control results would be inferior to those by the EPA study. However, the data in Table 6 show that no

TABLE 5

Total error (%) expressions for 0.5 μg Hg l^{-1} (as CH_3HgCl) solutions preserved with 1% H_2SO_4 + 0.05% $K_2Cr_2O_7$ for a duration of 60 days in different containers

Sample	Container material[a]							
	CPE	PP	LPE	Teflon	Soft glass	BOD	Pyrex glass	Soveril bottles
Synthetic water	8	12	11	10	10	11	8	7
Spiked natural water	29	14	11	12	17	18	20	18

[a]CPE = Common polyethylene. PP = Polypropylene. LPE = Linear polyethylene. BOD = Biological oxygen demand (glass).

TABLE 6

Comparison of EPA and present interlaboratory quality control studies

EPA study [28]				Round-robin study [27]			
Sample[a]	Designed value ($\mu g\ l^{-1}$)	Mean recovery ($\mu g\ l^{-1}$)	s_r (%)	Sample	Designed value ($\mu g\ l^{-1}$)	Mean recovery ($\mu g\ l^{-1}$)	s_r (%)
DW	0.21	0.418	66.9	NS	—	0.131	89.0
NW	0.21	0.349	78.9				
DW	0.27	0.450	72.2				
NW	0.27	0.414	67.5				
DW	0.51	0.653	57.5	NS	NS + 0.25	0.389	36.0
NW	0.51	0.674	80.3				
DW	0.60	0.744	62.6	NS	NS + 0.94	1.05	23.0
NW	0.60	0.709	55.0	S	1.40	1.11	35.0
DW	3.4	3.40	37.9	NS	NS + 4.84	4.91	25.0
NW	3.4	3.41	43.7				
DW	4.1	4.26	33.2	NS	NS + 18.54	18.54	15.0
NW	4.1	3.81	29.3				

[a]DW — Distilled water. NW — Natural water by difference. S — Synthetic sample. NS — Natural sample.

deterioration in preservation occurred with the recommended preservative for the duration of the experiment.

REFERENCES

1 P. D. Goulden and B. K. Afghan, Technicon International Congress Vol. II, Nov. 2—4, 1970, Futura, New York, 1970, p. 317.
2 R. M. Rosain and C. M. Wai, Anal. Chim. Acta, 65 (1973) 279.
3 R. A. Carr and P. E. Wilkniss, Environ. Sci. Technol., 7 (1973) 63.
4 G. N. Gaston and A. K. Lee, J. Am. Water Works Assoc., 66 (1974) 495.
5 J. F. Kopp, M. C. Longbottom and L. B. Lobring, J. Am. Water Works Assoc., 64 (1972) 20.
6 R. V. Coyne and J. A. Collins, Anal. Chem., 44 (1972) 1093.
7 M. H. Bothner and D. E. Robertson, Anal. Chem., 47 (1975) 592.
8 H. V. Weiss and K. Chew, Anal. Chim. Acta, 67 (1973) 444.
9 M. S. Masri and M. Friedman, Environ. Sci. Technol., 7 (1973) 951.
10 D. W. Newton and R. Ellis, Jr., J. Environ. Qual., 3 (1974) 20.
11 I. R. Jonasson, J. J. Lynch and L. J. Trip, Geol. Surv. Can. Paper, 73-21, 1973.
12 T. Y. Toribara, C. P. Shields and L. Koval, Talanta, 17 (1970) 1025.
13 S. Shimomura and A. Kise, Bunseki Kagaku, 18 (1969) 1412.
14 P. Avotins and E. A. Jenne, J. Environ. Qual., 4 (1975) 515.
15 C. Feldman, Anal. Chem., 46 (1974) 99.
16 J. M. Lo and C. M. Wai, Anal. Chem., 47 (1975) 1869.
17 A. A. El-Awady, R. B. Miller and M. J. Carter, Anal. Chem., 48 (1976) 110.
18 D. R. Christmann and J. D. Ingle, Jr., Anal. Chim. Acta, 86 (1976) 53.
19 E. F. McFarren, R. J. Lishka and J. H. Parker, Anal. Chem., 42 (1970) 358.

20 P. D. Goulden, private communication, Canada Centre for Inland Waters, 867 Lakeshore Rd., Burlington, Ontario, Canada.
21 E. A. Jenne and P. Avotins, J. Environ. Qual., 4 (1975) 427.
22 Y. Dokiya, S. Yamazaki and K. Fuwa, Environ. Lett., 7 (1974) 67.
23 H. V. Weiss, W. H. Shipman and M. A. Guttman, Anal. Chim. Acta, 81 (1976) 211.
24 S. Shimomura, Y. Nishihara and Y. Tanase, Bunseki Kagaku, 18 (1969) 1072.
25 H. Agemian and A. S. Y. Chau, Anal. Chim. Acta, 75 (1975) 297.
26 G. L. Baughman, J. A. Gordon, N. Lee Wolfe and R. G. Zepp, Chemistry of Organomercurials in Aquatic Systems, EPA-660/3-73-012 Sept. 1973; U.S. Government Printing Office, Washington, D.C. 20402, U.S.A.
27 K. I. Aspila and J. Carron, Interlaboratory Quality Control Study No. 16 — Total Mercury in Natural Water, Report Series No. 53 (1977), Inland Waters Directorate, Dept. of the Environment, Burlington, Ontario.
28 J. A. Winter and H. A. Clements, Interlaboratory Study of the Cold Vapor Technique for Total Mercury in Water, Water Quality Parameters, ASTM STP 573, American Society for Testing and Materials, 1975, pp.566—580.

Analytica Chimica Acta, 92 (1977) 71—77

DETERMINATION OF TOTAL MERCURY IN AIR BY ATOMIC ABSORPTION SPECTROMETRY AFTER COLLECTION ON MANGANESE DIOXIDE

J. H. JANSSEN, J. E. VAN DEN ENK, R. BULT and D. C. DE GROOT

Akzo Zout Chemie Nederland bv Research, Analytical Department, Boortorenweg 18, Hengelo 7700 (The Netherlands)

(Received 21st January 1977)

SUMMARY

A method has been developed for the routine determination of total mercury in air. Mercury and its compounds are collected on manganese dioxide, the manganese dioxide is dissolved and the mercury is determined by atomic absorption spectrometry (cold vapour technique). The method was tested with standard samples containing elemental mercury, mercury(II) and organomercurials. The collection efficiency of the manganese dioxide is greater than 95% for concentrations up to 2 mg of mercury per m^3 of air. The lowest quantity of mercury that can be determined is 0.02 μg. The relative standard deviation calculated from experiments done in an alkali chloride electrolysis plant equipped with mercury cells, is 1.4% at the 25 $\mu g\ m^{-3}$ level (collection time, 4 h).

The method by which mercury and its compounds are collected on carbon-loaded paper [1] was developed originally for the determination of mercury by x-ray fluorescence spectrometry (x.r.f.s.). The mercury sampled on the paper could also be determined by atomic absorption spectrometry (a.a.s.), but a drawback of this procedure is the essential filtration of the solution. To avoid this filtration, the collection of mercury and its compounds on manganese dioxide [2] has been investigated.

EXPERIMENTAL

Preparation of the collection tube (sampler) and the sampling procedure

The design of the sampler is shown schematically in Fig. 1. Clean the empty tube and the required quartz wool carefully with hot nitric acid (ca. 14 M), rinse with water and dry in an oven. Insert a quartz wool plug by means of a glass rod into the tube, followed by 1.0 g of manganese dioxide, tamp, insert another quartz wool plug, followed by 1.0 g of manganese dioxide, tamp, and insert a third quartz wool plug to keep the manganese dioxide in place. Cap the sampler at both ends when not in use. For sampling, connect the sampler to a vacuum pressure pump (e.g. Millipore XX 60.220.50), paying attention to the direction of the air flow.

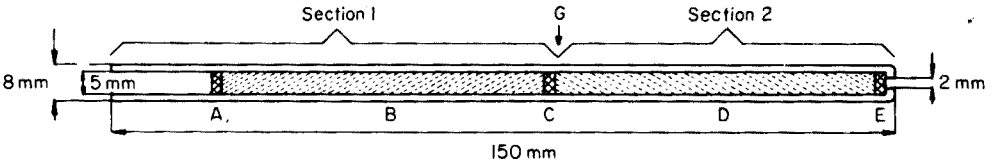

Fig. 1. MnO_2 sampler. A, C, E: quartz wool. B, D: manganese dioxide (1 g). G: point for cutting after sampling.

Connect the outlet of the pump to a wet gas meter. Sample the air at a flow rate of about 3 l min^{-1}. To prevent contamination, cap the sampler after sampling.

Cold-vapour atomic absorption spectrometry

Clean the outside of the sampler with water and dry with tissue. Cut the tube in two parts (see Fig. 1). Transfer the manganese dioxide and the two quartz wool plugs of section 1 to a 200-ml conical flask. Rinse the inner wall of the emptied part of the sampler successively with 20 ml of hydrochloric acid (1 + 1), 2 ml of nitric acid (ca. 14 M) and a little water, and transfer these into the flask. Cover the flask with a watch glass, heat to boiling and boil until the manganese dioxide has dissolved. If dissolution is incomplete after 10 min, cool and add a few drops of hydrogen peroxide (30%); then destroy the hydrogen peroxide in excess by boiling. Cool and transfer the solution to a 50-ml volumetric flask. Section 2 can be used as a check on complete collection of the mercury in section 1. For a blank determination, use 1.0 g of manganese dioxide. Transfer equivalent aliquots (a maximum aliquot of 25 ml) of sample and blank solution to 100-ml conical flasks containing 1 ml of potassium permanganate solution (40 g l^{-1}) and 1 ml of sulphuric acid (1 + 4). Rinse the walls with 5 ml of distilled water.

Heat to boiling, boil for a few seconds, and cool. Add 0.5 ml of sodium chloride solution (300 g l^{-1}). Decolourize the solution by dropwise addition of hydroxyammonium chloride solution (100 g l^{-1}). After transferring the solution to an aeration flask, determine the mercury content by the procedure recommended by the Mercury Analysis Working Party of BITC [3]. For calibration, the method of standard additions must be used to correct for any matrix effects, unless it has been proved that there are no matrix effects.

Reagents

All chemicals were selected for low mercury content. Manganese dioxide (10—25-mesh B.S.; micro-analytical grade; Hopkin & Williams; for specification see [4]) was used. The fraction retained by a 710-μm (22-mesh B.S.) sieve was used to achieve almost the same pressure drop across each sampler, which is of interest when samplers are connected in parallel. Quartz wool (Heraeus GmbH Hanau, number Mikro RZ 112) was employed to hold

the adsorbent in position. Mercury-free hydrochloric acid (1 + 1) was obtained by distillation (constant boiling hydrochloric acid).

Mercury, mercury(II) chloride, methylmercury chloride, phenylmercury chloride and methylmercury benzoate were applied in evaluation of sampling.

RESULTS AND DISCUSSION

Collection efficiency

To investigate the collection efficiency of the MnO_2 samplers, several experiments were done. Initially, a sampler provided with carbon-loaded paper [1] was placed in series behind a MnO_2 sampler. This combination was used for sampling air from a cell room in an alkali chloride electrolysis plant; the sampling rate was 120—180 l h^{-1}. In three experiments done at different times, the amounts of mercury found in the MnO_2 samplers were 50, 40 and 39 μg, respectively, and no mercury could be detected (<0.2 μg) on the carbon-loaded paper. In other experiments the two sections of the MnO_2 samplers, loaded with mercury in the cell room were analyzed separately. In each experiment, three samplers were used in parallel in the plant. No significant amounts of mercury were detected in the downstream MnO_2 sections (Table 1).

In laboratory experiments, a permeation tube [5] was used to spike a test gas (argon) with selectable but time-constant concentrations of mercury and mercury compounds. The mercury concentrations of the test gas, before and after passing through the MnO_2 samplers, were determined by emission spectrometry with a microwave-induced plasma source [6]. Recoveries were calculated from the initial and breakthrough values in the gas. Carbon-loaded paper [1] was also tested in this way. For all compounds the collection efficiency was very high (>95%, Table 2). To check the influence of moisture on the sampling, air containing elemental mercury was sucked through a

TABLE 1

Results of the determination of mercury in the two sections of MnO_2 samplers (Sample: cell-room air at a flow rate of 3 l min^{-1}. The quantity of air sampled varied.)

Exp.	Hg in section 1 (μg)	Hg in section 2 (μg)	Exp.	Hg in section 1 (μg)	Hg in section 2 (μg)
	14	0.02		210	0.05
1	14	0.02	4	211	0.02
	15	<0.02		199	<0.02
	30	0.17		598	0.05
2	31	0.19	5	597	<0.02
	33	0.21		604	<0.02
	97	0.31			
3	101	0.23			
	101	0.42			

TABLE 2

Collection efficiency for mercury and mercury compounds with manganese dioxide and carbon-loaded paper
(Initial concentration was determined by emission spectrometry with a microwave-induced plasma source.)

Compound	Argon flow (l min^{-1})	Initial Hg concn. ($\mu g\ m^{-3}$)	Total Hg offered (μg)	Recovery MnO_2 (%)	Recovery C-loaded paper (%)
Mercury	2.8	220	73	>99	>97
Mercury(II) chloride	3	2600	950	>95	>98
Mercury(II) chloride	0.5	250		>99	
Methylmercury chloride	0.9	3100	200	>99	>99
Methylmercury chloride	2.7	2600	200	>99	>99
Phenylmercury chloride	3	69	25	>98	>97
Methylmercury benzoate	0.9	250	50	>99	>99

MnO_2 sampler via a desiccant (magnesium perchlorate); mercury was generated by reducing mercury(II) with tin(II) chloride in an aeration flask and passing air through [1]. In series with the MnO_2 sampler were placed successively a sampler fitted with carbon-loaded paper and two bubblers containing sulphuric acid—permanganate solution [3]. No mercury was detected in the carbon-loaded sampler or in the bubblers after sampling of 100 μg of mercury after 20 min. This procedure was repeated without the desiccant. The results proved that water does not decrease collection efficiency (Table 3).

Recovery of collected mercury

To prevent losses caused by violent reaction, azeotropic hydrochloric acid (1 + 1) must be used for dissolving the MnO_2 instead of 12 M. Nitric acid (ca. 14 M) is added and the solution is boiled to accelerate the decomposition rate.

TABLE 3

Influence of drying of the air on the collection of 100 μg of elemental mercury

Exp.	μg Hg (→ direction of air flow)[a]								
	Desiccant	Sampler section[b]					C-loaded paper	Bubbler 1	Bubbler 2	Total
		A	B	C	D	E				
1	$Mg(ClO_4)_2$	0.6	93.9	<0.1	0.3	<0.1	<0.2			95
2	$Mg(ClO_4)_2$	1.2	96.8	<0.1	<0.1	<0.1	<0.2			98
3	None	4.3	90.8	<0.1	0.2	<0.1	<0.2	<0.1	<0.1	95
4	$Mg(ClO_4)_2$	0.9	97.9	<0.1	<0.1	<0.1		<0.1	<0.1	99

[a] Air flow = 3 l min^{-1} during 20 min.
[a] See Fig. 1.

To test for possible losses of mercury by adsorption on the quartz wool plugs, 50 μg of mercury (as Hg^{2+} in solution) was added to 1.0 g of manganese dioxide and 2 plugs of quartz wool. After dissolution of the MnO_2, the solution was filtered on a membrane filter (cellulose acetate, 0.8 μm). The quartz wool was washed on the filter with water and then boiled with nitric acid (ca. 14 M). In three separate tests, 0.01, 0.02 and 0.04 μg of mercury were found in the nitric acid (corrected for a blank). These results are in accordance with the recovery experiments described above.

The retention of mercury and its compounds present in the gas phase is good (Table 2). However, these results were calculated from the initial and breakthrough mercury contents in the gas; the manganese dioxide was not analyzed. In order to be sure that the total mercury present on MnO_2 will be recovered (e.g. no losses of organic mercury compounds by incomplete mineralization), different amounts of mercury and some of its compounds were introduced to 1 g of MnO_2 and determined. Although it was unlikely that the air under investigation would contain organomercurials, the determination of these compounds was also evaluated because of the possibility of using the method for imission measurements near the plant (or other applications).

A known amount of mercury was generated by the reduction of mercury(II) chloride with tin(II) chloride [1] and drawn from the generating system through the MnO_2 adsorbent; mercury(II) chloride was added as Hg^{2+} in solution, mercury(I) chloride as a solid, and the organic mercury compounds as solutions in methanol. Tables 3, 4 and 5 show that no mercury was lost during analysis. Free chlorine created on dissolving MnO_2 destroyed the added organic mercury compounds, producing a solution containing only inorganic mercury species.

The manganese dioxide used contained 0.15 ± 0.01 μg Hg g^{-1}. The lower limit of detection, based on the threefold, overall standard deviation of the blank determination, is 0.02 μg of mercury.

Collection capacity of the samplers

The maximum amount of mercury that can be collected on a sampler was not determined. In some experiments, samplers were loaded with 200 μg

TABLE 4

Recovery of mercury added to MnO_2

Exp.	Hg added as $HgCl_2$ (μg)	Hg found (μg)	Exp.	Hg added as Hg_2Cl_2 (μg)	Hg found (μg)
1	50.6	49.0	6	8200	8500
2	50.6	49.0	7	8900	9000
3	50.1	50.0	8	11300	11200
4	1.0	0.95			
5	1.0	0.94			

TABLE 5

Recovery of organomercurials added to MnO_2

Compound	Hg added (μg)	Recovery (%)
Methylmercury chloride	100	101
	0.21	112
Phenylmercury chloride	100	100
	0.21	105
Methylmercury benzoate	100	101
	0.21	100

of elemental mercury or 1000 μg of mercury(II); significant amounts of mercury were not detected in the air passing from the sampler.

Because the mercury was introduced at a much faster rate (mercury(II), 8 $\mu g\ min^{-1}$, Table 2; mercury(0), 5 $\mu g\ min^{-1}$, Table 3) than during actual sampling, the collection capacity should suffice for most environmental problems.

The loaded samplers mentioned in Table 3 were analyzed after storage for two weeks at room temperature. No significant loss of mercury was detected.

Results for cell-room air

The results for mercury in cell-room air obtained by collection on manganese dioxide and on carbon-loaded paper are in good agreement (see Table 6). Samples taken in the plant gave a relative standard deviation of about 1.4% [7].

TABLE 6

The determination of mercury in cell-room air after collection on manganese dioxide and carbon-loaded paper. For each experiment 6 samples were taken simultaneously

Exp.	MnO_2		C-loaded paper		Exp.	MnO_2		C-loaded paper	
	Air flow ($l\ min^{-1}$)	Hg ($\mu g\ m^{-3}$)	Air flow ($l\ min^{-1}$)	Hg ($\mu g\ m^{-3}$)		Air flow ($l\ min^{-1}$)	Hg ($\mu g\ m^{-3}$)	Air flow ($l\ min^{-1}$)	Hg (μg
	2.9	49	2.7	50		2.6	27	2.7	25
1	2.9	50	2.7	50	3	2.5	26	2.7	25
	3.0	50	2.7	52		2.5	27	2.7	25
	2.5	27	2.5	25		2.9	20	0.9	22
2	2.6	27	2.5	26	4	2.9	20	0.9	20
	2.6	26	2.5	26		2.8	20	0.9	21

Conclusions

The method of collecting mercury and its compounds on manganese dioxide followed by determination by a.a.s. is suitable for cell-room air of a mercury cell electrolysis plant. The lower limit of detection is 0.02 μg of mercury. The method can also be applied to air containing organic mercury compounds such as methylmercury chloride, methylmercury benzoate and phenylmercury chloride.

The advantages of this method compared with the earlier method [1] are that the filtration step can be omitted, the limit of detection is lower, and the method is applicable for wet air. However, for large series, the carbon-loaded paper method in combination with x.r.f.s. is preferable because of its speed.

The help of Mr. S. Coffa is gratefully acknowledged.

REFERENCES

1 J. H. Janssen, J. E. van den Enk, R. Bult and D. C. de Groot, Anal. Chim. Acta, 84 (1976) 319.
2 M. K. Pakter, Gig. Sanit., 34 (1969) 401.
3 Mercury Analysis Working Party of BITC, Anal. Chim. Acta, 72 (1974) 37.
4 The Joint Panel of the Microchemical Methods Group and the Analytical Standards Sub-Committee of the Society for Analytical Chemistry, Analyst, 97 (1972) 740.
5 F. P. Scaringelli, A. E. O'Keefe, E. Rosenberg and J. P. Bell, Anal. Chem., 42 (1970) 871.
6 G. Kaiser, D. Götz, P. Schoch and G. Tölg, Talanta, 22 (1975) 889.
7 Instructions for statistical treatment of series of observations, Nederlands Normalisatie Instituut, NEN 1047, UDC 311.1; 519.24, blad 3.4.

Analytica Chimica Acta, 92 (1977) 79—83

ATOMIC ABSORPTION SPECTROMETRIC DETERMINATION OF ALUMINIUM IN WHOLE BLOOD

F. J. LANGMYHR* and D. L. TSALEV†

Department of Chemistry, University of Oslo, Oslo 3 (Norway)

(Received 15th February 1977)

SUMMARY

Two methods are described for atomic absorption spectrometric determinations of aluminium in heparinized and haemolyzed samples of undiluted whole human blood. In the direct method 2 μl of blood are pipetted into a graphite cup atomizer; after a drying and two ashing steps aluminium is determined by atomization at 2500°C. In the second method, 15 μl of blood are decomposed by nitric acid in polytetrafluoroethylene tubes; 2-μl portions of the solution are then analyzed with the graphite tube atomizer. The direct method was applied to the determination of aluminium in whole blood from 48 Norwegian workers occupationally unexposed to the element; the concentrations of aluminium ranged from 0.05—0.59 p.p.m. (mean value, 0.20 p.p.m.). For 0.35 p.p.m. aluminium, the relative standard deviation of both methods was 8%. The detection limit of the direct method is 0.05 p.p.m. aluminium.

During recent years the universal interest in trace elements has stimulated a number of studies of their concentration and distribution in the human body, with the purpose of establishing the normal values, and to detect illnesses, occupational diseases and toxic effects.

Whole human blood contains small amounts of aluminium (of the order of one or more tenths of 1 p.p.m.); the concentration has been found to vary during certain diseases [1]. At present, nothing definite can be said about the toxicity of aluminium, for this question is still being debated.

The determination of aluminium in biological materials is complicated by the low concentration of the element, the limited amounts of sample available, and the large number of analyses required in clinical situations.

Various methods, such as spectrophotometry [2], emission spectroscopy [3], neutron activation analysis [4, 5], and atomic absorption spectrometry (a.a.s.) [6—11], have been used for the determination of aluminium in biological materials. The furnace a.a.s. technique has been applied to the determination of aluminium in serum [11], but, to the authors' best knowledge, it has not been used for determining the metal in undiluted whole blood.

---

†On leave from Faculty of Chemistry, University of Sofia, Sofia 26, Bulgaria.

The purpose of the present work was to develop a direct, rapid and simple method for the determination of aluminium in undiluted whole human blood.

EXPERIMENTAL

Apparatus

The measurements were made with a Perkin-Elmer 400 S atomic absorption spectrophotometer, the cup and tube version of the Varian-Techtron CRA-63 resistance-heated graphite furnace and a Perkin-Elmer single-channel recorder. The instrument was equipped with two lamps for background correction; however, as apparent from the preliminary investigations (vide infra), the analyses can be made without using a background corrector.

The furnace was heated by a four-step power supply constructed in the laboratory. Temperature calibration curves for the furnaces were recorded with an Ircon radiation thermometer.

Sample and standard solutions were introduced into the cup with a 2-μl Ultra-Micro pipette (Oxford Labs. Intern.), and a 5—50-μl adjustable Finnpipette (Kemistien OY, Finland).

For the decomposition of whole blood, 100-μl tubes with stoppers were made from rods of a dense quality of polytetrafluoroethylene (PTFE). During heating the tubes were placed in holes drilled in a circular steel plate, and the stoppers were pressed into the tubes by a second plate fastened to the perforated plate with a screw in the centre. The tubes were heated in a drying oven.

Reagents and standard solutions

A primary 1000-p.p.m. aluminium standard solution was prepared by dissolving 1 g of high-purity metal (Johnson Matthey, London) in 200 ml of (1 + 9) sulphuric acid (Suprapur, Merck), and diluting the solution to 1 l with deionized water.

Secondary standard solutions were prepared daily by dilution.

Concentrated nitric acid (Suprapur, Merck) was employed for the decomposition of blood.

The graphite furnace was purged with argon of purity 99.9% (by volume).

Samples

The feasibility of the proposed direct method was demonstrated by the analysis of whole blood samples from 48 Norwegian workers who were not occupationally exposed to aluminium. The samples were collected in heparinized "Vacutainer" tubes and were haemolyzed by the addition of four drops of Triton X-100.

Preliminary work

Some introductory measurements were made to establish the best conditions for the ashing and atomization steps. It was found that aluminium is not lost by ashing whole blood samples in the furnace at 1200°C.

When the proposed direct method was used, the peak heights were the same whether the background corrector was used or not; consequently, the non-specific absorption of radiation during atomization of aluminium can be considered to be negligible.

When calibration curves were plotted for aluminium in a whole blood matrix, and from aqueous aluminium standard solutions, it was observed that the slope of the curves varied considerably. In the direct method, the measurements should therefore be based either on the tedious and time-consuming standard addition technique, or on employing one or more carefully analyzed whole blood samples as the standard. The latter approach was used in the present direct analyses.

After the wet-ashing of whole blood by nitric acid, the matrix consists of a dilute solution of simple salts; in such cases aqueous aluminium solutions can be used as standards.

Procedures

Before the start of the measurements, the hollow-cathode lamp was heated for about 15 min. The flow of argon was adjusted to 4 l min^{-1}. The measurements were made at 309.3 nm. All analyses were based on measuring peak heights.

Direct analysis. Undiluted whole blood (2 μl) was transferred to the graphite cup of the atomizer; during the introduction of the sample, the pipette tip should not touch the interior walls of the cup. The samples were analyzed with the following heating program: drying at 90°C for 40 s, first ashing at 400°C for 30 s, second ashing at 1200°C for 30 s, and atomization at 2500°C for 7 s.

Two blood samples were employed as standards, the content of aluminium in these being established by the standard addition technique. To three of a series of four 1-ml portions of the blood to be used as standard, 10 μl of 10, 20 or 50 p.p.m. aluminium standard solutions were added; the concentrations in the blood of the aluminium added thus corresponded to 0.1, 0.2 and 0.5 p.p.m., respectively.

Analysis by wet-ashing. In addition to the analyses by the above direct method, aluminium was also determined in some samples decomposed by wet-ashing. Portions (15 μl) of whole blood were transferred to 100-μl PTFE tubes, 15 μl of nitric acid were added, and the tubes were stoppered. The contents were mixed vigorously and heated at 90°C for 2 h. After being cooled to room temperature, the contents were again mixed by shaking.

Portions (2 μl) of the solutions were pipetted into the graphite tube atomizer, and aluminium was determined as described in the above procedure. The analyses were made with aqueous aluminium solutions as standards.

Other analyses

For comparison some samples were also analyzed in another laboratory (Institute of Occupational Health, Oslo). The equipment employed was a Perkin-Elmer 300 atomic absorption spectrophotometer with a HGA-76 graphite furnace. Portions of diluted whole blood samples (1 + 10) were analyzed by the standard addition technique, and with the following heating program: drying at 90°C, rate 2, for 30 s; first ashing at 500°C, rate 2, for 30 s; second ashing at 1200°C, rate 1, for 30 s; and atomization at 2700°C, rate 0, for 10 s with gas stop for 7 s.

RESULTS

The above direct procedure was employed in the analysis of 48 undiluted whole blood samples. The results ranged from 0.05 to 0.59 p.p.m. with a mean value of 0.20 p.p.m. The distribution of the results was as follows: 23% in the range 0.05—0.10 p.p.m.; 42% in the range 0.11—0.20 p.p.m.; 12% in the range 0.21—0.30 p.p.m.; 15% in the range 0.31—0.40 p.p.m.; 4% in the range 0.41—0.50 p.p.m.; and 4% in the range 0.51—0.60 p.p.m.

Two of the samples were analyzed by three different methods. The data from these analyses are listed in Table 1.

DISCUSSION

The results of the present investigation lie in the range covered by the data from the following previous studies: 0.13 p.p.m. [12], 0.21—0.94 p.p.m. (mean value 0.53 p.p.m.) [3], and 1.40 p.p.m. [13].

As is apparent from Table 1, the data obtained by the direct method are in good agreement with those of the two other procedures. Statistical calculations confirmed that the differences between the mean values are explained by the presence of random errors alone.

TABLE 1

Analytical results (in p.p.m.) for aluminium in two samples of whole human blood analyzed by three atomic absorption spectrometric methods. The figures tabulated are the mean values ± one standard deviation as calculated from N analyses

Sample	Method I[a]	Method II[b]	Method III[c]
A	0.35 ± 0.03 $N = 6$	0.36 ± 0.03 $N = 8$	0.39 ± 0.03 $N = 6$
B	0.16 ± 0.03 $N = 10$	0.14 ± 0.04 $N = 4$	0.13 ± 0.04 $N = 4$

[a] Method I — Direct analysis of undiluted whole blood.
[b] Method II — Analysis by wet-ashing.
[c] Method III — Direct analysis of diluted whole blood (1 + 10), (Institute of Occupational Health, Oslo).

The precision of the direct method is satisfactory. It was found to be ±0.03 p.p.m., i.e. a relative standard deviation of 8% at a concentration 0.35 p.p.m. aluminium. The detection limit of the direct method is approximately 0.05 p.p.m. aluminium.

The main advantages of the proposed direct method are that the analyses are made without the addition of reagents and without any separation and/or concentration steps; the risks of introducing contaminations and of losing aluminium are thus considerably reduced.

The authors are indebted to Dr. N. Gundersen, The Institute of Occupational Health, Oslo, for providing the blood samples and for critical comments on the manuscript.

REFERENCES

1 J. R. J. Sorenson, I. R. Campbell, L. B. Tepper and R. D. Lingg, Environ. Health Perspectives, 8 (1974) 3.
2 M. Seilbold, Klin. Wochschr., 38 (1960) 117.
3 H. Wolff, Biochem. Z., 319 (1948) 1.
4 K. Fritze and R. Robertson, J. Radioanal. Chem., 7 (1971) 213.
5 H. Galenkamp, J. van Leeuwen and H. A. Das, Reactor Cent. Nederland Rep., RCN-208 (1974) 19.
6 E. Berman, Appl. Spectrosc., 29 (1975) 1.
7 F. Dolinšek, J. Štupar and M. Špenko, Analyst, 100 (1975) 884.
8 S. S. Krishnan, K. A. Gillespie and D. R. Crapper, Anal. Chem., 44 (1972) 1469.
9 J. R. McDermott and J. Whitehill, Anal. Chim. Acta, 85 (1976) 195.
10 H. A. Schroeder and A. P. Nason, Clin. Chem., 17 (1971) 461.
11 C. Fuchs, M. Brasche, K. Paschen, H. Nordbeck and E. Quellhorst, Clin. Chim. Acta, 52 (1974) 71.
12 R. A. Kehoe, J. Cholak and R. V. Story, J. Nutr., 19 (1940) 579.
13 F. Burriel Marti, C. Alvarez Herrero and M. P. Martin Mateo, Rev. Clin. Esp., 113 (1969) 413.

Analytica Chimica Acta, 92 (1977) 85—93

INVESTIGATIONS OF REACTIONS INVOLVED IN FLAMELESS ATOMIC ABSORPTION PROCEDURES

Part IV. A Theoretical Study of Factors Influencing the Determination of Aluminium

JAN-ÅKE PERSSON, WOLFGANG FRECH and ANDERS CEDERGREN*
Department of Analytical Chemistry, University of Umeå, S-901 87 Umeå (Sweden)
(Received 17th February 1977)

SUMMARY

High-temperature equilibrium calculations are used to study potential interferences in the determination of aluminium by flameless a.a.s. The conditions for the formation of interfering aluminium compounds like AlO(g), $Al_2O(g)$, $Al_2O_3(s)$, AlOH(g), AlH(g), $AlHO_2(g)$, AlS(g), AlN(g), AlN(s) and AlCl(g) have been calculated. The influence of kinetic parameters on the equilibrium calculations for the reactions involving carbon—oxygen and carbon—sulphur has been established by varying the input amount of carbon. The results indicate that even in the nanomole range the presence of elements like H, O, N, Cl and S may cause severe interferences during the atomization step (2300—2900 K).

Several papers have appeared on the determination of aluminium by flameless a.a.s. but very little fundamental research on interferences has been published. Aggett and Sprott [1] showed that the appearance temperature for aluminium is the same for both carbon and tantalum atomizers; they concluded that Al(g) must be formed by thermal decomposition of $Al_2O_3(s)$, i.e., carbon is not involved in the reaction. Sturgeon et al. [2] studied the mechanisms of free atom formation in a graphite furnace, and suggested that the thermal decomposition of $Al_2O_3(g)$ is a two-step reaction. The first step was considered to include the formation of Al(g) and AlO(g) and the second step the dissociation of AlO(g). However, the model of atom formation presented [2] deals with a simplified chemical system, for the only compounds present at the start of the atomization procedure were assumed to be C(s), Ar(g) and trace amounts of $Al_2O_3(s)$. In practice, the chemical system is far more complicated because of the presence of other substances, e.g. water. Water has been reported to be tenaciously held by graphite; even at 1200°C the fraction of water retained by the graphite after 15 min in vacuum was reported to be 0.05 [3]. This means that water must be present in a large excess over aluminium oxide at the start of the atomization.

The influence of various gases on the atomic absorption signal for aluminium has been described by several authors. Atsuya and Sugiura [4]

found a negative effect of argon on the peak height; they used a Perkin-Elmer HGA 70 graphite furnace, but their results do not agree with those reported in other papers which show a positive influence in the use of argon as the sheathing gas. Thus, Maruta et al. [5] recommended a flow rate of argon of 3.4 l min^{-1} on a Varian CRA 63; they concluded that more oxide is formed at low flow rates because of inefficient sheathing of the graphite from atmospheric oxygen. Brodie and Matoušek [6] found that the ratio of the peak absorbance in helium, nitrogen and argon was 1 : 1.5 : 3, respectively, when the flow rate of each gas was about 1.5 l min^{-1}. The depressing effect of nitrogen on the atomic absorption signal of aluminium has also been observed by Sturgeon et al. [2] and Manning and Fernandez [7]. The interferences in the presence of nitrogen were thought to be due to the formation of solid aluminium nitride which is stable up to 2500 K. The lower sensitivity for aluminium in helium compared to argon reported by Brodie and Matoušek [6] was assumed to depend on different rates of diffusion of the metal atoms in these gases. Parker and Shrader [8] using a Varian-Techtron CRA 63, investigated the effect of hydrogen on 31 elements in various matrices, and showed that the sensitivity for aluminium in an aqueous sample in the presence of hydrogen could be doubled. Maximum sensitivity was obtained when 0.5 l min^{-1} of hydrogen was mixed with the argon, but higher flow rates of hydrogen caused negative errors compared to the use of argon alone. Ohta and Suzuki [9] found that different flow rates of hydrogen—argon mixtures had very little effect on the sensitivity for aluminium in a micro-tube metal atomizer within a glass chamber.

The interference from hydrochloric and nitric acids has been reported to depend on the type of matrix [4, 10, 11]. Atsuya and Sugiura [4] found no interference from hydrochloric acid in the range 0—3 M. For more than 0.5 M nitric acid, the atomic absorption signal from aluminium decreased by about 70%. These latter results agree with those reported by Shaw and Ottaway [10], who found, however, that the interference from nitric acid was slight when iron was present, although a solution containing 1% of iron and 8% of hydrochloric acid caused erratic signals. However, Persson et al. [11] showed that the interference from hydrochloric acid could be almost eliminated by adding ammonium sulphate to a solution of a steel dissolved in a mixture of hydrochloric acid and nitric acid. They obtained maximum sensitivity by charring the ammonium sulphate-containing sample in the range 1200—1400°C. The convenient dissolution procedure including nitric and hydrochloric acid for high-alloy steels could therefore be used.

Calcium has also been reported to influence the sensitivity for aluminium. Dolinšek et al. [12] and Thompson et al. [13] using carbon cup atomizers both found a positive effect with a maximum sensitivity for 0.7% of calcium present. In contrast, Maruta et al. [5] found a negative interference from calcium using the Varian-Techtron Model CRA 63 carbon rod atomizer.

However, the interference could be completely eliminated by ashing the sample at 1200°C.

As is obvious from the above review, methods for the determination of aluminium lack basic systematic study of the factors influencing the determination. In this paper high-temperature equilibrium calculations have been used to obtain a general idea of the behaviour of the system. These results will be further discussed on the basis of experimental observations in Part V of this series [14].

HIGH-TEMPERATURE EQUILIBRIUM CALCULATIONS

The high-temperature equilibria were calculated in the same way as described in Part I of this series [15]. To obtain a survey of potential interfering elements, the elements selected were: H, O, N, Ar, Cl, S, C, Al, Si and Fe. The amounts of elements used in the calculations (the input amounts) and the temperatures were varied over a wide range, so that a general idea of the critical parameters controlling the formation of Al(g) could be obtained. To simulate a heavy matrix, iron and silicon were included in the calculations. The main components considered are given in Table 1. The input amounts of the elements used in the calculations were chosen so that a volume approximately equivalent to the volume of the Perkin-Elmer HGA 2100 graphite tube was obtained at 2600 K, assuming a total pressure of 1 atm.

RESULTS AND DISCUSSION

Effects of oxygen

It is well known that aluminium forms stable oxides. Maruta et al. [5] reported that oxygen might interfere with the determination of aluminium in a graphite atomizer. The partial pressure of oxygen inside the graphite tube during atomization is governed by several factors such as the kinetics of the reactions involved in the system, the total amount of elements initially present, and time. Therefore, it is difficult to estimate the true partial pressure of oxygen during atomization of an oxygen-containing matrix. To estimate the extent of interferences caused by oxygen, the

TABLE 1

Species considered in the equilibrium calculations

Gaseous	H, H_2, O, O_2, OH, H_2O, N_2, Cl, Cl_2, Ar, S, S_2, SO, HS, H_2S, COS, C, CS, CS_2, HCl, CH_4, CO, CO_2, AlCl, AlClO, $AlCl_2$, $AlCl_3$, AlH, AlOH, $AlHO_2$, AlO, AlO_2, Al_2O, AlN, AlS, Al, Fe, FeCl, $FeCl_2$, $FeCl_3$, Si
Liquid	SiO_2, Fe, Al, Si, $FeCl_2$
Solid	C, Al_2O_3, Fe_2O_3, AlN

distribution of aluminium and aluminium oxide compounds was calculated as a function of the partial pressure of oxygen. For clarity, the simplified system used omits elements like chlorine and sulphur. Figure 1 shows the results obtained at 2600 K (which approximately corresponds to the atomization temperature for aluminium). The formation of aluminium oxides was less than 1% of the input amount of aluminium for partial pressures of oxygen less than 10^{-8} atm. For higher values significant amounts of aluminium oxides were obtained. Al_2O_3(cond) was always found to be present at equilibrium for partial pressures of oxygen larger than 10^{-5} atm. It should be observed that the distribution of the aluminium compounds between the condensed and gaseous phases depends on the volume of the system as well as the input amount of aluminium. This was outlined in Part I of this series [15].

Effects of hydrogen

Hydrogen has been reported to influence the sensitivity of aluminium determination [8]. Figure 2 shows the effect of hydrogen on the formation of aluminium oxides. The input amount of oxygen corresponds to a partial pressure of oxygen of 10^{-5} atm with regard to Fig. 1. As can be seen, the formation of AlO(g) and AlO_2(g) decreases with increasing input amounts of hydrogen. Despite this, the formation of Al(g) also decreases up to about 0.1 μmol (pH_2 = 0.01 atm) of hydrogen added, because of the formation of AlOH(g) and $AlHO_2$(g). The latter compounds are present in maximum amounts in a range coinciding with the maximum amount of OH(g) present. For the conditions assumed for the calculations shown in Fig. 2, the percent fraction of aluminium (Al(g) + Al(l)) varies between 46 and 83% depending on the input amounts of hydrogen chosen. It must be concluded that hydrogen cannot completely suppress the formation of potential interfering amounts of aluminium oxides.

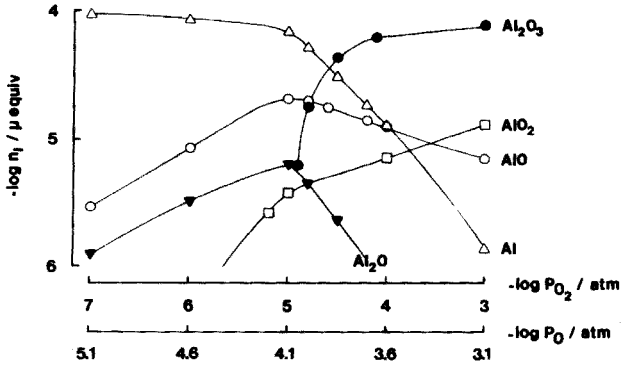

Fig. 1. The distribution of aluminium compounds at equilibrium and at a total pressure of 1 atm as a function of the partial pressure of O_2 at 2600 K. The input amounts (μmol) used in the calculations were: $H_2 = 1 \cdot 10^{-10}$, $Cl_2 = 0$, $S_2 = 0$, $N_2 = 2 \cdot 10^{-2}$, Ar = 4, C = 1, Fe = 2, Si = $2 \cdot 10^{-5}$, Al = $1 \cdot 10^{-4}$.

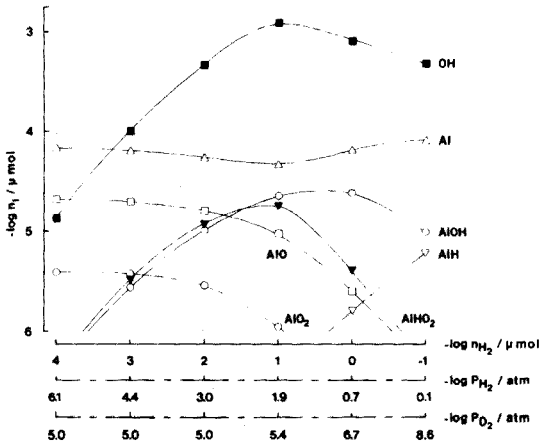

Fig. 2. The distribution of aluminium compounds and OH at equilibrium and at a total pressure of 1 atm as a function of the input amount of H_2 at 2600 K. The input amounts (μmol) used in the calculations were: $O_2 = 0.52$, $Cl_2 = 0$, $S_2 = 0$, $N_2 = 2 \cdot 10^{-2}$, Ar = 4, C = 1, Fe = 2, Si = $2 \cdot 10^{-5}$, Al = $1 \cdot 10^{-4}$.

Effects of chlorine

Figure 3a shows the influence of chlorine on the formation of aluminium chloride compounds at 2600 K for a low partial pressure of hydrogen (10^{-18} atm). To show the single effect of chlorine the input amount of oxygen was chosen to be deficient in carbon, which resulted in an equilibrium partial pressure of oxygen of the order of 10^{-20} atm. As can be seen, even extremely small input amounts of chlorine allow the formation of significant amounts of aluminium chlorides. Figure 3b shows that the formation of aluminium chloride compounds is only slightly decreased in the presence of as much as 0.18 atm of hydrogen.

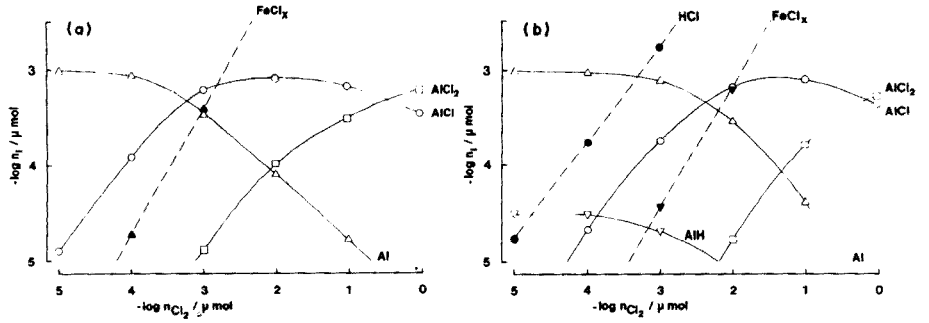

Fig. 3 (a, b). The distribution of aluminium compounds, HCl and $FeCl_x$ ($FeCl + FeCl_2$) at equilibrium and at a total pressure of 1 atm as a function of the input amounts of Cl_2 and H_2 at 2600 K. The input amounts (μmol) used in the calculations were: $O_2 = 2 \cdot 10^{-3}$, $S_2 = 0$, $N_2 = 2 \cdot 10^{-2}$, Ar = 4, C = 100, Fe = 2, Si = $2 \cdot 10^{-5}$, Al = $1 \cdot 10^{-3}$, H_2 = (a) $1 \cdot 10^{-10}$, (b) 1.

Effects of sulphur

Figure 4 shows the distribution of aluminium compounds at 2600 K as a function of the input amount of sulphur. For the results given in Fig. 4(a), carbon was always in excess of oxygen and sulphur. Clearly, large amounts of sulphur must be present for the formation of significant amounts of AlS(g). This happens because CS(g) and CS_2(g) are thermodynamically very stable, which results in a low partial pressure of sulphur, the latter being the factor governing the formation of AlS(g). The presence of as much as 0.2 atm of hydrogen did not significantly change the shape of the curves shown in Fig. 4(a). In order to simulate incomplete or slow reactions in the carbon—sulphur system, the input amount of carbon was chosen to be in deficit of sulphur. In these calculations, the input amount of carbon was always chosen in excess of oxygen, because the effect of incomplete reaction between carbon and oxygen has already been shown in Fig. 1. The results (Fig. 4b) show that very small amounts of sulphur are needed for the formation of significant amounts of AlS(g). As is evident from Fig. 4b, the formation of AlS(g) does not decrease significantly when the input amount of hydrogen is increased from 10^{-10} to 4 μmol; the latter amount correspond to an equilibrium partial pressure of 0.9 atm of hydrogen.

Effects of nitrogen

Interferences caused by nitrogen have been reported for graphite furnace systems [2] but not for atomization devices consisting of tantalum or tungsten [2]. The theoretical conditions for the formation of aluminium nitride (AlN(s)) were therefore studied. Carbon was assumed to be in excess of oxygen. The calculations were performed for 2300 K because the formation of AlN(s) is known to occur in the presence of carbon at this

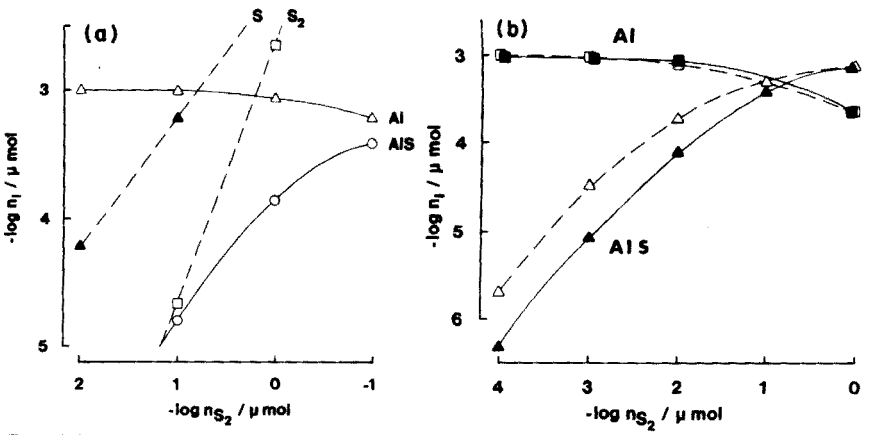

Fig. 4 (a, b). The distribution of aluminium compounds, S and S_2 at equilibrium and at a total pressure of 1 atm as a function of the input amounts of S_2, H_2 and C at 2600 K. The input amounts (μmol) used in the calculations were: $O_2 = 2 \cdot 10^{-3}$, $Cl_2 = 0$, $N_2 = 2 \cdot 1$ Ar = 4, Fe = 2, Si = $2 \cdot 10^{-5}$, Al ≙ $1 \cdot 10^{-3}$, C = (a) 100, (b) $4.1 \cdot 10^{-3}$, H_2 = (a) $1 \cdot 10^{-10}$, (b) unfilled symbols $1 \cdot 10^{-10}$, (b) filled symbols 4.

temperature. Figure 5 shows the amount of AlN(s) formed as a function of the partial pressure of nitrogen for two different input amounts of iron. The assumption for the formation of AlN(s) at 2300 K is that $p_{Al(g)} \cdot p_{N_2(g)}^{1/2} > 3 \cdot 10^{-3}$ atm$^{3/2}$. Since $p_{Al(g)} = 7 \cdot 10^{-2}\, a_{Al(l)}$ at this temperature, the formation of AlN(s) will depend critically on the activity of aluminium in the liquid phase, which will depend on the amounts of other elements present in this phase at equilibrium. A lower activity of iron in the liquid phase will result in a higher activity of Al(l). Consequently, the increase in the formation of AlN(s) at lower input amounts of iron (see Fig. 5) is due to an increased activity of Al(l).

If a tantalum or tungsten atomizer is used instead of graphite, the partial pressure of oxygen is likely to be at least of the order of 10^{-10} atm, so that the main aluminium compound at 2300 K is Al_2O_3(s). Complete dissociation of this oxide occurs at a temperature too high for the formation of AlN(s). This may explain why there are no interferences from the formation of AlN(s) in a tantalum atomizer. A further discussion of this interference from nitrogen will be given in Part V [14].

Combined effects

The preceding discussion proves that the formation of Al(g) is theoretically affected by many elements. The extent of incomplete reactions in the graphite furnace as well as the real amounts of trace elements present (corresponding to the input amounts) are very difficult to estimate. Figure 6 shows the influence of temperature on the distribution of aluminium compounds for certain input amounts of the elements, which correspond to an ashed (1200°C) sample of a low alloy steel dissolved in aqua regia with ammonium sulphate added. The input amount of carbon was chosen so that a partial pressure of oxygen of $10^{-6.4}$ atm was obtained at 2600 K, i.e. the reaction between carbon and oxygen was assumed to be incomplete, which is reasonable with regard to experimental results [5, 16, 17]. The input amounts of H_2, O_2, N_2, Cl_2, S_2 and Al used are in the nanomole range which

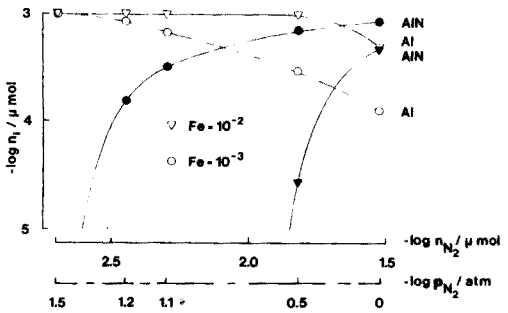

Fig. 5. The distribution of aluminium compounds at equilibrium and at a total pressure of 1 atm as a function of the input amounts of N_2 at 2300 K. The input amounts (μmol) used in the calculations were: $H_2 = 1 \cdot 10^{-10}$, $O_2 = 1 \cdot 10^{-8}$, $S_2 = 0$, $Cl_2 = 0$, Ar = $6 \cdot 10^{-2}$, $C = 1 \cdot 10^{-5}$, Si = 0, Al = $1 \cdot 10^{-3}$, Fe = (▽▼) $1 \cdot 10^{-2}$, (○●) $1 \cdot 10^{-3}$.

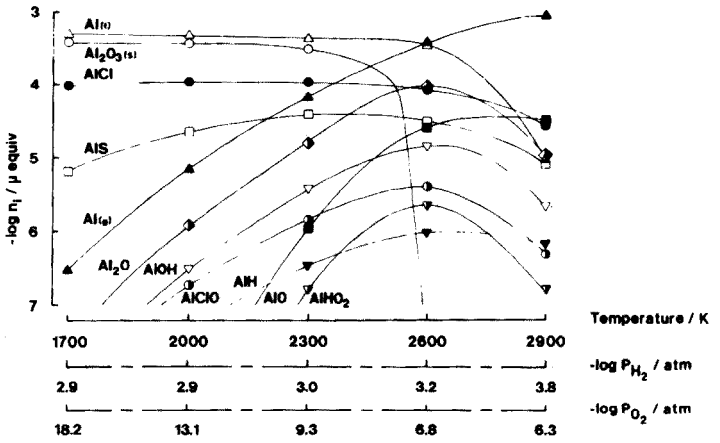

Fig. 6. The distribution of aluminium compounds at equilibrium and at a total pressure of 1 atm as a function of temperature. The input amounts (μmol) used in the calculations were: $H_2 = 5 \cdot 10^{-3}$, $O_2 = 3 \cdot 10^{-4}$, $N_2 = 5 \cdot 10^{-3}$, $Cl_2 = 1 \cdot 10^{-4}$, Ar = 4, $S_2 = 1 \cdot 10^{-3}$, $C = 4 \cdot 10^{-6}$, Fe = 2, $Si = 2 \cdot 10^{-5}$, $Al = 1 \cdot 10^{-3}$.

corresponds to realistic amounts of such elements present during atomization. To illustrate what happens during heating of the graphite tube from the ashing temperature to the preset atomization temperature, Al(g), Al(l) as well as Al_2O_3(s) are represented in Fig. 6. Since iron is always present in the liquid phase at equilibrium, the activity of Al(l) will be less than unity and will therefore depend on the input amount of aluminium. Consequently, the amount of Al(g) will increase for increasing input amounts of aluminium, because the ratio of the activities for Al(l) and Al(g) is constant. For the calculations represented in Fig. 6, corrections were not made for losses of volatile compounds at the lower temperatures. According to the Figure, aluminium compounds might be already lost at 1700 K. Therefore it should be advantageous to reach the final temperature as rapidly as possible.

The partial pressures of oxygen as well as hydrogen are also given in Fig. 6 as a function of the temperature. At about 2300 K, Al_2O_3(s) decomposes and this is the main reason for the relatively large increase in the partial pressure of oxygen in the interval 2300—2600 K.

As shown in this paper, the formation of Al(g) is likely to be decreased by a large number of elements even when they are present in extremely small amounts. This implies that it is difficult to discuss some of the experimental results mentioned in the introduction of this paper because the details for the experiments are not reported completely enough. During this work, a continuous feed-back from experiments was found to be necessary in order to check the relevance of the calculations. The inputs used in the calculations could thus be altered realistically. The experimental results and a discussion based on these high-temperature calculations will be presented in Part V of this series.

The authors thank Dr. Gunnar Eriksson for valuable discussions and Dr. Franklin Smyth for linguistic revision of the manuscript.

REFERENCES

1 J. Aggett and A. J. Sprott, Anal. Chim. Acta, 72 (1974) 49.
2 R. E. Sturgeon, C. L. Chakrabarti and C. H. Langford, Anal. Chem., 48 (1976) 1792.
3 R. Henning, J. Chim. Phys., 58 (1961) 12.
4 J. Atsuya and N. Sugiura, Japan Analyst, 23 (1974) 1170.
5 T. Maruta, K. Minegishi and G. Sudoh, Anal. Chim. Acta, 81 (1976) 313.
6 K. G. Brodie and J. P. Matoušek, Anal. Chem., 43 (1971) 1557.
7 D. C. Manning and F. Fernandez, At. Absorpt. Newsl., 9 (1970) 65.
8 C. Parker and D. Shrader, Paper presented at the Fifth International Conference on Atomic Spectroscopy, Australia, 1975.
9 K. Ohta and M. Suzuki, Talanta, 22 (1975) 465.
10 F. Shaw and J. M. Ottaway, Analyst, 100 (1975) 217.
11 J.-A. Persson, W. Frech and Å. Cedergren, Anal. Chim. Acta, 89 (1977) 119.
12 F. Dolinšek, J. Štupar and M. Špenko, Analyst, 100 (1975) 884.
13 K. C. Thompson, R. G. Godden and D. R. Thomerson, Anal. Chim. Acta, 74 (1975) 289.
14 J.-A. Persson, W. Frech and A. Cedergren, Anal. Chim. Acta, 92 (1977) 95.
15 W. Frech and A. Cedergren, Anal. Chim., Acta 82 (1976) 83.
16 W. Frech and A. Cedergren, Anal. Chim. Acta, 82 (1976) 93.
17 W. Frech and A. Cedergren, Anal. Chim. Acta, 88 (1977) 57.

Analytica Chimica Acta, 92 (1977) 95—104

INVESTIGATIONS OF REACTIONS INVOLVED IN FLAMELESS ATOMIC ABSORPTION PROCEDURES

Part V. An Experimental Study of Factors Influencing the Determination of Aluminium

JAN-ÅKE PERSSON, WOLFGANG FRECH and ANDERS CEDERGREN*

Department of Analytical Chemistry, University of Umeå, S-901 87 Umeå (Sweden)

(Received 17th February 1977)

SUMMARY

An experimental study of various factors influencing the flameless a.a.s. determination of aluminium in graphite furnaces is reported. Even in very low amounts, oxygen, hydrogen, chlorine, sulphur and nitrogen cause interferences during atomization. In addition, hydrogen and chlorine interfere during the ashing step. The interferences are discussed on the basis of high-temperature equilibrium calculations. The interferences can be minimized by using an ashing temperature as high as possible. Hydrogen, in particular, significantly lowers the ideal ashing temperature; its interference increases with the age of the graphite tube and in the presence of iron. The exclusion of atmospheric gases such as oxygen and nitrogen from the tube is an essential requirement for obtaining reliable results.

A theoretical treatment of the aluminium system based on equilibrium calculations was given in Part IV of this series [1]. The criteria for the formation of several aluminium compounds decreasing the sensitivity for aluminium were reported. It was shown that elements like H, O, N, Cl and S might under certain conditions give rise to severe interferences even when present in the nanomole range.

The aim of the work described here was to check the relevance of these predictions experimentally. This is of fundamental importance since the validity of the calculations is based primarily on the assumption that an equilibrium state is obtained. For aluminium, the probability of achieving a state close to the true equilibrium is high, because of the high atomization temperature of about 2600 K, at which most reactions are known to be rapid. Nevertheless, the kinetics of several reactions were considered in the equilibrium calculations, because results reported in the literature indicated slow reactions involving carbon. Slow kinetics were simulated by the use of varying input amounts of carbon in the calculations. Another source of error in the equilibrium calculations is the use of unreliable thermodynamic data, the extent of which is difficult to estimate. There is, of course, no

guarantee that all the species actually present at equilibrium were taken into account in the calculations.

Single as well as combined effects of various parameters influencing the determination of aluminium are discussed below. The investigations are presented with special reference to the problems associated with the determination of aluminium in steel dissolved in aqua regia.

EXPERIMENTAL

Instrumentation

A Perkin-Elmer HGA 2100 graphite furnace connected to a research spectrophotometer [2] was used. The instrument was provided with facilities for background correction and peak integration. Peak absorbances were registered on a Houston Instrument recorder. Since peak absorbance values did not differ significantly from the integrated values, only peak absorbances are given here. The furnace temperature was controlled. [3]. Temperature settings referring to the surface of the graphite tube were calibrated with a NiCr—Ni (below 1000°C) or with a PtRh—El 18 (below 1700°C) thermocouple. A pyrometer was used for higher temperatures. The instrumental parameters are given in Table 1.

Reagents and materials

The following reagents were used: 30% hydrochloric acid and concentrated nitric acid (Merck Suprapur); ammonium sulphate (Baker p.a.); carbon tetrachloride and carbon disulphide (Merck p.a.). The JK 1C ultrapure steel standard served as the sample. Gases were of SR-grade purity. All vessels were washed in 4 M nitric acid. Solutions were stored in polyethylene bottles.

TABLE 1

Instrumental parameters

	Time (s)	Temp (°C)
Drying	40	90
Ashing	40	1250
Delay	4	—
Atomization	8	2300
Cleanout	6	max

Wavelength (nm)	309.3
Slit width (μm)	150
Metal lamp current (mA)	5
Hydrogen lamp current (mA)	20
Sample volume (μ l)	20
Gas flow argon (l min^{-1})	
internal	0.25[a]
external	1
Integration time (s)	7

[a]For the experiments in which gas mixtures were used, the flow rate was 0.06 l min^{-1}. Gas stop during atomization except for the experiments with gas mixtures.

Preparation of gas mixtures

Oxygen, nitrogen, hydrogen or carbon monoxide were added to the internal flow of argon leading to the graphite tube. Flow rates were measured with a "dose-vent" (Leybold-Heraeus, Cat. No. 17317). The gas flows were calibrated with a soap-bubble meter or a rotameter. Mixtures of argon—carbon tetrachloride or argon—carbon disulphide were prepared by passing a controlled flow of argon through the respective liquids; the gas mixtures were added to the internal flow of argon and calibrated by gravimetric determinations of the carbon tetrachloride or carbon disulphide losses. This simple procedure should provide an accuracy of concentration of the prepared gas mixtures within 10%.

Determination of losses of aluminium during ashing

Ultrapure steel (0.5 g) was dissolved in aqua regia as described by Persson et al. [4]. Aluminium was added so that the concentration of the solution was 5 μg Al ml^{-1}. One of two aliquots of this sample solution was prepared to contain 0.5 M ammonium sulphate. An aliquot (0.1 ml) of each solution was dried at 90°C for 100 s and ashed at 1250°C for 40 s in the graphite furnace. The graphite tube was then transferred to a small reagent bottle and the aluminium left in the tube was redissolved in 2 ml of a solution containing 0.5 M ammonium sulphate and 0.1 M nitric acid. This solution was analyzed according to the parameters given in Table 1. The values given in Table 5 are referred to a reference solution which was prepared by adding 0.1 ml of the sample solution to 1.9 ml of 0.5 M ammonium sulphate and 0.1 M nitric acid. Blank values for the whole procedure were corrected for. One experimental series was discarded because the values obtained for aluminium indicated serious contamination.

Influence of hydrogen during ashing

Aluminium (10 μg) in aqueous solution was dried and charred for 50 s. The charring temperature started from 80°C and the average increase was 44°C per second up to 1750°C. The temperature of the graphite tube was monitored by a photosensitive diode, the signal of which was registered on a dual chart recorder. Simultaneously the absorbance during ashing was measured. The sample was charred in the presence of argon, or argon with 10 vol.% hydrogen added, at an inner flow rate of 50 ml min^{-1}. After ashing and flushing with argon, the samples were atomized. Other parameters were as given in Table 1.

RESULTS AND DISCUSSION

The precision of the experiments described lay in the range 2—5%, depending on the condition of the graphite tube and the matrix.

Effects of oxygen

Figure 1 shows the decrease in sensitivity for the determination of 4 ng of aluminium in water as a function of the concentration of oxygen in the internal flow of argon. An addition of 0.5% of oxygen decreased the sensitivity by about 10%. According to the equilibrium calculations [1], this decrease corresponds to a partial pressure of oxygen (p_{O_2}) in the range 10^{-6} 10^{-5} atm. This implies that about 0.1% of the amount of oxygen added is left unreacted in the graphite tube, assuming equilibrium between aluminium and oxygen. The shape of the curve shown in Fig. 1 depended on the condition of the graphite. The interference caused by oxygen was less for aged tubes, indicating different reaction rates between graphite and oxygen because of differences in the surface structures.

These results prove that a fundamental requirement for the determination of aluminium by flameless a.a.s. is an atomization device from which oxygen can be excluded. For the determination of aluminium in oxygen-containing matrices, oxygen will interfere if even minute amounts are left unreacted during atomization. To minimize the interference, the charring temperature should be made as high as possible, because the reaction rate between carbon and oxygen increases considerably at higher temperatures [5].

Effects of hydrogen

Figure 2 shows the effect of hydrogen on the sensitivity for aluminium. For the highest concentration of hydrogen shown, the decrease in the signal should be about 10%, because of different diffusion rates in the argon—hydrogen gas mixture compared to argon. No aluminium was lost at the selected ashing temperature of 1250°C (see below) so that the interferences seen in the Figure refer to reactions at higher temperatures. According to the equilibrium calculations [1], the formation of AlOH(g) should be responsible

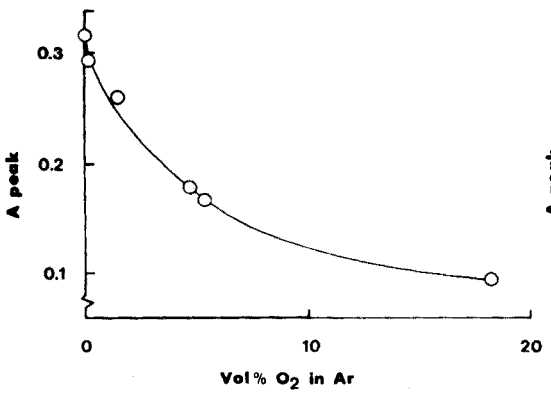

Fig. 1. Effect of oxygen on the peak absorbance for 4 ng of aluminium.

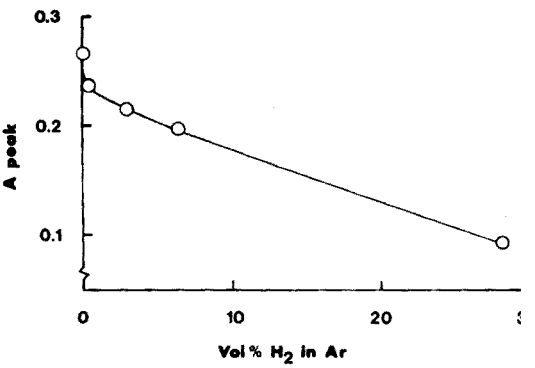

Fig. 2. Effect of hydrogen on the peak absorbance for 4 ng of aluminium.

for the decreased sensitivity. For example, if the partial pressure of oxygen during the initial part of the atomization (2000 K) is assumed to be 10^{-12} atm, the mole fraction of AlOH(g) is within the range 1—10%, depending on the equilibrium partial pressure of hydrogen.

Figure 3 shows the influence of hydrogen on the atomic absorption signal for aluminium in the temperature interval 1000—1750°C. Significantly lower signals were obtained in the presence of hydrogen, and the total loss of aluminium was much larger. This indicates that aluminium is lost as a molecule between 1250 and 1750°C, probably as AlOH(g).

The effect of hydrogen was further evaluated by studying the value of the peak absorbance as a function of the charring temperature. In these experiments the sample was first charred in the presence of the gas mixture; during a second ashing step, only argon was supplied. Gas stop was used during the atomization step. Figure 4 shows that hydrogen caused a marked decrease in sensitivity for ashing temperatures above 1400°C. If hydrogen was not added there were no losses for temperatures below 1600°C. The addition of carbon monoxide also resulted in losses of aluminium at relatively low temperatures. The lowest temperature at which aluminium was lost coincides with that obtained in the presence of hydrogen. Because water is still retained by graphite at these temperatures [6], the addition of CO(g) will increase the partial pressure of hydrogen according to the water gas equilibrium reaction. The latter reaction is known to be catalyzed by heavy metals like iron, so that the partial pressure of hydrogen will be increased in the presence of such metals. Therefore the temperature at which aluminium is lost will depend on the presence of catalyzing elements.

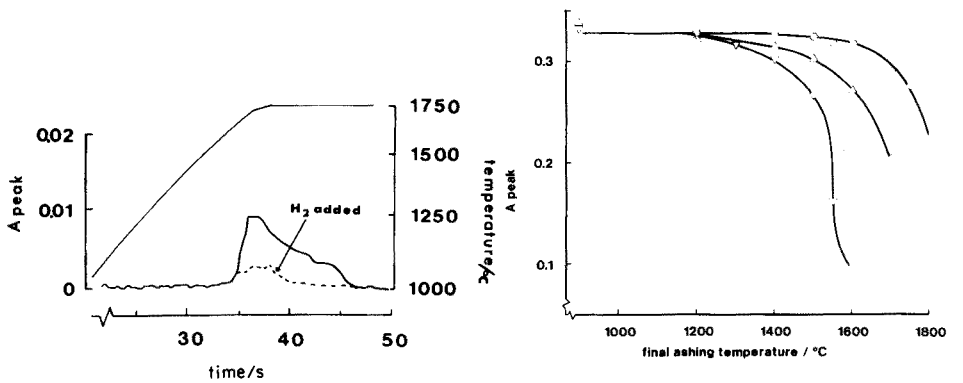

Fig. 3. Absorbance obtained for 10 ng of aluminium as a function of temperature. The upper curve shows the output signal from the photosensitive diode referred to the right hand scale. Middle curve: absorbance without hydrogen added. Lower curve: absorbance with hydrogen added. The peak absorbances obtained during atomization at 2300°C were 0.242 without hydrogen, and 0.075 with hydrogen added during ashing.

Fig. 4. Peak absorbance for 4 ng of aluminium as a function of the final ashing temperature for gas mixtures of (○) argon, (▽) 3% hydrogen in argon, (△) 3% carbon monoxide in argon. Gas stop was used during atomization.

Effects of chlorine

As mentioned previously [1], severe interferences from chlorine have been reported. The effect of chlorine was first investigated by determining aluminium in aqueous solution containing various amounts of hydrochloric acid. Figure 5 shows the decrease of the peak absorbance value as a function of the concentration of hydrochloric acid; the interferences caused can be minimized by selecting an ashing temperature of 1470°C (see inset, Fig. 5). However, the sensitivity for hydrochloric acid solutions was always less than that obtained in aqueous solutions. The interferences from hydrochloric acid can be minimized by prolonging the ashing time (Table 2), but no significant increase in sensitivity was obtained for ashing times longer than 160 s. It can be concluded that the amount of chlorine left in the graphite tube depends on the ashing temperature as well as the time of ashing.

The effect of chlorine was further investigated by adding carbon tetrachloride to the internal gas flow of argon. A significant decrease in sensitivity

TABLE 2

Comparison of sensitivity for aluminium in 0.5 M HCl or 0.01 M HNO_3 for two ashing times and at a charring temperature of 1470°C.

	Ashing time (s)	
Matrix	60	160
0.5 M HCl	74.6%	93.3%
0.01 M HNO_3	94.3%	100.0%

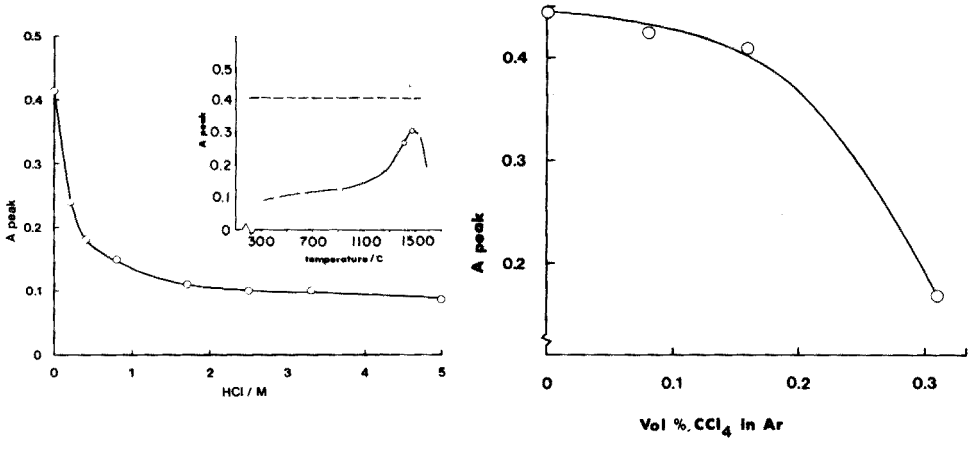

Fig. 5. Peak absorbance for 4 ng of aluminium as a function of the concentration of hydrochloric acid in the sample. The inset shows the peak absorbance as a function of the ashing temperature (---- 0.01 M HNO_3; —o— 0.5 M HCl).

Fig. 6. Effect of carbon tetrachloride on the peak absorbance for 4 ng of aluminium.

was obtained for 0.1% of carbon tetrachloride added (Fig. 6). At 2600 K (the temperature at which the equilibrium calculations were performed [1]) this concentration of carbon tetrachloride will give rise to a partial pressure of chlorine ($p_{Cl(g)}$) of about $4 \cdot 10^{-3}$ atm. Theoretically, at this equilibrium pressure of chlorine, 85—90% of the aluminium will be in the form of AlCl(g), depending on the partial pressure of hydrogen. Thus the correlation between the calculations and the results of this experiment is poor. However, for higher concentrations of carbon tetrachloride there is much better agreement between the theoretical and experimental results. Since the reaction rate varies with the concentration of the reactants, the discrepancy between the theoretical and experimental results at the lower partial pressures of chlorine probably depends on the kinetics of formation of AlCl(g). However, even in the nanomole range, chlorine clearly causes severe interferences. The effects of iron and hydrogen on this disturbance are discussed later.

Effects of sulphur

Figure 7 shows the sensitivity for aluminium as a function of the concentration of carbon disulphide in argon. The agreement is poor between these results and the equilibrium calculations based on the assumption that carbon is in equilibrium with sulphur. But the correlation between theory and practice is very good if carbon is assumed not to react with $CS_2(g)$, i.e., if the reaction $CS_2(g) \Leftrightarrow CS(g) + S(g)$ determines the partial pressure of sulphur. This reaction is displaced well to the right at higher temperatures, so that the resulting partial pressure of sulphur will be approximately equal to the concentration of carbon disulphide in argon. The equilibrium calculations indicated that hydrogen did not significantly suppress the formation of AlS(g), hence the effect of hydrogen was not investigated.

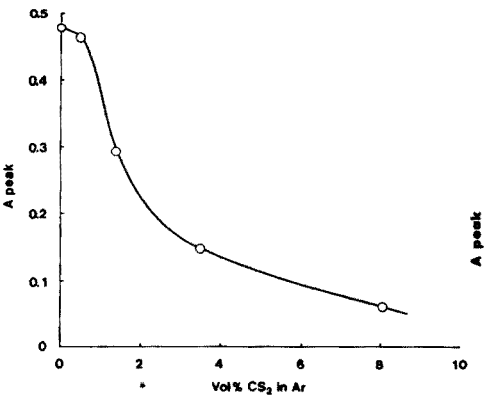

Fig. 7. Effect of carbon disulphide on the peak absorbance for 4 ng of aluminium.

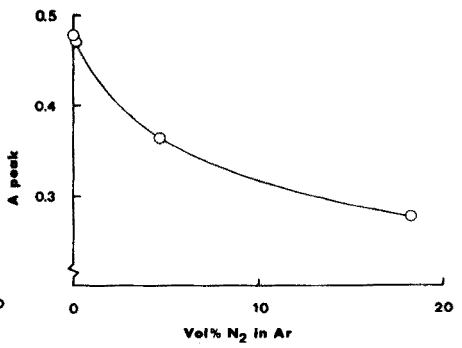

Fig. 8. Effect of nitrogen on the peak absorbance for 4 ng of aluminium.

Effects of nitrogen

Figure 8 shows the influence of nitrogen on the peak absorbance value for aluminium. The experimental results are in line with those reported by other authors [7]. The decrease in the formation of Al(g) was found theoretically to be caused by the formation of AlN(s). Separate experiments proved that this interference should be referred to the atomization sequence. As was predicted [1] the activity of aluminium in the liquid phase is the critical parameter controlling the formation of AlN(s). For the results reported in Fig. 8 it is reasonable to assume that the activity of Al(l) is close to unity. The effect of nitrogen in the presence of other elements capable of decreasing the activity of Al(l) will be discussed below.

Combined effects

Figure 9 shows the influence of nitric acid on the peak absorbance value for aluminium. The change in sensitivity is given as a function of the concentration of nitric acid as well as the charring temperature. Clearly the interferences could be minimized by thermal treatment (see inset). The increase in sensitivity with increasing ashing temperatures (up to about 1450°C) is due to the gradual removal of nitric acid from the graphite tube. This was proved in a separate experiment in which the sensitivity for aluminium in aqueous solution was determined after a nitric acid solution had been charred without being atomized; this pretreatment resulted in a significantly lower sensitivity compared to a determination including a preceding atomization step. According to the equilibrium calculations [1] it seems reasonable to assume that the interference in the presence of nitric acid is caused by nitrogen. The sensitivity was considerably enhanced in the presence of iron (Fig. 9), possibly because the formation of AlN(s) is depressed in an iron matrix. The latter hypothesis was tested by studying the effect of iron on the interference caused by nitrogen. The results are summarized in Fig. 10, which also includes a comparison between used and new graphite tubes. It can be seen that the effect of nitrogen was similar for aqueous solutions in both types of tubes. For a used tube, nitrogen did not significantly change the sensitivity in the presence of iron, but for new tubes the sensitivity in the presence of iron was larger. Nitrogen significantly decreased the sensitivity in the presence of iron. These results do not support the theoretical predictions that the activity of Al(l) decreases in the presence of iron resulting in a decreased formation of AlN(s). As discussed earlier [8], the production of hydrogen from the reaction of adsorbed water with graphite depends on the structure of the graphite; more hydrogen is generated in a used tube than in a new one. Moreover, iron increases the formation of hydrogen by a catalytic action on the reaction between carbon and water. Therefore it can be concluded that the main interference in used tubes in the presence of iron is caused by hydrogen, while in new tubes the main interference is caused by nitrogen. This conclusion was confirmed by the following experiment. The peak absorbance determined for aluminium

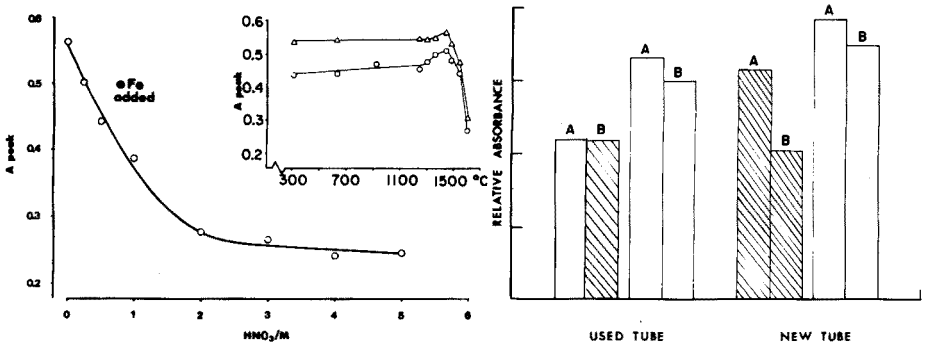

Fig. 9. Peak absorbance for 4 ng of aluminium as a function of the concentration of nitric acid in the sample. The inset shows the peak absorbance as a function of the ashing temperature (○, 0.5 M HNO_3; △, 0.01 M HNO_3).

Fig. 10. Comparison of the sensitivity obtained for 4 ng of aluminium in the absence (A) and presence (B) of 1% of nitrogen added to the inner flow of argon. The open blocks represent aqueous solution, and the lined blocks represent samples with 100 μg of iron added.

(4 ng) in aqueous solution in an argon flow was 0.300, but when 3 vol.% of hydrogen was added to the argon, the absorbance decreased to 0.208. When hydrogen and nitrogen (each 3 vol.%) were both added, the absorbance was not changed significantly (0.213). When only nitrogen (3 vol.%) was added, the peak absorbance was 0.244.

The above results show that the combined effects of nitrogen, hydrogen and iron are difficult to evaluate because of varying conditions of the graphite and catalytic effects caused by elements like iron. A more detailed study of these combined effects is necessary.

Finally, the interferences involved in the determination of aluminium in a steel sample dissolved in aqua regia were studied. Table 3 shows the relative absorbance values obtained for iron in various solutions. The single effect of ammonium sulphate on the sensitivity obtained in a solution of iron dissolved in nitric acid was rather small. In contrast, the interference caused by hydro-

TABLE 3

Relative absorbance values for 4 ng of aluminium in various sample solutions

Sample solution	Relative absorbance	Sample solution	Relative absorbance
0.01 M HNO_3	100	0.4 M HNO_3, 0.5 M HCl, 0.5 M $(NH_4)_2SO_4$, 0.09 M Fe	62
0.8 M HNO_3	64		
0.8 M HNO_3, 0.09 M Fe	87	0.4 M HNO_3, 0.5 M HCl, 0.09 M Fe	31
0.8 M HNO_3, 0.09 M Fe, 0.5 M $(NH_4)_2SO_4$	80		

chloric acid was severe but was almost removed by ammonium sulphate. Separate experiments on a steel sample dissolved in aqua regia showed that 13—24% of the aluminium (3 results) was lost during the ashing step, probably as $AlCl_3(g)$, whereas significantly lower amounts of aluminium (7—18%) were lost when 0.5 M ammonium sulphate was added. Attempts to minimize the interferences caused by chloride by the addition of hydrogen during the ashing step were unsuccessful. It was concluded that the decreased sensitivity in the presence of hydrochloric acid is in part due to losses of $AlCl_3(g)$ at low temperatures, since hydrogen has been found to be effective in removing chloride in a similar matrix [8]. However, amounts of chloride in the low nanomole range may still remain in the graphite tube before atomization, and the equilibrium calculations have shown that such amounts of chloride may allow the formation of significant amounts of AlCl(g).

CONCLUSIONS

The ashing temperature should be as high as possible to eliminate potentially interfering elements. Hydrogen, in particular, significantly lowers the ideal ashing temperature. The interference from hydrogen increases with the age of the tube and with presence of iron therein. The total exclusion of atmospheric gases such as oxygen and nitrogen from the tube greatly improves the sensitivity of the method.

The authors wish to thank Dr. W. Franklin Smyth for linguistic revision of the manuscript.

REFERENCES

1 J.-Å. Persson, W. Frech and A. Cedergren, Anal. Chim. Acta, 00 (1977) 00.
2 G. Lundgren and G. Johansson, Talanta, 21 (1974) 257.
3 G. Lundgren, L. Lundmark and G. Johansson, Anal. Chem., 46 (1974) 1028.
4 J.-Å. Persson, W. Frech and A. Cedergren, Anal. Chim. Acta, 89 (1977) 119.
5 J. N. Ong, Jr., Carbon, 2 (1964) 281.
6 R. Henning, J. Chim. Phys., 58 (1961) 12.
7 R. E. Sturgeon, C. L. Chakrabarti and C. H. Langford, Anal. Chem., 48 (1976) 1792.
8 W. Frech and A. Cedergren, Anal. Chim. Acta, 82 (1976) 93.

Analytica Chimica Acta, 92 (1977) 105—109

ATOMIC ABSORPTION SPECTROMETRIC DETERMINATION OF THIRTEEN MINOR AND TRACE METALS IN PHOSPHATE ROCK CONCENTRATES

F. J. LANGMYHR, R. SOLBERG and Y. THOMASSEN

Department of Chemistry, University of Oslo, Oslo 3 (Norway)

(Received 22nd January 1977)

SUMMARY

Atomic absorption spectrometric methods are described for the determination of thirteen minor and trace elements in phosphate rock concentrates from Florida (U.S.A.), Kola (U.S.S.R.) and Morocco. The techniques employed are atomization of solid or liquid samples in two types of graphite furnace, and conventional atomization in the flame or the cold-vapour cell.

In agriculture it is important to know, and to be able to adjust, the contents of the minor and trace constituents of soils. Commercial fertilizers contain small concentrations of a number of components, some of which, e.g. the heavy metals, are undesirable. Several minor and trace metals in commercial fertilizers originate from the phosphate rocks added during production.

The present paper describes atomic absorption spectrometric methods for the determination of thirteen minor and trace metals in phosphate rock concentrates. The analyses are based on atomization of solid or liquid samples in two types of graphite furnace, conventional atomization in the flame, and the cold-vapour technique. The feasibility of the methods is demonstrated by analyses of phosphate rock concentrates from Florida (U.S.A.), Kola (U.S.S.R.), and Morocco.

EXPERIMENTAL

Apparatus

The measurements were made with a Perkin-Elmer (P-E) 303 or 400 S atomic absorption spectrophotometer. Both instruments were equipped with arc source deuterium lamps for background correction; the 400 S instrument also had a tungsten lamp for corrections in the 300—700 nm range.

Solid samples were atomized directly in a home-made graphite furnace heated by a high-frequency generator, the construction of which has been described elsewhere [1]. The h.f. furnace was used in combination with the P-E 303 instrument. Analyses were based on measuring peak areas.

Sample solutions were atomized in the tube version of the Varian-Techtron Model 63 graphite furnace heated by a power supply constructed in this Department. Analyses were done with the P-E 400 S instrument and were based on measuring peak heights.

The P-E 400 S instrument (equipped with a standard single-slot burner) was employed for atomizing sample solutions in an air-acetylene flame. Mercury was determined with the equipment and by the procedure described by Omang and Paus [2].

Samples were decomposed in polytetrafluoroethylene (PTFE)-lined aluminium bombs heated on thermostatically controlled hot plates.

Samples were weighed on semi-micro or micro balances. All grinding was done in agate mortars. Liquids were introduced into the furnace with 1 and 2-μl ultramicro pipettes (Oxford Labs.) or 10 and 25-μl Hamilton syringes.

Reagents, solid and liquid standards

Standard solutions were prepared from high-purity metals. Nitric acid was added to dilute standard solutions to maintain pH $\leq$ 2.0.

All acids were of "Suprapur" quality from E. Merck.

To prolong the life of the home-made graphite tubes, the solid samples and some of the solid standards were mixed with graphite of the quality used for making the tubes. After being pulverized, the graphite powder was heated for 60 s at 1950°C.

The solid standards were: hydroxyapatite (lead content, 2.4 ppm [3]), the U.S. Geological Survey Reference rock GSO-1 (thallium content, 1.3 p.p.m. [4]), the Nordic reference rock ASK-Schist (silver content, 0.43 ppm [5]), and calcined animal bone (zinc content, 183 ppm [6]).

A solid synthetic standard for mercury was prepared by homogenizing known amounts of mercury(II) sulfide and iron(II) sulfide in an agate mortar, the concentration of mercury corresponding to 1.0 ppm. The content of mercury and the homogeneity of the preparation were checked by analysis.

Sample preparation

The particle size of the samples from Kola and Morocco was sufficiently small for the decomposition of about 1-g portions in the bombs, but the sample from Florida had to be ground to pass a 100-mesh sieve.

The very small samples taken for direct atomizations in the graphite furnace made a further reduction of the particle size necessary. Suitable portions of the three samples and three of the solid standards (hydroxyapatite, GSP-1 and calcined animal bone) were first ground to pass a 270-mesh sieve; 300-mg portions were then intimately mixed in an agate mortar with an equal amount of graphite powder. The solid standard ASK-Schist was ground as described above; however, its content of carbon made it unnecessary to add graphite

Decompositions

The Florida and Morocco samples (1-g portions), and the Kola sample (0.8-g portions) were transferred to the PTFE vessels of the bombs, the samples were moistened with some drops of water, and 1.0 ml of concentrated hydrochloric and 7.0 ml of concentrated nitric acid were added. After the initial reaction with the carbonates present, the bombs were closed; they were then heated to and maintained at 180° C for 30 min. After being cooled to room temperature, the bombs were opened, the covers and the interior sides were washed with water, and the contents were transferred to 50-ml volumetric flasks and made up to volume with water. The solutions were stored in plastic bottles.

The sample from Morocco was completely decomposed by the above treatment, whereas the other two materials gave a residue weighing a few tenths of a milligram. The residues from several decompositions were collected and submitted to emission spectrography. The residues were found to contain the following major or minor components: silicon, aluminium, iron, titanium, magnesium, calcium, sodium, manganese and zirconium. The trace elements detected were copper, hafnium, boron, vanadium and ytterbium, and possibly lanthanum, yttrium and cerium. It was concluded that the residues consisted mainly of unattacked silicates.

Procedure

Before the start of the measurements, the radiation sources (the deuterium, tungsten, hollow-cathode and/or electrodeless lamps) were heated for about 0.5 h. The flow of argon was adjusted to 360 ml min^{-1} and 4.0 l min^{-1} for the home-made and the Varian-Techtron furnaces, respectively. The solid sample-graphite, or standard-graphite mixture (1—40 mg) were weighed in a small tantalum scoop and placed in the middle of the home-made furnace by means of a specially constructed adjustable inserting device. The scoop was re-weighed and the furnace was moved to its pre-adjusted position.

Silver, lead, thallium, mercury and zinc were determined with the home-made graphite furnace, and with the ASK-Schist, hydroxyapatite, GSP-1, calcined animal bone and the synthetic mercury standard, respectively, as the solid standards. Bismuth, cadmium and indium were determined by the standard addition technique, liquid standards being added to weighed portions of the solid samples.

Cobalt, nickel, chromium, lead and silver were determined by atomizing sample solutions in the Varian-Techtron tube furnace, the measurements being made by the standard addition technique.

Cadmium, chromium, cobalt, copper, manganese and zinc were determined in the air—acetylene flame; the standard addition method and a modified version of the small volume sampling technique described by Manning, [7] were used.

The operating conditions for the spectrophotometers and graphite furnaces are listed in Table 1.

TABLE 1

Operating conditions for the spectrophotometers and graphite furnaces

Element	Wavelength (nm)	Temperatures (°C) and times (s) of atomization[a]	
		CRA-63	H.f.-furnace
Ag	328.1	2200-5	1900-30
Bi	223.1	—	1700-30
Cd	228.8	—	1700-30
Co	240.7	2600-5	—
Cr	357.9	2500-6	—
Cu	324.8[b]	—	—
Hg	253.7	—	1500-40
In	303.9	—	1900-30
Mn	279.5[b]	—	—
Ni	232.0	2600-5	—
Pb	283.3	2000-5	1800-30
Tl	276.8	—	1700-30
Zn	213.9[b]	—	—
Zn	307.6[c]	—	1700-30

[a]For all elements except mercury, and for both furnaces, the atomization step was preceded by 15 s drying at 80°C.
[b]The wavelength for atomization in the flame.
[c]The wavelength used during measurements with the h.f. furnace. When this line is employed, a multielement hollow-cathode lamp containing iron should not be used, because it is then difficult to distinguish the zinc line from the adjacent iron line(s).

RESULTS

The results of the analyses of the three phosphate rock concentrates are given in Table 2. Each sample was analysed 2—5 times.

It should be noted that direct atomization in graphite furnaces gives the total contents, while the two other methods used give the amounts brought into solution by the mixture of hydrochloric and nitric acid.

Commercial furnaces such as the P-E HGA-76, have been successfully applied to the analysis of phosphate rock concentrates by the present solid sampling technique.

TABLE 2

Results for thirteen minor and trace metals in three phosphate rock concentrates. (All data are mean values given in p.p.m.)

Element	Florida, U.S.A.			Kola, U.S.S.R.			Morocco		
	Solid sampling	Sample solutions in the		Solid sampling	Sample solutions in the		Solid sampling	Sample solutions in the	
		furnace	flame		furnace	flame		furnace	flame
Ag	0.84	0.83	—	0.017	<0.03	—	2.8	2.5	—
Bi	0.44	—	—	<0.05	—	—	<0.05	—	—
Cd	7.3	—	6.8	0.0097	—	<1	13	—	11
Co	—	5.0	6.0	—	<3	<5	—	<3	<5
Cr	—	—	69	—	1.7	<2	—	—	306
Cu	—	—	14	—	—	40	—	—	39
Hg	<0.5	0.14[a]	—	<0.5	0.30[a]	—	<0.5	0.094[a]	—
In	<0.03	—	—	<0.03	—	—	0.06	—	—
Mn	—	—	771	—	—	266	—	—	10.4
Ni	—	39	—	—	<2	<20	—	69	—
Pb	14	15	16	2.4	2.4	<5	3.3	3.2	<5
Tl	1.2	—	—	<0.03	—	—	0.14	—	—
Zn	92	—	94	25	—	24	229	—	222

[a]Determined by the cold-vapour technique

The authors gratefully acknowledge the gift of samples of phosphate rock concentrates from Norsk Hydro A/S.

REFERENCES

1 F. J. Langmyhr and Y. Thomassen, Z. Anal. Chem., 264 (1973) 122.
2 S. H. Omang and P. E. Paus, Anal. Chim. Acta, 56 (1971) 393.
3 F. J. Langmyhr, A. Sundi and J. Jonsen, Anal. Chim. Acta, 73 (1974) 81.
4 F. J. Flanagan, Geochim. Cosmochim. Acta, 37 (1973) 1189.
5 F. J. Langmyhr, J. R. Stuberg, Y. Thomassen, J. E. Hanssen and Jan Doležal, Anal. Chim. Acta, 71 (1974) 35.
6 International Atomic Energy Agency, P. O. Box 590, A-1011, Vienna, Austria, Information Sheet dated 1 October, 1974.
7 D. C. Manning, At. Absorpt. Newslett., 14 (1975) 99.

Analytica Chimica Acta, 92 (1977) 111—116

HIGH-PRESSURE LIQUID CHROMATOGRAPHY OF DIBENZO-18-CROWN-6 COMPLEXES WITH MERCURY(II) HALIDES

ALESSANDRO MANGIA and GIOVANNI PAROLARI*
Istituto di Chimica Generale ed Inorganica, Università di Parma
ENRICO GAETANI and CARLO F. LAURERI
Istituto di Chimica Farmaceutica e Tossicologica, Università di Parma, Parma (Italy)
(Received 25th January 1977)

SUMMARY

The chromatographic behaviour of dibenzo-18-crown-6 complexes with mercury chloride, bromide and iodide on a Micropak CH column, with methanol—10^{-2} M phosphate or borate buffer mixtures as mobile phase, is reported. Mercury and halides are extracted by dibenzo-18-crown-6 into methylene chloride. The detector response at 254 nm was linear in the range 0.1—10 μg of metal or halide.

In the last few years several examples of the application of high pressure liquid chromatography (h.p.l.c.) to inorganic and organometallic compounds [1, 2] have been reported. In most cases ion-exchange techniques were used, but chromatographic separations of metals as complexes of polydentate ligands have also been recorded. Bidentate diketone derivatives [3—5] and tetradentate β-ketoamine [1, 2, 6] and salicylaldimine [1, 6] derivatives have been used in liquid—liquid or liquid—solid chromatography. In contrast, few examples of analytical applications of h.p.l.c. to inorganic anions (e.g. chloride [7], nitrate and nitrite [8, 9], thiosulphate and polythionates [10]) have been proposed. For the application of h.p.l.c. to metal chelates, the hexadentate ligand dibenzo-18-crown-6 (2,3,11,12-dibenzo-1,4,7,10,13,16-hexaoxacyclooctadeca-2,11-diene) (DBC) has now been considered. This macrocyclic polyether [11] is still of interest in different fields of chemistry, e.g. extraction and chromatography [12—14], determination of stability constants of its complexes [15, 16], spectral and structural studies [17, 18].

The aims of the present work were to study the behaviour of complexes of this ligand in reverse-phase liquid—liquid partition chromatography and to test the use of this crown compound in h.p.l.c. of both metals and anions. For this purpose, halides of lead, cadmium, silver and mercury were chosen to obtain complexes with DBC. Of these, mercury(II) halide derivatives

*Present address: Stazione Sperimentale per l'Industria delle Conserve Alimentari, Viale Tanara 33, Parma, Italy.

showed interesting chromatographic behaviour; the dependence of the detector response on the amount of mercury and halide in aqueous solutions was obtained.

EXPERIMENTAL

Preparation of the ligand and complexes

Dibenzo-18-crown-6, prepared from catechol and bis(2-chloroethyl)-ether [11], was recrystallized from toluene. The complexes were prepared by refluxing methanol—water solutions of the crown compound and the inorganic salts in a molar ratio of 1:1; $HgI_2 \cdot$ DBC was prepared by adding solid HgI_2 to a methanolic solution of the polyether. All compounds were characterized by elemental analysis, m.p., and mass spectrum.

Instrumentation

A Perkin-Elmer Model 402 u.v.—visible spectrophotometer was used in the range 200—360 nm; methylene chloride and ethanol (spectroscopic grade) were used as solvents. A Perkin-Elmer Model 503 atomic absorption spectrophotometer was used for mercury determination in aqueous solutions at 254 nm. Mass spectra were run on a Varian MAT CH5 spectrometer with ionizing voltage of 70 eV, source temperature 220—300°C; solid samples were used and were introduced into the source by a direct insertion probe system.

High-pressure liquid chromatography

A Varian Aerograph 8500 equipped with a single wavelength u.v. detector (254 nm) was used (full-scale sensitivity, 5×10^{-3} absorbance units; flow cell volume, 8 μl). The columns were stainless steel, 25 cm × 0.2 cm i.d., packed with Micropak CH (octadecylsilane on silica gel, 10 μm diameter). The mobile phase was methanol—phosphate or borate (10^{-2}M) buffer mixtures with a pH range 7.0—10.0; the flow rate was 1 or 1.5 $cm^3\ min^{-1}$ at 225—275 atm. Spectroscopic grade solvents were used.

RESULTS AND DISCUSSION

The crown polyether provides a partition of the inorganic salts between the polar phase (methanol—water mixture) and the non-polar phase (ODS). The chromatograms of crown complexes with Cd, Pb, Ag halides show one peak, corresponding to the free ligand, at every pH value of the mobile phase; with mercury halide complexes a peak well-separated from that corresponding to the ligand is obtained.

Figure 1a shows the chromatogram of a mixture of $HgCl_2 \cdot$ DBC and DBC in methylene chloride; the mobile phase is 60/40 (v/v) methanol—phosphate buffer (pH 7.8). The resolution factor is 2.7. Increasing the pH value lengthens the retention time, particularly that of the free ligand. Below pH 7.0

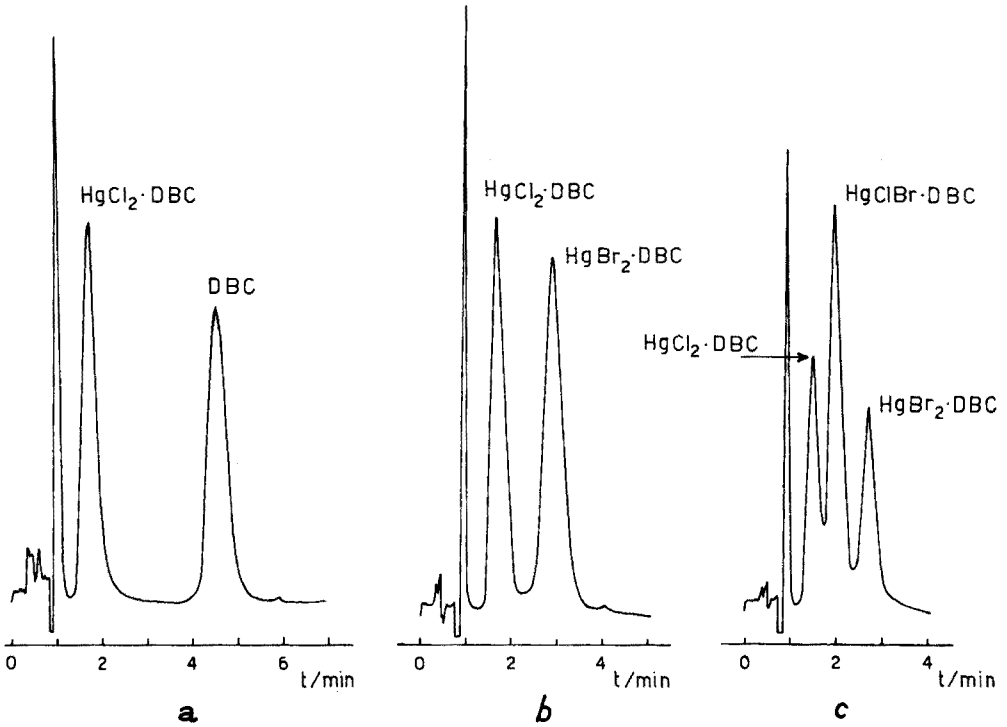

Fig. 1. (a) Separation of $HgCl_2 \cdot DBC$ and DBC in CH_2Cl_2. Column, Micropak CH, 25 cm × 0.2 cm; mobile phase, methanol—0.01 M phosphate buffer (pH 7.8) 60:40 (v/v); flow rate, 1 cm^3 min^{-1}. Theoretical plate number for DBC, 596. (b) Separation of $HgCl_2 \cdot DBC$ and $HgBr_2 \cdot DBC$ in CH_2Cl_2 on the same column. Mobile phase, methanol—0.01 M borate buffer (pH 8.8) 63:37 (v/v); flow rate, 1.5 cm^3 min^{-1}. Theoretical plate number for $HgBr_2 \cdot DBC$, 290. (c) Chromatogram of CH_2Cl_2 solution, obtained by extraction of aqueous mixture of Cl^- and Br^- with Hg^{2+} and DBC. Conditions as in (b).

decomposition occurs in the column and a new broad peak appears in addition to the peak corresponding to the complex.

Analogous behaviour is shown by $HgBr_2 \cdot DBC$, the retention time of which allows a good separation from $HgCl_2 \cdot DBC$. Figure 1b shows the separation of the two complexes in methylene chloride solution with a mixture (63/37, v/v) of methanol—borate buffer (pH 8.8) as mobile phase. The resolution factor $HgBr_2 \cdot DBC/HgCl_2 \cdot DBC$ is 1.8.

Identical chromatograms were obtained after the extraction of $HgCl_2$ and $HgBr_2$ from aqueous solution by DBC in CH_2Cl_2. In contrast, different behaviour was observed when the complexes were obtained from an aqueous solution of alkaline chloride and bromide; in this procedure mercury acetate was added to the aqueous chloride—bromide solution and the aqueous phase was shaken with a CH_2Cl_2 solution of the polyether. The chromatogram of the organic phase shows three peaks in addition to that attributable to the free ligand (Fig. 1c) which has, under these conditions, a much higher

retention time. The first and third peaks correspond to $HgCl_2 \cdot DBC$ and $HgBr_2 \cdot DBC$. The second, of double the intensity, can be attributed to the formation of the DBC complex with the mixed halide HgClBr.

The existence of HgClBr has been known for a long time [19, 20]; the formation of its complex with DBC (probably with the halogen atoms on opposite sides of the plane of the crown compound) is indicated by the mass spectrum of the solid product obtained by drying a methylene chloride solution of the complexes, extracted by the same procedure (Table 1); in addition to the peaks corresponding to $HgCl_2^+$ and $HgBr_2^+$, a strong peak with m/e = 316 ($HgClBr^+$) and a weak one corresponding to $HClBr \cdot DBC^+$ are present. These peaks are not present in the mass spectrum, run under the same conditions, of a mixture of solid $HgCl_2 \cdot DBC$ and $HgBr_2 \cdot DBC$.

The chromatogram of $HgI_2 \cdot DBC$ shows, under the same conditions, a lower retention time and the peak is overlapped by that of methylene chloride when it is used as solvent; Fig. 2a shows the chromatogram of $HgI_2 \cdot DBC$ in ethanol, with a mixture of methanol and borate buffer (pH 8.8) as the mobile phase. Since $HgCl_2 \cdot DBC$ and $HgBr_2 \cdot DBC$ are not soluble in ethanol or methanol, the separation of the three complexes requires a change of solvent. In fact, when methylene chloride is used as solvent, excessive tailing of the $HgCl_2 \cdot DBC$ and $HgBr_2 \cdot DBC$ peaks occurs if the retention times are increased sufficiently to avoid the overlapping of the $HgI_2 \cdot DBC$ peak and the signal of the solvent.

Analytical applications

In order to test the possibility of an analytical application of h.p.l.c. for the determination of mercury or halides, the dependence of the detector response on the concentration of aqueous solutions of the inorganic salts was obtained.

Mercury(II) chloride (5—100 p.p.m.) was extracted from aqueous solutions with an excess of polyether in methylene chloride (CH_2Cl_2 : water = 1 : 5, v/v). The extraction was carried out three times and the organic phases were mixed before injection into the chromatograph; five injections were

TABLE 1

Principal features of mass spectral fragmentation patterns of the extraction product of Cl^- and Br^- by Hg^{2+} and DBC
(m/e values given for ^{35}Cl, ^{79}Br, ^{202}Hg)

m/e	R.I.	Fragment
676	4	$HgClBr \cdot DBC^+$
360	100	$HgBr_2^+$ and/or DBC^+
316	40	$HgClBr^+$
281	5	$HgBr^+$
272	10	$HgCl_2^+$
237	2	$HgCl^+$

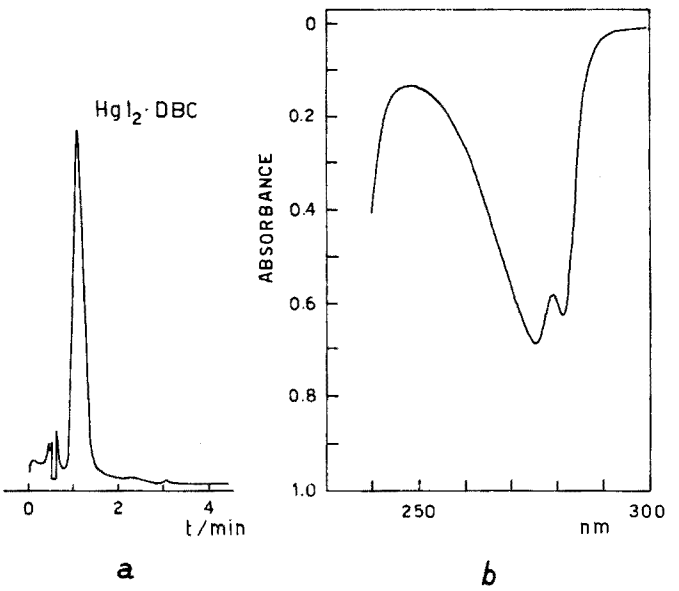

Fig. 2. (a) Chromatogram of methanolic solution of HgI_2 · DBC. Conditions as in Fig. 1 (b). (b) U.v. spectrum of 10^{-4} M solution of $HgCl_2$ · DBC in methylene chloride.

made for each sample. The calibration plot is linear over the concentration range studied; the relative standard deviation of the mean value of the peak area is ca. 4% for 5 p.p.m. mercury(II) in the aqueous phase. This concentration corresponds to about 0.1 μg of metal injected, with 5-μl injections. The detection limit, corresponding to a signal-to-noise ratio of 3:1, is about 15 ng of mercury injected, corresponding to a concentration of ca. 0.5 p.p.m. in the aqueous phase. This plot is coincident, within experimental error, with that obtained analogously for methylene chloride solutions of the complex $HgCl_2$ · DBC.

With aqueous solutions of other mercury salts (acetate, nitrate, sulfate), the amount of mercury extracted by DBC in CH_2Cl_2 is only 10—15%. However, complete extraction of the mercury can be achieved by adding to the aqueous solution of Hg^{2+} (nitrate or acetate) an excess of potassium iodide and extracting with DBC into methylene chloride or chloroform. No mercury remains in the aqueous phase as determined by a.a.s., and the calibration plot obtained by extraction is coincident with that obtained starting from methanolic solutions of HgI_2 · DBC. With this method it is necessary to evaporate the extract to dryness and redissolve HgI_2 · DBC in methanol or ethanol before injection into the column.

A more straightforward procedure is possible for obtaining the dependence of the detector response on the concentration of chloride, bromide or iodide in the aqueous phase. An excess (10—50 fold) of mercury acetate was added to slightly acidic aqueous solutions (5—100 p.p.m.) of chloride. The aqueous

phase was shaken with a solution containing an excess of DBC in CH_2Cl_2 (volume ratio, 5:1) and the organic phase was injected into the chromatograph. Extractions and injections were replicated several times for each concentration. The relationship between the u.v. detector response and the concentration of chloride in water is linear over the range examined; the corresponding plot is not significantly different from that obtained directly from the CH_2Cl_2 solutions of $HgCl_2 \cdot$ DBC, and therefore the extraction step does not appear to influence the formation of the complex. The estimated standard deviation at the lowest concentration level is 5%; the detection limit is ca. 25 ng of chloride injected, i.e. about 1 p.p.m. in the aqueous phase.

An analogous procedure, with similar results, can be followed for bromide. For iodide the low retention time of $HgI_2 \cdot$ DBC makes it necessary to change the solvent after the extraction.

The extracted methylene chloride solutions of the complexes can be concentrated easily because of the high volatility of the solvent. This allows the use of very dilute aqueous solutions of the halides for carrying out successive extractions, even if the estimated experimental detection limits are relatively high because of the low absorbance. At 275 nm the spectrum of all complexes (Fig. 2b) shows a maximum ($\epsilon \simeq 5200$ l mol^{-1} cm^{-1}); $\epsilon \simeq 1300$ l mol^{-1} cm^{-1} at 254 nm, therefore the detector response is more sensitive at 275 nm.

REFERENCES

1 P. C. Uden and F. H. Walters, Anal. Chim. Acta, 79 (1975) 175, and references therein.
2 E. Gaetani, C. F. Laureri, A. Mangia and G. Parolari, Anal. Chem., 48 (1976) 1725, and references therein.
3 J. F. K. Huber, J. C. Kraak and H. Veening, Anal. Chem., 44 (1972) 1554.
4 P. Heizmann and K. Ballschmiter, Fresenius Z. Anal. Chem., 266 (1973) 206.
5 D. R. Jones IV and S. E. Manahan, Anal. Lett., 8 (1975) 569.
6 P. C. Uden, D. M. Parees and F. H. Walters, Anal. Lett., 8 (1975) 795.
7 T. A. Maldacker and L. B. Rogers, Sep. Sci., 9 (1974) 27.
8 R. J. Davenport and D. C. Johnson, Anal. Chem., 46 (1974) 1971.
9 G. L. Wheeler and P. F. Lott, Microchem. J., 19 (1974) 390.
10 A. W. Wolkoff and R. H. Larose, Anal. Chem., 47 (1975) 1003.
11 C. J. Pedersen, J. Am. Chem. Soc., 89 (1967) 2495.
12 K. H. Pannel, D. C. Hambrick and G. S. Lewandos, J. Organomet. Chem., 99 (1975) C21.
13 A. Sadakane, T. Iwachido and K. Tôei, Bull. Chem. Soc. Jpn., 48 (1975) 60.
14 E. Blasius, K. P. Janzen and G. Klautke, Fresenius Z. Anal. Chem., 277 (1975) 374.
15 E. Shchori, N. Nae and Jagur-Grodzinski, J. Chem. Soc., Dalton Trans., (1975) 2381.
16 N. Matsuura, K. Umemoto, Y. Takeda and A. Sasaki, Bull. Chem. Soc. Jpn., 49 (1976) 1246.
17 G. F. Pedulli and A. Alberti, J. Chem. Soc. Perkin Trans. 2, (1976) 137.
18 D. Live and S. I. Chan, J. Am. Chem. Soc., 98 (1976) 3769.
19 L. Losana, Gazz. Chim. Ital., 56 (1926) 309.
20 Y. Marcus and A. S. Kertes, Ion Exchange and Solvent Extraction of Metal Complexes, Wiley-Interscience, London, 1968, p. 444.

Analytica Chimica Acta, 92 (1977) 117—122

THE DETERMINATION OF TRACES OF ORGANOHALOGEN COMPOUNDS IN AQUEOUS SOLUTION BY DIRECT INJECTION GAS CHROMATOGRAPHY—MASS SPECTROMETRY AND SINGLE ION DETECTION

TOSHIHIRO FUJII

Division of Chemistry and Physics, National Institute for Environmental Studies, Yatabe, Tsukuba, Ibaraki 300-21 (Japan)

(Received 7th February 1977)

SUMMARY

By means of gas chromatography—mass spectrometry with direct injection, a diglycerol column and single ion detection, a detection limit of 2 $\mu g\ l^{-1}$ can be obtained for chloroform and other organohalogen compounds in aqueous solutions: no concentration or extraction is required.

Gas chromatography—mass spectrometry with direct aqueous injection, developed by Harris et al. [1], offers the potentially significant advantage of instantaneous analysis, but does not meet the sensitivity requirements. Even though the single ion detection technique of g.c.—m.s. provides a sensitivity that often surpasses that of the g.c. electron capture detector, it is not adequate when a minimum detectable limit is required for specific compounds. Ion counting, which permits the measurement of very small ion currents, enables the sensitivity requirements to be met.

The improved single ion detection technique and direct aqueous injection involving a liquid diglycerol phase (to make the organic peaks appear before the large water peak) have been applied to the determination of organohalogen compounds in tap water at the p.p.b. level; in addition to being quantitative the method avoids the use of time-consuming and error-producing cleanup, preconcentration, and extraction stages.

EXPERIMENTAL

Apparatus

A Finnigan 3300F gas chromatograph—quadrupole mass spectrometer, with glass column and glass jet separator, was employed. A spiral electron multiplier (Galileo Electro-Optics, Model H751) and a single ion counting device (SSR Instruments) for ion counting [2, 3] were used. Single ion detection in the d.c. mode can be made with a conventional d.c. amplifier.

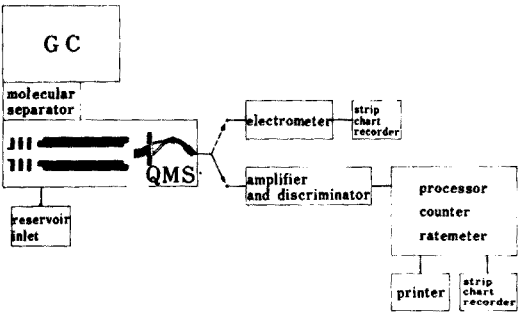

Fig. 1. Block diagram: gas chromatograph—mass spectrometer with ion counting device.

A block diagram of the instrumentation is shown in Fig. 1. The ion counting device, consisting of an amplifier/discriminator (Model 1100) and a processor (Model 1120) provides fast pulse amplification (maximum gain, 100) with the output discriminator threshold range variable from 10 to 1000 mV. A 100-mV discriminator setting was used throughout the experiments. The processor includes a timer to control integration time, a counter for a digital output, and a ratemeter for an analog output. The processor can operate in the automatic subtraction mode. Additional details on the operational characteristics of ion counting g.c.—m.s. are described elsewhere [4].

Operating conditions

A glass column (2 m) packed with 10% diglycerol on 60/80 mesh Gaschrom G.NAW. (Johns-Manville) was used. Other conditions held constant throughout the analyses were: helium carrier gas flow rate, 35 ml min^{-1}; injection port, 190°C; column temperature, 40°C.

The quadrupole mass spectrometer (q.m.s.) operating conditions were: pressure, $6 \cdot 10^{-6}$ torr; emission current, 430 μA; ion energy, 5 eV; the applied voltage of the electron multiplier was 1800 V when the counting plateau range [3] was 1600—2050 V. An electron energy of 70 eV was chosen in the d.c. mode operation; an electron energy of 23 eV, at which ionization of the relatively large volume of helium carrier-gas in the q.m.s. does not occur, was chosen in the ion counting mode. High count rates were observed [4] when the helium was ionized.

Standard solutions

Water, free of interfering organic compounds, was prepared by double distillation. Standard stock solutions were prepared by injecting 10 mg of the compound to be determined, i.e., $CHCl_3$, CCl_4, $CHCl_2Br$ (Wako chemicals, special grade), into a 100-ml volumetric flask filled with distilled water. The stock solutions were diluted further as required.

Procedure

The test sample (10 μl) was injected (10-μl Hamilton syringe) into the diglycerol column. This has an extremely long retention time for water; water is eluted after the organohalogen compounds, which are eluted in less than 5 min. After detection of the organic compounds, the column was kept at 100°C for at least 40 min to eliminate water and less volatile materials before the next analysis; during this period the column was uncoupled from the q.m.s.-side connection to avoid saturating the q.m.s. with water.

The q.m.s. was set at unit resolution (10% valley between adjacent nominal masses). To observe a single mass ion, the mass scan switch of the q.m.s. was set at the no scan position, and the instrument was tuned to a selected mass. The selected mass ions were integrated for 2 s and counted with the ion counting device; the processor, in the automatic subtraction mode, subtracted the constant counts from background counts. As the resulting integrated counts were printed, the ratemeter output (log scale) was recorded simultaneously as a single ion chromatogram. Quantitative information was obtained from the total integrated counts for each substance.

Positive identification of the dissolved compounds was obtained from the retention times of standards and from the selectivity afforded by the single ion detection. The ion chosen to monitor $CHCl_3$ was $CHCl_2^+$. Thus, from the chlorine isotope cluster, a ratio of 3:2 would be expected at masses 83 and 85. Several such checks for each compound (*m/e* 117 and 119 for CCl_4, *m/e* 83, 85, 127 and 129 for $CHCl_2Br$) were made periodically to confirm the absence of interferences.

RESULTS AND DISCUSSION

Detection limit

Figures 2 and 3 show the single ion chromatograms (*m/e* 83) in the ion counting mode and d.c. mode resulting from injections (10 μl) of prepared $CHCl_3$ standards. The practical detection limit of $CHCl_3$ in the ion counting mode (the concentration producing integrated counts five times higher than the standard deviation of the background counts in the integration time) was 2 p.p.b.: in the d.c. mode (with at least 5:1 signal-to-noise ratio) the limit was calculated to be 10 p.p.b. The same detection limit (2 p.p.b.) was obtained for CCl_4 and $CHCl_2Br$ by monitoring *m/e* 119 and *m/e* 83, respectively, in the ion counting mode. The detection limit does not directly reflect the response of single ion detection for these compounds. The implication of the result obtained in the ion counting mode is significant for applications in which the concentration of the substances to be analyzed is low. Although *m/e* 127 for $GHCl_2Br$ can also be monitored, the detection limit is 5 p.p.b., even in the ion counting mode.

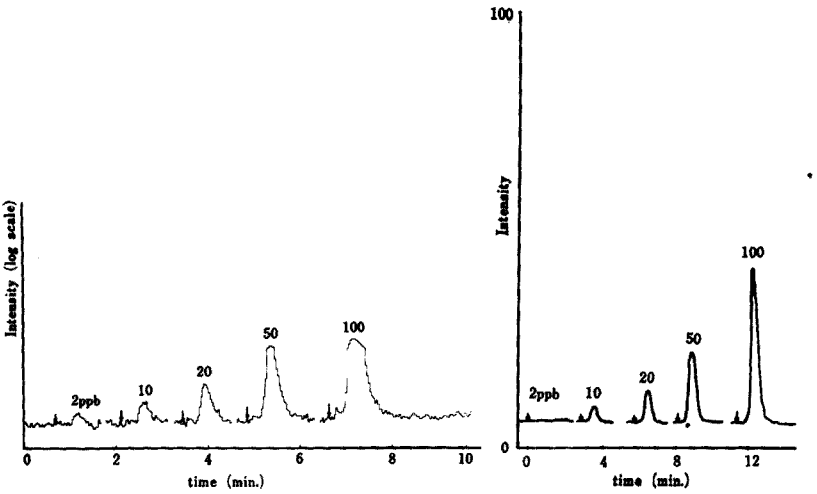

Fig. 2. Single ion chromatogram obtained (ion counting mode) for a series of concentration of $CHCl_3$ (p.p.b.) in water (10-μl injections).

Fig. 3. Single ion chromatogram (d.c. mode) for a series of concentrations (p.p.b.) of $CHCl_3$ (10-μl injections).

TABLE 1

Measurements on tap water spiked with $CHCl_3$

$CHCl_3$ added (p.p.b.)	$CHCl_3$ found (p.p.b.)	$CHCl_3$ recovered (p.p.b.)
0	24	0
10	34.5	10.5
50	74	50

Linear concentration range, accuracy and precision

Figure 4 shows working curves for measurements in the ion counting mode. The total integrated counts were linear over the chosen range (2—100 p.p.b.) of standard concentrations for each compound; a decrease in precision is observed at the detection limit level.

The accuracy of the ion counting mode was determined by measurements on samples spiked with $CHCl_3$ (Table 1).

The precision in the ion counting mode was determined from 10 replicate injections of the standard sample at the 50 p.p.b. $CHCl_3$ level. The standard deviation was ca. 2600 (counts) and the relative standard deviation 3.5% for total integrated counts; these values are close to the optimum performance generally accepted for a microliter syringe in the hands of an experienced operator. Similar results were obtained for $CHCl_2Br$ and CCl_4.

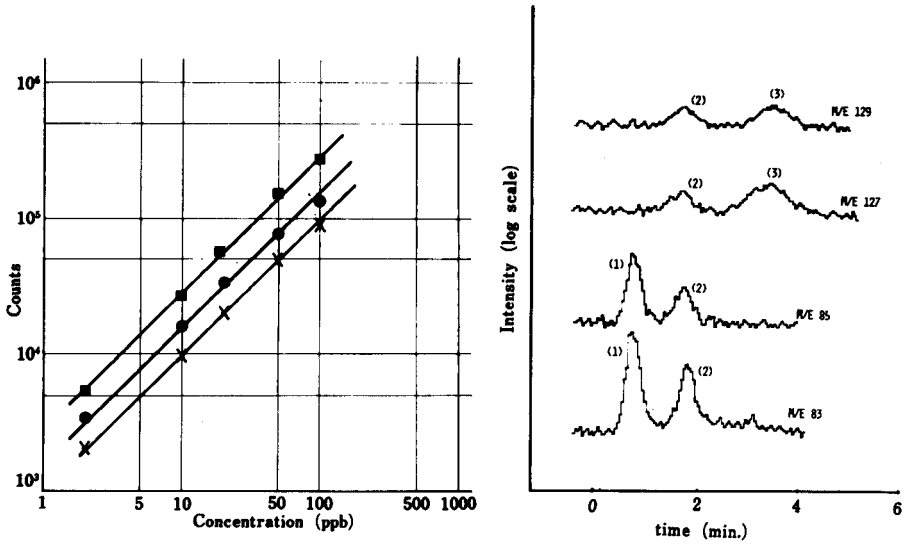

Fig. 4. Total integrated counts (response) vs. sample size, showing linearity of response for $CHCl_3$(•), $CHCl_2Br$ (▪) and CCl_4(×). (Selected ions: *m/e* 83 for $CHCl_3$ and $CHCl_2Br$, *m/e* 119 for CCl_4).

Fig. 5. Single ion chromatograms from four individual injections (10 μl) of tap water taken at Tsuchiura City. The peaks are: (1) $CHCl_3$, 61 p.p.b. (2) $CHCl_2Br$, 24 p.p.b. (3) $CHClBr_2$.

Application to tap water samples

$CHCl_3$, $CHCl_2Br$, $CHClBr_2$ and CCl_4 are commonly found [5—8] in chlorinated water supplies in the concentration range 1—100 μg l^{-1}. These compounds are of interest; some are suspected of being toxic and/or carcinogenic.

As the method described proved to be sensitive, accurate and precise, with good stability throughout the analysis period, it was applied to the determination of these compounds. Tap water (10 μl) taken at Tsuchiura City, Ibaraki Prefecture, was injected directly. The single ion chromatograms of *m/e* 83, *m/e* 85, *m/e* 127 and *m/e* 129 in the ion counting mode (four individual injections) shown in Fig. 5 prove that there is no interference from other organic compounds. Peak (3) in Fig. 5 was identified as $CHClBr_2$ by interpretation of the mass spectra (it is necessary to concentrate the sample). Quantitative analysis was not possible because a suitable reagent-grade standard was not available at the time of analysis. Even single ion detection in the d.c. mode was sufficient for this sample. The analysis for CCl_4 indicated a concentration of less than 2 p.p.b. i.e. the detection limit in the ion counting mode.

This report may stimulate further improvements in methodology, e.g. combination of the multiple ion detector with a multichannel analyzer in the scaling mode [9].

REFERENCES

1 L. E. Harris, W. L. Budde and J. M. Eichelberger, Anal. Chem., 46 (1974) 1912.
2 E. Yellin, L. I. Yin and I. Adler, Rev. Sci. Instrum., 41 (1970) 18.
3 W. E. Potter and K. Mauersberger, Rev. Sci. Instrum., 43 (1972) 1327.
4 T. Fujii, Shitsuryo Bunseki (Mass Spectrom.), in press.
5 B. Dowty, D. Carlisle and J. L. Laseter, Science, 187 (1975) 75.
6 R. D. Kleopfer and B. J. Fairless, Environ. Sci. Technol., 6 (1973) 1063.
7 T. A. Bellar, J. J. Lichtenberg and R. C. Kroner, J. Am. Water Works Ass., 66 (1974) 703.
8 K. Grob, K. Grob, Jr. and G. Grob, J. Chromatogr., 106 (1975) 299.
9 H. Miyake and M. Michijima, Shitsuryo Buseki (Mass Spectrom.), 19 (1971) 110.

Analytica Chimica Acta, 92 (1977) 123—128

NUCLEAR MAGNETIC RESONANCE ANALYSIS OF PHARMACEUTICALS*
Part XV. Determination of Sulfamethoxazole and Trimethoprim in Combination in Tablets

JOHN W. TURCZAN

Food and Drug Administration, Department of Health, Education, and Welfare, 850 Third Avenue, Brooklyn, New York 11232 (U.S.A.)

(Received 16th November 1976)

SUMMARY

The determination of sulfamethoxazole and trimethoprim as a mixture in tablets by n.m.r. spectrometry is reported. Formamide containing 8% formic acid is the solvent system with t-butanol as the internal standard. The resonances for the hydrogens on all three methyl groups of the methoxyl functions together with hydrogens of the lone methylene group are integrated as a measure of trimethoprim, whereas the hydrogens of the methyl group of the oxazole heterocycle are integrated to determine sulfamethoxazole. A mixture of two standards and representative commercial tablets were analyzed by the procedure; the results are satisfactory.

A mixture of sulfamethoxazole (N^1-(5-methyl-3-isoxazole) sulfanilamide) (I) and of trimethoprim (2,4-diamino-5-(3,4,5-trimethoxybenzyl) pyrimidine) (II) is a synthetic antibacterial combination product which acts by inhibiting the biosynthesis of folic acid in bacteria [1]. Several approaches to the determination of the sulfonamide component of this therapeutic mixture are available. The most widely discussed approach to the determination of (I) is a colorimetric procedure based on the Bratton—Marshall reaction [2] and its application [3] to automated systems to provide speed. Other techniques utilized to improve selectivity for determination of (I), in both pharmaceutical preparations and biological samples, include potentiometry [4], t.l.c. [5—8], g.l.c. [9], h.p.l.c. [10] and partition chromatography [11].

Approaches to the determination of (II) include differential pulse polarography [12—14], spectrofluorimetry [15—17], gas chromatography [18], spectrophotometry [19], t.l.c. with spectrophotometry [20], and t.l.c. with fluorescence [21]. The only specific assays for (II) are those including t.l.c. separation followed either by isolation from the t.l.c. adsorbent or by direct measurement of the absorbance on silica gel plates.

*Part XIV. J. W. Turczan and T. Medwick, J. Pharm. Sci., 65 (1976) 235.

The procedure for mixtures of (I) and (II) in tablets proposed here uses n.m.r. spectrometry, a very specific measurement technique. The scheme used is simple: it involves dissolving a tablet powder containing (I) and (II), addition of an internal standard and a drop of a reference standard (TMS), n.m.r. spectral scan of the solution, and integration. Good quantitative results are obtained together with a positive identification of the active components in terms of the n.m.r. spectrum. A more complete identification with no interference from the solvent can be accomplished by obtaining the spectrum in DMSO-d_6 solvent.

EXPERIMENTAL

Chemicals, reagents, solutions and tablets

Sulfamethoxazole and trimethoprim were working laboratory standards. The internal standard was t-butanol (>99 mol %, Matheson, Coleman and Bell), and the reference standard was tetramethylsilane (TMS).

Formic acid (Fisher Scientific, certified ACS) was distilled before use. Formamide (Fisher Scientific, reagent grade) was distilled under reduced pressure (about 3—4 mm Hg). Deuterated dimethylsulfoxide (DMSO-d_6, 99.5% isotopic purity, Mallinckrodt) and trifluoroacetic acid (reagent grade, Eastman white label) were also used.

Internal standard solution. Carefully weigh enough t-butanol to give a final concentration of 20 mg ml^{-1}, and dissolve in 8% (v/v) formic acid in formamide.

Tablets containing (I) and (II) were obtained from commercial sources.

Procedure

Weigh and finely powder not less than 20 tablets. Weigh accurately a portion of the powder equivalent to about 400 mg of sulfamethoxazole and 80 mg of trimethoprim into a glass-stoppered centrifuge tube. Add 2.0 ml of internal standard solution and stopper. Place on a steam bath for about 1 min, remove from the bath and shake well, using a laboratory shaker, for about 1 min. Shaking should not be so vigorous as to permit the solution to touch the stopper. Centrifuge to separate the solution from the insoluble solids. Using a capillary pipet, transfer about 0.4 ml of the solution to an analytical n.m.r. tube and add 1 drop of TMS. Place in an n.m.r. spectrometer (Varian EM 390 Spectrometer) and obtain the spectrum, adjusting the spin-rate so that no spinning side-bands interfere with the peaks of interest at approximately 1.3, 2.3 and 2.6—2.9 p.p.m. regions. (All field positions are referred to TMS at 0 p.p.m.) Expand the spectrum from 10 p.p.m. to 5 p.p.m. Integrate each of the peaks of interest at least 5 times.

The amounts of (I) and (II) are calculated from:

$$\frac{\text{mg (I) or (II)}}{\text{tablet}} = \frac{A_{\text{(I) or (II)}}}{A_{tb}} \times \frac{\text{EW}_{\text{(I) or (II)}}}{\text{EW}_{tb}} \times \frac{\text{mg t-butanol}}{\text{mg sample}} \times \text{A.T.W.}$$

where $A_{(I) \text{ or } (II)}$ = integral value of the signal representing sulfamethoxazole (I) or trimethoprim (II); A_{tb} = integral value of the signal representing t-butanol; $EW_{(I) \text{ or } (II)}$ = formula weight of sulfamethoxazole (I)/3 = 84.436 or formula weight of trimethoprim (II)/11 = 26.39; EW_{tb} = formula weight of t-butanol/9 = 8.236; and A.T.W. = average tablet weight.

RESULTS AND DISCUSSION

The choice of a solvent, which would easily and quantitatively dissolve a large quantity of (I) and (II) in tablets, and yet not interfere with the integration in the region of interest, was not easy. Difficulties were especially encountered with (I), which will hydrolyze partially in acidic or basic solutions. One of the many organic solvents tried was formic acid. The solubility of (I) and (II) in formic acid is very good; however, within about 20 min a white precipitate (5-methyl isoxazole ring) appears, indicating hydrolysis of (I). DMSO-d_6 was also tried but quantitative extraction of (I) and (II) from tablets was impossible. However, the latter solvent was found to be an excellent choice for the identification of these two active ingredients in admixture (Fig. 1a).

The solvent finally chosen was 8% formic acid in formamide; with this solvent, (I) and (II) dissolved completely, interferences in the 0—5 p.p.m. region were eliminated and hydrolysis of (I) was not evident for at least 1 h, allowing reliable, uncomplicated analysis. The 8% formic acid in formamide solvent proved to be satisfactory for the determination of (I) and (II). The 8% formic acid increases the solubility of (I) and (II), and shifts all exchangeable protons downfield. This proton shift eliminates the possiblility of interference with integration, for these protons would otherwise overwhelm the near region where the nine methoxy protons together with the lone methylene protons on (II) resonate. Perhaps the only feature of this solvent that might be considered a limitation is that both the formic acid and formamide used contained small amounts of methanol and methyl formate as impurities which manifested themselves at ca. 3.8 p.p.m. and 3.4 p.p.m., respectively. The field position of the three methyl protons of methanol interferes with the integration of the multiplet in the 2.6—2.9 p.p.m. region from the eleven protons of (II). However, considering the advantages of the proposed solvent system in the assay of tablets, these impurities are not a severe limitation, since they can easily be removed by prior distillation of the solvent; alternatively, purer solvents may be purchased.

A single internal standard, t-butanol, was satisfactory for the analysis of this mixture. This alcohol is easily soluble in the chosen solvent and provides a strong signal at a convenient upfield position (1.3 p.p.m.), giving an unambiguous identification and interference-free quantitative analysis.

Figure 1b is the spectrum obtained under the recommended conditions of a mixture of (I) and (II). The quantities of each component are calculated from the integration of the multiplet in the region 3.6—4.1 p.p.m. from the nine methoxy protons together with the two protons of the lone methylene moiety of (II), the singlet at ca. 2.3 p.p.m. attributed to the three methyl protons of (I), and the singlet at ca. 1.3 p.p.m. from the nine

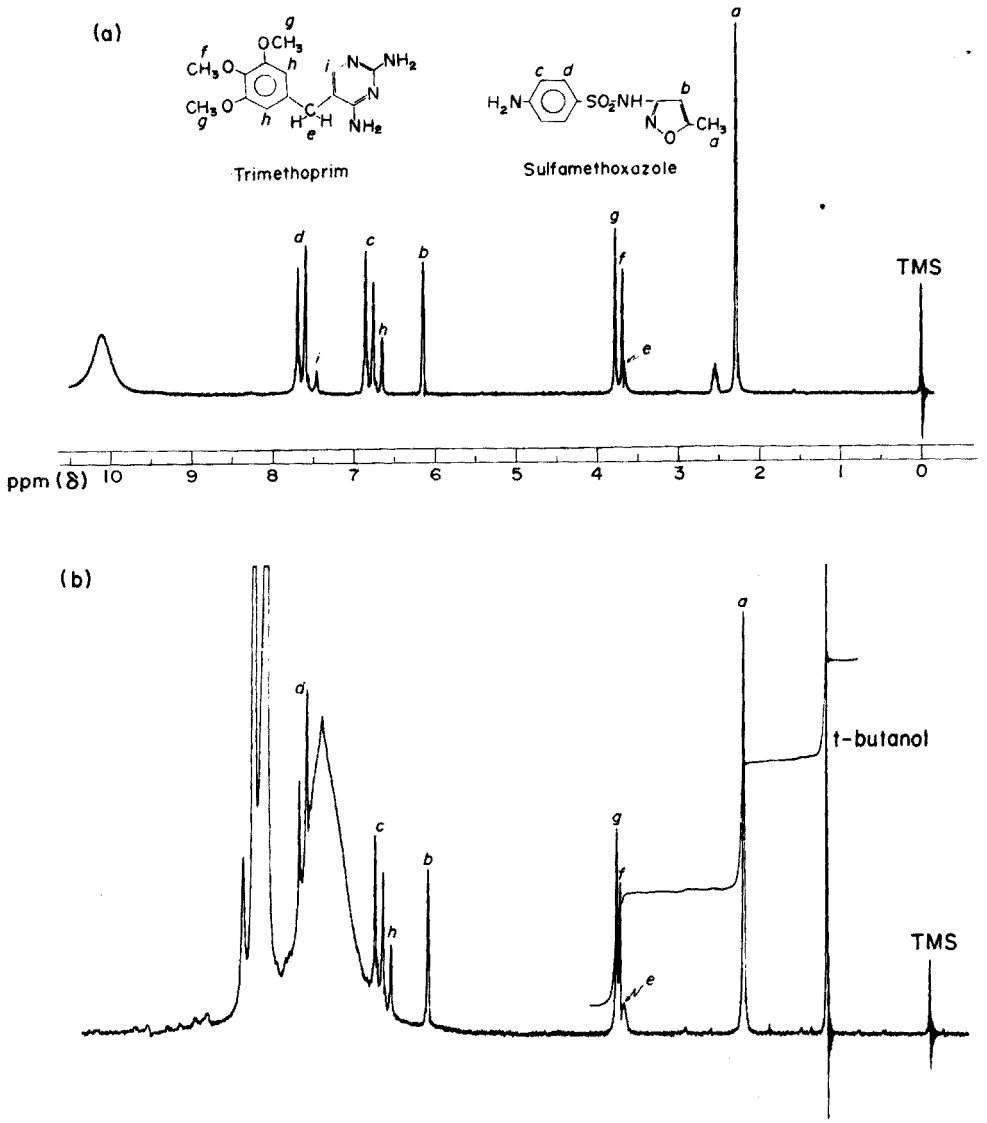

Fig. 1. N.m.r. spectra (a) and (b) of sulfamethoxazole and trimethoprim mixture in 8% formic acid in formamide solvent containing t-butanol (upper-b) and DMSO-d_6 with 2—3 drops of t-butanol (lower-a). TMS = tetramethylsilane.

methyl protons of t-butanol. The other resonance peaks of interest that are useful in identification of (I) and (II) are related to the appropriate structural component in Fig. 1.

A group of mixtures with known (I) and (II) content was analyzed; the results are summarized in Table 1. The n.m.r. results were compared with those obtained by the NF XIV method [4] and by a differential pulse polarography (d.p.p.) technique modified from the original report [13].

TABLE 1

Determination of known amounts of sulfamethoxazole and trimethoprim in mixtures by n.m.r.

No.	t-Butanol added (mg)	Sulfamethoxazole (mg)		Recovery (%)	Trimethoprim (mg)		Recovery (%)
		Added	Found		Added	Found	
1	34.7	402.5	399.7	99.3	83.1	82.2	98.9
2	36.6	410.0	414.6	101.1	86.4	86.0	99.5
3	36.2	421.6	420.0	99.6	85.4	85.9	100.6
4	35.1	412.0	418.2	101.5	85.6	85.2	99.5
5	36.0	420.1	415.9	99.0	86.3	86.5	100.2
6	35.7	404.6	400.1	98.9	85.1	84.3	99.1
7	36.1	415.7	420.3	101.1	85.6	86.5	101.1
8	48.5	405.3	401.7	99.1	87.1	88.7	101.8
9	55.0	601.5	588.5	97.8	100.5	98.6	98.1
10	25.0	406.1	411.0	101.2	84.3	83.4	98.9
Average				99.9			99.8
Range				97.8—101.5			98.1—101.8
S.d.				99.9 ± 1.3			99.8 ± 1.1
R.s.d. %				1.3			1.1
NF XIV Procedure				99.4			—
DPP				—			99.1

TABLE 2

Determination of sulfamethoxazole and trimethoprim in commercial tablets by n.m.r. and alternative procedures
(Sulfamethoxazole, 400 mg/tablet, trimethoprim, 80 mg/tablet.)

No.	Sulfamethoxazole found				Trimethoprim found			
	N.m.r.		NF XIV		N.m.r.		D.p.p.	
	mg/tab	Declared (%)	mg/tab	Declared (%)	mg/tab	Declared (%)	mg/tab	Declared (%)
1	407.6	101.9	396.0	99.0	80.7	100.9	79.6	99.5
2	402.0	100.5	400.4	100.1	79.4	99.3	79.1	98.9
3	398.4	99.6	406.0	101.5	80.5	100.6	80.6	100.8
4	396.0	99.0	398.8	99.7	80.2	100.3	79.5	99.4
5	400.8	100.2	395.6	98.9	79.2	99.0	79.0	98.8
6	394.4	98.6	392.4	98.1	81.0	101.3	79.0	98.8
7	392.4	98.1	391.6	97.9	80.6	100.8	81.0	101.3
8	391.2	97.8	394.0	98.5	79.0	98.8	79.4	99.3
9	393.2	98.3	397.6	99.4	80.3	100.4	79.1	98.9
10	391.6	97.9	393.2	98.3	81.3	101.6	79.6	99.5

The d.p.p. analysis was conducted in a pH 4 acetate buffer; the peak at −1.275 V vs. SCE from the reduction of the >C=N-moiety was used. The results obtained by the different methods show close agreement. However, the proposed n.m.r. procedure is advantageous in that it is simpler, faster, and more selective, giving confidence that only (I) and (II) are being determined and completely identified in a single operation. The n.m.r. procedure is accurate and precise with a relative standard deviation of 1.3% for (I) and 1.1% for (II). The relative proportion of (I) and (II) to t-butanol has no significant bearing on the results (Table 1).

Some 13 commercial tablet preparations were analyzed by n.m.r. Ten of these preparations were also analyzed by NF XIV method for (I) and d.p.p. for (II). The results (Table 2) are in good agreement.

The author is grateful to Dr. Thomas Medwick, Science Advisor, FDA, New York District and Professor of Pharmaceutical Chemistry, College of Pharmacy, Rutgers University, New Brunswick, New Jersey, for encouragement and many valuable discussions in the preparation of this manuscript.

Note added in proof. After acceptance of this paper, another study of the n.m.r. analysis of trimethoprim—sulfamethoxazole mixtures appeared (M. Rodriguez, M. Pizzorno and S. Albonico, J. Pharm. Sci., 66 (1977) 121). In this laboratory, DMSO was discarded because of a solvent impurity peak whicl appeared close to the sulfamethoxazole methyl peak selected for integration, and because the spectra of tablet extracts were complicated by an unidentified peak at 3.5 p.p.m. close to the peak cluster selected for trimethoprim measure ments. The solvent system described above avoids these shortcomings.

REFERENCES

1 M. Finland and E. H. Kass, Trimethoprim—Sulfamethoxazole, The University of Chicago Press, Chicago and London, 1974.
2 A. C. Bratton and E. K. Marshall, Jr., J. Biol. Chem., 128 (1939) 537.
3 M. Kraml and A. Boudreau, Clin. Biochem., 4 (1971) 123.
4 The National Formulary, Mack Publishing, Easton, Pa., 14th edn, (1975) 665.
5 C. W. Sigal, M. E. Grace, C. A. Nichol and G. H. Hitching, J. Pharm. Sci., 63 (1974) 120
6 M. Sarsunova, V. Schwartz, E. Feketova and J. Protiva, Pharmazie, 21 (1966) 219.
7 C. A. Brunner, J. Ass. Offic. Anal. Chem., 53 (1973) 689.
8 U. R. Cieri, J. Chromatogr., 49 (1970) 493.
9 S. Crisp, Analyst (London), 96 (1971) 671.
10 T. C. Kram, J. Pharm. Sci., 61 (1972) 254.
11 H. M. Miller, J. Ass. Offic. Anal. Chem., 53 (1970) 1100.
12 D. L. Smith and P. J. Elving, J. Am. Chem. Soc., 84 (1962) 2710.
13 M. A. Brooks, J. A. F. deSilva and L. M. D'Arconte, Anal. Chem., 45 (1973) 263.
14 M. A. Brooks, J. A. F. deSilva and M. R. Hackman, Am. Lab., 5 (1973) 23—6, 28—30, 32, 34—8.
15 D. E. Schwartz, W. Velter and G. Engler, Arzneim.-Forsch., 20 (1970) 1867.
16 D. E. Schwartz, B. Koechlin and R. E. Weinfeld, Chemotherapy, (Basel), Suppl., 14 (1969) 22.
17 S. A. Kaplan, R. E. Weinfeld and T. L. Lee, J. Pharm. Sci., 62 (1973) 1865.
18 E. Roeder and W. Stuthe, Dtsch. Apoth.-Ztg., 15 (1975) 1461.
19 S. M. R. Bushly and G. H. Hitching, Br. J. Pharmacol. Chemother., 33 (1968) 72.
20 M. Bidlo and D. Bobak, Lucr. Conf. Nat. Chim. Anal., (3rd), 4 (1971) 199.
21 C. W. Sigal and M. E. Grace, J. Chromatogr., 80 (1973) 11.

Analytica Chimica Acta, 92 (1977) 129—138

A SPECTRAL AND POLAROGRAPHIC STUDY OF THE ACID—BASE AND COMPLEXING BEHAVIOUR OF BROMAZEPAM

MALCOLM R. SMYTH†, TAN S. BENG and W. FRANKLIN SMYTH*

Chemistry Department, Chelsea College, Manresa Road, London SW3 (England)

(Received 16th February 1977)

SUMMARY

A spectral and polarographic study of bromazepam yielded pK_a values of 2.5, 5.2 and 11.8, corresponding to protonation at the azomethine and pyridine nitrogen atoms, and deprotonation at the nitrogen atom in position 1, respectively. These acid—base equilibrium reactions are discussed with reference to the hydrolysis and complexing properties of this compound. An indirect analytical method, based on the complexation of bromazepam with Cu^{2+} ions, has been investigated by differential pulse anodic stripping voltammetry.

Bromazepam, 7-bromo-1,3-dihydro-5-(2-pyridyl)-2H-1,4-benzodiazepin-2-one (I), has aroused clinical interest as an anti-anxiety agent [1—3]. Its metabolic fate has been investigated [4—6]; whereas benzophenone and hydroxylated metabolites exist predominantly in urine, only the parent compound is present in blood after therapeutic administration. Both gas chromatographic [6] and differential cathode ray polarographic [7] methods exist for the determination of bromazepam in plasma with detection limits of 5—10 and 50 ng ml^{-1}, respectively. Only differential pulse polarography, however, has been applied successfully to the determination of its metabolites in urine [6].

The presence of the pyridine moiety results in bromazepam having unique physico-chemical properties compared with other therapeutically important 1,4-benzodiazepines. Unlike other 1,4-benzodiazepines with electron-withdrawing substituents in the 5-phenyl ring, the rate of acidic hydrolysis of bromazepam increases in solutions of pH < pK_1 value [8]. The rapidity of this reaction, which eventually results in the formation of the 2-benzoyl-pyridine derivative (II) (also found [6] as a metabolite in urine) is believed to be

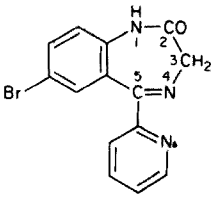

I

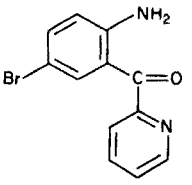

II

†Present Address: Department of Microbiology, Colorado State University, Fort Collins, Colorado 80523, U.S.A.

particularly dependent on the state of protonation of the pyridyl and azomethine nitrogen atoms. A systematic study of the acid—base equilibria existing in aqueous solutions of bromazepam was therefore undertaken; similar studies have been carried out for other 1,4-benzodiazepines [9—13]. The polarographic properties of bromazepam were also investigated.

The existence of the $-N=\overset{H}{\underset{|}{C}}-\overset{H}{\underset{|}{C}}=N-$ moiety (similar to that found in α,α′-dipyridyl) enables bromazepam to complex some divalent metal ions. This behaviour has been studied spectrophotometrically in relation to Fe^{2+} ions [14] and applied to the determination of iron [15] and haemoglobin [16] in serum. It was decided, therefore, to investigate the effect of complexation of bromazepam with ions such as Cu^{2+} and Co^{2+} by u.v. spectrophotometry and polarography.

EXPERIMENTAL

Apparatus

Ultraviolet spectra were recorded with a Perkin-Elmer Model 124 Double Beam Spectrophotometer and 1-cm matched silica cells. A PAR Model 174A Polarographic Analyzer was used with a 3-electrode cell system, the counter electrode being platinum and the reference electrode calomel. The dropping mercury electrode had an outflow velocity of 1.92 mg s^{-1} and a drop time of 3.9 s at the potential of the s.c.e. and a mercury pressure h = 55 cm in 1 M KCl. A PAR Model 9323 Hanging Mercury Drop Electrode (h.m.d.e.) was used for the anodic stripping voltammetric investigations.

Reagents

A stock solution (10^{-3} M) of bromazepam (Roche Products Ltd., Welwyn Garden City) was prepared in AnalaR methanol and stored in the dark under refrigeration.

A stock Britton—Robinson (BR) buffer solution, which was 0.04 M in glacial acetic acid, phosphoric acid and boric acid, was prepared from analytical grade reagents; buffer solutions of varying pH (2—12) were prepared by dropwise addition of 0.2 M NaOH. All other compounds were of analytical grade.

Procedures

Solutions were prepared for spectrophotometry by diluting 0.5 ml of the stock solution of bromazepam to 10 ml with the appropriate buffer. To extend the pH range at either end of the scale, 1 M HCl, 0.1 M, HCl 0.1 M NaOH and 1 M NaOH were used. Each solution was scanned from 370 to 210 nm and pK_a values were determined from plots of absorbance vs. pH at the appropriate wavelength. For the complexation studies, the concentration of bromazepam was kept constant at $5 \cdot 10^{-5}$ M while that of the metal ion (i.e. Fe^{2+}, Cu^{2+}, or Co^{2+}) was varied from $1 \cdot 10^{-5}$ M to $2 \cdot 10^{-4}$ M. The nature

of complexation was then derived from plots of absorbance vs. the molar ratio.

Polarographic studies of the variation of $E_{\frac{1}{2}}$ and i_{lim} with pH were carried out in the sampled d.c. mode on $5 \cdot 10^{-5}$ M solutions of bromazepam (previously degassed for 10 min with O_2-free N_2) at a scan rate of 5 mV s^{-1}, drop time 1 s, modulation amplitude 100 mV, and time constant 0.3 s. For solutions of pH < 4, the supporting electrolyte (9.5 ml) was degassed for 10 min prior to adding 0.5 ml of the stock solution and degassing for a further 30 s. This was done to minimize the interference caused by the hydrolytic side-reaction.

The effect of complexation on polarographic behaviour was studied with 10^{-5} M solutions of bromazepam using differential pulse polarography (d.p.p.), linear potential sweep anodic stripping voltammetry (l.p.s.a.s.v.) and differential pulse anodic stripping voltammetry (d.p.a.s.v.). In the former case, the conditions were the same as those employed in the Sampled d.c. investigation. For l.p.s.a.s.v. investigations, reproducible electrode surfaces of the h.m.d.e. were obtained by dialling out 6 divisions on the micrometer screw gauge each time. The solutions to be analyzed were first degassed for 10 min before holding the 'plating' potential for 3 min and scanning in a positive direction at 50 mV s^{-1}. For d.p.a.s.v. measurements, a scan rate of 2 mV s^{-1} and a drop time of 1 s were employed for the construction of the calibration graph.

RESULTS AND DISCUSSION

U.v. spectral behaviour; pK_a values and mechanism of hydrolysis

The u.v. spectral characteristics of the four forms of bromazepam existing across the pH range 0—14 are given in Table 1. The pK_a values relating to these equilibria, determined from a plot of absorbance vs. pH at 235 nm, were 2.5 (pK_1) and 11.8 (pK_3), in good agreement with the values obtained for other 1,4-benzodiazepines [9—13] and corresponding to protonation of the N atom in the azomethine group, and deprotonation of the N atom in position 1, respectively.

Protonation of the pyridyl N atom is not observed spectrally because of the expected low absorptivities of the protonated and deprotonated species, e.g. 2-picoline absorbs at 260 nm ($\epsilon = 4 \cdot 10^{-3}$) and 260.5 nm ($\epsilon = 5.2 \cdot 10^{-3}$) in the deprotonated and protonated states, respectively [17]. A pK_a value of 5.2 (pK_2) obtained in the polarographic studies agrees well with the tabulated pK_a value for pyridine itself (pK_a = 5.23).

A study of the variation in the rate of hydrolysis with pH shows that for bromazepam the rate is relatively slow in solutions of pH 3—4, but increases rapidly on passing through the pK_1 value until, at pH 1.0 and 0, the process goes to completion in 1 and 0.5 h, respectively [8]. This behaviour has not been observed for other 1,4-benzodiazepines with electron-withdrawing substituents in the 5-phenyl ring, e.g. 5-*o*-fluorophenyl-1,4-benzodiazepines

TABLE 1

U.v. spectral characteristics and pK_a values of the different forms of bromazepam existing across the pH range

Form	λ_{max} (nm)	$\epsilon(\cdot 10^4)$	pK_a
H_3A^{2+}	240	2.3	
	275(S)	1.0	
		⟶	2.5
H_2A^+	235	3.4	
	260(S)	1.2	
	320	0.2	
		⟶	5.2 (Pol)
HA	235	3.4	
	260(S)	1.2	
	320	0.2	
		⟶	11.8
A^-	238	2.8	
	260(S)	1.7	
	350	0.2	

(S) = shoulder
(Pol) = from polarographic results

hydrolyse more rapidly in 0.1 M HCl than 1 M HCl. Groves [8] has postulated that compounds such as *N*-desalkyl flurazepam (III) undergo acid-catalyzed hydrolysis, but that species

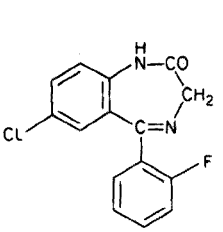

III

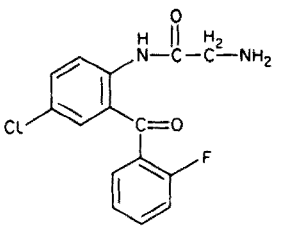

IV

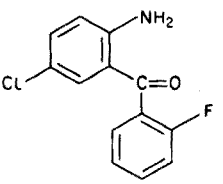

V

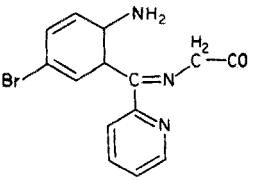

VI

containing a non-protonated azomethine group are more susceptible to this process than when they are protonated; hydrogen bonding between the protonated azomethine group and the fluorine atom may stabilize this structure towards hydrolytic attack. Indeed, at pH in the vicinity of the pK_1 value, benzophenones such as (IV) are produced; under more vigorous conditions (e.g. 4 M HCl at 100°C for 2 h) glycine is eliminated to give the aminebenzophenones such as (V) that are more commonly encountered in the analytical chemistry of the 1,4-benzodiazepines. This is in agreement

with the findings of deSilva et al. [18, 19].

In contrast, bromazepam is hydrolysed more rapidly when its azomethine group is protonated; this suggests that hydrogen bonding between the protonated pyridyl group and the azomethine nitrogen lone pair in the unprotonated state stabilizes this structure towards hydrolytic attack. The product of acid hydrolysis in the pH region 0—1.0 is likely to be (VI) since Groves [8] has observed that the half-wave potential of the azomethine group only shifts from —0.198 V to —0.232 V at pH 0. In contrast, other 1,4-benzodiazepines which form benzophenones (like (IV) or (V)) on acid hydrolysis undergo shifts in potential of ca. 130—140 mV at pH 0 [8]. Bromazepam is hydrolysed to the benzophenone (II) under more vigorous conditions [6].

Polarographic behaviour

Bromazepam exhibits two cathodic waves across the pH range 1—12 (Fig. 1). A wave is also observed for the hydrolysis product in solutions of pH < 4. The first wave i_a, corresponds to the $2e^-$ reduction of the azomethine group and exhibits two linear portions, of slopes 79 and 53 mV pH^{-1}, which intersect at the pK_1' value of 7.4. This behaviour is observed for other 1,4-benzodiazepines [8, 9, 12, 13]. The $E_{\frac{1}{2}}$ values obtained for this wave across the pH range occur ca. 300—400 mV more positive than the corresponding waves obtained for non-pyridine-containing 1,4-benzodiazepines; this has permitted a scheme to be devised for the identification of bromazepam in the presence of other 1,4-benzodiazepines [20]. In that scheme, only the

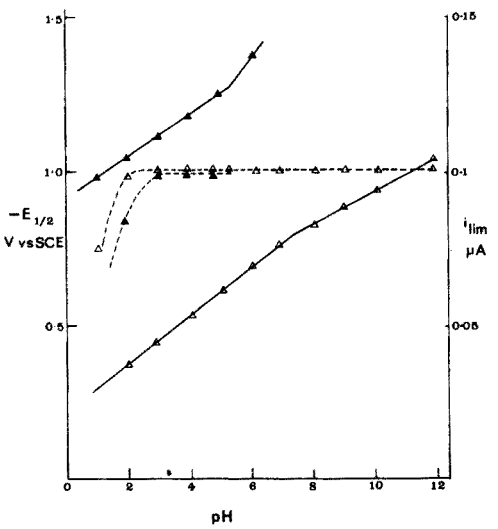

Fig. 1. Plots of $E_{\frac{1}{2}}$ (——) and i_{lim} (------) vs. pH for waves i_a (-△-△-) and i_b (-▲-▲-) exhibited by bromazepam across the pH range.

N-oxide reduction in chlordiazepoxide was shown to occur at the same potential as that of the $\backslash C{=}N-/$ reduction of bromazepam in BR buffer, pH 4.0, but since the *N*-oxide reduction depends on a preceding protonation reaction [9], the compounds can be resolved in alkaline media.

The second wave, i_b, exists only over the pH range 1—6 and also corresponds to a $2e^-$ reduction. The $E_{\frac{1}{2}}$ vs. pH plot consisted of two linear portions. The main portion gave 66 mV pH^{-1} at pH < 5.2, at which pH the slope changed to a higher value. This gave $pK_a = 5.2$ for the pyridyl nitrogen atom (pK_2) and indicates that only the protonated form of pyridine is reduced in this second wave which is given by a reduction process rather than catalytic hydrogen evolution since the height of the wave was independent of pH. A plot of $E_{d.e.}$ vs. $\log i/(i_d - i)$ at pH 3 for i_b yielded a value for αn of 1.02; this suggests that the rate-determining step could be reversible and involve $1e^-$.

A possible mechanism for this reduction is given below

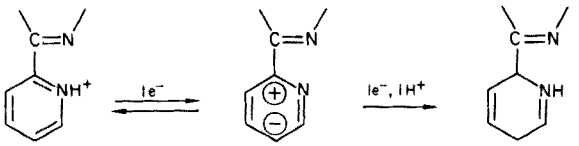

U.v. spectrophotometric and polarographic study of the complexation of bromazepam with Cu^{2+} ions

An earlier study [14] showed that bromazepam formed a 1:3 complex with Fe^{2+} ions when the concentration of the ligand was maintained at 10^{-3} M. This complex exhibits a distinctive violet-purple colour; that formed with Cu^{2+} ions (with SO_4^{2-} as the anion) at the same concentration exhibits a slight yellowish-green colour. Figure 2 shows the change in u.v. absorption of bromazepam in the presence of varying concentrations of Cu^{2+} ions. A plot of absorbance (at 280 nm) vs. the molar ratio yielded a sharp inflexion corresponding to a 1:1 stoichiometry. A 1:1 complex was also observed for the bromazepam—Fe^{2+} complex when the concentration of bromazepam was maintained at $5 \cdot 10^{-5}$ M; the stoichiometry of the complexation process is therefore governed to a great extent by the ligand concentration.

Difficulty was encountered, however, in the determination of the conditional formation constant (K_{ML}) from these data as a wavelength could not be found where the absorbance was due solely to the complex (Fig. 2). A rough estimate was obtained, however, from readings at 350 nm (a wavelength where, although the absorption of the complex is weak, bromazepam itself does not absorb and there is only slight interference by free Cu^{2+} ions) by first calculating the molar absorptivity of the complex (assuming that in a solution containing a 5:1 excess of bromazepam, all the Cu^{2+} ions are in a complexed state) and then substitution into the Beer—Lambert equation to find the concentration of complex in solutions containing approximately equimolar concentrations of bromazepam and Cu^{2+} ions. The concentrations

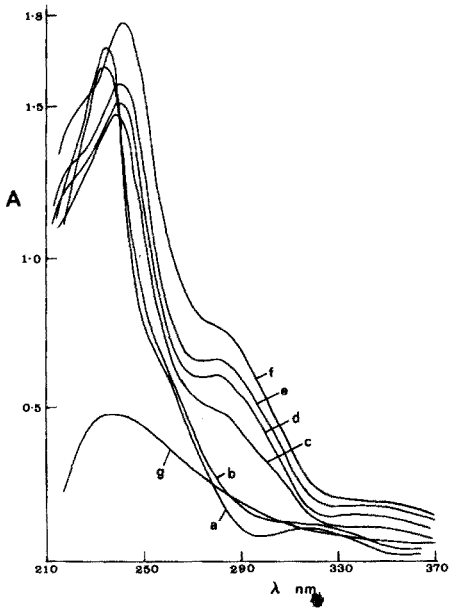

Fig. 2. U.v. spectral behaviour of bromazepam in the presence of Cu^{2+} ions: (a) $5 \cdot 10^{-5}$ M bromazepam; (b) a + $1 \cdot 10^{-5}$ M Cu^{2+}; (c) a + $4 \cdot 10^{-5}$ M Cu^{2+}; (d) a + $8 \cdot 10^{-5}$ M Cu^{2+}; (e) a + $1 \cdot 10^{-4}$ M Cu^{2+}; (f) a + $2 \cdot 10^{-4}$ M Cu^{2+}; (g) $2 \cdot 10^{-4}$ M Cu^{2+}.

of free ligand and metal ion were then obtained by subtraction and K_{ML} was calculated from $K_{ML} = [ML]/([M][L])$. A value of $(6.5 \pm 1.5) \cdot 10^5$ was obtained; a relatively strong complex is therefore formed between bromazepam and Cu^{2+} ions at these concentrations.

The complexation process was further investigated by differential pulse polarography. When an equimolar concentration of Cu^{2+} ions was added to 10^{-5} M bromazepam, polarography of the resulting solutions showed that i_a decreased by 14.5% in BR buffer pH 9 and that i_a and i_b decreased by 11.4% and 11.7% respectively in BR buffer, pH 4.0. This indicates that a slightly stronger complex was formed between Cu^{2+} ions and the neutral form of bromazepam (HA) than when the pyridyl nitrogen atom was protonated. No shifts in the potential(s) of reduction of bromazepam were observed in either case and no further decreases in the peak height (at either pH) resulted when Cu^{2+} ions were added in excess. Complexation of bromazepam with Fe^{2+} ions at pH 9 caused a much smaller decrease in the peak height (2—3%) of i_a; Cu^{2+} ions are therefore more strongly complexed to bromazepam than Fe^{2+} ions when the ligand is present at these concentrations.

The behaviour of the bromazepam—Cu^{2+} complex was further studied by anodic stripping voltammetry. The results for a plating potential of —1.0 V are shown in Fig. 3. This shows that whereas copper exhibits a single stripping peak at —0.05 V, copper in the presence of an equimolar concentration of

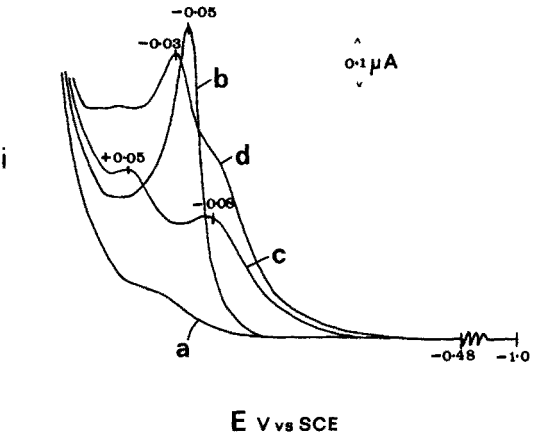

Fig. 3. Effect of bromazepam on stripping current of Cu^{2+} ions: (a) blank BR buffer, pH 9.0; (b) $1 \cdot 10^{-5}$ M Cu^{2+}; (c) $1 \cdot 10^{-5}$ M Cu^{2+} + $1 \cdot 10^{-5}$ M bromazepam; (d) $2 \cdot 10^{-5}$ M Cu^{2+} + $1 \cdot 10^{-5}$ M bromazepam.

bromazepam at 10^{-5} M in pH 9 buffer gives two peaks of relatively similar height at −0.08 V and +0.05 V, probably corresponding to the processes $Cu^0 \rightarrow Cu^+ \rightarrow Cu^{2+}$. This double wave behaviour occurs in the reduction of Cu^{2+} complexes of ammonia and pyridine [21, 22].

Effect of Co^{2+} ions on the polarographic behaviour of bromazepam

The addition of Co^{2+} ions did not change the u.v. spectral behaviour of bromazepam across the pH range, but did change markedly its polarographic behaviour. In BR buffer, pH 4.0, i_a decreased in height at the expense of i_b, whereas in BR buffer, pH 9.0, i_a decreased and a double wave appeared at more negative potentials (Fig. 4). The potential of the second portion of this double wave corresponded to the reduction of free Co^{2+} ions (i.e. −1.33 V) whereas the wave height of the first portion did not vary linearly with increasing concentration of Co^{2+} ions but gave a plot indicative of an adsorption isotherm. This has been observed for other processes involving catalytic hydrogen evolution [23].

These results indicate that although Co^{2+} does not form a complex with bromazepam in the same manner as Cu^{2+}, it is involved as a catalyst in the evolution of hydrogen. Although bromazepam obviously participates in this reaction (as shown by the decrease in the height of wave i_a) its role in this reaction is not yet fully understood since the production of hydrogen from pyridine derivatives generally occurs only when these derivatives exist in the protonated form [24]. In this case, catalytic hydrogen evolution is observed when the pyridyl group in bromazepam is both protonated and deprotonated.

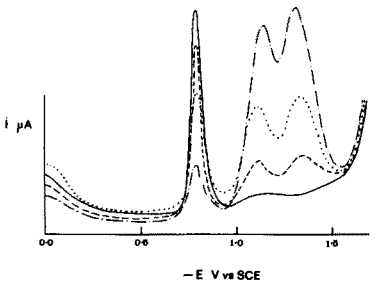

Fig. 4. Effect of Co^{2+} ions on d.p.p. behaviour of bromazepam in BR buffer, pH 9.0: (——) $1 \cdot 10^{-5}$ M bromazepam; (------) $1 \cdot 10^{-5}$ M bromazepam + $1 \cdot 10^{-5}$ M Co^{2+}; (·····) $1 \cdot 10^{-5}$ M bromazepam + $2 \cdot 10^{-5}$ M Co^{2+}; (-·-·-) $1 \cdot 10^{-5}$ M bromazepam + $1 \cdot 10^{-4}$ M Co^{2+}

Analysis of bromazepam by differential pulse anodic stripping voltammetry

As can be seen in Fig. 3, addition of an equimolar amount of bromazepam to a 10^{-5} M Cu^{2+} solution caused a decrease in the stripping peak height corresponding to the oxidation of copper. It was decided, therefore, to investigate whether this behaviour could be applied to the indirect low level determination of bromazepam by d.p.a.s.v.

A series of different supporting electrolytes was investigated; BR buffer, pH 9.0, gave the lowest blank in the region of the stripping potential of copper. Ammonia, phosphate and tartrate buffers of pH 9.0 were inferior in this potential region. BR buffer, pH 9.0, did however, show a small interference at −0.07 V which was removed by the addition 20% methanol. Stirring the solutions during deposition resulted in an increase in the background current between −0.2 V and +0.1 V and so this was omitted, in the analytical determination.

A calibration plot was constructed by plotting the decrease in the peak height arising from stripping of free copper against the concentration of bromazepam (in the range $1 \cdot 10^{-7}$ M—$5 \cdot 10^{-7}$ M) in solutions containing a fixed concentration of Cu^{2+} ions ($5 \cdot 10^{-7}$ M). This is represented in Fig. 5; although the curve obeys an overall sigmoidal relationship, there is linearity in the concentration range $1.5—4 \cdot 10^{-7}$ M for bromazepam. It was impossible to measure bromazepam concentrations of 10^{-7} M because of the interference caused by the oxidation of mercury.

Since this method does not provide greater sensitivity than a direct d.p.p. or g.c. procedure, it is unlikely to be of great application in analytical determinations of bromazepam in body fluids. It may, however, provide a means for investigating the degree to which this compound is complexed to various metal ions and thus help in an understanding of its pharmacological behaviour.

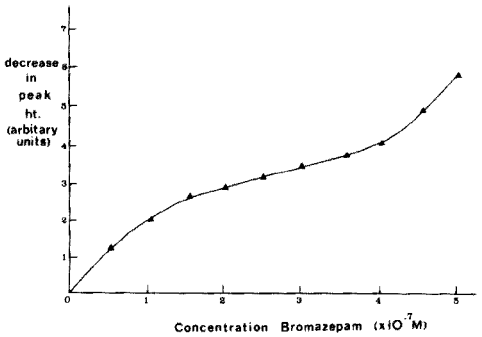

Fig. 5. Calibration plot of decrease in stripping peak height of free Cu^{2+} against concentration of bromazepam.

The authors thank Mr. L. Spencer for technical assistance throughout this work.

REFERENCES

1 E. Stovehill, H. Lee, and T. A. Ban, Dis. Nerv. Syst., 27 (1966) 411.
2 R. J. Kerry, F. A. Jenner, and I. B. Pearson, Psychosomatics, 13 (1972) 122.
3 K. Rickels, J. A. Pereira-Ogan, H. R. Chung, P. E. Gordon, and W. Laudis, Curr. Ther. Res., 15 (1973) 679.
4 H. Sawada, Experienta, 28 (1972) 393.
5 H. Sawada, H. Yano, and A. Kido, J. Pharm. Soc. Jpn., 92 (1972) 1237.
6 J. A. F. deSilva, I. Bekersky, M. A. Brooks, R. E. Weinfeld, W. Glover, and C. V. Puglisi, J. Pharm. Sci., 63 (1974) 1440.
7 F. E. Senguen and H. Oelschlager, Arch. Pharm. (Weinheim), 308 (1975) 720.
8 J. A. Groves, PhD Thesis, Univ. of London (1976).
9 J. M. Clifford and W. Franklin Smyth, Z. Anal. Chem., 264 (1973) 149.
10 J. Barrett, W. F. Smyth, and I. E. Davidson, J. Pharm. Pharmacol., 25 (1973) 387.
11 J. Barrett, W. Franklin Smyth, and J. P. Hart, J. Pharm. Pharmacol., 26 (1974) 9.
12 J. A. Goldsmith, H. A. Jenkins, J. Grant, and W. Franklin Smyth, Anal. Chim. Acta, 66 (1973) 427.
13 W. Franklin Smyth and B. Leo, Anal. Chim. Acta, 76 (1975) 289.
14 J. D. Sabatino, O. W. Weber, G. R. Padmanabhan, and B. Z. Senkowski, Anal. Chem., 41 (1969) 905.
15 B. Klein, L. B. Lucas, and R. L. Searcy, Clin. Chim. Acta, 26 (1969) 517.
16 B. Klein, B. K. Weber, L. Lucas, J. K. Foreman, and R. L. Searcy, Clin. Chim. Acta, 26 (1969) 77.
17 H. H. Jaffe and M. Orchin, Theory and Applications of Ultraviolet Spectroscopy, New York, J. Wiley, (1962) p. 257.
18 J. A. F. deSilva, C. V. Puglisi, M. A. Brooks, and M. R. Hackman, J. Chromatogr., 99 (1974) 461.
19 J. A. F. deSilva and N. J. Strojny, J. Pharm. Sci., 60 (1971) 1303.
20 M. R. Smyth, J. A. Groves, T. S. Beng, and W. Franklin Smyth, Analyst, to be published.
21 I. M. Kolthoff and J. J. Lingane, in Polarography 2nd edn. Interscience, N.Y., (1952) p. 227
22 M. Stulikova and F. Vydra, J. Electroanal. Chem., 44 (1973) 117.
23 S. G. Mairanovskii, in Catalytic and Kinetic Waves in Polarography, Plenum Press, N.Y., (1968) p. 241.
24 C. L. Perrin, in P. Zuman and C. L. Perrin (Eds.), Organic Polarography, Interscience, 1969, p. 280.

Analytica Chimica Acta, 92 (1977) 139—148

DETERMINATION OF ETHYLENEDIAMINETETRAACETATE AND NITRILOTRIACETATE IN PHYTOPLANKTON MEDIA BY DIFFERENTIAL PULSE POLAROGRAPHY

RICHARD J. STOLZBERG

Harold Edgerton Research Laboratory, New England Aquarium, Central Wharf, Boston, MA 02110 (U.S.A.)

(Received 1st December 1976)

SUMMARY

A technique for the analysis of synthetic sea water and phytoplankton media for ethylenediaminetetraacetate (EDTA) and nitrilotriacetate (NTA) by differential pulse polarography has been developed. The addition of approximately $2.4 \cdot 10^{-4}$ M cadmium to the analyte converts a large fraction of either ligand to the reducible cadmium complex. With $5 \cdot 10^{-6}$ M ligand present, the standard deviation is approximately $6 \cdot 10^{-7}$ M for NTA and $4 \cdot 10^{-7}$ M for EDTA. The presence of competing metal cations, including copper, is not detrimental if the method of standard additions is used.

During investigation of the effects of trace metal speciation on phytoplankton productivity, the concentrations of small quantities of strong organic ligands had to be measured. The ligands included ethylenediaminetetraacetate (EDTA), nitrilotriacetate (NTA), and tris(hydroxymethyl)aminomethane (Tris) added to the waters, and some less well-defined extracellular metal-binding organics (EMBO) contributed by the phytoplankton. Artificial ligands have traditionally been added by physiologists because a wide variety of algae can be grown in media containing complexed trace metals. In addition, precipitation of the medium is reduced, enabling more reproducible media to be prepared [1]. It has been suggested that plankton may produce EMBO for much the same reason — to improve the medium for growth either by detoxifying potentially toxic metals such as copper [2] or by making iron available as a soluble chelated species [3, 4].

Our work currently involves correlating the concentration of complexed and uncomplexed species of copper with phytoplankton productivity and the production of EMBO. Well-defined artificial media that lend themselves to convenient chemical manipulation and which support a good growth of algae are used. Accurate determination of trace metal speciation requires verification of ligand concentration, particularly at low ($<10^{-5}$ M) levels. Loss of ligand by photodegradation is a distinct possibility, particularly in long-term experiments under high light intensity. The sensitivity of iron(III)—EDTA to photodegradation is well known [5], and the susceptibilities of

both iron(III)— and copper(II)—NTA to photodegradation have been documented recently [6, 7, 8]. Sorption of ligands can also present experimental difficulties in dense algal cultures. Changes in metal speciation can be expected from any of these mechanisms that might reduce ligand or metal concentrations. Finally, the production of EMBO by the cells must be considered when calculating speciation. The quantity of EMBO produced by the cells can be determined by the difference in total complexing capacity [9] and the quantity of EDTA or NTA present.

The analytical methodology for specific and sensitive determinations of EDTA and NTA in saline waters is not well developed despite the wide range of techniques developed for NTA in fresh water and sewage sludge [10]. The most widely used techniques for non-saline water are gas chromatography [11—13] and electrochemistry [14—18]. The presence of large quantities of dissolved salts in sea water clearly favors electrochemical techniques. Electrochemical reduction of the Cd—NTA complex, first used analytically for the determination of NTA in EDTA [14], and later adapted for NTA determination in lake and river waters [16, 17] is the system of choice. Reduction of NTA complexes of lead, bismuth, and indium [15, 18] has been used analytically, but the electrochemistry of the Cd—NTA [19, 20] and Cd—EDTA [21, 22, 23] complexes has been characterized in detail and is straightforward.

Classical d.c. polarography has been used to measure 1—10 p.p.m. NTA in lake water [16], but this technique could not be used in sea water. The reduction current from the large quantity of cadmium added to displace calcium from the NTA swamps the small current increments from Cd—NTA reduction. Differential pulse polarography (d.p.p.) is more sensitive than d.c. polarography, and can be used to measure small currents at a potential cathodic of an electrochemically active species present at much greater concentration.

THEORETICAL CONSIDERATIONS

Equation 1 describes the generalized competition reaction between cadmium and competing metal (M) for EDTA or NTA (L). Charges have been omitted for clarity. Concentration stability constants and molar concentrations are used throughout.

$$CdL + M \rightleftharpoons Cd + ML\ ;\ K_c = K_{ML}/K_{CdL} \qquad (1)$$

where $K_{ML} = [ML]/[M][L]$ and $K_{CdL} = [CdL]/[Cd][L]$. If Ringbom's concept of conditional stability constants and his notation [24] are used, the competition stability constant, K_C, can be rewritten as a conditional competition constant.

$$K'_c \equiv K'_{ML}/K'_{CdL} = [Cd'][ML]/[M'][CdL] \qquad (2)$$

[M′] and [Cd′] are the concentrations of all M and Cd species not present as ML and CdL. When the total competing metal concentration, C_M, and the total cadmium concentration, C_{Cd}, are in excess of the total ligand concentration, C_L, and the values of the conditional stability constants, K'_{ML} and K'_{CdL}, are large enough to ensure formation of ML and CdL in preference to H_nL ($n = 0, 1, 2 \ldots$), the following approximation is valid

$$[ML] \approx C_L - [CdL] \tag{3}$$

Substituting eqn. (3) into eqn. (2) and rearranging gives

$$[CdL] = [Cd'] \cdot C_L/(K'_c[M'] + [Cd']) \tag{4}$$

If the definitions, $[M'] = C_M - [ML]$ and $[Cd'] = C_{Cd} - [CdL]$ are used, eqn. (4) can be rewritten in the generally applicable form

$$[CdL] = \{C_{Cd} - [CdL]\} \cdot C_L/\{K'_c(C_M - [ML]) + C_{Cd} - [CdL]\} \tag{5}$$

Under the conditions of analysis in sea water where C_L should be much less than C_M or C_{Cd}, the following approximations are valid: $C_{Cd} - [CdL] \approx C_{Cd}$ and $C_M - [ML] \approx C_M$. Substitution of these equations into eqn. (5) produces

$$[CdL] = C_{Cd} \cdot C_L/(K'_c C_M + C_{Cd}) \tag{6}$$

Equation (6) predicts that the concentration of the electroactive CdL species in the bulk solution is a linear function of the analytical concentration of L when C_M and C_{Cd} are constant. Care must be taken to ensure that the approximation $C_{Cd} - [CdL] \approx C_{Cd}$ is valid when NTA is determined, otherwise a non-linear response is observed. This non-linear response is not observed for EDTA determinations because of the smaller value of K'_c for EDTA ($10^{-4.3}$) compared to that for NTA ($10^{-2.2}$); see the appendix for calculation of these values. For EDTA, the value of $K'_c(C_M - [ML]) \ll (C_{Cd} - [CdL])$ unless C_L is nearly as great as C_{Cd}. In most cases eqn. (5) reduces to $[CdL] \approx C_L$, i.e. EDTA is completely associated with cadmium at most values of C_L. The $K'_c(C_M - [ML])$ term is important for NTA, but only when the value of [Cd′] is reduced below ca. $1.4 \cdot 10^{-4}$ M in synthetic sea water (SSW) by complexation with L. Changes in the fraction of L associated with Cd occur at higher values of [Cd′], but the magnitude of the change is small. In SSW containing $2.4 \cdot 10^{-4}$ M Cd, approximately 80% of the NTA is associated with cadmium when $C_{Cd} - [CdL] \approx C_{Cd}$ is valid. Figure 1 plots the fraction of NTA and EDTA associated with cadmium as a function of [Cd′]. To insure that response is linear within the precision of the technique (ca. 5%), the total concentration of strong ligands in solution should not exceed 10^{-4} M during NTA determination.

EXPERIMENTAL

Apparatus

The electrochemical system used was a Princeton Applied Research Model 174 Polarographic Analyzer and a Model 172A mercury drop-timer. Output was to a Houston Instruments Omnigraphic 2000 X-Y recorder. The electrochemical cell was similar to that described by Gilbert and Hume [25], but a dropping mercury electrode (DME) was used rather than a wax-impregnated graphite electrode. Solutions were stirred magnetically with a Teflon-coated bar. Data were analyzed with a Wang 600 programmable calculator.

Reagents

Glass distilled, deionized water; reagent-grade chemicals; and triple distilled mercury were used. Prepurified nitrogen gas presaturated with water was used to deoxygenate samples. The pH of the $8.6 \cdot 10^{-2}$ M Tris buffer was adjusted to 8.0 with HCl. The 1 M Ca^{2+} solution was made from the chloride salt.

The synthetic sea water (SSW) contained $4.3 \cdot 10^{-1}$ M NaCl, $9.4 \cdot 10^{-3}$ M KCl, $2.7 \cdot 10^{-2}$ M $MgSO_4$, and $9.5 \cdot 10^{-3}$ M $CaCl_2$. The medium Cu-IV was prepared by the addition of nutrients, trace metals and vitamins to SSW.

Procedure

Optimum conditions for the determination of NTA and EDTA differ. Samples containing NTA are spiked with 0.6 ml of 500-p.p.m. cadmium solution. Those containing EDTA are spiked with either 0.1 or 0.6 ml of 500-p.p.m. cadmium solution and with sufficient 1 M $CaCl_2$ to increase the calcium concentration to approximately 0.1 M. With the smaller quantity of cadmium added, baseline noise in the region of the Cd—EDTA wave is reduced. However, the top of the linear range is extended from $3.3 \cdot 10^{-5}$ M to $2.0 \cdot 10^{-4}$ M EDTA if the cadmium spike is increased from 0.1 ml to 0.6 ml.

A 10.00-ml sample is added to the polarographic cell with 1.00 ml of Tris buffer and the appropriate volume of 500-p.p.m. cadmium solution. The solution is deoxygenated for approximately 10 min, after which the nitrogen flow is directed into the head space. A pulse amplitude of 25 or 50 mV, a scan rate of 5 mV s^{-1}, and a drop time of 1 s are used. Instrument sensitivity in the range of 0.5—2 μA full scale produces peaks of convenient size. The cathodic scan begins at −0.7 V for NTA and −1.0 V for EDTA. Peak potentials for the Cd—NTA and Cd—EDTA reductions are observed at −0.90 V and ca. −1.25 V, respectively. Standard additions of NTA or EDTA are made with a microsyringe, deoxygenation is repeated for 1 min, and the scan is repeated after each addition. Peak current values are used in quantification. In many cases, a calibration curve can be constructed and standard additions are not necessary.

Simultaneous determination of both ligands is possible if the sum of the strong ligands present at the end of the standard addition series is less than $1 \cdot 10^{-4}$ M. Calcium should not be added because the sensitivity of the NTA determination drops precipitously. The quantity of cadmium added should be 0.6 ml to ensure adequate sensitivity in the NTA determination. A complete standard addition series with four voltage scans can be run in less than 30 min, including deoxygenation time.

The pH should be kept between 7 and 8. Above pH 8 the added cadmium tends to precipitate, and below pH 6 or 7 the rapid dissociation reaction of the protonated Cd—HNTA species becomes important [20]; dissociation of Cd—NTA is slow. The sensitivity of the technique is reduced in acidic solution because the concentration of the species reduced at −0.9 V, Cd—NTA, is diminished. Formation of the Cd—$HEDTA^-$ species below pH 5 plays a similar role in decreasing the reduction current at ca. −1.25 V.

RESULTS AND DISCUSSION

Linearity

As predicted, a plot of EDTA concentration in SSW vs. peak current at approximately −1.25 V is linear from 10^{-5} M to $2.0 \cdot 10^{-4}$ M in the presence of $2.4 \cdot 10^{-4}$ M Cd. Response at $5 \cdot 10^{-6}$ M is generally below that expected by extrapolating the linear portion of the calibration curve back toward the origin. This decrease in relative response is due to the slow reaction between micromolar quantities of cadmium and EDTA. Maljkovic and Branica [26] observed that the reaction between $2 \cdot 10^{-6}$ M Cd and $2—7 \cdot 10^{-6}$ M EDTA in natural sea water proceeds only 31—69% of the way to the equilibrium value in 10 min. In the presence of $2.5 \cdot 10^{-5}$ M EDTA the reaction is rapid, however. In the usual analytical technique, the EDTA present in the sample reacts with the cadmium for only the 10-min deoxygenation period. It was observed that the reaction is incomplete in 10 min in spite of the relatively high concentration of cadmium if the EDTA concentration is $\leqslant 10^{-5}$ M. When the sample is equilibrated with the cadmium spike for 1 h, the decreased response was not observed.

Within the limits of the accuracy of the technique, the peak current at −0.9 V is a linear function of NTA concentration from zero to $1 \cdot 10^{-4}$ M in SSW containing $2.4 \cdot 10^{-4}$ M Cd. Solution of eqn. (5) predicts that the fraction of NTA associated with cadmium decreases from 0.80 to 0.73 in that range because of calcium competition, but this decrease was not observed in the experimental data. A definite decrease in relative response was observed above 10^{-4} M NTA. Figure 2 compares the observed behavior with that predicted with no competition ($K_c' = 0$), and with two non-zero values of K_c'. The value of K_c' calculated for calcium competition from Ringbom's constants [24] is $10^{-2.2}$. The good fit of the observed data to the line calculated for $K_c' = 10^{-2.2}$ suggests that the system behaves as predicted in SSW. Figure 3 shows typical polarograms of Cd—NTA and Cd—EDTA in SSW.

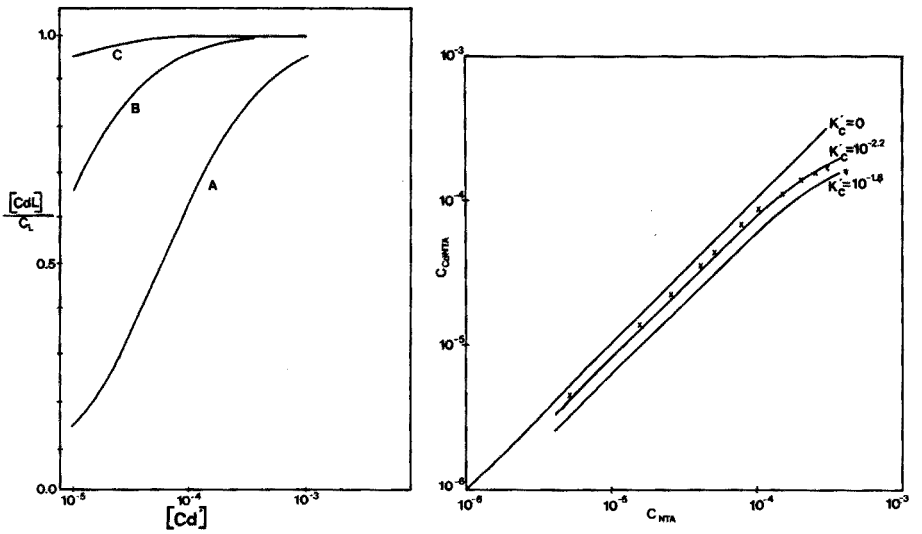

Fig. 1. Fraction of L associated with Cd in SSW as function of [Cd']. (A) NTA, $K'_c C_M$ = $6.0 \cdot 10^{-5}$ (B) EDTA, 0.1 M Ca^{2+} added, $K'_c C_M = 5.1 \cdot 10^{-6}$ (C) EDTA, $K'_c C_M = 4.8 \cdot 10^{-7}$.

Fig. 2. Concentration of Cd—NTA as function of total NTA concentration. C_{Cd} = $2.67 \cdot 10^{-4}$ M; x, experimental points. The lines are calculated from eqn. (5) for various values of K'_c assuming [ML] + [CdL] ≈ C_L.

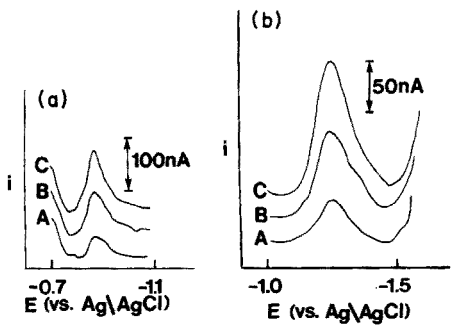

Fig. 3. Differential pulse polarograms. (a) NTA: (A) 1.6 μM NTA in SSW; (B) +1.6 μM NTA spike; (C) +3.2 μM NTA spike. (b) EDTA: (A) 5.0 μM EDTA in SSW; (B) +5.0 μM EDTA spike; (C) +10.0 μM EDTA spike. 25 mV pulse height, 5 mV s^{-1} scan rate, 1 s drop time. For EDTA, the calcium concentration was increased by 0.1 M and the sample was equilibrated with the cadmium spike for 1 h.

Precision and accuracy

The precision of the analysis for NTA in SSW was determined by replicate analysis of samples of NTA alone and in the presence of EDTA (Table 1). The standard deviation in the 1.5—5 μM NTA range is approximately 0.6 μM. Accuracy is excellent in this range and also in media containing larger amounts of ligand.

TABLE 1

Precision and accuracy of NTA determination
(25 mV pulse amplitude, 5 mV s^{-1} scan rate, 0.6 ml of 500-p.p.m. Cd solution per 10-ml sample.)

Sample	NTA found[a] (μM)	Standard deviation (μM)	No. of detns.
1.57 μM NTA in SSW	1.63	0.68	6
5.24 μM NTA in SSW	5.40	0.68	5
5.24 μM NTA in Cu-IV medium	5.44	0.42	10
5.00 μM NTA + 50 μM EDTA in SSW	4.77	0.48	6

[a]Standard addition analysis — only NTA added.

Table 2 presents analogous results for EDTA determinations in SSW and in the medium Aquil [27], which resembles Cu-IV. The accuracy is excellent for $5 \cdot 10^{-6}$—$5 \cdot 10^{-5}$ M EDTA. Sensitivity and precision increase with the addition of 10^{-1} M Ca^{2+}, but accuracy is not affected. The effects of alkaline earth metals on Cd—EDTA reduction have been described [21]. Addition of 0.1 M calcium ion minimizes variation in relative reduction current between samples caused by variations in major cation concentration. If the cadmium spike is allowed to equilibrate with the sample, satisfactory analyses can be made of samples containing $5 \cdot 10^{-6}$ M EDTA.

TABLE 2

Precision and accuracy of EDTA determination
(25 mV pulse amplitude, 5 mV s^{-1} scan rate, 0.6 ml of 500-p.p.m. Cd solution added per 10 ml sample with no equilibrium time allowed except where noted; standard addition analysis.)

Sample	EDTA found	Standard deviation	No. of detns.
$5.0 \cdot 10^{-6}$ M EDTA in Aquil, 0.1 M Ca^{2+} added[a]	$4.48 \cdot 10^{-6}$ M	$0.42 \cdot 10^{-6}$ M	4
$1.00 \cdot 10^{-5}$ M EDTA in SSW, no Ca^{2+} added	$0.93 \cdot 10^{-5}$ M	$3.5 \cdot 10^{-6}$ M	6
$5.00 \cdot 10^{-5}$ M EDTA + $5.24 \cdot 10^{-6}$ M NTA in SSW, no Ca^{2+} added[b]	$5.09 \cdot 10^{-5}$ M	$5.0 \cdot 10^{-6}$ M	5
$5.00 \cdot 10^{-5}$ M EDTA in SSW, 0.1 M Ca^{2+} added	$5.13 \cdot 10^{-5}$ M	$1.1 \cdot 10^{-6}$ M	5

[a]0.1 ml of 500 p.p.m. Cd solution added per 10-ml sample; cadmium spike equilibrated for 1 h before analysis.
[b]Simultaneous additions of NTA and EDTA.

The sensitivity of the technique is not as good as one might expect, considering the inherent sensitivity of d.p.p. The irreversible nature of the Cd—NTA and Cd—EDTA reductions results in currents only about 0.3 of those expected for a reversible reaction. Nonetheless, the technique is sufficiently precise and sensitive for use in the analysis of relatively poorly enriched media, which generally contain no less than 5 μM EDTA or 5 μM NTA, in addition to more traditional media which contain more than 10^{-4} M ligand.

Metal cation effects

Much of the work done here on phytoplankton productivity deals with copper speciation. The values of log K'_c with copper as the competing metal are 1.3 for NTA and 1.2 for EDTA. In a solution where $C_{Cu} > C_L$, the ligand should be associated primarily with copper unless $[Cd'] \geqslant 16[Cu']$ (for EDTA) or $[Cd'] \geqslant 20[Cu']$ (for NTA). This fact is of concern because only ligand associated with cadmium at the electrode surface will be reduced at the proper potential to be measured. In practice, the effect of copper is not predictable simply from its competition with cadmium in the bulk solution. The proposed technique is applicable to media containing sufficient copper to dissociate 95% of the Cd—NTA or Cd—EDTA complex in the bulk of solution [28]. Non-uniform distribution of ligand species within the polarographic cell reduces the effective copper competition. A slight decrease in sensitivity and precision is observed. Linearity is maintained, and the method of standard additions is used to obtain accurate results.

The presence of 10^{-5} M Ni, Zn or Co has no effect on the Cd—EDTA wave when $2.4 \cdot 10^{-4}$ M Cd is present. The cobalt and Cd—EDTA waves overlap only slightly. The same is true for the NTA wave, except that the nickel and Cd—NTA waves occur at nearly the same potential. This quantity of nickel is quite high for a phytoplankton medium, but if it were present it would likely reduce the sensitivity of the technique to a large extent by out-competing the cadmium for the NTA. No effect analogous to that observed in copper competition for NTA and EDTA or in Ni competition for EDTA was observed because the nickel complex is not reduced at a potential anodic of —0.9 V.

Iron is often added to phytoplankton media as the 1:1 complex with EDTA to satisfy the requirement of the organism for soluble iron. Often less iron is added. The effect of iron on the Cd—EDTA wave was examined in Tris-buffered SSW containing $2.3 \cdot 10^{-5}$ M EDTA and 0.1 M calcium. The addition of $2.3 \cdot 10^{-5}$ or $4.6 \cdot 10^{-5}$ M iron(III) caused no change in the Cd—EDTA peak height when $2.4 \cdot 10^{-4}$ M Cd was present. The effect of iron on NTA was not tested because 10^{-5} M NTA cannot effectively compete with hydroxide for Fe(III) and is therefore not associated with the iron.

Analysis of media

The preparation of a phytoplankton growth medium requires the addition of nutrients (N, P, Si) and micronutrients (trace metals, ligands, vitamins) to

SSW. Results presented in Tables 1 and 2 demonstrate the applicability of the technique to samples of medium containing $\geqslant 5$ μM ligand as well as synthetic sea water. No significant differences in precision or accuracy were observed between SSW and Cu-IV or Aquil analyses. The relative standard deviation of the technique is ca. 10% for 5 μM NTA or 5 μM EDTA.

Photodegradation of the artificial medium ASP 7 ($8.1 \cdot 10^{-5}$ M EDTA, $3.66 \cdot 10^{-4}$ M NTA) was examined under rather extreme conditions (direct sunlight, mid-summer, no temperature controls); rapid, but sometimes erratic disappearance of both NTA and EDTA (ca. 90% reduction in both ligands in 4 days) was observed. No such decreases were observed under normal culturing conditions over a period of two weeks. The relative standard deviation of replicate analyses was less than 5%.

The presence of 10^6 cells/ml of *Skeletonema costatum*, a marine diatom, in the medium decreases the reliability of measurements. Centrifugation of the sample is desirable when analyzing growing cultures.

This technique is useful for monitoring the ligand concentrations in a wide variety of media. It can be used for determinations of NTA and EDTA in Cu-IV and EDTA in Aquil, and is necessary if photodegradation or sorption of the ligand occurs in the culture. Although photodegradation was not observed in our experiments, it could occur in long-term experiments performed under higher light intensity. In addition, some pure cultures of marine phytoplankton have been reported to metabolize EDTA [29]. However, the precision of the technique limits its ability to measure reliably submicromolar changes in complexing capacity. If degradative processes do not occur, another technique [9] with somewhat better precision can be used to measure the production of EMBO. However, if degradation of ligand does occur, or if more than one strong ligand is present in the medium, this technique is applicable for specific measurement of $\geqslant 5 \cdot 10^{-6}$ M EDTA and NTA in media similar to sea water.

This research was supported by the Oceanography Section, National Science Foundation, Grant DES74-21642. The author thanks D. Rosin for aid in the experimental work.

APPENDIX

The conditional competition constants for Ca and Cd complexes of NTA and EDTA at pH 8 were determined from data applicable at $\mu = 0.1$ [24]. Corrections to change constants applicable at $\mu = 0.1$ to constants applicable at $\mu = 0.58$ were made by using Fig. 2.1 in the same reference.

	$\mu = 0.1$	$\mu = 0.58$
$\log K_{CdNTA}$	10.1	9.5
$\log K_{CdEDTA}$	16.5	16.0
$\log K_{CaNTA}$	6.4	5.8
$\log K_{CaEDTA}$	10.7	10.2
$\log \alpha_{NTA(H^+)}$	1.8	1.7
$\log \alpha_{EDTA(H^+)}$	2.3	2.2
$\log \beta_{CdCl}$	1.6	1.4
$\log \beta_{CdCl_2}$	2.1	1.9
$\log \alpha_{Cd(Cl)}$	—	1.5

$\log K'_{CdNTA} = 9.5-1.7-1.5 = 6.3$ ($\mu = 0.58$)
$\log K'_{CaNTA} = 5.8-1.7 = 4.1$ ($\mu = 0.58$)

$\log K'^{NTA}_{Cd,Ca} = 4.1-6.3 = -2.2$ ($\mu = 0.58$)
$\log K'_{CdEDTA} = 16.5-2.2-1.5 = 12.8$ ($\mu = 0.58$)
$\log K'_{CaEDTA} = 10.7-2.2 = 8.5$
$\log K'^{EDTA}_{Cd,Ca} = 8.5-12.8 = -4.3$ ($\mu = 0.58$)

REFERENCES

1 L. Provasoli, J. J. A. McLaughlin, and M. R. Droop, Archiv Mikrobiol., 25 (1957) 392.
2 E. Steemann Nielsen and S. Wium-Andersen, Physiol. Plant, 24 (1971) 480.
3 T. P. Murphy, D. R. S. Lean, and C. Nalewajko, Science, 192 (1976) 900.
4 M. Levandowsky and S. H. Hutner, Ann. N.Y. Acad. Sci., 245 (1974) 16.
5 S. S. Jones and F. Long, J. Phys. Chem., 56 (1952) 25.
6 R. J. Stolzberg and D. N. Hume, Environ. Sci. Technol., 9 (1975) 654.
7 C. Langford, M. Wingham, and V. Sastri, Environ. Sci. Technol., 7 (1973) 820.
8 T. Trott, R. Henwood, and C. Langford, Environ. Sci. Technol., 6 (1972) 367.
9 R. J. Stolzberg and D. Rosin, Anal. Chem., 49 (1977) 226.
10 H. A. Mottola, Toxicol. Environ. Chem. Rev., 2 (1974) 99.
11 R. J. Stolzberg and D. N. Hume, Anal. Lett., 6 (1973) 829.
12 W. Aue, C. Hastings, K. Gerhard, J. Pierce, H. Hill and R. Moseman, J. Chromatogr., 72 (1972) 259.
13 C. Warren and E. Malec, J. Chromatogr., 64 (1972) 219.
14 R. Daniel and R. LeBlanc, Anal. Chem., 31 (1959) 1221.
15 B. Afghan and P. Goulden, Environ. Sci. Technol., 5 (1971) 601.
16 J. Asplund and E. Wänninen, Anal. Lett., 4 (1971) 267.
17 J. Wernet and K. Wahl, Fresenius' Z. Anal. Chem., 251 (1970) 373.
18 J. P. Haberman, Anal. Chem., 43 (1971) 63.
19 J. Koryta and I. Kössler, Collect. Czech. Chem. Commun., 15 (1950) 241.
20 B. Raspor and M. Branica, J. Electroanal. Chem., 59 (1975) 99.
21 B. Raspor and M. Branica, J. Electroanal. Chem., 45 (1973) 79.
22 B. Raspor and M. Branica, J. Electroanal. Chem., 60 (1975) 335.
23 R. W. Schmid and C. N. Reilley, J. Am. Chem. Soc., 80 (1958) 2101.
24 A. Ringbom, Complexation in Analytical Chemistry, Interscience (1963).
25 T. R. Gilbert and D. N. Hume, Anal. Chim. Acta, 65 (1973) 451.
26 D. Maljkovic and M. Branica, Limnol. Oceanogr., 16 (1971) 779.
27 F. M. M. Morel, J. C. Westall, J. G. Reuter, and J. P. Chaplick, Technical Note No. 16, Ralph M. Parsons Laboratory, M.I.T., Cambridge, Mass., Sept. 1974.
28 R. J. Stolzberg, Anal. Chim. Acta, 92 (1977) 193.
29 W. R. Taylor, Biol. Bull., 127 (1964) 392.

Analytica Chimica Acta, 92 (1977) 149—154

VINYLOGE ACYLVERBINDUNGEN
Mitt. XVI. Spektrophotometrische Bestimmung toxikologisch relevanter 2-Halogenvinylketone mittels 4-(4-Nitrobenzyl)-pyridin [1]

GERHARD W. FISCHER

Forschungsstelle für chemische Toxikologie der Akademie der Wissenschaften der DDR, Johannesallee 20, DDR-701 Leipzig (D.D.R.)

(Eingegangen am 8. März 1977)

ZUSAMMENFASSUNG

2-Halogenvinylketone des Typs R—CO—CH=CH—X bilden mit überschüssigem 4-(4-Nitrobenzyl)-pyridin (NBP) bereits ohne Anwendung einer zusätzlichen Base NBP-Farbstoffe und lassen sich daher auch in Gegenwart alkylierender Agentien spektrophotometrisch bestimmen. Die Empfindlichkeit der Methode liegt für $E = 0.001$ bei $1.8—4.0 \cdot 10^{-4}$ μmol ml^{-1} cm^{-1}, die ebenfalls variierende Bestimmungsgrenze unterhalb 0.01 μmol ml^{-1} cm^{-1} und die relative Standardabweichung im mittleren Extinktionsbereich unterhalb ± 2%. Es werden Störmöglichkeiten diskutiert und für die Bestimmung von 20 *trans*-konfigurierten 2-Halogenvinylketonen Absorptionsmaxima, Extinktionswerte und deren relative Standardabweichungen mitgeteilt.

SUMMARY

Vinylogous acyl compounds. Part XVI. Spectrophotometric determination of toxicologically relevant 2-halovinyl ketones with 4-(4-nitrobenzyl)pyridine

2-Halovinyl ketones of the type R—CO—CH=CH—X react with excess of 4-(4-nitrobenzyl)pyridine (NBP) to give NBP-dyes without using an additional base, and can therefore be determined spectrophotometrically even in the presence of alkylating agents. The sensitivity of the method lies at $1.8—4.0 \cdot 10^{-4}$ μmol ml^{-1} cm^{-1} for $E = 0.001$, and the determination limit below 0.01 μmol ml^{-1} cm^{-1}; the relative standard deviation in the middle absorbance range is below ± 2%. Possible interferences are discussed and wavelengths of maximum absorption, absorbance values and their relative standard deviation for the determination of 20 *trans*-2-halovinyl ketones are given.

Für die spektrophotometrische Bestimmung alkylierender Agentien hat ihre Umsetzung mit 4-(4-Nitrobenzyl)-pyridin (NBP) zu farblosen 1-Alkyl-4-(4-nitrobenzyl)-pyridiniumsalzen (I) und deren anschließende Deprotonierung zu tieffarbigen 1-Alkyl-4-(4-nitrobenzyliden)-1,4-dihydropyridinen (II) Bedeutung erlangt [2]. Diese auf Koenigs et al. [3] zurückgehende und im Arbeitskreis um Epstein [4] eingehender auf analytische Brauchbarkeit

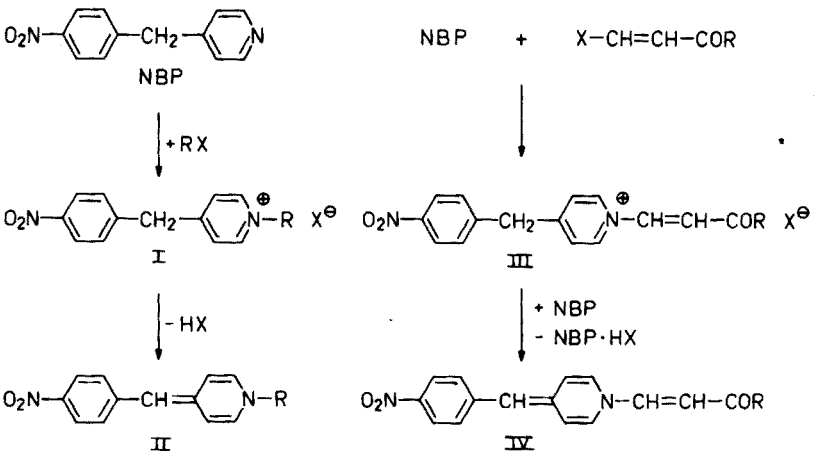

untersuchte Farbreaktion wurde angesichts der ausgedehnten Verbreitung alkylierender Agentien in der menschlichen Umwelt und der damit verbundenen toxischen Risiken [5] in den vergangenen Jahren wiederholt mit dem Ziel modifiziert, höhere Nachweisempfindlichkeiten zu erreichen [6, 7] ode weitere Verbindungsklassen mit alkylierenden Eigenschaften zu erfassen [8,

Die Frage nach geeigneten Nachweis- und Bestimmungsverfahren erhob sich auch bei Vinylhalogeniden der Struktur R—CO—CR′=CR″—X, die in jüngster Zeit als reaktive Synthesebausteine [10—15] zunehmend an Interes gewinnen, wegen ihrer teils beträchtlichen akuten Giftigkeit [16] sowie ihre haut-bzw. schleimhautschädigenden Wirkung [17—19] toxikologisch jedoch nicht unbedenklich sind. Nachdem in vorangegangenen Arbeiten die Umsetzung aktivierter Vinylhalogenide zu NBP-Farbstoffen [20] und ein darauf beruhendes dünnschichtchromatographisches Detektionsverfahren [1 mitgeteilt wurden, soll im folgenden über die spektrophotometrische Bestimmung von 2-Halogenvinylketonen R—CO—CH=CH—X mittels einer modifizierten NBP-Reaktion berichtet werden.

EXPERIMENTELLES

Geräteausrüstung

Die Untersuchungen wurden mit Hilfe eines mit einem Digitalvoltmeter gekoppelten Pye Unicam SP 8000 UV-Spektrophotometers unter Verwendu von 1 cm-Küvetten durchgeführt. Die Messungen erfolgten im Meßbereich $E = 0$ bis 1.

Chemikalien

Die *trans*-konfigurierten 2-Halogenvinylketone R—CO—CH=CH—X wurde nach bekannten Methoden hergestellt: im Falle R = Alkyl, X = Cl aus Acylchloriden und Acetylen [12, 18], im Falle R = Aryl, X = Cl aus 2-Hydroxyvinylketonen und Thionylchlorid [12] und im Falle R = Aryl,

X = J aus entsprechenden Aroylvinylphosphaten und Natriumjodid [21]. NBP kam als Präparat der EGA-Chemie KG Keppler u. Reif (Steinheim, B.R.D.) zum Einsatz. Als Lösungsmittel dienten absolutes Benzol p.A. und absolutes Äthanol p.A.

Standardvorschrift für die Bestimmung von 2-Halogenvinylketonen des Typs R—CO—CH=CH—X

Die benzolische Probelösung (0.5 ml mit 0.005—0.1 μmol 2-Halogenvinylketon) wird in einem 5 ml-Maßkolben mit 2 ml äthanolischer 5% NBP-Lösung 30 Min auf 60°C erhitzt. Nach dem raschen Abkühlen auf Raumtemperatur füllt man mit absolutem Äthanol auf 5 ml auf, mißt die Extinktion bei der für den jeweiligen Farbstoff charakteristischen Wellenlänge (vgl. Tab. 1) gegen eine analog behandelte Vergleichslösung ohne 2-Halogenvinylketon und ermittelt den Gehalt an letzterem aus der mit Standardlösungen erhaltenen Eichgeraden (Beispiele s. Abb. 2).

ERGEBNISSE UND DISKUSSION

Die Farbstoffbildung aus NBP und 2-Halogenvinylketonen vollzieht sich nach dem gleichen Schema wie im Falle alkylierender Agentien. Während dort jedoch die Abwandlung der primär entstehenden Pyridiniumsalze (I) zu den meist blauvioletten Dihydropyridinen (II) gewöhnlich stärkere Basen wie Triäthylamin, Piperidin oder Alkali erfordert, bilden 2-Halogenvinylketone entsprechende Farbstoffe (IV) bereits ohne Anwendung einer Fremdbase. Die Deprotonierung der Quartäsalze (III) erfolgt hier auf Grund der stark acidifizierten Benzyl-CH_2-Gruppe bereits durch überschüssiges NBP selbst [20].

Der Auswahl der Reaktionsbedingungen liegen Untersuchungen über den zeitlichen Verlauf der Farbstoffbildung sowie über die Stabilität der entstehenden Farbstoffe (IV) zugrunde. Wie aus Abb. 1 hervorgeht, sind unter den in der Standardvorschrift angegebenen Bedingungen die reaktiveren 2-Halogenvinyl-arylketone (Beispiele A und B) bereits nach 30 Min soweit umgesetzt, daß längeres Erhitzen keine wesentliche Extinktionserhöhung mehr bewirkt. Bei Einhaltung der genannten Reaktionszeit, Begrenzung der Reaktionstemperatur auf 60°C und Verwendung eines geeigneten Lösungsmittelgemisches wie Benzol—Äthanol als Reaktionsmedium fällt die bei drastischeren Bedingungen zu beobachtende Farbstoffzersetzung noch nicht ins Gewicht.

Abbildung 2 demonstriert an einigen Beispielen die Linearität der Eichkurven bei Einsatz von 2-Halogenvinylketonen in Konzentrationen bis zu 0.2 μmol ml^{-1}. Die Empfindlichkeit [22] der Bestimmungsmethode variiert je nach Reaktivität der Halogenverbindungen und Größe des molaren Extinktionskoeffizienten der betreffenden NBP-Farbstoffe, im Falle der bisher untersuchten Verbindungen im Bereich von $1.8—4.0 \cdot 10^{-4}$ μmol ml^{-1} cm^{-1} für $E = 0.001$. Für 2-Chlorvinyl-phenylketon (Beispiel A) liegt die Empfindlichkeit z.B. mit $1.98 \cdot 10^{-4}$ μmol ml^{-1} cm^{-1} ($E = 0.001$) doppelt so hoch wie

TABELLE 1

Angaben zur NBP-Reaktion verschiedener *trans*-2-Halogenvinylketone (Umsetzung von 0.05 μmol 2-Halogenvinylketon gemäß Vorschrift S. 151.)

2-Halogenvinylketon	λ_{max} (nm)	E^a	s_r (%)
CH_3—CO—CH=CH—Cl	480	0.251	1.9
C_2H_5—CO—CH=CH—Cl	482	0.292	1.8
n—C_3H_7—CO—CH=CH—Cl	485	0.347	1.2
i—C_3H_7—CO—CH=CH—Cl	484	0.362	1.3
C_6H_5—CO—CH=CH—Cl	498	0.506	0.9
4—CH_3—C_6H_4—CO—CH=CH—Cl	498	0.509	0.6
4—C_2H_5—C_6H_4—CO—CH=CH—Cl	498	0.512	0.7
4—CH_3O—C_6H_4—CO—CH=CH—Cl	498	0.508	0.5
4—F—C_6H_4—CO—CH=CH—Cl	496	0.532	0.8
4—Cl—C_6H_4—CO—CH=CH—Cl	498	0.542	0.8
4—Br—C_6H_4—CO—CH=CH—Cl	500	0.552	0.7
4—J—C_6H_4—CO—CH=CH—Cl	501	0.502	0.8
4—O_2N—C_6H_4—CO—CH=CH—Cl	512	0.493	0.4
4—C_6H_5—C_6H_4—CO—CH=CH—Cl	502	0.501	0.8
2,4—$(CH_3)_2C_6H_3$—CO—CH=CH—Cl	490	0.500	0.9
2,4,6—$(CH_3)_3C_6H_2$—CO—CH=CH—Cl	480	0.417	0.4
1—$C_{10}H_7$—CO—CH=CH—Cl[b]	493	0.490	0.6
2—C_4H_3S—CO—CH=CH—Cl[c]	502	0.538	0.3
4—CH_3—C_6H_4—CO—CH=CH—J	498	0.520	0.7
4—Cl—C_6H_4—CO—CH=CH—J	498	0.561	0.7

[a] Mittelwert aus 20 Bestimmungen. [b] 1—$C_{10}H_7$ = 1—Naphthyl. [c] 2—C_4H_3S = 2—Thienyl.

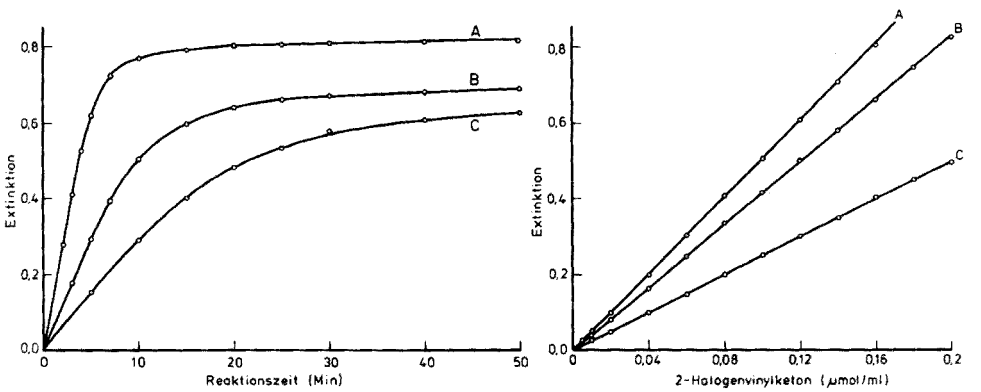

Abb. 1. Zeitlicher Verlauf der Farbstoffbildung. Umsetzung von 0.08 μmol 2-Chlorvinyl-phenylketon (A), 2-Chlorvinyl-2,4,6-trimethylphenylketon (B) und 2-Chlorvinyl-isopropylketon (C) unter den Bedingungen der Standardvorschrift (Absorptionsmaxima s. Tab. 1).

Abb. 2. Eichkurven für die Bestimmung von 2-Chlorvinyl-phenylketon (A), 2-Chlorvinyl-2,4,6-trimethylphenylketon (B) und 2-Chlorvinyl-methylketon (C) (Absorptionsmaxima s. Tab. 1).

für 2-Chlorvinyl-methylketon (Beispiel C) mit $3.98 \cdot 10^{-4}$ μmol ml^{-1} cm^{-1} ($E = 0.001$). Die ebenfalls variierende Bestimmungsgrenze [22] liegt bei Benutzung des Meßbereiches $E = 0$ bis 1 für die meisten 2-Halogenvinylketone unterhalb 0.01 μmol ml^{-1} cm^{-1}, für 2-Chlorvinyl-phenylketon z.B. bei 0.002 μmol ml^{-1} cm^{-1} ($S_1 = 95\%$).

Die unter den angegebenen Reaktionsbedingungen für eine Reihe *trans*-konfigurierter 2-Halogenvinylketone charakteristischen Farbstoffmaxima sowie die nach Umsetzung von jeweils 0.05 μmol 2-Halogenvinylketon gemessenen Extinktionen und deren relative Standardabweichungen sind in Tabelle 1 zusammengestellt. Die s_r-Werte der niederen aliphatischen 2-Chlorvinylketone (1.2 bis 1.9%) liegen höher als die der aromatischen Derivate (0.3 bis 0.9%) und steigen mit zunehmender Flüchtigkeit der Verbindungen an. Die Art des reaktiven Halogens (z.B. Cl oder J) in den 2-Halogenvinylketonen hat erwartungsgemäß auf die Lage des Absorptionsmaximums keinen Einfluß. Hingegen bedarf es bei Änderung der Lösungsmittelzusammensetzung einer Neubestimmung der Absorptionslage, da die NBP-Farbstoffe (IV) ebenso wie die 1-Alkyldihydropyridine (II) als typische Merocyanine eine ausgeprägte Solvatochromie zeigen [20].

Durch ihre spontane Farbstoffbildung unterscheiden sich 2-Halogenvinylketone charakteristisch von alkylierenden Agentien und sind daher in deren Gegenwart bestimmbar. Wie aus Tabelle 2 am Beispiel des 2-Chlorvinylphenylketons ersichtlich, bleibt der Einfluß eines äquimolaren Zusatzes Dimethylsulfat innerhalb der $3s_r$-Grenze. Das reaktionsträgere Diäthylsulfat ist noch in 10fachem Überschuß ohne signifikanten Einfluß und viele Alkylhalogenide stören selbst in 100fachem Überschuß nicht.

Eine Beeinträchtigung der Bestimmung von 2-Halogenvinylketonen ist dagegen generell durch solche Verbindungen zu erwarten, die wie erstere zur

TABELLE 2

Einfluß alkylierender und acylierender Agentien auf die NBP-Reaktion von 0.05 μmol 2-Chlorvinyl-phenylketon
($\lambda_{max} = 498$ nm, $E_o = 0.506$[a], $s_r = 0.9\%$, $3s_r = 2.7\%$)

Zugesetztes Agens	E[b]	s_r (%)	$\frac{E_o - E}{E_o}$ (%)
0.05 μmol Dimethylsulfat	0.493	1.5	−2.6
0.1 μmol Diäthylsulfat	0.504	1.6	−0.4
0.5 μmol Diäthylsulfat	0.500	1.7	−1.2
5.0 μmol n-Propylbromid	0.495	1.2	−2.2
5.0 μmol n-Butylbromid	0.498	1.7	−1.6
5.0 μmol Benzylchlorid	0.505	1.0	−0.2
0.05 μmol Benzoylchlorid	0.510	0.6	+0.8
0.5 μmol Benzoylchlorid	0.554	0.9	+9.5

[a] E_o = Extinktion ohne Zusatz. [b] Mittelwert aus 20 Bestimmungen.

elektronegativen NBP-Quarternierung befähigt sind und daher ebenfalls ohne Anwendung einer Fremdbase zu NBP-Farbstoffen führen. Hierzu gehören neben anderen aktivierten Vinylhalogeniden (z.B. vinylogen Vilsmeier-Reagentien [20]) auch aktivierte Arylhalogenide (z.B. 2,4-Dinitrochlorbenzol) und Carbonsäurehalogenide [4, 6, 7, 20, 23]. Im Falle der letzteren erfolgt die glatte Bildung der Farbstoffe allerdings nur in hydroxylgruppenfreien Medien [20, 23], andernfalls kommt es zur teilweisen Solvolyse der reaktiven Pyridinium-Intermediate. Bei Verwendung eines äthanolhaltigen Reaktionsmediums gemäß eingangs angegebener Standardvorschrift machen sich daher Carbonsäurehalogenide meist erst in größerem Überschuß störend bemerkbar (vgl. Tab. 2). 2-Chlorvinylcarbonylverbindungen mit Alkyl- oder Arylsubstituenten in 2-Stellung treten unter gleichen Bedingungen nicht mit NBP in Reaktion.

LITERATUR

1 G. W. Fischer, J. Chromatogr., 177 (1976) 137 [XV. Mitt.].
2 B. Kakáč und Z. J. Vejdělek, Handbuch der photometrischen Analyse organischer Verbindungen, Verlag Chemie, Weinheim/Bergstr., 1974, S. 612, 662, 694, 720 und 739.
3 E. Koenigs, K. Köhler und K. Blindow, Ber. Deut. Chem. Ges., 58 (1925) 933.
4 J. Epstein, R. W. Rosenthal und R. J. Ess, Anal. Chem., 27 (1955) 1435.
5 W. C. J. Ross, Biological Alkylating Agents, Butterworth, London, 1962; A. Loveless, Genetic and Allied Effects of Alkylating Agents, Butterworth, London, 1966; B. W. van Duuren (Hrsg.), Ann. N.Y. Acad. Sci., 163 (1969) 589.
6 E. Sawicki, D. F. Bender, T. R. Hauser, R. M. Wilson und J. E. Meeker, Anal. Chem., 35 (1963) 1479.
7 E. Sawicki und C. R. Sawicki, Ann. N.Y. Acad. Sci., 163 (1969) 895.
8 R. Preussmann, H. Hengy und H. Druckrey, Justus Liebigs Ann. Chem., 684 (1965) 57.
9 R. Preussmann, H. Schneider und F. Epple, Arzneim. Forsch., 19 (1969) 1059.
10 N. K. Kochetkov, Usp. Khim., 24 (1955) 32; C. A., 49 (1955) 7544; deutsche Version in: Chem. Tech. (Leipzig), 7 (1955) 518.
11 N. K. Kochetkov, Prakt. Chem. (Wien), 12 (1961) 336.
12 A. E. Pohland und W. R. Benson, Chem. Rev., 66 (1966) 161.
13 M. I. Rybinskaja, A. N. Nesmejanov und N. K. Kochetkov, Usp. Khim., 38 (1969) 961; C.A., 71 (1969) 48884.
14 H. Teufel, Chem. Ztg., 98 (1974) 606.
15 M. Pulst und M. Weißenfels, Z. Chem., 16 (1976) 337.
16 G. W. Fischer und F. Riemer, unveröffentlichte Ergebnisse.
17 Ch. C. Price und J. A. Pappalardo, J. Am. Chem. Soc., 72 (1950) 2613.
18 R. Gipp, in E. Müller (Hrsg.), Methoden der organischen Chemie (Houben-Weyl), Georg Thieme Verlag, Stuttgart, 4. Aufl., 1973, Bd. 7/2a, Ketone I, S. 480, insbesondere S. 483.
19 B. Cavalchi, D. Landini und F. Montanari, J. Chem. Soc. C, (1969) 1204.
20 G. W. Fischer, J. Prakt. Chem., 317 (1975) 779.
21 G. W. Fischer und P. Schneider, Chem. Ber., 106 (1973) 435.
22 O. G. Koch und G. A. Koch-Dedic, Handbuch der Spurenanalyse, 2. Aufl., Springer-Verlag, Berlin, 1974, S. 19.
23 A. M. Agree und R. L. Meeker, Talanta, 13 (1966) 1151.

Analytica Chimica Acta, 92 (1977) 155—161

SULFONEPHTHALEIN DYES
Part VI. Protolytic Equilibria of Glycinethymol Blue*

K. VYTŘAS** and F. J. LANGMYHR

Department of Chemistry, University of Oslo, Oslo - Blindern (Norway)

(Received 21st January 1977)

SUMMARY

Glycinethymol blue has been studied spectrophotometrically and by using complementary tristimulus colorimetry over the whole region of its protolytic equilibria. The purification of commercial preparations is described. The seven dissociation constants were determined; the means of the pK_a (H_iI) values for i = 7, 6, 5, etc., were found to be —2.61, —1.42, —0.6, 1.2, 6.98, 10.50, and 12.62, respectively.

About 40 papers dealing with glycinethymol blue have been published since 1957 when this sulfonephthalein dye was first prepared by Körbl et al. [2] during a search for new metallochromic indicators. The compound was originally recommended as an indicator for the complexiметric titration of copper(II), but has lately found broader application as a sensitive reagent for the spectrophotometric determination of a number of metals. Some of these papers also deal with the compositions of the complexes.

For analytical applications of glycinethymol blue and in detailed studies of its metal complex equilibria, it is highly desirable that the protolytic equilibria are known. Unfortunately, data are available only for a limited pH region [3, 4]. In view of the fact that metallochromic indicators are often impure, it is to be regretted that the latter two papers give no information on the purity or purification of the reagent employed.

EXPERIMENTAL

Instrumentation and methods of measurement

A Cary 14 spectrophotometer was used to record the absorption spectra. Britton—Robinson buffer solutions with addition of sodium chloride to ionic strength 0.2 were used. The pH values were measured with a Radiometer pH-meter 26 equipped with glass (Radiometer G202 B) and saturated calomel electrodes, and calibrated with buffer solutions of the conventional activity

*Part V: see ref. 1.

**On leave from Department of Analytical Chemistry, College of Chemical Technology, Pardubice, Czechoslovakia.

scale [5]. H_0 (or H_-) acidity functions [6] were used in the strongly acidic (or alkaline) region in media of sulphuric and formic acids (or sodium hydroxide). Calculations were made on a CDC 6500 computer with the FORTRAN IV transcription of the procedures published earlier [7]. The weighted ordinate method ($\Delta\lambda = 10$ nm) was used for the calculation of tristimulus values.

Glycinethymol blue

The purity of two commercial preparations (Fluka, Switzerland, and Lachema, Czechoslovakia) was tested by ascending paper chromatography. Whatman No. 2 paper was used with a mobile phase of acetic acid, butanol, and water (1:2:1). Both the reagents provided two colour components (Fig. 1): the first spot with the R_F value 0.60—0.64 (glycinethymol blue) and the second one with $R_F \approx 0.8$ (semi-glycinethymol blue). A spot of thymol blue, the parent compound (glycinethymol blue is synthesized from it, glycine, and formaldehyde by Mannich condensation), was visible only if a very high concentration of the Fluka reagent was used; a check with a standard showed that it had $R_F \approx 0.9$. It was estimated from the colour intensity of the spots that the amount of the semi-form was about 30% (Lachema), or more than 50% (Fluka). It is self-evident that, since the semi-form has similar acid-base colour changes, the results of a study of the protolytic equilibria of glycinethymol blue would be greatly distorted.

The following procedure proved to be satisfactory for the preparation of chromatographically pure glycinethymol blue. The commercial preparation (ca. 5 g, Lachema) and an excess of glycine (2 g) were dissolved in glacial acetic acid (50 ml), and a small amount of sodium hydroxide (as catalyst) and 2 ml of formaldehyde (40%) were added. The mixture was kept at

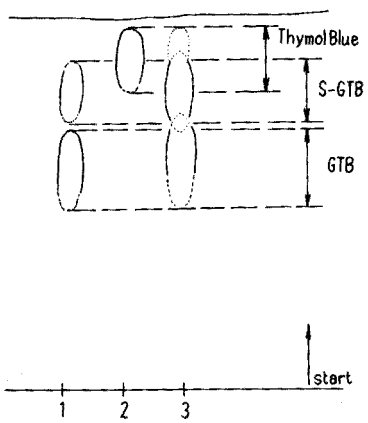

Fig. 1. Ascending paper chromatography of commercial preparations of glycinethymol blue (1, Lachema, 3, Fluka) and thymol blue (2, Riedel de Haën, West Germany). Whatman No. 2 paper, acetic acid—butanol—water (1:2:1).

50—60°C, and the progress of the reaction was checked by paper chromatography. When the intensity of the higher R_F spot was reduced to a minimum, the reaction mixture was allowed to stand overnight, and then the crude product was precipitated by adding ethanol (400 ml). The precipitate was separated by decantation, washed with ethanol, filtered, recrystallized from water, and dried at 50°C (first fraction, 12% of originally weighed amount). The ethanolic solution was mixed with diethyl ether; after standing, the sticky sediment formed on the bottom of the beaker was isolated by decantation, washed with an ethanol—ether (1 + 2) mixture, recrystallized from water, and dried at 50°C (second fraction, 18%). The remaining ethanolic solution was mixed with diethyl ether again and the precipitate isolated as described above (third fraction, 37%). The first and second fractions showed only one spot at $R_F \approx 0.6$ (the third fraction was negligibly contaminated by the semi-form), and the second had the highest absorptivity.

As the purified product could be a mixture of the acid (H_4I) and its monosodium salt, and in addition contain some sodium acetate, a strongly acidic cation-exchanger (Ionenaustauscher I, Merck) was applied to convert the dye completely to its acid form. About 200 mg of the above second fraction was dissolved in 15 ml of water, and the solution passed through a column containing some 5 ml of resin. As the free acid is less soluble in water than the sodium salt, it is partly precipitated in the column. The elution was therefore made by alternate passage of water and n-butanol. The eluates were collected, evaporated to dryness and dried in an oven at 50°C. The following results were obtained by elemental analysis (theoretical percentages for $C_{33}H_{40}O_9N_2S \cdot 2H_2O$ are given in parentheses): C, 59.3% (58.6%); H, 6.80% (6.55%); N, 3.57% (4·14%); S, 4.61% (4.74%); O (by difference), 25.8% (26.0%).

The stock solution of glycinethymol blue (0.1%, i.e. ca. $1.5 \cdot 10^{-3}$ M) was stabilized with a little nitric acid (5 drops/250 ml).

RESULTS AND DISCUSSION

Glycinethymol blue (H_4I) can take up (in acidic solutions) or lose (in alkaline solutions) several protons; thus its protolytic equilibria present a rather complicated system. The reactions and the colour changes connected with association or dissociation of hydrogen ions may be interpreted analogously to the equilibria of related sulfonephthalein dyes, e.g. xylenol orange [8, 9], methylthymol blue [10, 11], or methylxylenol blue [12], but the total number of dissociation constants of the present reagent is lower (see Fig. 2).

The first dissociation of the fully protonated cation H_7I^{3+} occurs in a concentrated sulphuric acid medium between $H_0 -5$ and -2.3. This dissociation of the hydrogen ion from the $-SO_3H$ group is accompanied by a decrease of the main absorption maximum at 551 nm and three isosbestic points (494, 427, ca. 385 nm) appear (Fig. 3A). The colour change accompanying the second dissociation is more distinctive, in agreement with the Schwarzenbach theory [13] of the molecular resonance system of sulfonephthalein dyes,

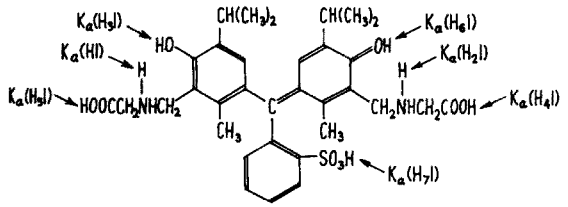

Fig. 2. Glycinethymol blue. Structure of the cation H_7I^{3+} with the dissociation constants marked.

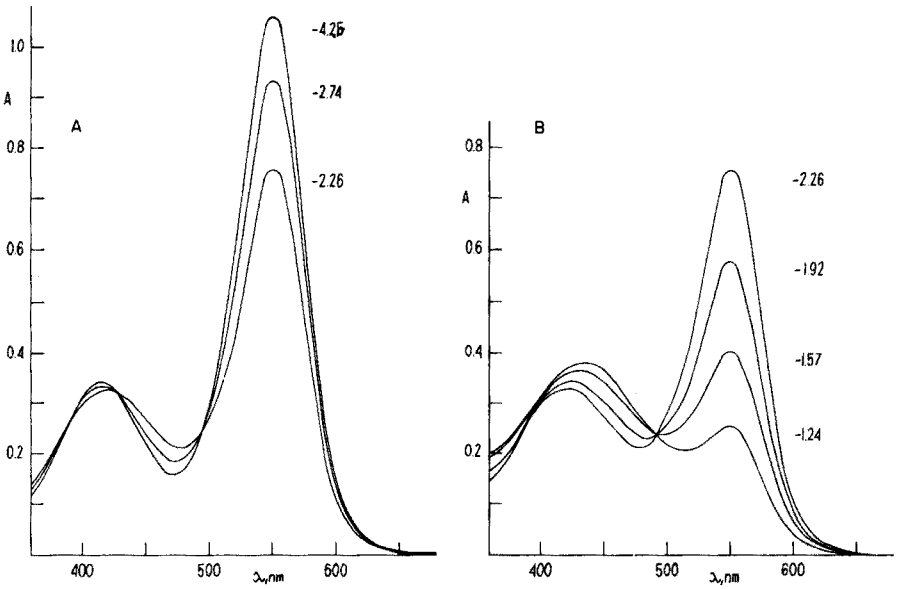

Fig. 3. Absorption spectra of glycinethymol blue in the H_0 (H_2SO_4) range marked. c_I = $3 \cdot 10^{-5}$ M, l = 10 mm, t = 20°C.

because the overall electron distribution in the chromophore system becomes asymmetrical after the hydrogen leaves the quinoid oxygen. With this colour transition from reddish purple to orange (the hue names are those proposed by Kelly [14]) there is an isosbestic point at 492 nm (Fig. 3B).

The colour changes accompanying the dissociation of the two protons from the carboxyl groups are not pronounced. Four absorption curves recorded between H_0 values of −1.18 and +0.13 showed an indistinct isosbestic point at 460—70 nm. Spectra taken at higher H_0 (or pH) values (+0.13 to +1.91) showed another isosbestic point at ca. 410 nm, and at this stage the maximum at 551 nm vanished. Solutions of pH 2—4 are yellow and do not exhibit any differences in their absorption spectra (λ_{max} = 437 nm).

Another marked colour change is observed between pH 5 and 9 when the hydroxyl proton dissociates and a symmetric molecule is formed again (Fig. 4A). This colour transition to purplish blue is characterized by a new absorption band at 603 nm and by an isosbestic point at 487 nm. Further

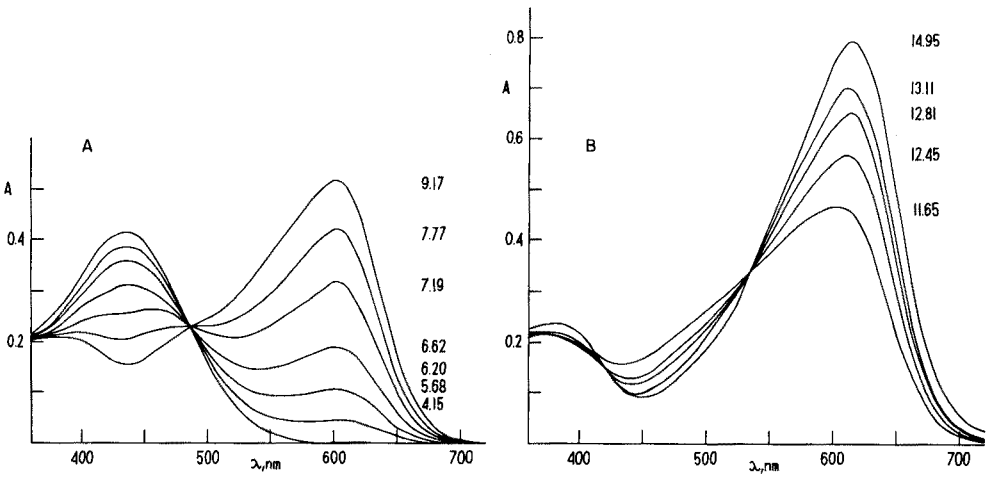

Fig. 4. Absorption spectra of glycinethymol blue at the marked values of pH (4.15—12.81) or H_ function. $c_I = 3 \cdot 10^{-5}$ M, $l = 10$ mm, $I = 0.2$ (except the value 14.95), $t = 20°C$.

increase of pH from 9.5 to 11 causes dissociation of the protons on the nitrogen atoms which are hydrogen-bonded to the oxygens in the 4 and 4′-positions (see Fig. 2). In accordance with the statement of Körbl et al. [2], the decrease in colour intensity which attends the formation of the asymmetric ion HI in the case of methylthymol blue [10, 11] is not sufficiently marked in glycinethymol blue to be distinguished visually (there is only a small colour difference between the purplish blue and bluish purple hues, with three ill-defined isosbestic points at 540, 420, and 375 nm). However, the last dissociation (Fig. 4B; isosbestic points at 533 and ca. 420 nm) is characterized by the formation of a pure blue colour ($\lambda_{max} = 614$ nm).

In strongly alkaline solutions ($H_- > 16$) the colour faded on standing, which may be connected with carbinol formation as reported [15] for a number of sulfonephthalein dyes.

It has been found very useful to represent the protolytic equilibria of glycinethymol blue by calculating the values of the complementary tristimulus system. Although the colour changes connected with some dissociations are not easily distinguished, they can be read quite well from the course of the overall transition curve in the complementary Q_xQ_y triangle (Fig. 5).

The dissociation constants were evaluated from the values of the tristimulus components X_c, Y_c, Z_c (their pH dependence is shown in Fig. 6), or the modified tristimulus values were used; for the methods of evaluation of equilibrium constants by complementary tristimulus colorimetry, see refs 16—18 or a review [19]. The graphical evaluation was completed by statistical treatment based on linear regression analysis. It is, however, evident that the constants of the equilibria connected with small colour changes ($H_5I \rightleftharpoons$

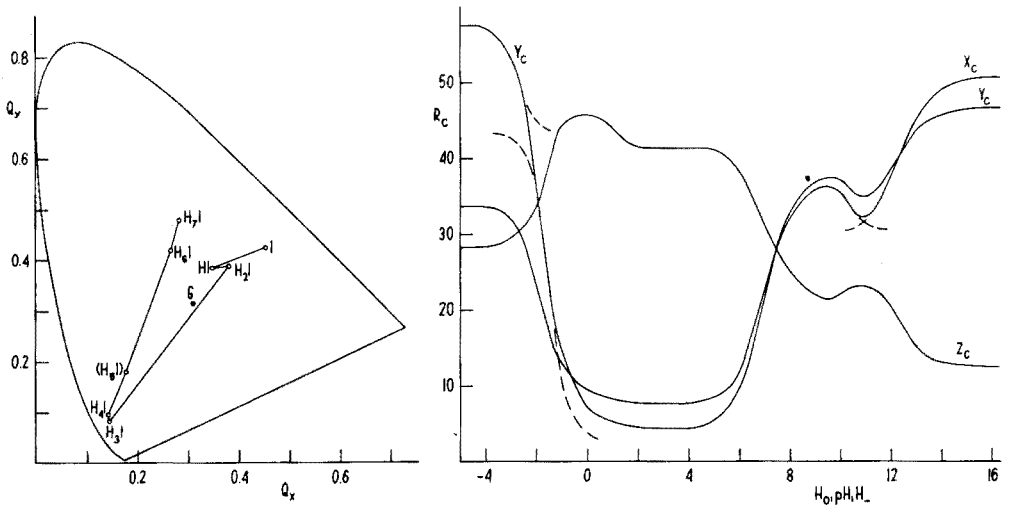

Fig. 5. Colour transitions of glycinethymol blue in the Q_xQ_y complementary tristimulus diagram with marked colour points of the individual species. G - grey point (corresponding to the CIE standard source C).

Fig. 6. R_c—pH curves of glycinethymol blue solutions.

$H_4I \rightleftharpoons H_3I$) are of low precision. All the results are summarized in Table 1.

Of the present data only two could be compared with values published earlier Akhmedli and Babaeva [3] have reported a $pK_a(H_3I)$ value of 6.05, 6.9, or 7.05, and a $pK_a(H_2I)$ value of 8.3, 9.7, or 10.05; these values were obtained by three different methods and their mutual agreement is not very satisfactory. The distribution diagram for glycinethymol blue given by Akhmedli et al. (see Fig. 2b in ref. 20) differs considerably from the constants evaluated [3]. A $pK_a(H_3I)$ value of ca. 7.3 was estimated from the absorption spectra

TABLE 1

Dissociation constants of glycinethymol blue[a]

Equilibrium	$pK_a(H_iI)$		
	n	$\bar{x}$	s
$H_7I^{3+} \rightleftharpoons H_6I^{2+} + H^+$	4	−2.61	0.08
$H_6I^{2+} \rightleftharpoons H_5I^+ + H^+$	5	−1.42	0.02
$H_5I^+ \rightleftharpoons H_4I + H^+$	4	−0.6	0.3
$H_4I \rightleftharpoons H_3I^- + H^+$	4	1.2	0.2
$H_3I^- \rightleftharpoons H_2I^{2-} + H^+$	10	6.98	0.02
$H_2I^{2-} \rightleftharpoons HI^{3-} + H^+$	5	10.50	0.03
$HI^{3-} \rightleftharpoons I^{4-} + H^+$	8	12.62	0.03

[a]For statistical evaluation, see ref. 21; n, number of points considered; $\bar{x}$, average value; s, standard deviation.

reported by Zielinski et al. [4]. In the latter investigation unpurified reagent was used and this may explain the discrepancy.

REFERENCES

1 K. Vytřas, V. Mach and M. Malcová, Chem. Zvesti, in press.
2 J. Körbl, E. Kraus and R. Přibil, Chem. Listy, 51 (1957) 1809; Collect. Czech. Chem. Commun., 23 (1958) 1219.
3 M. K. Akhmedli and T. R. Babaeva, Uch. Zap. Azerb. Gos. Univer., Ser. Khim. Nauk, (3) (1965) 31.
4 S. Zielinski, L. Lomozik and J. Andrzejewska, Zh. Neorg. Khim., 20 (1975) 329.
5 D. D. Perrin and B. Dempsey, Buffers for pH and Metal Ion Control, Chapman and Hall, London, 1974, p. 40.
6 C. H. Rochester, Acidity Functions, Academic Press, London, 1970, pp. 28, 54, 237.
7 K. Vytřas and S. Kotrlý, Sb. Věd. Pr., Vys. Šk. Chemickotechnol., Pardubice, 26 (1971) 3.
8 B. Řehák and J. Körbl, Collect. Czech. Chem. Commun., 25 (1960) 797.
9 M. Murakami, T. Yoshino and S. Harasawa, Talanta, 14 (1967) 1293.
10 J. Körbl and B. Kakáč, Chem. Listy, 51 (1957) 1680; Collect. Czech. Chem. Commun., 23 (1958) 889.
11 T. Yoshino, H. Imada, S. Murakami and M. Kagawa, Talanta, 21 (1974) 211.
12 K. Vytřas and J. Vytřasová, Chem. Zvesti, 28 (1974) 779.
13 G. Schwarzenbach, M. Brandenberger, G. H. Ott and O. Hagger, Helv. Chim. Acta, 20 (1937) 490.
14 K. L. Kelly, J. Res. Natl. Bur. Standards, 31 (1943) 271; J. Opt. Soc. Am., 33 (1943) 627.
15 S. Hochberg and V. K. LaMer, J. Am. Chem. Soc., 63 (1941) 3110.
16 C. N. Reilley and E. M. Smith, Anal. Chem., 32 (1960) 1233.
17 H. Flaschka, Talanta, 8 (1961) 342.
18 M. Morin, M. M. Petit-Ramel, J. P. Scharff and M. R. Paris, Can. J. Chem., 51 (1973) 2186.
19 K. Vytřas, J. Vytřasová and S. Kotrlý, Chem. Listy, 70 (1976) 234.
20 M. K. Akhmedli, A. E. Klygin, L. I. Ivanova and E. A. Bashirov, Zh. Neorg. Khim., 19 (1974) 2007.
21 K. Eckschlager, Errors, Measurements and Results in Chemical Analysis, Van Nostrand, London, 1969, p. 142.

Analytica Chimica Acta, 92 (1977) 163—169

SIMPLE CONDITIONS FOR THE USE OF FERROIN INDICATOR IN CERIMETRIC TITRATIONS OF ANTIMONY(III) ALONE AND IN MIXTURES WITH ARSENIC(III)

G. GOPALA RAO* and S. G. VISWANATH

Department of Chemistry, Andhra University, Waltair (India)

(Received 25th September 1976)

SUMMARY

The titration of antimony(III) with cerium(V) sulphate in the presence of ferroin indicator at room temperature is entirely satisfactory in media consisting of 50% (v/v) acetic acid and 1—3 M hydrochloric acid. In the absence of acetic acid, ferroin reacts with the antimony(V) formed in the very early stages, to give a sparingly soluble red complex, which remains in suspension and resists oxidation by cerium(IV). This titration provides a rational method for sequential visual titrations of antimony(III) and arsenic(III). The composition of the ferroin—antimony(V) complex is discussed. Titrations of antimony(III) in 0.5—1 M sulphuric acid medium do not require acetic acid but need iodine monochloride catalyst.

Willard and Young [1] reported that antimony(III) can be titrated accurately at 50°C with cerium(IV) sulphate in the presence of ferroin indicator and iodine monochloride catalyst in a medium containing 15% (v/v) hydrochloric acid. Later workers [2, 3] found ferroin to be very unsatisfactory and recommended the use of irreversible indicators. During developmental work here, it was observed that, if a few drops of 0.1 M cerium(IV) sulphate solution were added to a solution of antimony(III) in 1—3 M hydrochloric acid containing 1—2 drops of ferroin, the solution became turbid; the turbidity did not disappear nor did the red colour of ferroin fade on adding further quantities of cerium(IV) sulphate. However, when the titration medium contained acetic acid (50% v/v), no turbidity appeared and the usual alternate fading and reappearance of the ferroin colour occurred as cerium(IV) sulphate was added, up to the stoichiometric end-point, where the pale blue colour of ferriin remained stable for over 90 min. This observation allows accurate titrations of antimony(III) to be achieved with ferroin as indicator at room temperature.

EXPERIMENTAL

Reagents

Antimony(III) solutions (0.05 N). A solution in 3 M hydrochloric acid was prepared from AnalaR antimony(III) chloride and standardized with cerium(IV)

sulphate [4] and by the bromate method [5]. For the solution in 2 M sulphuric acid, the requisite quantity of antimony(III) oxide was dissolved in hot concentrated sulphuric acid, cooled and treated with sufficient hydrochloric acid to give a solution 2 M in sulphuric acid and 0.7 M in hydrochloric acid after dilution to 1 l; this was standardized as below.

Potassium antimony tartrate. An aqueous solution, 0.05 N with respect to antimony(III), was prepared from the AnalaR salt (tartar emetic).

Cerium(IV) sulphate solution (0.05 M). A solution in 0.05 M sulphuric acid was prepared from cerium(III) carbonate (Indian Rare Earths Ltd.) and standardized against AnalaR arsenic(III) oxide [6].

The acetic acid used was Merck's pro analysi grade. It must be noted that some brands of acetic acid, although labelled analytical reagent grade, contain traces of impurities which react with cerium(IV) sulphate in the presence of ferroin indicator.

The indicator solutions (0.01 M) contained the iron(II) complexes of 1,10-phenanthroline or 2,2′-bipyridine, prepared as described by Kolthoff and Belcher [7].

Recommended procedure for the titration of antimony(III) in hydrochloric acid medium

Treat 4—10 ml of 0.05 N antimony(III) solution with enough hydrochloric acid and glacial acetic acid to give the required acidity (1—3 M) in hydrochloric acid and 50% (v/v) in acetic acid. Dilute to 50 ml and add 1—2 drops of ferroin or bipyridine solution. Titrate with 0.05 M cerium(IV) sulphate solution at the usual speed in the early stages and with a wait of 5 s between drops 0.2—0.3 ml before the end-point. In this region the reduction of pale blue ferriin by antimony(III) to the red ferroin is somewhat slow. This is an advantage as it warns of the approach of the end-point, in contrast to titrations of iron(II), etc. After the end-point, the pale blue colour of ferriin is stable for over 90 min, when the ferroin colour slowly returns. In the case of the bipyridine indicator, the oxidized indicator decomposes irreversibly about 2 min after the end-point.

A concentration of acetic acid less than 50% (v/v) does not give satisfactory results in titrations of 0.05 N antimony(III) solutions. However, 30% (v/v) suffices in the titration of 0.01 N antimony(III) solutions with 0.01 M cerium(IV) sulphate, provided that a suitable indicator correction is applied. Typical results (Table 1) show that the procedure is subject to a relative error of ± 0.2%.

Interferences. Sulphuric acid or sulphate ion does not interfere up to a concentration of 0.05 M. Copper(II) and manganese(II) do not interfere up to 0.5 meq. Phosphoric acid interferes because cerium(IV) forms a gelatinous precipitate which adsorbs ferroin. Even large amounts of lead do not interfere, so that even small quantities of antimony can be determined in lead. If iron(II) is present, the titration volume corresponds to the total of antimony(III) and iron(II).

TABLE 1

Titration of antimony(III) in 1—3 M hydrochloric acid plus acetic acid with cerium(IV) sulphate in the presence of ferroin indicator

Titration with 0.05 M solutions		Titrations with 0.01 M solutions	
Antimony(III) taken (meq)	Antimony(III) found (meq)	Antimony(III) taken (meq)	Antimony(III) found (meq)
0.1816	0.1817	0.0363	0.0363
0.2271	0.2270	0.0454	0.0451
0.2725	0.2729	0.0545	0.0547
0.2956	0.2960	0.0636	0.0639
0.3179	0.3184	0.0727	0.0729
0.4088	0.4090	0.0817	0.0820
0.3633	0.3638		

Recommended procedure for the determination of antimony in pig lead

Weigh accurately ca. 1 g of the finely divided pig lead into a beaker, add 20—30 ml of concentrated sulphuric acid, heat, allow to cool, dilute to 50 ml and stand. Decant the clear liquid from the lead sulphate into a wide-mouthed conical flask, and boil for 5 min while passing carbon dioxide to expel all sulphur dioxide. Boil the lead sulphate with 50—60 ml of (1 + 1) hydrochloric acid until the lead sulphate dissolves completely; wash back quantitatively into the main antimony solution, disregarding any lead salt which may have reprecipitated. Transfer to a 100-ml standard flask and dilute to the mark with water. Titrate 25 ml of this solution with 0.05 M cerium(IV) sulphate as described above.

The results (Table 2) show that this assay is accurate and reproducible, giving results agreeing with those of the bromate method. The permanganate assay gives somewhat higher values.

Recommended procedure for the determination of antimony(III) in tartar emetic

The assay of antimony in tartar emetic was conducted in 1—2 M hydrochloric acid in the presence of 50% acetic acid. The results obtained agree closely with those obtained by titration with cerium(IV) in the presence of diphenylamine indicator in sulphuric acid medium [6]. When ferroin was used as indicator, the pale-blue ferriin was stable for only 2—3 min after the end-point; the orange-red ferroin then reappeared. This is in marked contrast with the much longer stability of ferriin observed in titrations of simple antimony(III) and may be due to the reduction of ferriin by tartaric acid.

Recommended procedure for the sequential titration of antimony(III) and arsenic(III) in mixtures

To 4—9 ml of the mixture, add enough hydrochloric acid and glacial acetic acid to give 1 M and 50% concentrations, respectively, after dilution

TABLE 2

Assay of antimony in pig lead

Amount of pig lead taken (g)	Antimony found (%)		
	Cerium(IV) sulphate	Potassium bromate	Potassium permanganate
1.0000	4.76	4.73	5.05
1.2014	4.73	4.75	4.95
1.5000	4.74	4.78	4.90

to 50 ml. Add 2 drops of ferroin indicator and titrate with 0.05 M cerium(IV) sulphate solution, until the colour changes to pale-blue; this end-point corresponds to antimony(III). Then add 0.5—1.0 ml of 0.005 M iodine monochloride solution, heat to 50°C and continue the titration at the usual speed until 0.3—0.4 ml before the end-point; then titrate dropwise, allowing 5—10 s between drops. If the titration is done at room temperature, a wait of 20—25 s is necessary between drops near the end-point.

The volume of cerium(IV) sulphate consumed between the first and second end-points corresponds to the amount of arsenic(III). Typical results are presented in Table 3. The pale-blue colour of ferriin after the first end-point is stable only for 60 s. If the concentration of hydrochloric acid is increased beyond 1 M, there is a slightly increased interference of arsenic(III).

Recommended procedure for the determination of antimony(III) in sulphuric acid medium

The stock solution of antimony(III) prepared from antimony oxide was used. For these titrations, the addition of acetic acid is unnecessary but a catalyst is needed. For this purpose, 1 ml of 0.005 M iodine monochloride was added for 50 ml of the titration mixture, containing 0.5—1 M sulphuric acid. The titrations can be done at the usual speed up to 0.2—0.1 ml short of the equivalence point. As the reduction of ferriin by antimony(III) is slow in this region, a wait of 15 s is required between drops of titrant. After the end-point, the ferroin colour returns in 4—5 min. When titrations are conducted in 1.5 M sulphuric acid medium, the reduction of ferriin by antimony(III) before the end-point becomes very slow.

RESULTS AND DISCUSSION

The failure by previous workers to achieve a titrimetric determination of antimony(III) in hydrochloric acid medium with cerium(IV) sulphate when ferroin serves as the indicator, is due to the formation of a sparingly soluble red precipitate in which the ferroin is bound in an unreactive form. This red precipitate can be centrifuged and dissolved in nitrobenzene to give a red colour. Ferroin alone does not dissolve in nitrobenzene. This precipitate is,

TABLE 3

Sequential titration of antimony(III) and arsenic(III)

Sample No.	Antimony(III)(meq)			Arsenic(III)(meq)		
	Taken	Found	% Error	Taken	Found	% Error
1	0.1960	0.1970	+0.5	0.3392	0.3390	−0.1
2	0.2450	0.2460	+0.4	0.2907	0.2900	−0.3
3	0.2940	0.2940	nil	0.2423	0.2420	−0.1
4	0.4430	0.4450	+0.4	0.1938	0.1940	−0.1
5	0.3920	0.3930	+0.3	0.3876	0.3865	−0.2

therefore, similar to that of ferroin perchlorate [8—11] to which is ascribed the formula $[Fe(phen)_3](ClO_4)_2$. Under suitable conditions, anionic metal complex anions such as tetrachloromercurate(II) and tetrachloroaurate(III) [12] form sparingly soluble complexes with ferroin. In the present work, a red precipitate was observed when ferroin was added to 6—8 M hydrochloric acid containing antimony(V) but not antimony(III). The red precipitate was not formed when ferroin was added to a solution of antimony(V) in 1—4 M hydrochloric acid kept for 24 hours. Neumann [13] and Kambare et al. [14] concluded from spectrophotometric studies that antimony(V) exists as $SbCl_6^-$ and $SbCl_4(OH)_2^-$ ions in hydrochloric acid solutions, the former preponderating in concentrated acid and the latter in dilute acid. The polarographic studies of Lingane and Nishida [15] and the extraction studies of Dakar et al. [16] show that the unhydrolyzed complex ion $SbCl_6^-$ predominates in more concentrated hydrochloric acid. These considerations make it reasonable to conclude that the red precipitate formed on adding ferroin to antimony(V) in concentrated acid is the ion association complex $[Fe(phen)_3](SbCl_6)_2$.

If the $SbCl_6^-$ anion is stable only in strong hydrochloric acid solutions, it is not immediately obvious how the red precipitate $[Fe(phen)_3](SbCl_6)_2$ can appear in the titration of antimony(III) with cerium(IV) sulphate in 1—3 M hydrochloric acid. However, from their polarographic investigations, Lingane and Nishida [15] concluded that antimony(III) exists in these solutions as $SbCl_4^-$; This reacts with cerium(IV) according to the equation $SbCl_4^- + 2Cl^- - 2e^- \rightarrow SbCl_6^-$. The resulting $SbCl_6^-$ reacts with the ferroin cation $[Fe(phen)_3]^{2+}$ before it hydrolyses to $SbCl_4(OH)_2^-$. Clearly, the hydrolysis of $SbCl_6^-$ is slower than is usually believed; this was proved as follows. When 2.5 ml of a dilute equilibrated solution of potassium antimonate in 4 M hydrochloric acid was added to 47.5 ml of 2 M hydrochloric acid and then treated with 0.1 ml of ferroin, no red precipitate was formed. In contrast, when 2.5 ml of the antimony(V) solution was added to 8 ml of concentrated hydrochloric acid, which was then immediately mixed with 39.5 ml of water containing 0.1 ml of ferroin, a red precipitate appeared. The spectrophotometric studies of Neumann and Nishida also indicated that the hydrolysis of $SbCl_6^-$ is not fast.

It remains to elucidate the mechanism of the rôle of acetic acid in making the titration facile. Potentiometric titration curves showed that the redox potentials of the Sb(V)/Sb(III) couple decrease in the presence of acetic acid. For instance, in 1.65 M hydrochloric acid, the potential has the value 0.945 V; on addition of 25% acetic acid, the value falls to 0.895 V, and with 50% acetic acid to 0.840 V. It is evident, therefore, that preferential complexation of antimony(V) occurs with acetic acid. This conclusion is amply supported by the ultraviolet absorption spectra of antimony(V) and antimony(III) in hydrochloric acid alone and in mixtures with 50% acetic acid (Fig. 1); the absorption of antimony(III) in 3 M hydrochloric acid is not significantly altered by the addition of acetic acid, whereas the absorption of antimony(V) is greatly increased. Thus the presence of acetic acid in the titration medium prevents the formation of $SbCl_6^-$, which alone is capable of binding ferroin in an unreactive form.

The procedure described here for the sequential titration of antimony(III) and arsenic(III) is simple and more rational than the empirical procedures proposed by Přibil [2] for differentiating mixtures of antimony(III) and arsenic(III).

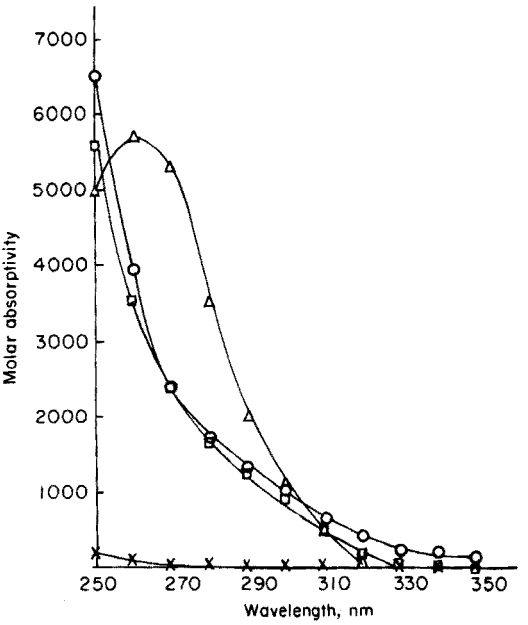

Fig. 1. Absorption spectra of antimony(III) and antimony(V). ○ Antimony(III) in 3 M HCl; × antimony(V) in 3 M HCl; □ antimony(III) in 3 M HCl + 50% HAc; △ antimony in 3 M HCl + 50% HAc.

REFERENCES

1 H. H. Willard and P. Young, J. Am. Chem. Soc., 55 (1933) 3268.
2 R. Přibil, Chem. Listy, 39 (1945) 19.
3 E. H. Swift, Introduction to Quantitative Analysis, Prentice-Hall, New York, 1950, p. 169 ff.
4 G. Gopala Rao, Muralikrishna Gandikota and S. G. Viswanath, Anal. Chim. Acta, 87 (1976) 511.
5 A. I. Vogel, Text Book of Quantitative Inorganic Analysis, Longman, London, 1973, p. 366.
6 G. Gopala Rao, S. G. Viswanath and Muralikrishna Gandikota, Anal. Chim. Acta, 79 (1975) 273.
7 I. M. Kolthoff and R. Belcher, Volumetric Analysis, Vol III, Interscience, New York, 1957, p. 127.
8 Z. Gregorowicz, F. Buhl and Z. Klima, Mikrochim. Ichoanal. Acta, (1963) 116.
9 J. S. Fritz, J. E. Abbink and P. A. Campbell, Anal. Chem., 36 (1964) 2123.
10 Y. Yamamoto and K. Kotsuji, Bull. Chem. Soc. Jpn., 37 (1964) 785.
11 Y. Yamamoto, K. Kotsuji, S. Kinuwaki and H. Sawa Mura, Nippon Kagaku Zasshi, 85 (1964) 869.
12 N. S. Poluektov and V. A. Nazarenko, J. Appl. Chem. (U.S.S.R.), 10 (1937) 2105.
13 H. M. Neumann, J. Am. Chem. Soc., 76 (1954) 2612.
14 T. Kambara, K. Yamaguchi and S. Yasuba, Exchange Reactions, International Atomic Energy Agency, Vienna, 1965.
15 J. J. Lingane and S. Nishida, J. Am. Chem. Soc., 71 (1949) 2719.
16 G. M. Dakar, B. Z. Iofa and A. N. Nesmeyanov, Radiokhimiya, 5 (1963) 428.

Analytica Chimica Acta, 92 (1977) 171—181

RECOVERY OF PLATINUM, PALLADIUM, RHODIUM, IRIDIUM, AND GOLD AFTER LEAD FUSION AND PERCHLORIC ACID PARTING

A. DIAMANTATOS

J. C. I. Minerals Processing Research Laboratory, Knights 1413, Transvaal (South Africa)

(Received 26th January 1977)

SUMMARY

A method is described for the wet analysis of the lead—noble metals button which is parted with perchloric acid after heating at 160—180°C, thus resulting in the complete dissolution of platinum, palladium, rhodium, and gold; iridium remains totally unattacked. Quantitative group precipitation of the precious metals from the diluted lead perchlorate filtrate solution is possible with 2-mercaptobenzothiazole as precipitant. The noble metals precipitated are isolated by filtration and are easily determined. The proposed procedure is rapid, precise, and applicable to a wide variety of platiniferous materials.

Little attention seems to have been paid to the development of an efficient wet analytical method for the determination of all the precious metals, directly from the lead button collector. Beamish [1] has repeatedly expressed surprise at the lack of such a procedure and urged chemists to extend their research in this field because the direct wet analysis of the lead—noble metals button offers advantages over the classical silver bead method. Losses from the cupellation stage of the classical method indeed occur; this time-honoured smelting technique of removing lead results in large losses of ruthenium [2, 3], osmium [4] and iridium [3, 5] and usually in relatively small losses of platinum [3, 6], palladium [7], rhodium [8], and gold [3, 9]. An attempt by Agrawal and Beamish [10] to determine all seven noble metals in the nitric acid parting solution, derived from the dissolution of the lead button, failed because of the complexity of the partial attack of the nitric acid on all the precious metals [11, 12]. In this respect, the use of perchloric acid as a parting acid for the lead button collector is distinctly advantageous. The behaviour of the platinum metals and gold during the perchloric acid parting treatment of the lead—noble metals button has been studied [13, 14]. By dissolving the button with perchloric acid in the presence of a little acetic acid, after heating at 160—180°C, the platinum, palladium, rhodium, and gold are quantitatively dissolved into the lead perchlorate solution; all the iridium and ruthenium, as well as a portion of the osmium, remain unattacked and thus can be easily retained by filtration and subsequently determined. However, no method

appears to have been recorded for the recovery of the platinum, palladium, rhodium, and gold from the lead perchlorate filtrate solution, despite the early use of perchloric acid by Thiers et al. [2] and by Allan and Beamish [4] for determining the ruthenium and osmium, respectively, directly from the lead collector. Nevertheless, the provision of a method for the recovery of the non-volatile noble metals from the perchloric acid medium is worth investigating. Instead of attempting to separate the large quantities of lead from the parting acid solution, it appeared to be preferable to separate the microquantities of the noble metals from the lead perchlorate solution. This approach demands a precipitant which gives: (a) quantitative simultaneous precipitation of platinum, palladium, rhodium, and gold, (b) no precipitation of lead.

This paper describes optimal conditions for the above purpose with 2-mercaptobenzothiazole as precipitant.

EXPERIMENTAL

Apparatus and reagents

The fire-assay equipment included an electric furnace with silicon carbide element, fireclay crucibles, and cast iron conical moulds (150-ml capacity).

A Zeiss model PMQ II Spectrophotometer, Varian-Techtron AA5 atomic-absorption spectrophotometer, and Philips PW 1220 x-ray fluorescence spectrometer were used.

The assay lead flux contained (parts by weight) litharge 50, borax 20, soda ash 60, silica 20, flour 5—6.

The standard copper—nickel matte comprised Pt 958 p.p.m., Pd 536 p.p.m., Rh 93 p.p.m., Ir 24.6 p.p.m., Ru 205 p.p.m., Os 19 p.p.m., Au 47.9 p.p.m., Ag 81 p.p.m., Cu 28.9%, Ni 48.2%, S 22.4%, Fe 1.4%, Co 0.45%, Se 0.06%, Te 0.02%, silica, etc.

Standard stock hydrochloric acid solutions of platinum, palladium, rhodium, iridium, ruthenium, osmium, and gold were prepared as described previously [15].

2-Mercaptobenzothiazole was used as a 1% (w/v) solution in glacial acetic acid.

Recommended procedure (see Fig. 1)

Mix thoroughly 2—60 g of the sample (leach and/or roast, if necessary) with 150—180 g of lead flux and transfer to a suitable size of fireclay crucible. Fuse at 1200°C for 1 h and pour the molten fluid into a conical iron mould. After cooling, detach the lead button from the slag by tapping. (Re-fuse the slag if high quantities of iridium are present.) Place the button in 100 ml of 30% (w/v) sodium hydroxide solution and boil to remove completely any adhering slag. Compress the button to produce a disc of ca. 4 mm thickness. Place the lead disc in a 1-l squat beaker and add 300 ml of perchloric acid (70%) and 30 ml of acetic acid (glacial). Cover the beaker.

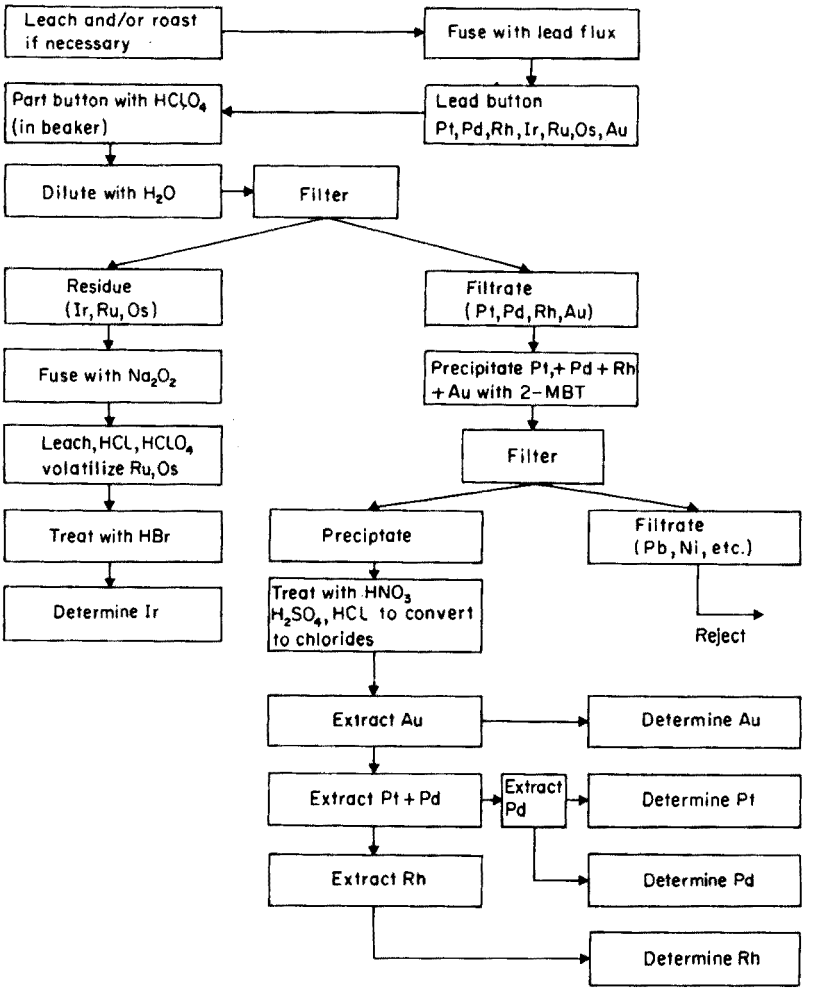

Fig. 1. Flow-sheet. Determination of Pt, Pd, Rh, Ir, Au.

Heat to 180°C initially, remove the heat source for a time, then maintain at 160—180°C until all the lead has dissolved. Continue heating for 20 min at ca. 150°C to ensure complete dissolution of platinum, palladium, rhodium, and gold. Cool to 70°C, and dilute the perchlorate solution slowly with 200 ml of water while stirring. Boil this solution for 5 min, and cool. Filter the solution through a No. 540 filter paper into a 1-l beaker. Retain the black residue containing the iridium, ruthenium, and osmium for later use. Dilute the filtrate to ca. 600 ml with water, and bring to the boil gently (use a boiling rod). Then cool the solution and carefully add 20 ml of the 2-mercaptobenzothiazole solution. Boil gently for 30 min, and then cool in cold water for at least 40 min to ensure complete precipitation of the gold

complex. Separate the noble metals precipitate on a No. 540 filter paper, and wash precipitate and beaker at least three times with hot water. (It is not necessary to transfer the precipitate quantitatively to the filter.) Wash the precipitate quantitatively from the wet filter paper to the bottom of the beaker with a thin stream of acetone. Reject the paper. Evaporate the acetonic solution to dryness on a steam bath, blowing air onto the solvent surface. Destroy the organic residue by boiling for 10—15 min with 10 ml of concentrated nitric acid and evaporate to dryness in the presence of a little sodium chloride. Add 5 ml of concentrated sulphuric acid, heat strongly for 20—30 min, and again fume to dryness. Dissolve, and convert the residue to a hydrochloric acid solution by boiling with 20 ml of 12 M hydrochloric acid for 15 min and evaporating to incipient dryness. Repeat the hydrochloric acid treatment once more. Finally, add 20 ml of 12 M hydrochloric acid and 3—5 drops of 100-vol hydrogen peroxide, boil for 5—6 min, and cool. Determine the platinum, palladium, rhodium, and gold either directly in the hydrochloric acid mixture by a.a.s. [16] or after extraction of the noble metals, as described previously [17]. To determine the iridium in the unattacked residue, transfer the filter paper to a zirconium crucible, char, ignite, and fuse the residue with 2—3 g of sodium peroxide. Cool, leach the melt with water, acidify with hydrochloric acid and evaporate to dryness. Add 10 ml of perchloric acid (70%), boil for 10 min, and fume to complete dryness to volatilize all ruthenium and osmium. Proceed with the extraction and determination of iridium as detailed previously [18].

RESULTS AND DISCUSSION

The choice of 2-mercaptobenzothiazole as precipitant

The "standard" matte (25 g) was leached with 300 ml of 12 M hydrochloric acid and 100 g of ammonium chloride to remove the bulk of the copper and nickel; the mixture was filtered, and the residue fused in the usual way with 180 g of lead flux. The lead disc was parted with perchloric acid and acetic acid as described above, until complete dissolution was achieved (ca. 1 h). The solution was then cooled, diluted to 600 ml, and again heated for a few minutes to obtain a clear yellow solution; only the small amounts of iridium, ruthenium, and osmium which had remained unattacked remained on the bottom of the beaker. The solution was finally cooled to room temperature, filtered through a Whatman no. 540 filter paper into a 1-l volumetric flask, and made up to the mark with water.

Two 100-ml aliquots of this solution were transferred to 400-ml beakers; 10 and 80 ml of perchloric acid (70%) respectively, were added, and each solution was finally diluted to about 250 ml with water. The solutions were boiled and 20 ml of 1% 2-mercaptobenzothiazole in acetic acid was added slowly while stirring. An orange precipitate formed almost instantaneously. The solutions containing the coagulated precipitates were kept boiling gently for 1 h, cooled for 30 min, and filtered through Whatman no. 540 papers;

the precipitates were thoroughly washed with hot water. The filtrates were almost colourless. However, to check the efficiency of the precipitation of platinum, palladium, rhodium, and gold at the two different perchloric acid concentrations, the filtrates were analyzed for these metals. The filtrates were evaporated and fumed to dryness. The organic matter was destroyed by heating the residues strongly with sulphuric acid, as usual, and then evaporating to complete dryness. To each dry residue, 25 ml of 12 M hydrochloric acid was added. The solution was boiled and evaporated to a small volume. Finally an additional 10 ml of 12 M hydrochloric acid was added and the mixtures were boiled again for a few min. The cooled solutions were filtered to remove the precipitated lead, and the filtrates were diluted to 10 ml in 5—6 M hydrochloric acid and tested qualitatively by a.a.s. Platinum, palladium, and gold were not detected in any of the solutions. Rhodium was detected in the first solution (low concentration of perchloric acid), but not in the second solution. In another test, two 100-ml aliquots of the above working solution were pipetted into 400-ml beakers and 80 ml of perchloric acid (70%) was added to each before diluting to 250 ml with water. The addition of 2-mercaptobenzothiazole and the boiling treatment, were performed as in the previous experiment, but the first aliquot was filtered hot (15—20 min after removing from the hot plate) and the second aliquot was filtered after cooling in cold water for 30 min. Both filtrates were examined for unprecipitated precious metals. Platinum, palladium, rhodium, and gold were not detected in the filtrate of the "cold" sample; but 26% of the original gold content was found in the "hot" filtrate. These initial tests indicated that 2-mercaptobenzothiazole is suitable for precipitating the noble metals from the lead perchlorate-perchloric acid medium; that for the quantitative precipitation of rhodium, a certain minimum concentration of perchloric acid is necessary; and that the filtration of the (Pt, Pd, Rh, Au)-2-mercaptobenzothiazole precipitate should be performed after the solution has cooled to ensure complete retention of gold.

Effect of perchloric acid concentration on the precipitation of platinum, palladium, rhodium, and gold with 2-mercaptobenzothiazole

A lead button, obtained after fire-assay fusion of 25 g of "standard matte" sample, was parted with 300 ml of perchloric acid and 30 ml of acetic acid, and the resulting lead perchlorate solution was treated and diluted to 1 l as described previously. Aliquots (100 ml) were treated with different added amounts (10—90 ml) of perchloric acid (70%), and diluted to ca. 250 ml with water. The precipitation of platinum, palladium, rhodium, and gold with 2-mercaptobenzothiazole, and the following steps, were done as above. Platinum, palladium and gold were not detected in the filtrates from any of these tests. The amount of rhodium detected decreased from 1.29% for 10 ml extra of perchloric acid to 0.43% for 50 ml; rhodium was not detected when more than 60 ml extra was used. These results show quantitative precipitation of platinum, palladium, and gold over a wide range of perchloric acid concen-

trations; but precipitation of rhodium was quantitative only under conditions of high acidity. If this precipitation procedure were used in an overall separation scheme, precipitation of the noble metals would be performed on the original solution after parting, and not on aliquots; high perchloric acid concentrations would therefore be the rule as large amounts of perchloric acid are required initially to disintegrate the lead button. Sufficient perchloric acid would then already be present; in practice, it would be advisable to dilute the solution obtained after parting with an equal volume of water before attempting precipitation of the noble metals. This would ensure that the perchloric acid would not cause decomposition of any organic reagent added at a later stage.

Effect of acetic acid on rhodium precipitation

The previous experiment was repeated on a similar button, but the lead was dissolved with only 300 ml of perchloric acid (70%). This was done to check any effect of acetic acid on the precipitation of the precious metals. Again platinum, palladium and gold were not detected in any filtrate. When 20 ml extra perchloric acid was added, 4.7% of the rhodium appeared in the filtrate, and 100 ml extra had to be used before rhodium was not detected in the filtrate.

The difference in the behaviour of rhodium when acetic acid was not used led to the investigation of the case where acetic acid was excluded completely. A lead button was parted with 300-ml of perchloric acid only and the 2-mercaptobenzothiazole was dissolved in ethanol instead of acetic acid. Again, platinum, palladium and gold were not detected in any filtrate. The results for rhodium (Table 1) show that the absence of acetic acid has a detrimental effect on the precipitation of rhodium, especially in low perchloric acid concentrations.

A comparison of the results below leads to the conclusion that the presence of acetic acid is essential during the precipitation stage. Acetic acid is thus used as the solvent for 2-mercaptobenzothiazole.

Effect of the boiling time on precipitation

A lead button containing the precious metals in 25 g of "standard" matte was dissolved in 300 ml of perchloric acid in the presence of 30 ml of acetic acid, as previously described; the filtrate was diluted to 1 l with water.

TABLE 1

Rhodium found in the filtrate after precipitation in the absence of acetate ion (2.39 mg Pt, 1.34 mg Pd, 0.232 mg Rh, 0.12 mg Au; 0.3 g of reagent in 20 ml ethanol; 1 h boiling; 250 ml final volume)

Aliquot	1	2	3	4	5	6
Extra $HClO_4$ (ml)	30	50	70	80	90	100
Unretained Rh (%)	24.0	15.4	6.0	3.9	2.6	2.1

Six 100-ml aliquots of this solution were pipetted into 400-ml beakers; 100 ml of perchloric acid (70%) was added to each, before dilution to ca. 250 ml with water. The solutions were boiled, and each was treated with 0.2 g of 2-mercaptobenzothiazole dissolved in 20 ml of glacial acetic acid. Each solution was boiled for a known period of 10—60 min. After cooling in running tap water for 30 min, the yellow precipitates were retained on No. 542 filter papers and each filtrate was analyzed for unprecipitated noble metals, as described previously.

Although platinum, palladium, and gold were quantitatively precipitated after boiling for 10 min, rhodium required boiling for at least 25 min for complete precipitation. A boiling time of 30 min was therefore chosen.

Effect of reagent concentration on precipitation

Six 100-ml aliquots, similar to those for the boiling time experiments, were used to examine the precipitation of the precious metals with different amounts of 2-mercaptobenzothiazole dissolved in 20 ml of acetic acid. The experimental data and results are shown in Table 2.

The results indicate that a large excess of reagent is required for the quantitative precipitation of all the noble metals. The addition of 200 mg of 2-mercaptobenzothiazole for the precipitation of 4 mg of total precious metals appears to be satisfactory for this sample. Although less than 25 mg of reagent was necessary to precipitate all the platinum, palladium and gold, and part of the rhodium, a further 125 mg was required to complete the precipitation of rhodium. Thus, for samples containing more rhodium, the quantity of precipitant might need to be increased. It was decided, however, as a first step, to standardize the amount of 2-mercaptobenzothiazole used at 50 times the total mass of noble metals to be precipitated.

TABLE 2

Effect of reagent concentration on the precipitation
(2.39 mg Pt, 1.34 mg Pd, 0.232 mg Rh, 0.12 mg Au; 100 ml $HClO_4$ added; 30 min boiling; 250 ml final volume)

Aliquot	Reagent added (g)	Unprecipitated			
		Pt (%)	Pd (%)	Rh (%)	Au (%)
1	0.01	4.18	4.55	38.79	ND<0.33
2	0.025	ND<0.01	ND<0.03	26.29	ND<0.33
3	0.05	ND<0.01	ND<0.03	3.45	ND<0.33
4	0.10	ND<0.01	ND<0.03	2.59	ND<0.33
5	0.15	ND<0.01	ND<0.03	ND<0.17	ND<0.33
6	0.20	ND<0.01	ND<0.03	ND<0.17	ND<0.33

Precipitation of the gold—2-mercaptobenzothiazole complex

The solubility of the gold—2-mercaptobenzothiazole precipitate in hot perchloric acid solution has been mentioned; it was apparently necessary to filter the precipitate of the noble metals after the solution had been cooled, if gold was to be removed completely. To investigate this particular phase of the operation more thoroughly, a "black sands" sample (chosen because of its high gold content in comparison with other noble metals: 200 p.p.m. Au, 14 p.p.m. Os, 6 p.p.m. Ir, 5 p.p.m. Pt, 2 p.p.m. Ru) was used to study the loss of gold with variation in temperature of the solution to be filtered.

The sample (25 g) was fire-assayed, and the resulting 50-g lead button was dissolved with 300 ml of perchloric acid (70%) and 30 ml of glacial acetic acid as usual. The solution was finally diluted to 1 l with water. Aliquots (100 ml) of this solution, each containing 0.5 mg of gold, were pipetted into 400-ml beakers; 80 ml of perchloric acid (70%) was added to each before dilution with water to ca. 250 ml. The solutions were boiled, removed from the hot plate, and then 20 ml of 1% 2-mercaptobenzothiazole—acetic acid solution was added carefully with stirring. The solutions were boiled again for 30 min. No precipitate formed during the boiling, but some precipitate appeared during the cooling and standing of the solutions, prior to their filtration. The pre-filtration conditions used are shown in Table 3, together with the corresponding values for the gold content of each filtrate. The results show the effect of a combined time—temperature relationship on the solubility of the gold—reagent complex; a period of more than 40 min of

TABLE 3

Filtration conditions for gold—2-mercaptobenzothiazole complex (0.5 mg Au, 0.2 g reagent, 30 min boiling, 250 ml final volume)

Aliquot	Period and manner of cooling	Final temperature (°C)	Au in filtrate	
			(mg)	(%)
1	15 min in air[a]	80	0.253	50.6
2	30 min in air[a]	60	0.157	31.4
3	60 min in air[a]	47	0.094	18.8
4	5 min in cool water[b]	33	0.216	43.2
5	15 min in cool water[b]	22	0.093	18.6
6	30 min in cool water[b]	18	0.006	1.2
7	45 min in cool water[b]	18	ND<0.0015	ND<0.3
8	5 min in ice water[c]	38	0.184	36.8
9	15 min in ice water[c]	10	0.008	1.6
10	30 min in ice water[c]	5	ND<0.0015	ND<0.3

[a]Beakers were allowed to cool on the bench. [b]Beakers were cooled in running water (ca. 18°C). [c]Beakers were cooled in an ice-water bath (±2°C).

cooling in running water should be observed to achieve quantitative retention of the gold precipitate on the filter. This precaution is necessary only for the precipitation of gold.

Application of the precipitation to platiniferous materials

The precipitation procedure was applied to a South African ore (Pt 4.0 p.p.m., Pd 1.7 p.p.m., Rh 0.33 p.p.m., Au 0.34 p.p.m.); to a Canadian ore (Pd 13.1 p.p.m., Pt 1.3 p.p.m., Au 1.0 p.p.m., Cu 0.12%, Ni 0.22%); to a platinum—rhodium silicate material (1600 p.p.m. Pt, 365 p.p.m. Rh, 70% SiO_2, 20% Al_2O_3) and to a spent platinum catalyst (silicate material containing ca. 0.7% Pt). These platiniferous materials were chosen because of their different origin, composition, and ratio of precious metal content. The noble metal—2-mercaptobenzothiazole precipitates were retained by filtration; the filtrates, after the usual treatment, were analyzed for any unprecipitated precious metal by a.a.s. The presence of any unprecipitated precious metal was not detected in any of these samples, thus confirming the wide applicability of the method.

Co-precipitation of foreign elements

A platiniferous concentrate (12 g) containing 2.8% Cu, 5.1% Ni, 18.2% Fe, 11.8% S, 36% SiO_2, 3.3% Al_2O_3, 3% CaO, 12.6% MgO, and a total of 132 p.p.m. of platinum-group metals and gold was fused with lead flux without prior leaching, but after being roasted at 900°C for 1 h. The parting and precipitation steps were performed as usual and the precipitate was examined by x-ray fluorescence spectrometry. Of the most common base metals normally occurring in platiniferous materials (Cu, Ni, Fe, Cr, Co), only copper co-precipitates with the noble metals when the procedure outlined is followed. There is also some co-precipitation of tellurium. The content of copper in ores and most other platiniferous materials is in the region 0.1—0.3%; for copper—nickel mattes, concentrates etc., with an initially high copper content, a preliminary leach with hydrochloric acid and ammonium chloride eliminates the bulk of copper prior to the fire assay lead fusion. Thus the button should contain only relatively small quantities of copper. When determining the precious metals by a.a.s., the presence of copper is not undesirable; copper sulphate is often added to minimize depressive inter-element effects [19—21]. If the extraction procedure [17] for the separation of platinum, palladium, rhodium, and gold is followed, copper remains behind with the platinum raffinate, and the moderate amount of copper present has no effect on the subsequent colorimetric determination of platinum with tin(II) chloride [22]. Tellurium would be co-extracted with gold from 6 M hydrochloric acid solutions by methyl isobutyl ketone [23, 24]

Conversion of the (Pt, Pd, Rh, Au)—2-mercaptobenzothiazole precipitate to a chloro complex solution

The obvious way to treat the (Pt, Pd, Rh, Au)—2-mercaptobenzothiazole precipitate retained on the filter, would involve transfer to a crucible, drying,

ignition, fusion with sodium peroxide, dissolution in dilute hydrochloric acid, separation and determination of the individual noble metals. This procedure, however, introduces undesirable quantities of sodium salts, contaminates the noble metal solution with scale from the crucible, and is time-consuming. An alternative technique was sought to obviate the peroxide fusion. In an attempt to find a suitable solvent for the precipitated noble metal complexes, methyl isobutyl ketone, chloroform, acetone, and ethanol were tried: of these, acetone was the most suitable; it is miscible with water, dissolves the precipitate almost instantaneously, and can be evaporated easily. The technique of dissolving the noble metal precipitate in acetone, and the conversion of that solution to a hydrochloric acid solution before the determination of the precious metals, are described in the recommended procedure.

Determination of the noble metals in a standard platiniferous copper—nickel matte

The applicability, accuracy and precision of the proposed method were evaluated by analyzing ten 5-g portions of the "standard" matte, for the platinoid metals and gold, following the recommended procedure. The results given in Table 4 confirm the satisfactory accuracy and reproducibility of the method for the five noble metals.

The accuracy was also evaluated as follows: lead fluxes were "salted" with standard hydrochloric acid solutions of noble metals, transferred to fireclay crucibles, and fused as usual. The lead buttons were parted with perchloric acid and analyzed by the recommended procedure. The average recoveries obtained are shown in Table 5.

TABLE 4

Statistical data for the analysis of 10 samples of Cu—Ni matte
(4.790 mg Pt, 2.680 mg Pd, 0.465 mg Rh, 0.123 mg Ir, 0.239 mg Au)

	Pt (mg)	Pd (mg)	Rh (mg)	Ir (mg)	Au (mg)
Average	4.784	2.670	0.463	0.120	0.235
s	0.03	0.02	0.006	0.007	0.006
s_r	0.6	0.6	1.33	5.7	2.5
Recovery (%)	99.87	99.63	99.57	97.56	98.33

TABLE 5

The recovery of precious metals added as pure solutions to lead flux

Element	Added (mg)	Recovery (mg)	Recovery (%)
Pt	2.004	1.998	99.7
Pd	1.008	1.008	100.0
Rh	0.203	0.204	100.4
Ir	0.1006	0.0986	98.0
Au	0.202	0.197	98.5

The author expresses his gratitude to Prof. A. A. Verbeek (University of Natal) for helpful discussions and suggestions.

REFERENCES

1 F. E. Beamish, Analytical Chemistry of the Noble Metals, Pergamon Press, 1966.
2 R. Thiers, W. Craydon and F. E. Beamish, Anal. Chem., 20 (1948) 831.
3 G. T. Georgiev and D. Apostolov, Zh. Anal. Khim., 27 (1972) 506.
4 W. J. Allan and F. E. Beamish, Anal. Chem., 24 (1952) 1569.
5 R. R. Barefoot and F. E. Beamish, Anal. Chem., 24 (1952) 840.
6 I. Hoffman and F. E. Beamish, Anal. Chem., 28 (1956) 1188.
7 J. G. Fraser and F. E. Beamish, Anal. Chem., 26 (1954) 1474.
8 W. F. Allen and F. E. Beamish, Anal. Chem., 22 (1950) 451.
9 C. H. Coxon, C. J. Verwey and D. N. Lock, J. S. Afr. Inst. Mining Met., 62 (1962) 546.
10 K. C. Agrawal and F. E. Beamish, Talanta, 11 (1964) 1449.
11 H. Ste-C. Deville and J. S. Stass, Procés-verbaux, Comité International de Poids et Mésures, 2 (1877) 162.
12 L. K. Shubochkin, V. N. Pichkov, A. F. Morgunov and N. I. Kolomiets, Zh. Prikl. Khim. (Leningrad), 45 (1972) 2327.
13 A. Diamantatos, Anal. Chim. Acta, 90 (1977) 179.
14 A. Diamantatos, Anal. Chim. Acta, 91 (1977) 281.
15 A Diamantatos, Anal. Chim. Acta, 66 (1973) 147.
16 R. C. Mallett, D. C. G. Pearton, E. J. Ring and T. W. Steele, Talanta, 19 (1972) 181.
17 A. Diamantatos, Anal. Chim. Acta, 67 (1973) 317.
18 A. Diamantatos and A. A. Verbeek, Anal. Chim. Acta, 86 (1976) 169.
19 A. Strasheim and G. J. Wessels, Appl. Spectrosc., 17 (1963) 65.
20 M. N. Schnepfe and F. S. Grimaldi, Talanta, 16 (1969) 591.
21 V. M. Apolitskii, L. P. Yudina, Yu. P. Latysheva and V. A. Pronin, Zh. Anal. Khim., 30 (1975) 141.
22 E. B. Sandell, Colorimetric Determination of Traces of Metals, Interscience, New York, 1944.
23 H. Goto, Y. Kakita and T. Furukawa, Nippon Kagaku Zasshi, 79 (1958) 1513.
24 Y. Uzumasa, K. Hayashi and S. Ito, Nippon Kagaku Zasshi, 36 (1963) 301.

Analytica Chimica Acta, 92 (1977) 183—192

THE STRUCTURE OF THE NICKEL—8-QUINOLINOL COMPLEX IN SOME ORGANIC SOLVENTS

E. SEKIDO* and K. KUNIKIDA

Department of Chemistry, Faculty of Science, Kobe University, Nada, Kobe 657 (Japan)

(Received 6th December 1976)

SUMMARY

The ultraviolet and visible absorption spectra of the nickel—8-quinolinol complex in chloroform are significantly affected by traces of water. Absorption spectra of the complex in mixed solvents, e.g. dioxane—water, dioxane—methanol and chloroform—methanol, and in chloroform solution containing water, pyridine, or 8-quinolinol are compared. An addition compound is formed in which the mole ratio of the nickel—8-quinolinol complex to the solvent or the base is 1:1 or 1:2. Polymerization occurs by mutual interaction between the nickel—8-quinolinol complexes. A degree of polymerization of 2.2 was obtained; this indicates that the binuclear compound predominates. The structure of the nickel—8-quinolinol complex in organic solvents is discussed.

Most of the 8-quinolinol complexes of metals such as copper, cobalt, manganese, zinc, and palladium have two well-separated bands [1] in the wavelength region above 300 nm, assigned at ^1L_a and ^1L_b bands [2]. The nickel 8-quinolinol complex, however, has three absorption bands in the same region [1, 3], and it does not give a reproducible spectrum in chloroform purified in the usual manner [4]. Recently, two species of nickel—8-quinolinol complex were extracted from perchlorate and sulfate solutions with chloroform [5]; these were the ion-association complex from perchlorate solution at low pH and the neutral binuclear complex from perchlorate solution at high pH or from sulfate solution.

To elucidate the characteristic spectrophotometric behavior and to confirm the formation of the binuclear complex in chloroform, the absorption spectra of the nickel—8-quinolinol complex in organic solvents under various conditions were examined and compared, and the structure of the nickel—8-quinolinol complex in organic solvents was investigated. The study of the nickel—8-quinolinol complex in solution is important in clarifying the mechanism of solvent extraction.

EXPERIMENTAL

Reagents

Chloroform (analytical reagent grade) was shaken three times with water to remove ethanol, allowed to stand for one night over calcium chloride, then shaken with phosphorus pentoxide and separated by decantation. Phosphorus

pentoxide was again added to the chloroform; the mixture was distilled and stored carefully with the exclusion of humidity and light. The purified chloroform is not stable and was used within 6 h. Dioxane and methanol (analytical-reagent grade) were purified by distillation after reflux over sodium. 8-Quinolinol was recrystallized twice from 50% ethanol. Other reagents, including buffer components, were of analytical grade.·

Preparation of the nickel—8-quinolinol hydrate and anhydride

8-Quinolinol (HQ) in ethanol ($2 \cdot 10^{-2}$ M) was added in slight excess to the nickel sulfate solution ($1.0 \cdot 10^{-2}$ M) adjusted to pH 5.0 (acetate buffer). The precipitate, $NiQ_2 \cdot 2H_2O$, was filtered, washed with hot water, and dried in air. The anhydride, NiQ_2, was prepared by heating at 130°C for 5 h over phosphorus pentoxide in vacuo.

Preparation of solutions of the complex and measurement of absorption spectra

Since a trace of water affects appreciably the absorption spectra of the nickel—8-quinolinol complex, completely desiccated solvents and reagents were used. A definite amount of the nickel—8-quinolinol complex anhydride was dissolved in the appropriate solvent to give a final concentration of $1.0 \cdot 10^{-3}$—$5.0 \cdot 10^{-4}$ M. The u.v. and visible absorption spectrum of the complex was measured with a Hitachi-124 spectrophotometer, with the pure solvent as a blank, in cells of 10, 20, 50, or 100-mm path-length.

RESULTS AND DISCUSSION

Effect of the decomposition of chloroform and of traces of water on the absorption spectra

Pure chloroform is decomposed by oxygen and light. The influence of the decomposition of chloroform on the absorption spectrum of NiQ_2 was examined; the absorption spectrum of NiQ_2 varied gradually with the period that the pure chloroform had been stored after distillation, although there was no variation for periods of less than 6 h. Hydrogen chloride and phosgene, formed as decomposition products of chloroform, probably react with the NiQ_2.

The absorption spectra of NiQ_2 in chloroform saturated with water and treated with various desiccants are shown in Fig. 1. In chloroform saturated with water, absorption maxima exist at 460, 390, and 340 nm (curve 1); in chloroform treated with desiccants, the maxima at 460 and 340 nm become stronger and that at 390 nm becomes weaker in the order $Na_2SO_4 < CaCl_2 < P_2O_5$ (curves 2, 3, and 4). In almost completely dry chloroform, only the maxima at 460 and 340 nm (curve 4) exist. This absorption spectrum may correspond to NiQ_2, because the tetrahedral structure [6] confirmed for solid NiQ_2 will be maintained in non-polar solvents containing no trace of water, but $NiQ_2 \cdot 2H_2O$, with the distorted octahedral structure [7] will be formed when a non-polar

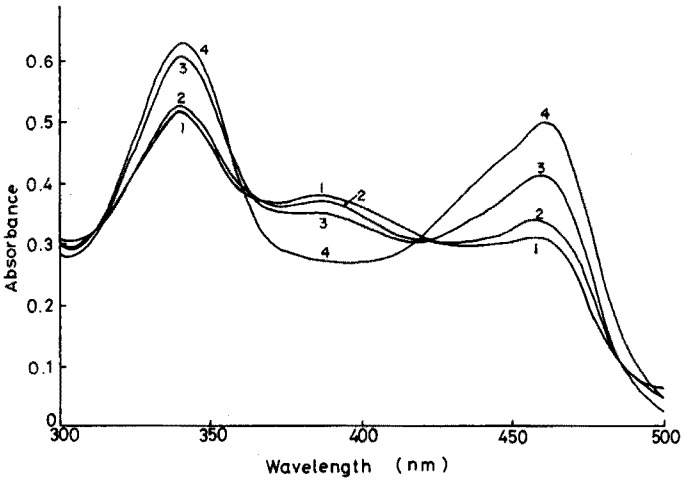

Fig. 1. Absorption spectra of the nickel—8-quinolinol complex in chloroform. (1) Saturated with water. (2) Dried with sodium sulphate. (3) Dried with calcium chloride. (4) Dried with phosphorus pentoxide. Nickel—8-quinolinol complex, $1.0 \cdot 10^{-4}$ M.

solvent contains a trace of water. It seems reasonable to consider that the addition of two molecules of water corresponds to the change in the absorption spectra. However, immediately after dissolution of the nickel—8-quinolinol complex in chloroform saturated with water (curve 1), the spectrum does not represent that of $NiQ_2 \cdot 2H_2O$ alone but that of the mixture of NiQ_2 and $NiQ_2 \cdot 2H_2O$ although $NiQ_2 \cdot 2H_2O$ is sparingly soluble in chloroform; $NiQ_2 \cdot 2H_2O$ was gradually precipitated in chloroform treated with calcium chloride, but no precipitate was formed in chloroform treated with phosphorus pentoxide.

Absorption spectra of the complex in various solvents

A stoichiometric study of the absorption spectra of the nickel—8-quinolinol complex in chloroform solutions containing water was impossible because water is almost immiscible and $NiQ_2 \cdot 2H_2O$ is sparingly soluble in chloroform. Therefore, the absorption spectra of the complex were measured and compared in chloroform solution containing methanol, pyridine, or 8-quinolinol, and in dioxane solution containing water or methanol; completely desiccated solvents and reagents were used. The absorption data are shown in Table 1.

The absorption spectra of the complex in chloroform containing various amounts of methanol are shown in Fig. 2. When the methanol content increases, the absorption maximum appears around 390 nm with isosbestic points at 423 and 361 nm (curves 1—4). When the methanol concentration exceeds 0.5 M, the absorption curves deviate from the isosbestic points; the absorption maximum around 390 nm increases with a shift to shorter wave-

TABLE 1

Absorption spectra data for the nickel—8-quinolinol complex in various chloroform and dioxane solutions

Solvent	Added reagent and its concn. range (M)	λ and ε at absorption maxima (nm) ($l\ mol^{-1}\ cm^{-1}$)		Isosbestic points (nm)	Approximate concn. of reagent at which the absorption around 460 nm disappears (M)
		No reagent	Added reagent		
Chloroform	Methanol (0—5.0)	340(6300) 460(5100)	337(4400) 383(5500) disappear	361 423	5.0
Chloroform	Pyridine ($0—5.0 \cdot 10^{-2}$)	340(6300) 460(5100)	342(5500) 400(5700) disappear	368 430	$5.0 \cdot 10^{-2}$
Chloroform	8-Quinolinol ($0—1.0 \cdot 10^{-2}$)	—[b] 460(5100)	—[b] —[b] disappear	— 422 (414)	$1.0 \cdot 10^{-2}$
Dioxane	Water (0—13.9)	343(6300) 400(4100) 463(3300)	337(4400) 385(5800) disappear	361 423	12.2
Dioxane	Methanol (0—19.8)	343(6400) 396(3900) 463(3800)	337(4400) 386(6000) disappear	365 (362) 425	19.8

[a]Concentration of NiQ_2: $1.0 \cdot 10^{-4}$ M.
[b]Difficult to measure below 380 nm.

lengths and that at 340 nm decreases with a slight shift to shorter wavelengths (curves 5—9). In chloroform solution containing 5.0 M methanol, the absorption maximum at 460 nm almost disappears and absorption maxima exist at 337 and 383 nm. Such a change in absorption suggests that there are at least three species in the chloroform solution containing various amounts of methanol; these species are discussed below. A similar change in absorption spectra was seen for chloroform solutions of the complex when a small amount of pyridine or 8-quinolinol was added: in the former, the absorption maxima around 340 and 390 nm shift to slightly lower wavelengths with increase in the pyridine content; in the latter, the absorption band for the complex cannot be measured below 400 nm because of the absorption of the added 8-quinolinol. The concentrations at which the absorption maximum at 460 nm disappears are $5.0 \cdot 10^{-2}$ M for pyridine and $1.0 \cdot 10^{-2}$ M for 8-quinolinol. These values are much lower than that for methanol (5.0 M). Slight amounts of pyridine or 8-quinolinol, which are stronger bases than methanol in chloroform, make a significant change in the

absorption spectra of the complex, which, in chloroform treated with phosphorus pentoxide, exists as the tetrahedral structure (structure I, Fig. 10). The addition of methanol, pyridine, and 8-quinolinol transforms the complex to the adduct of the nickel—8-quinolinol complex with a distorted octahedral structure (structures V and VIII, Fig. 10). When the absorption maximum around 460 nm disappears, almost all of the nickel—8-quinolinol complex is in the adduct form.

The absorption spectra of the nickel—8-quinolinol complex in dioxane, and in dioxane solution containing water or methanol, are shown in Figs. 3 and 4. Although the change in the spectra with increased water or methanol content is similar to the chloroform—methanol system mentioned above (cf. Fig. 2), there are absorption maxima at 463, 400, and 343 nm in pure dioxane (curve 1); this is similar to the spectrum of the nickel—8-quinolinol complex in chloroform saturated with water (curve 1, Fig. 2). The weak absorption maximum at 400 nm may be attributed to the ether group of dioxane.

Effect of the concentration of the complex on its absorption spectra

The absorption spectra of the complex at various concentrations in completely dry chloroform are shown in Fig. 5; the concentration range of the complex is restricted by its solubility in chloroform. If the state of the complex in chloroform is independent of its concentration, the same absorption spectrum should be obtained as long as the molar absorptivity is used as the abcissa. However, as the concentration of the complex decreases, the molar absorptivities at 460 and 340 nm increase and that around 390 nm decreases; they become almost constant below $1 \cdot 10^{-5}$ M nickel—8-quinolinol complex.

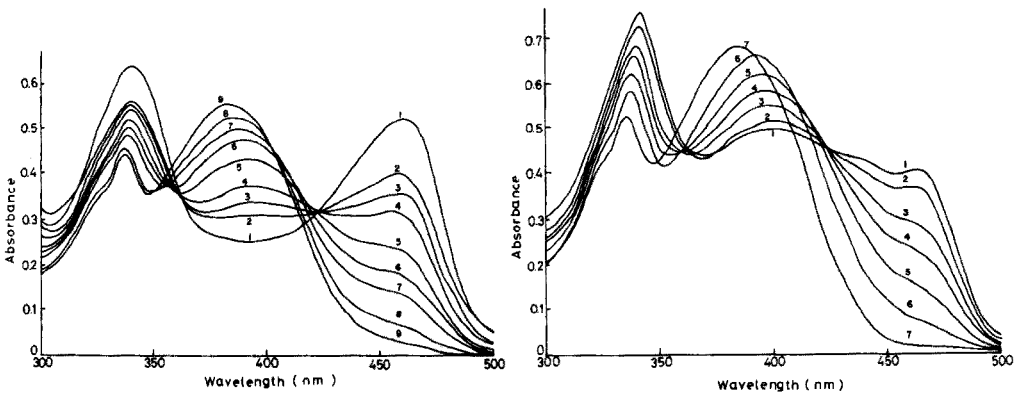

Fig. 2. Absorption spectra of the nickel—8-quinolinol complex in chloroform containing various amounts of methanol. Concentration of methanol: (1) 0; (2) 0.1 M; (3) 0.2 M; (4) 0.3 M; (5) 0.5 M; (6) 0.8 M; (7) 1.0 M; (8) 2.0 M; (9) 5.0 M. Nickel—8-quinolinol complex, $1.0 \cdot 10^{-4}$ M.

Fig. 3. Absorption spectra of the nickel—8-quinolinol complex in dioxane containing various amounts of water. Concentration of water: (1) 0; (2) 0.22 M; (3) 0.44 M; (4) 0.67 M; (5) 1.1 M; (6) 2.2 M; (7) 1.39 M. Nickel—8-quinolinol complex, $1.0 \cdot 10^{-4}$ M.

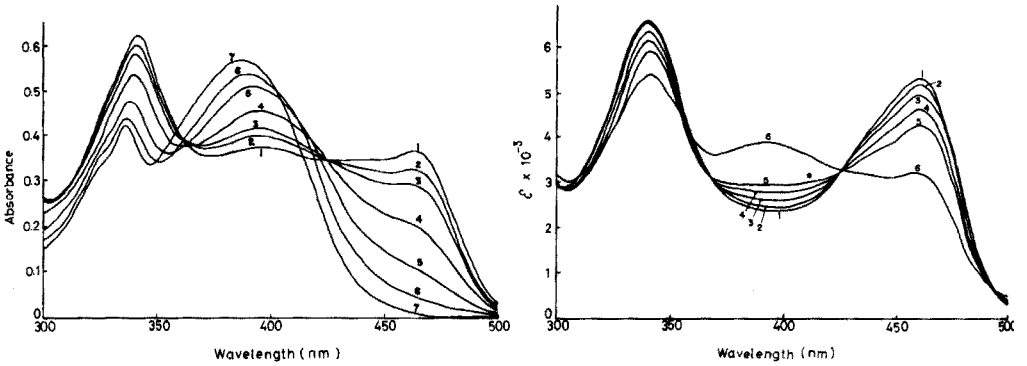

Fig. 4. Absorption spectra of the nickel—8-quinolinol complex in dioxane containing various amounts of methanol. Concentration of methanol: (1) 0; (2) 0.25 M; (3) 0.49 M; (4) 1.24 M; (5) 2.47 M; (6) 4.94 M; (7) 1.98 M. Nickel—8-quinolinol complex, $9.6 \cdot 10^{-5}$ M.

Fig. 5. Absorption spectra of the nickel—8-quinolinol complex in chloroform at various concentrations. (1) $1.0 \cdot 10^{-5}$ M; (2) $2.0 \cdot 10^{-5}$ M; (3) $1.0 \cdot 10^{-4}$ M; (4) $2.0 \cdot 10^{-4}$ M; (5) $3.0 \cdot 10^{-4}$ M.

This suggests that the monomer complex exists below $1 \cdot 10^{-5}$ M but the binuclear or trinuclear complex occurs at concentrations above $1 \cdot 10^{-5}$ M. Moreover, the absorption spectrum at concentrations above $1 \cdot 10^{-5}$ M is similar to that of the nickel—8-quinolinol complex in chloroform containing methanol or a trace of water. The oxygen atom of 8-quinolinol in a trans planar 1:2 nickel—8-quinolinol complex may coordinate weakly with the nickel atom of another 1:2 complex, so that the binuclear complex (e.g. structure II, Fig. 10) will be formed.

Effect of temperature on the absorption spectra of the complex

The effect of temperature in the range $-8°$ to 55°C is shown in Fig. 6. The volume change of chloroform with temperature was corrected by taking the volume at 18°C as standard. The change in the absorption spectra of the complex with the lowering of temperature is similar to the change in absorption spectra with increase in concentration, i.e. the absorption maximum at 460 nm increases with temperature and that at 390 nm decreases, with an isosbestic point at 426 nm. When the values of the absorbance at 460 and 400 nm were plotted against temperature, they became constant above 50°C. Such a change in the absorption spectra can be explained by the breaking of the weak intermolecular bond of the nickel—8-quinolinol complexes by the elevation of temperature. The nickel—8-quinolinol complex probably exists as the monomer at 60°C. It is well-known that the metal complex forms a polymer when interaction between the molecules increases, e.g. the copper—8-quinolinol complex forms the binuclear complex [8] by bridging involving the oxygen atom in an organic solvent; the binuclear complexes of nickel [5] and cobalt [9] 8-quinolinolates were extracted into chloroform under particular conditions.

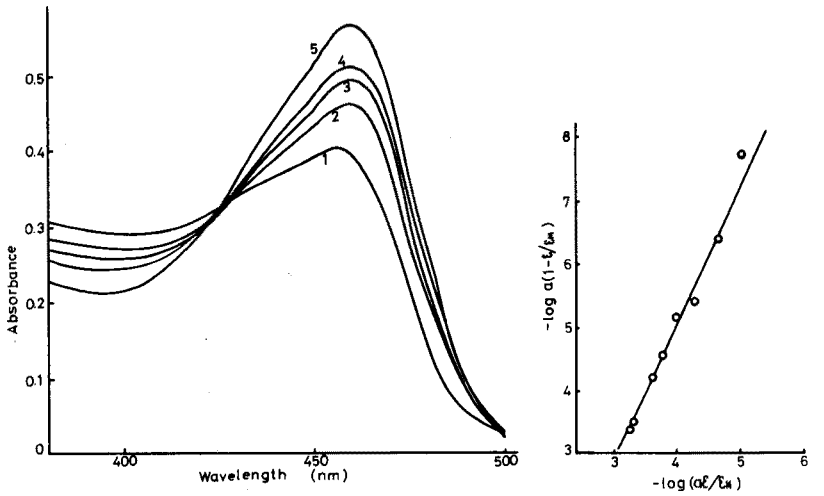

Fig. 6. Absorption spectra of the nickel—8-quinolinol complex in chloroform at various temperatures. (1) −8°C; (2) 3°C; (3) 15°C; (4) 25°C; (5) 55°C.

Fig. 7. Determination of degree of polymerization of nickel—8-quinolinol complex.

Degree of polymerization of the complex

The degree of polymerization resulting from the mutual interaction between molecules of the 1:2 nickel—8-quinolinol complex was studied. The degree of polymerization, n, and the equilibrium constant, K, were determined for $n\mathrm{NiQ}_2 \overset{K}{\rightleftharpoons} (\mathrm{NiQ}_2)_n$. When a is the initial concentration and x is the fraction of the concentration of the nickel—8-quinolinol complex in the equilibrium state, the equilibrium constant can be represented by $K = x/na^{n-1}(1-x)^n$, and the apparent molar absorptivity by $\epsilon = (1-x)\epsilon_M + x\epsilon_N$, where ϵ_M and ϵ_N are the molar absorptivities of the monomer and polymer, respectively. From these equations, with the simplification that $C = n(1-\epsilon_N/\epsilon_M)^{1-n}$, and with the approximation $\epsilon \gg \epsilon_N$, one obtains

$$\log a(1-\epsilon/\epsilon_M) = \log CK + n \log(a\epsilon/\epsilon_M) \qquad (1)$$

When $\log a(1-\epsilon/\epsilon_M)$ vs. $\log(a\epsilon/\epsilon_M)$ is plotted, a straight line with slope n should be obtained. When the wavelength 460 nm was selected to satisfy the approximation $\epsilon \gg \epsilon_N$, the molar absorptivity of the monomer complex, ϵ_M, was estimated as 5300, because plots of the apparent molar absorptivity vs. the concentration of the nickel—8-quinolinol complex are constant at concentrations less than ca. $1 \cdot 10^{-5}$ M. The plot of eqn. (1) is shown in Fig. 7. A straight line of slope 2.2 was obtained and $K = 2000$ was derived from the intercept. Two molecules of the nickel—8-quinolinol complex interact to form the binuclear complex.

Adduct formation constant of the complex

The absorption spectra of the nickel—8-quinolinol complex in organic solvents change progressively as increasing amounts of Lewis base are added,

as represented by $NiQ_2 + nB \rightleftharpoons NiQ_2 \cdot B_n$. The equilibrium constant of this equation and the amount of base added to the nickel—8-quinolinol complex, n, were determined. When the initial concentrations of the complex and the base in dioxane are a and b respectively, and the concentration of the adduct formed is x, the adduct formation constant K is represented by $K = x/(a-x)(b-nx)^n$. Then for $b \gg x$, one obtains $K = x/(a-x)b^n$, or $x = Kab^n/(1 + Kb^n)$.

The absorbance, As, at any wavelength is represented by $As = \epsilon_1(a-x) + \epsilon_2(b-nx) + \epsilon_3 x$, where ϵ_1, ϵ_2, and ϵ_3 are the molar absorptivities of the complex, the base, and the adduct, respectively. At the wavelengths involved, $\epsilon_2 = 0$, and this equation is simplified to $As = \epsilon_1(a-x) + \epsilon_3 x$.

The absorbance of the pure nickel—8-quinolinol complex, As_1, equals $\epsilon_1 a$, so that finally one obtains

$$a/(As - As_1) = 1/(\epsilon_3 - \epsilon_1) + 1/(\epsilon_3 - \epsilon_1)Kb^n \qquad (2)$$

When the relationship $a/(As - As_1)$ vs. $1/b^n$ is plotted for an appropriate integer, $n = 1$ or 2, a straight line should be obtained, and K can be obtained from values of the slope, the intercept and $\epsilon_1 = 3340$ at 460 nm. Plots for $n = 1$ and $n = 2$ for the chloroform—methanol system are shown in Fig. 8. Straight lines were obtained at methanol concentrations below ca. 1.0 M for $n = 1$, and above 1.0 M methanol for $n = 2$. This indicates that one molecule of methanol is added to the nickel—8-quinolinol complex below 1.0 M methanol; two molecules of methanol are added at higher concentrations of methanol (>1.0 M). This agrees with the previous conclusion, i.e. that there are three species at least in the chloroform solution containing various amounts of methanol. When dimerization of the nickel—8-quinolinol complex is taken into account, it is reasonable to consider the formation of methanol adducts; the 2:2 adduct is formed as shown (structure IV) in Fig. 10. The adduct formation constants $K_1 = 2.6$ and $K_2 = 3.9$ were obtained.

Similar plots were obtained for the dioxane—methanol system; $K_1 = 0.2$ and $K_2 = 0.4$. A straight line was obtained for $n = 2$ for the dioxane—water system (Fig. 9); $K = 2.4$ was derived. Two molecules of water are added to the nickel—8-quinolinol complex.

The structure of the complex in some organic solvents

The structures proposed for the nickel—8-quinolinol complex in organic solvents, on the basis of the above results, are represented in Fig. 10. When the complex, which has tetrahedral structure in the solid state, is dissolved in completely desiccated chloroform, the tetrahedral structure will be maintained as long as its concentration is low ($<10^{-5}$ M) at room temperature. However, at concentrations above 10^{-5} M, the binuclear complex, in which each nickel—8-quinolinol complex has the distorted octahedral structure, II, is formed. This binuclear complex tends to dissociate at higher temperature and appears to be solvated with chloroform(II), dioxane(VII), or methanol(IV). When the concentration of methanol or dioxane in chloroform becomes

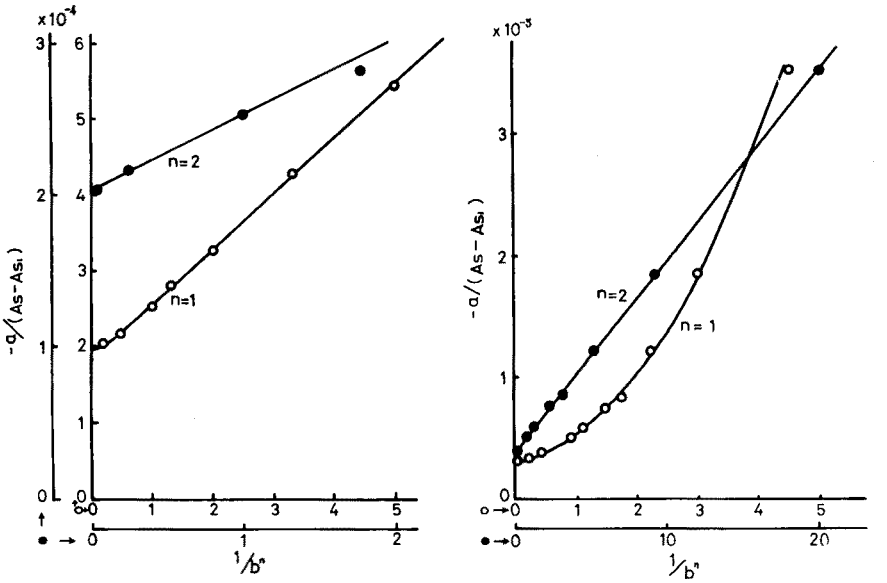

Fig. 8. Plots for chloroform—methanol system.

Fig. 9. Plots for dioxane—water system.

higher, the binuclear complex dissociates to form the 1:2 adduct complex (V or VI). When a stronger Lewis base, e.g. pyridine or 8-quinolinol, is added to the binuclear complex, the 1:2 adduct complex (VIII) is formed. When the Lewis base is water, the 1:2 adduct (III) is precipitated as $NiQ_2 \cdot 2H_2O$.

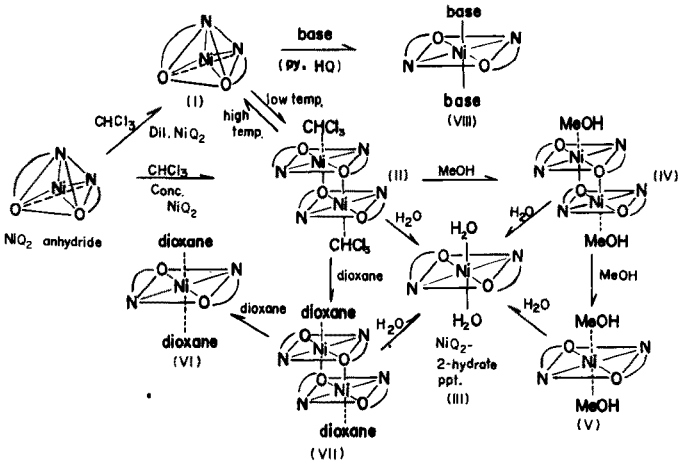

Fig. 10. Proposed structures of nickel—8-quinolinol complexes in organic solvents.

REFERENCES

1 K. Sone, J. Am. Chem. Soc., 75 (1953) 5207.
2 H. H. Perkampus and K. Kortum, Z. Anal. Chem., 190 (1962) 111.
3 E. Sekido, Nippon Kagaku Zasshi, 80 (1959) 871.
4 L. Morpurgo and R. J. P. Williams, J. Chem. Soc., A (1966) 73.
5 S. Oki and I. Terada, Anal. Chim. Acta, 66 (1973) 201.
6 N. Ohkaku and K. Nakamoto, Inorg. Chem., 10 (1971) 798.
7 E. Sekido, Nippon Kagaku Zasshi, 80 (1959) 1011.
8 C. M. Harris, E. Kokot and S. L. Lenzer, Nature, 196 (1962) 471.
9 E. Sekido and K. Fujita, Bull. Chem. Soc. Jpn., 49 (1976) 3073.

Analytica Chimica Acta, 92 (1977) 193—196

Short Communication

POTENTIAL INACCURACY IN TRACE METAL SPECIATION MEASUREMENTS BY DIFFERENTIAL PULSE POLAROGRAPHY

RICHARD J. STOLZBERG

Harold Edgerton Research Laboratory, New England Aquarium, Central Wharf, Boston, MA 02110 (U.S.A.)

(Received 1st December 1976)

The bio-availability and transport properties of trace metals in natural waters are determined largely by their chemical speciation [1]. Characterization of metal associations with natural organic ligands present in trace concentrations is an active area of research, and many attempts have been made to measure trace metal speciation in natural water. Anodic stripping voltammetry (a.s.v.) and differential pulse polarography (d.p.p.) have been widely used, and some success has been claimed [2—5]. The limitations of these techniques are often not considered. The roles of metal—ligand association and dissociation kinetics [6] and interfacial phenomena [7] are especially important. In addition, a number of assumptions must be made in interpreting ligand-induced shifts in peak potentials [8], and these assumptions are probably not valid in a typical natural water system containing only a small quantity of a variety of complex organic ligands.

This communication reports another limitation inherent in electrochemical measurement of speciation — non-uniform distribution of metal—ligand species within the polarographic cell. In examinations of the differential pulse polarographic behavior of the Cd complexes of nitrilotriacetate (NTA) and ethylenediaminetetraacetate (EDTA) in seawater [9], it was observed that the response of the electrode did not reflect the speciation of the ligand in the bulk solution when copper competed with cadmium for the ligand. Koryta [10] has described an analogous situation for the reduction of cyanide complexes in media without a sufficient excess of cyanide to form the most highly substituted complexes. The shape of the current—voltage curve was interpreted as being due to cyanide released at the electrode surface reacting with inward diffusing metal cyanide complexes to form more highly substituted species. Similar behavior would be expected in using d.p.p. to examine trace metal speciation in certain types of natural water and sewage sludge. For example, reduction of a copper—ligand complex will release uncomplexed ligand at the surface of the electrode. The uncomplexed ligand will diffuse out from the electrode surface and form complexes with inward diffusing metals. If lead were present as an uncomplexed species in the bulk solution, it could react with the ligand near the electrode, and the

reduction current or peak potential for lead would be the same as if a lead—ligand complex were present in the bulk solution.

The recent use of d.p.p. for measuring metal speciation [4] in the presence of humic acids demonstrates the technique to be sensitive enough to study some natural systems. Other results [9] show that speciation in the bulk solution is reflected in electrode response in many cases. However, if a metal—ligand complex is reduced at a potential anodic of the potential of interest, erroneous results will be obtained if the ligand is not present in excess.

Experimental

The apparatus and general analytical conditions have been described [9]. Competition experiments were carried out as follows. For calcium competition a sample of synthetic seawater ($4.3 \cdot 10^{-1}$ M NaCl, $9.4 \cdot 10^{-3}$ M KCl, $2.7 \cdot 10^{-2}$ M $MgSO_4$, $9.5 \cdot 10^{-3}$ M $CaCl_2$) was spiked with 4.75 μM NTA. The differential pulse polarogram was recorded with no cadmium added and subsequently at nine different concentrations of cadmium, the highest being $8.1 \cdot 10^{-4}$ M. For copper competition, a sample of synthetic sea water (SSW) was spiked with copper and $2.7 \cdot 10^{-4}$ M Cd. Polarograms were recorded at 6 levels of NTA and at 6 levels of EDTA. This was repeated for each ligand at four levels of copper.

Results and discussion

It has been shown [9] that the following relationship is true in the bulk solution of a sea-water sample spiked with cadmium and containing a competing metal ion, M.

$$[CdL] = (C_{Cd} - [CdL]) \cdot C_L / \{K'_c(C_M - [ML]) + C_{Cd} - [CdL]\} \quad (1)$$

(For definitions, see [9]). Since $(C_{Cd} + C_M) \gg C_L$ in SSW spiked with copper and $2.7 \cdot 10^{-4}$ M cadmium, and K'_{CdL} and K'_{ML} are large, the approximation $[ML] + [CdL] \approx C_L$ can be used. When this is substituted into eqn. (1), rearrangement gives

$$(K'_c - 1)\,[CdL]^2 + \{K'_c(C_M - C_L) + C_{Cd} + C_L\}\,[CdL] - C_{Cd}\,C_L = 0 \quad (2)$$

The solution of eqn. (2) for [CdL] was calculated for all values of C_{Cd}, C_M, C_L, and K'_c appropriate to the competition experiments done. With no copper present, calcium was the competing cation.

A comparison of the concentration of CdL species present in the bulk medium calculated from eqn. (2) and that "observed" by using polarographic peak current as an indicator of CdL concentration is presented in Table 1. Calcium is the competing metal. The value of the Student-t for the 11 pairs of data is 1.50. The critical value of t is 2.20 (11 degrees of freedom, $p < 0.05$). No significant difference is observable between the theoretically calculated and electrochemically observed values. The lack of bias between the values indicates that the electrode response reflects ligand speciation in the bulk solution.

Data presented in Table 2 (for NTA) and Table 3 (for EDTA) show the linear regression best fit to data calculated from eqn. (2) and to data

TABLE 1

Calcium competition experiment[a]

C_{Cd} (M)	[Cd—NTA] calculated from eqn. (2)[b] (μM)	[Cd—NTA] observed electro-chemically (μM)	C_{Cd} (M)	[Cd—NTA] calculated from eqn. (2) (μM)	[Cd—NTA] observed electro-chemically (μM)
0	0.0	0.0	$1.6 \cdot 10^{-4}$	3.4	3.1
$8.1 \cdot 10^{-6}$	0.5	0.2	$2.5 \cdot 10^{-4}$	3.8	4.0
$1.6 \cdot 10^{-5}$	0.9	0.6	$3.3 \cdot 10^{-4}$	4.0	4.0
$4.0 \cdot 10^{-5}$	1.8	1.3	$4.0 \cdot 10^{-4}$	4.1	4.5
$8.1 \cdot 10^{-5}$	2.7	2.1	$8.1 \cdot 10^{-4}$	4.4	4.8
$1.2 \cdot 10^{-4}$	3.1	2.9			

[a]In synthetic sea water, $C_{Ca} = 9.7 \cdot 10^{-3}$ M, $C_{NTA} = 4.75$ μM. Each value is the mean of 2 or 3 voltage scans in a single sample.)
[b]$K'_c = 10^{-2.2}$.

observed electrochemically with copper as the competing metal. With copper as the competing metal, the observed slope is from 1.6 to 16.5 times greater than expected from metal speciation in the bulk solution, i.e. the fraction of ligand associated with cadmium as observed electrochemically is 1.6 to 16.5 times greater than that calculated in the bulk solution. Only a 4.5% difference is observed for NTA when calcium is the competing cation in Table 2. No significant difference in the value of the expected and the observed slope can be seen for calcium competition for EDTA. (Table 3).

The copper competition experiments have thus shown that metal speciation measurements made by differential pulse polarography are

TABLE 2

Relation between [Cd—NTA] and C_{NTA}[a]

C_{Cu}		B	Standard deviation of B	A (μM)
0	Exp.[b]	0.803	0.004	0.004
	Obs.[c]	0.767	0.020	0.046
$5.2 \cdot 10^{-5}$ M	Exp.	0.377	0.029	−0.129
	Obs.	0.611	0.018	0.086
$1.2 \cdot 10^{-4}$ M	Exp.	0.148	0.009	−0.040
	Obs.	0.576	0.010	−0.008
$5.2 \cdot 10^{-4}$ M	Exp.	0.028	0.001	−0.002
	Obs.	0.461	0.018	−0.016

[a]Assuming a linear relation of [Cd—NTA] = A + B (C_{NTA}).
[b]Expected by solution of eqn. (2) at 0, 1.05, 2.1, 3.14, 4.2, $5.24 \cdot 10^{-5}$ M NTA; $\log K'_{C,Cu} = 1.3$; $\log K'_{C,Ca} = -2.2$; $C_{Cd} = 2.7 \cdot 10^{-4}$ M; $C_{Ca} = 9.5 \cdot 10^{-3}$ M.
[c]Observed by d.p.p. in solutions of composition noted in [b].

TABLE 3

Relation between [Cd—EDTA] and C_{EDTA}[a]

C_{Cu}		B	Standard deviation of B	A (μM)
0	Exp.[b]	0.997	0.0003	0.03
	Obs.[c]	0.999	0.007	0.03
$1.2 \cdot 10^{-4}$ M	Exp.	0.299	0.033	−3.46
	Obs.	0.604	0.064	−0.15
$3.7 \cdot 10^{-4}$ M	Exp.	0.061	0.003	−0.30
	Obs.	0.337	0.025	1.68
$6.2 \cdot 10^{-4}$ M	Exp.	0.033	0.001	−0.12
	Obs.	—[d]	—	—

[a] Assuming a linear relation of [Cd—EDTA] = A + B (C_{EDTA}).
[b] Expected by solution of eqn. (2) at 0, 2.5, 5, 7.5, 10 and $12.5 \cdot 10^{-5}$ M EDTA; log $K'_{c,Cu} = 1.2$; log $K'_{c,Ca} = -4.3$; $C_{Cd} = 2.7 \cdot 10^{-4}$ M; $C_{Ca} = 9.5 \cdot 10^{-3}$ M.
[c] Observed by d.p.p. in solutions of composition noted in [b].
[d] Very noisy, quantification difficult.

susceptible to errors from non-uniform distribution of ligand species in the polarographic cell. Reduction of the CuL species releases uncomplexed ligand at the electrode surface. The uncomplexed ligand in then able to react with inward diffusing metal cations. In this particular case, the recently complexed cadmium is reduced at a potential indicative of the presence of Cd—NTA or Cd—EDTA. In other cases, there may be a shift in reduction peak potential or changes in relative peak height or peak width [4]. Interpretation of differential pulse polarograms that suggest organic complexation of trace metals should include the possibility of non-uniform distribution of various metal—ligand complexes within the polarographic cell as being the cause of changes in peak height, position, or shape.

This research was supported by the Oceanography Section, National Science Foundation, Grant DES 74-21642.

REFERENCES

1 R. J. Stolzberg and D. Rosin, Anal. Chem., 49 (1977) 226.
2 W. R. Matson, Ph.D. Thesis, MIT (1968).
3 M. E. Bender, W. R. Matson and R. A. Jordan, Environ. Sci. Technol., 4 (1970) 520.
4 R. Ernst, H. E. Allen and K. H. Mancy, Water Res., 9 (1975) 969.
5 T. A. O'Shea and K. H. Mancy, Anal. Chem., 48 (1976) 1603.
6 M. S. Shuman and G. P. Woodward, Anal. Chem., 45 (1973) 2032.
7 G. E. Batley and T. M. Florence, J. Electroanal. Chem., 72 (1976) 121.
8 J. J. Lingane, Chem. Rev., 29 (1941) 1.
9 R. J. Stolzberg, Anal. Chim. Acta, 92 (1977) 139.
10 J. Koryta in P. Zuman (Ed.), Progress in Polarography, Vol. 1, Interscience, New York, 1962, p. 295.
11 A. Ringbom, Complexation in Analytical Chemistry, Interscience, 1963, p. 35 ff.

Analytica Chimica Acta, 92 (1977) 197—200

Short Communication

X-RAY FLUORESCENCE DETERMINATION OF TITANIUM IN GEOLOGICAL MATERIALS

A. E. HUBERT and T. T. CHAO*

U.S. Geological Survey, Denver, Colorado 80225 (U.S.A.)

(Received 6th January 1977)

The crustal abundance of titanium is estimated to be 0.44—0.61% according to Rosler [1]. Titanium is normally listed as one of the major rock-forming elements. The x-ray fluorescence method described here provides a sensitivity of 0.02%; the range of determination is 0.02—10%.

Titanium occurs in a variety of geological materials as well as in the detrital titanium-rich minerals ilmenite, anatase, rutile, and sphene, which are quite resistant to physical and chemical weathering. The particulate nature of these titanium minerals tends to cause homogeneity problems in powder and pelletization techniques. Lewis and Goldberg [2] mentioned some of the matrix effects encountered in the determination of titanium in powder samples of marine sediments. Mechanical segregation of titanium-rich minerals is also possible in a powder sample, because the various minerals tend to differ in specific gravity, which leads to sorting by density during processing. The solution technique used by Van Loon and Parissis [3] in the determination of titanium in silicates by atomic absorption has been adopted for sample preparation in this work, owing to the lack of the necessary molds for a fusion technique such as those described by Harvey et al. [4].

In the proposed method, the sample is decomposed with a mixture of hydrofluoric and sulfuric acids. The sample solution is dried on a filter-paper circle for analysis by x.r.f. Interferences, common to the analyses of powder samples, caused by particle-size variations and absorption of x-rays are thus eliminated or minimized.

Experimental

Apparatus and reagents. A Siemens SRS x-ray spectrometer was used. The operating conditions for the crystal-dispersive equipment are: Cr target, 35 kV, 20 mA; LiF 100 crystal; collimator, 0.4°; K_α line; flow counter; 2θ for peak, 86.13°; 2θ for background, 91.00°.

Other items used included 100-ml Teflon beakers, Eppendorf micropipets, x-ray cell film (Spex no. 3517), filter-paper circles (Whatman 540), plastic Caplugs EC-16 (Protective Closures Comp., Inc., Buffalo), and curtain rings (2.54 cm in diameter).

All chemicals were of reagent grade.

Titanium stock solution, 1000 μg ml⁻¹. Dissolve 1.668 g of titanium dioxide in a mixture (15 + 2) of hydrofluoric and sulfuric acids. Evaporate, dissolve the residue in 50 ml of hydrochloric acid and dilute to 1 l with water.

Titanium standard solutions. Make a series of standard solutions containing 0, 2, 5, 10, 20, 50, 100, 200, 500, and 1000 μg Ti ml^{-1} by dilution of the above stock solution with 5% (v/v) hydrochloric acid.

Procedure. Place a 0.50-g pulverized rock or soil sample in a 100-ml Teflon beaker and wet with 1 ml of water. Add 2 ml of concentrated sulfuric acid and 15 ml of 48% hydrofluoric acid. Allow to stand overnight if possible, and then heat to fumes of sulfuric acid. Cool the solution and add 10 ml of concentrated hydrochloric acid and 10 ml of water. Evaporate the solution to dryness below 250°C. Cool the residue, add 10 ml of water and 2.5 ml of concentrated hydrochloric acid, and warm to effect solution. Decant and wash the solution into a 50-ml screw-cap test tube. Add water to a volume of 50 ml and mix thoroughly. The sample solution is then ready to be pipetted onto a filter-paper circle.

Cover a Caplug with a layer of x-ray cell film which is held in place with a curtain ring. Place a filter-paper circle on top of the film. Using an Eppendorf micropipet, deliver 200 μl of the sample solution onto the filter-paper circle and allow to air-dry completely. Cover the filter-paper circle with another layer of the cell-film and secure with a second curtain ring. The sample is now ready for x-ray spectrometry. Treat a series of titanium standard solutions identically as the sample solution.

Each sample or standard is counted under vacuum in the x-ray spectrometer for a 100-s interval. The 100 μg Ti ml^{-1} standard has about 1200 cps above the 35—40 cps of the background. With a 0.50-g sample dissolved in 50 ml of solution, a 100-μg Ti ml^{-1} standard corresponds to 1% Ti in the sample. The standard series containing 2—1000 μg Ti ml^{-1} covers a range from 0.02 to 10% Ti in the sample. For practical purposes, two calibration curves should be prepared, one covering the range 0.02—1% Ti in the sample (using 0, 2, 5, 10, 20, 50, and 100 μg Ti ml^{-1} standard solutions), and the other covering the range 1—10% (using 0, 100, 200, 500, and 1000 μg Ti ml^{-1} standard solutions). The relationship between the counts per second of the standard solutions and the concentrations of titanium remains linear throughout the range of both calibration curves. The content of titanium of the sample can be determined directly from the calibration curves.

Results and discussion

Rock or soil samples containing organic matter or sulfides should first be roasted in a furnace at 800°C or on a Meker burner flame. As a substitute for roasting, an additional step can be added to the digestion. After the evaporation of the hydrofluoric acid, add very slowly about 3 ml of hydrogen peroxide (50%) to the sulfuric acid solution. Again evaporate the solution to fumes of sulfuric acid, cool, and proceed with the next step of the digestion.

After sample decomposition, all the sulfuric acid in the solution should be eliminated by evaporation to dryness. Sulfuric acid or water left on the filter-paper circle will cause the titanium values to be erratically low. To reduce variations in delivering sample or standard solutions, the same plastic tip is used for the Eppendorf micropipet. The tip is thoroughly rinsed between pipettings.

Table 1 presents the range and mean values of titanium for the USGS rock standards. The mean values for the six diverse rock types compare favorably with those published by Flanagan [5].

Table 2 lists the mean and relative standard deviations of six replicate analyses for titanium on the U.S. Geological Survey geochemical reference samples.

The data indicate that the analytical values obtained by this method define the amounts of titanium sufficiently well for geochemical studies. The method covers a range of titanium values both below and above the crustal abundance.

TABLE 1

Titanium values (%) on U.S. Geological Survey rock standards (average of six replicate analyses)

Sample	Rock Type	This work		Flanagan [5]
		Range	Mean	
G-2	Granite	0.29—0.33	0.30	0.32
GSP-1	Granodiorite	0.36—0.38	0.37	0.41
AGV-1	Andesite	0.65—0.66	0.65	0.65
PCC-1	Peridotite	<0.02	<0.02	0.01
DTS-1	Dunite	<0.02	<0.02	0.01
BCR-1	Basalt	1.30—1.38	1.33	1.34

TABLE 2

Six replicates analyses of U.S. Geological Survey geochemical reference standards [6] for titanium (%)

Sample	Material	Range	Mean	s_r(%)
GxR-1	Jasperoid	<0.02	<0.02	—
GxR-2	Soil	0.29—0.32	0.30	1.8
GxR-3	Spring deposit	0.11—0.14	0.12	1.4
GxR-4[a]	Cu-mill tailings	0.27—0.30	0.26	1.1
GxR-5	Soil	0.25—0.26	0.26	0.5
GxR-6	Soil	0.48—0.54	0.51	2.4

[a]Oxidized with hydrogen peroxide.

REFERENCES

1 H. J. Rosler, Geochemical Tables, Elsevier, New York, 1972.
2 G. J. Lewis and E. D. Goldberg, Anal. Chem., 28 (1956) 1282.
3 J. C. Van Loon and C. Parissis, Anal. Lett., 1 (1968) 249.
4 P. K. Harvey, D. M. Taylor, R. D. Hendry and F. Bancroft, X-ray Spectrom., 2 (1973) 33.
5 F. J. Flanagan, Geochim. Cosmochim. Acta, 33 (1969) 81.
6 G. H. Allcott and H. W. Lakin, Proc. 5th Int. Geochem. Expl. Symp., (1974) 659.

Analytica Chimica Acta, 92 (1977) 201—202

Short Communication

CATALYTIC ACTION OF CATION-EXCHANGE RESINS FOR THE DETECTION OF MICROGRAM AMOUNTS OF AMINO ACIDS

SAIDUL ZAFAR QURESHI and IZZATULLAH

Department of Chemistry, Aligarh Muslim University, Aligarh (India)

(Received 7th February 1977)

Ion-exchange resins can be used for the detection and determination of organic functional groups by means of the resin spot technique [1]. The present communication describes a sensitive test for the detection of α- and β-amino acids, and sulphur-containing amino acids.

Experimental

All chemicals were of reagent grade. Solutions of amino acids were prepared in demineralized water (free from ammonia).

Berthelot's reagent [2]. Dissolve 25 g of phenol in 54 ml of aqueous 20% (w/v) sodium hydroxide solution and make up to 100 ml. Store in a dark bottle in a cool place (Solution A). Saturate an aqueous 30% (w/v) sodium hydroxide solution with chlorine (Solution B). Use one drop of each solution in the test.

Resins. Dowex 50W-X8 (20-50 mesh, Na^+-form) was used after regeneration and washing with demineralized water until Berthelot's reagent gave no reaction.

Procedure. To the test solution (2—3 ml) add 1 drop of 1% potassium permanganate, and place the test tube in a boiling water bath for 2—3 min. Add 4—6 beads of ion-exchange resin (Na^+-form) and heat again. Decant the liquid and wash the resin with demineralized water two or three times. Place the beads on a white spot plate, and remove the excess of water with filter paper. Add one drop of Berthelot's reagent. In the presence of amino acids a blue colour develops at the surface of the resin beads.

Results and discussion

When an aqueous solution of an amino acid is heated with potassium permanganate in the presence of a few cation-exchange resin beads in the H^+-form, deamination with the evolution of ammonia takes place. A positive test is given by one drop of Berthelot's reagent on the resin beads. This test cannot be applied to the detection of amino acids as other functional groups, e.g. amines, amides, imides and nitriles, also give positive tests.

If resin beads in the Na^+-form are used, however, a positive test is given by amino acids only. In the regeneration of the resin in Na^+-form, H^+ ions are displaced from the resin phase, but it is difficult to eliminate them completely; even when the resin appears to have been fully converted to the Na^+-form, a few H^+ ions still remain in the resin phase. These enable potassium permanganate to act as a selective oxidant for amino acids; there is no oxidation or acid hydrolysis of other functional groups, e.g. amines, amides, imides, and nitriles. The method depends on the use of resins with a sulphonic acid group; weakly acidic resins do not give the test.

This function of a cation-exchange resin in the Na^+-form with a very low residual concentration of H^+ ions may be regarded as similar to that of hydrolytic enzymes [3].

The minimum amounts of the following amino acids detected by the recommended test were: glycine (4.50 μg), asparagine (4.50 μg), taurine (7.50 μg), lysine (8.70 μg), glutamic acid (13.76 μg), L-cystine (14.40 μg), methionine (8.9 μg), valine (9.36 μg), cysteine hydrochloride (18.40 μg), glycylglycine (7.92 μg), leucine (7.80 μg), DL-serine (6.30 μg), histidine (12.40 μg), α-alanine (13.55 μg), adenine (27.00 μg), L-proline (27.60 μg), aspartic acid (26.60 μg), β-alanine (26.70 μg), creatine (44.70 μg).

A positive test was given by anthranilic acid (27.00 μg), sulphanilic acid (38.50 μg), and sulphadiazine (50.00 μg) but barbituric acid and its derivatives gave a negative test. The ion-exchange test for microgram amounts of amino acid was performed in the presence of large amounts of foreign substances; no interference was given by hydrocarbons and their derivatives, alcohols, ethers, carboxylic acids, carbohydrates, phenols, heterocyclic bases, amides, nitriles, aldehydes, ketones and amines other than methylamine and ethylamine.

The authors thank W. Rahman for research facilities and the C.S.I.R. (India), for financial assistance to Izzatullah.

REFERENCES

1 S. Z. Qureshi, M. S. Rathi and S. Bano, Anal. Chem., 46 (1974) 1139.
2 F. D. Snell, Colorimetric Method of Analysis, 3rd edn., Vol. II; D. Van Nostrand, New York, (1959), p. 819.
3 C. Calmon and T. R. E. Kressman, Ion Exchange in Organic and Biochemistry, Interscience, New York, (1957), p. 388.

Analytica Chimica Acta, 92 (1977) 203—207

Short Communication

PROPRIÉTÉS D'ÉCHANGE D'IONS DU DIOXYDE D'ÉTAIN CRISTALLISÉ, FAIBLEMENT HYDRATÉ: ÉCHANGE DE L'ION Fe^{3+}

N. JAFFREZIC-RENAULT

Groupe de Recherche de Radiochimie Analytique, Laboratoire Pierre Sue, C.N.R.S., C.E.N./Saclay, B.P. nº 2, 91190, Gif-sur-Yvette (France)

(Reçu le 10 janvier 1977)

Les oxydes hydratés d'éléments tétravalents présentent des propriétés acides et échangeuses d'ions dues aux groupes acides de Brönstedt. Il semble que ces propriétés soient dues aux groupes hydroxyles de surface [1]. Les ions divalents de la première série de transition s'échangent avec une partie de ces protons acides suivant un équilibre réversible, de stoéchiométrie 1 M^{2+}: 1H^+ [1].

Dans ce travail, nous avons comparé le comportement de l'ion Fe^{3+} et des ions divalents. Nous avons fait une étude thermodynamique de la réaction de fixation de l'ion par les traceurs radioactifs, puis une étude du solide avant et après la fixation du fer(III), réalisée par e.s.c.a. et spectroscopie Mössbauer; celle-ci a permis de préciser le modèle du mécanisme de fixation.

Partie expérimentale

Les échantillons de dioxyde d'étain (Carlo-Erba, Milan) sont caractérisés par leur température de préparation. TDO est le dioxyde d'étain commercial.

Détermination de la réversibilité des équilibres et de la stoéchiométrie de la réaction d'échange. Une solution $NaNO_3$ 5,5 M (500 ml) de concentration initiale 10^{-4} M en élément et 0,03 M en acide, est mise en contact avec 20 g de dioxyde d'étain; 5 ml de solution sont prélevés à l'équilibre sur lesquels la quantité d'élément restant en solution est déterminée grâce à la détection de la radioactivité du traceur $^{59}Fe^*$. Par addition de 5 ml de soude, le pH d'équilibre est amené à des valeurs plus élevées. Le rapport volume de solution/masse de solide reste inchangé; la force ionique égale à 5,5 n'est pas modifiée de façon importante, la concentration en H^+ variant de 0,03 à 0,3. Ainsi, point par point on trace l'isotherme de la réaction (1)

$$Fe^{3+}_{soln.} + \alpha H^+_{SnO_2} \underset{\text{(réaction 2)}}{\overset{\text{(réaction 1)}}{\rightleftharpoons}} Fe^{3+}_{SnO_2} + \alpha H^+_{soln.}$$

Des additions successives de 5 ml d'acide nitrique ont permis de tracer l'isotherme de la réaction (2).

Détermination des capacités de rétention. La détermination des capacités de rétention est faite suivant la méthode de Glaeser [2]: le diagramme représentant la quantité de cation en excès en fonction de la quantité initiale est une droite de pente + 1 qui, prolongée jusqu'à l'axe des x, détermine la capacité de rétention. Les équilibres solution—solide sont réalisés en agitant 50 ml de solution $NaNO_3$ 0,6 M, contenant des concentrations initiales en élément de $3 \cdot 10^{-2}$ M à 10^{-1} M, avec 2 g de dioxyde d'étain.

Détermination des acidités de Brönstedt. Le principe du dosage est fondé sur la réaction: $H^+(SnO_2) + CH_3COONH_4$ (soln.) → CH_3COOH (soln.) + $NH_4^+(SnO_2)$. Il s'agit de doser l'acide acétique ainsi libéré. La méthode utilisée a été mise au point par De Mourgues [3]: solide (2 g) est mis en équilibre avec 50 ml de solution d'acétate d'ammonium 1 M, par une agitation de 30 min. Après centrifugation, on mesure le pH de la solution. Une courbe d'étalonnage permet de réaliser la correspondance entre le pH et la quantité d'acide acétique libérée.

E.s.c.a. Ces études ont été réalisées sur un spectromètre à émission électronique induite (IEE) Varian. Le rayonnement excitateur est l'émission K_α du magnésium d'énergie 1253,6 eV.

Pour l'estimation des quantités d'éléments fixées [4], seuls les ions situés dans la couche superficielle sont pris en compte. Une étude préalable a été effectuée sur les nitrates des métaux de transition afin de déterminer les coefficients d'intensité relative pour chacun d'entre eux; ceux-ci sont égaux au rapport de l'intensité de la raie 2*p* pour chaque élément à l'intensité de la raie 1*s* de l'azote. En utilisant le pic Sn 3*d* comme référence et à l'aide de ces coefficients d'intensité, le rapport de la capacité en Fe^{3+} à celle du manganèse a pu être calculée.

Pour caractériser l'environnement chimique du fer fixé à la surface du dioxyde d'étain, à partir des spectres e.s.c.a., il était nécessaire d'étudier à titre de comparaison, les énergies de liaison des électrons 2*p* dans la goethite, l'oxyde (Fe_2O_3), le sulfate, le nitrate.

Résultats et discussion

Relation entre la capacité de rétention et l'acidité de Brönstedt. Dans le cas des ions divalents, ces rapports étaient constants, ce qui permettait d'en déduire quelle proportion des groupes acides de Brönstedt dosés participait à l'échange.

Dans le cas du fer(III) nos résultats sont présentés dans le tableau 1. Pour des températures de préparation comprises entre 250°C et 600°C, le rapport $(Fe^{3+})/(A)$ est égal à environ 1,2. Ceci montre qu'il se fixe plus d'un ion Fe^{3+} par proton acide dosé.

Etude thermodynamique de la réaction d'échange. Si la réaction d'échange est réversible (réactions 1 et 2) nous pouvons appliquer la loi d'action de masse. En faisant l'approximation qu'à force ionique μ = 5,5, les coefficients d'activité des espèces sont peu différents de 1, nous pouvons écrire.

$$K_0' = [Fe^{3+}]_{SnO_2} [H^+]^{\alpha}_{soln.} / [Fe^{3+}]_{soln.} [H^+]^{\alpha}_{SnO_2}$$

TABLEAU 1

La capacité de rétention et l'acidité de Brönstedt

Température de préparation (°C)	Acidité de Brönstedt (A) Nb éq. H^+ par g SnO_2	Capacité en Fe^{3+} (Fe) Nb Ion.g Fe^{3+} par g SnO_2	$\frac{(Fe)}{(A)}$
100	$4{,}4 \cdot 10^{-4}$	$2{,}4 \cdot 10^{-4}$	$0{,}5_5$
200	$3{,}3 \cdot 10^{-4}$	$2{,}6 \cdot 10^{-4}$	0,8
250	$2{,}8 \cdot 10^{-4}$	$3{,}3 \cdot 10^{-4}$	1,2
400	$8{,}9 \cdot 10^{-5}$	$1{,}5 \cdot 10^{-4}$	1,7
500	$5{,}2 \cdot 10^{-5}$	$6{,}3 \cdot 10^{-5}$	1,2
600	$5{,}2 \cdot 10^{-5}$	$6{,}2 \cdot 10^{-5}$	1,2

Les symboles [ ] représentent les concentrations molaires des espèces. En faisant les mêmes approximations que pour les ions divalents, nous obtenons la relation

$$\log ([Fe^{3+}]_{SnO_2}/[Fe^{3+}]_{soln.}) = \log (K'_0 [H^+]^{\alpha}_{SnO_2}) - \alpha \log [H^+]$$

Si nous représentons les isothermes des réactions (1) et (2) sous la forme $\log ([Fe^{3+}]_{SnO_2}/[Fe^{3+}]_{soln.}) = f(-\log [H^+])$, nous devrions obtenir, avec ces hypothèses, deux droites confondues de pente α. La Fig. 1 montre que l'isotherme de la réaction (1) est une droite de pente +3,2. Lorsqu'un ion Fe^{3+} est fixé sur le dioxyde d'étain, trois ions H^+ sont libérés en solution. L'isotherme de la réaction (2) n'est pas confondue avec celle de la réaction (1); cet équilibre d'échange n'est pas réversible. D'après ces premiers résultats, il semble que le fer ne se fixe pas par une simple réaction d'échange d'ions comme les ions divalents.

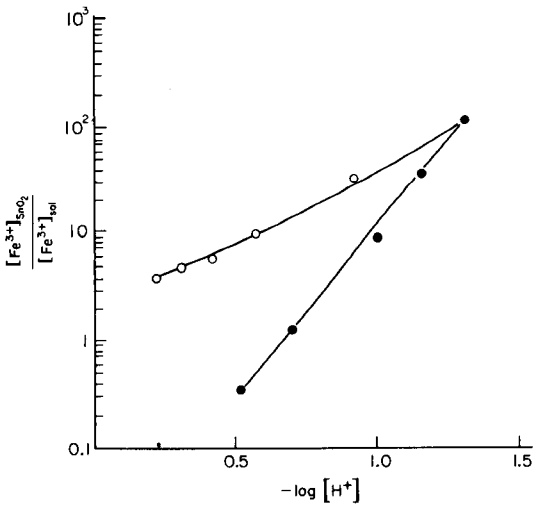

Fig. 1. Isothermes des réactions (1) (•) et (2) (○).

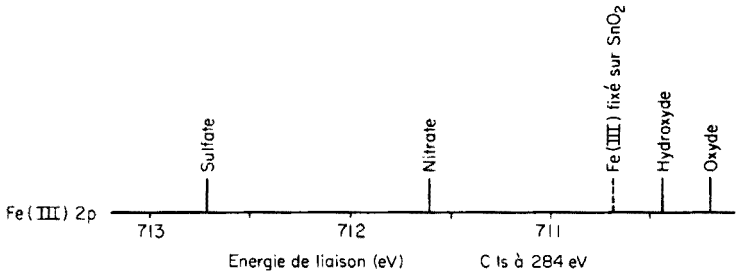

Fig. 2. Energies de liaison des électrons 2*p* dans les différents composés de fer(III).

Résultats de l'étude par spectroscopie Mössbauer. Le fer, fixé sur le dioxyde d'étain, est totalement trivalent, dans un environnement très asymétrique. Les distances Fe^{3+}—Fe^{3+} sont très petites, inférieures à celles rencontrées dans le nitrate de fer; en considérant la faible concentration en fer, la remarque précédente nous permet de conclure à la présence d'agglomérats de fer(III).

Résultats obtenus par e.s.c.a. Le rapport du nombre de cations détectés par e.s.c.a. au nombre d'atomes d'étain dans la couche superficielle est estimée à: Mn^{2+}, 1 (unités arbitraires); Fe^{3+}, 3,6 ± 0,9. Les mêmes rapports déterminés à l'aide des traceurs radioactifs sont les suivants: Mn^{2+}, 1 (unités arbitraires); Fe^{3+}, 15 ± 4. L'écart observé tient à la localisation des cations puisque l'e.s.c.a. n'est sensible qu'à la constitution superficielle alors que les traceurs renseignent sur la constitution massique.

Dans ce cas, nous pourrions attribuer cet écart à la présence d'agglomérats superficiels déjà mis en évidence par la spectroscopie Mössbauer, dont seule la surface serait prise en compte; la taille de ces agglomérats étant d'une centaine d'Angströms au minimum.

La comparaison des énergies de liaison des électrons 2*p* dans les différents composés (cf. Fig. 2) montre que pour l'ion Fe^{3+} fixé sur le dioxyde d'étain, l'énergie est proche de celle de l'hydroxyde (goethite) et de l'oxyde.

La largeur à mi-hauteur du pic de l'oxygène O 1*s* est particulièrement élevée (3,1 eV) alors qu'elle n'est que de 2,5 eV pour le dioxyde d'étain seul; ceci peut être attribué à des molécules d'eau de solvatation entourant les atomes de fer(III).

Proposition d'un mécanisme de fixation. D'après résultats, nous proposons un mécanisme de rétention qui ferait intervenir une réaction d'échange avec les protons acides du dioxyde d'étain pour tenir compte du rapport constant entre la capacité de rétention et l'acidité de Brönstedt:

(1) Echange d'ions:

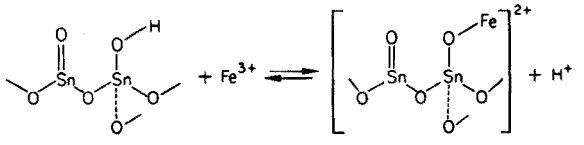

Puis une réaction d'hydrolyse rendant compte de la stoechiométrie de la réaction de fixation 1 Fe^{3+}: $3H^+$.

(2) Hydrolyse:

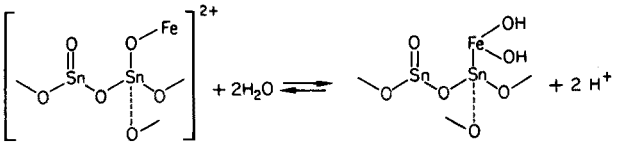

A partir de ce groupe hydroxyde ferrique, d'autres ions Fe^{3+} pourraient se fixer et donner naissance aux agglomérats.

Conclusion

La réaction de fixation du fer(III) n'était pas un simple équilibre d'échange d'ions comme pour les ions divalents: cette réaction est irréversible de stoéchiométrie 1 Fe^{3+}: 3 H^+.

Les études réalisées par spectroscopie Mössbauer et par e.s.c.a., ont montré que le fer fixé se trouvait vraisemblablement sous forme d'agglomérats bien que ceux-ci n'aient pas pu être mis en évidence à cause de leur taille.

Nous avons proposé un mécanisme se fixation; nous avons éliminé l'hypothèse d'une simple réaction d'hydrolyse vues nos conditions expérimentales (0,03 M < H^+ < 0,3 M) et vus les résultats obtenus par e.s.c.a. où le fer fixé sur le dioxyde d'étain a une position différente de l'hydroxyde (FeOOH). Cependant des phénomènes de coagulation de sols ou d'adsorption d'espèces hydroxylés peuvent avoir lieu, comme le propose Bilinski [5].

Nous remercions Monsieur J. M. Friedt du Laboratoire de Chimie Nucléaire de l'IN_2P_3 de Strasbourg qui a effectué l'étude par spectroscopie Mössbauer. Nous remercions Madame J. Escard et Monsieur D. Brion du Centre de Recherche de l'Ircha (Vert le Petit, France) qui ont réalisé l'étude par e.s.c.a.

BIBLIOGRAPHIE

1 N. Jaffrezic-Renault, Thèse, Orsay, 1976.
2 R. Glaeser, C.R. Acad. Sci. Ser. C, 222 (1946) 1179.
3 L. De Mourgues, Thèse, Lyon, 1957.
4 D. Brion, J. Escard et G. Mavel, Rapport DRGST n° 74-7-1386 (1976).
5 H. Bilinski, J. Inorg. Nucl. Chem., 38 (1976) 2001.

Analytica Chimica Acta, 92 (1977) 209—211

Short Communication

THE KINETIC DETERMINATION OF IRON(III) BASED ON THE IRON(III)-CATALYZED REDUCTION OF TRIS(OXALATO)COBALTATE(III) BY ASCORBIC ACID

KOUSABURO OHASHI, TERUHIKO SAGAWA, EIICHI GOTO and KATSUMI YAMAMOTO

Department of Chemistry, Faculty of Science, Ibaraki University, Mito 310 (Japan)

(Received 6th December 1976)

Kinetic determinations of metal ions are usually based on metal ion-catalyzed reactions [1]. Redox reactions are particularly useful, because they are extremely sensitive and often very selective. Kinetic studies have been made of the reduction of chloro- [2], oxalato- [3] and azido- [4] cobalt(III) complexes by iron(II). It seemed to be worthwhile to apply these reduction reactions of cobalt(III) complexes to the determination of metal ions based on their catalytic effects on the reduction rates. The rate of reduction of tris(oxalato)cobaltate(III) ($Co(ox)_3^{3-}$) by ascorbic acid is catalyzed by iron(III). Iron(III) can be determined in the range 0.28—7.80 $\mu g\ ml^{-1}$, based on the relationship between the rate of decrease of the absorbance of $Co(ox)_3^{3-}$ at 600 nm and the concentration of iron(III). The mechanism of the iron(III)-catalyzed reduction of $Co(ox)_3^{3-}$ by ascorbic acid is discussed.

Experimental

Apparatus and chemicals. A Hitachi EPS-3 spectrophotometer was used.

$K_3[Co(ox)_3] \cdot 3H_2O$ was prepared by the method of Sommer [5]. The identity and purity of the complex were confirmed by microanalysis and spectrophotometry.

Iron(III) solution ($1.0 \cdot 10^{-1}$ M). Iron wire (99.99% pure) was dissolved in perchloric acid and oxidized with bromine solution; hydrobromic acid was removed by fuming. Working solutions were prepared by dilution with redistilled water.

Procedures. Solutions of iron(III), ascorbic acid, $Co(ox)_3^{3-}$, and perchloric acid were thermostated at 25°C. For the iron(III) determination, 5 ml of a series of iron(III) solutions were placed in 25-ml measuring flasks. Then, 5 ml of $1.5 \cdot 10^{-2}$ M $Co(ox)_3^{3-}$, 5 ml of 0.60 M perchloric acid, and 5 ml of $1.5 \cdot 10^{-1}$ M ascorbic acid in 0.2 M perchloric acid were added successively to the solution. The final concentration of perchloric acid was maintained at 0.20 M. The solution was transferred to a quartz 1-cm cell which was thermostated by circulating water through the cell holder.

The plots of the absorbance at 600 nm vs. time showed straight lines up to at least 10% of the whole reaction. Therefore, the rates of the iron(III)-catalyzed reduction of $Co(ox)_3^{3-}$ by ascorbic acid were obtained from the slopes of these plots. The calibration curve was prepared by plotting the rate vs. the concentration of iron(III).

Results and discussion

Determination of iron(III). The relation between the rate of reduction of $Co(ox)_3^{3-}$ and the concentration of iron(III) was rectilinear in the range 0.28—7.8 μg Fe ml^{-1}; at the upper end of the range, the rate was about $8 \cdot 10^{-6}$ M s^{-1}.

Iron(III)-catalyzed reduction of $Co(ox)_3^{3-}$ by ascorbic acid. Although $Co(ox)_3^{3-}$ is reduced by ascorbic acid, the rate of this reduction is negligible compared to that of the iron(III)-catalyzed reduction in acid solution ($[H^+] > 0.10$ M). The effect of the concentration of perchloric acid was examined; the rate increases slightly with increase in the concentration of perchloric acid from 0.1 M to 0.5 M, and a 0.2 M acidity was chosen. The dependence of the reduction rate on the concentration of ascorbic acid or $Co(ox)_3^{3-}$ was examined at 0.20 M perchloric acid (Fig. 1). The reduction rate increases with increase in the concentration of ascorbic acid or $Co(ox)_3^{3-}$, but the dependence of the rate on the concentration of ascorbic acid or $Co(ox)_3^{3-}$ is complicated. Therefore, the rate law cannot be obtained.

In 0.20 M perchloric acid, ascorbic acid exists as the neutral form, because the first and second dissociation constants of ascorbic acid are $10^{-4.14}$ mol l^{-1} and $10^{-11.75}$ mol l^{-1}, respectively [6]. Therefore, initiation of the iron(III)-catalyzed reduction of $Co(ox)_3^{3-}$ by ascorbic acid in the strong acid solution would take place by the reaction $Fe^{3+} + H_2A \rightarrow Fe^{2+} + H_2A^{\cdot}$, where H_2A and $H_2A^{\cdot}$ represent the neutral and radical forms of ascorbic acid. Subsequently, the following reaction paths may be possible:

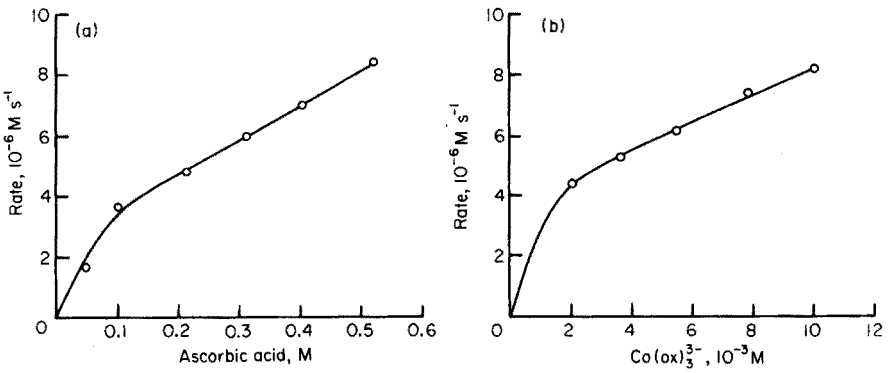

Fig. 1. The relation between the rate of the reduction and the concentration of ascorbic acid (a) or $Co(ox)_3^{3-}$ (b) $[Fe(III)] = 8.00 \cdot 10^{-5}$ M, $[HClO_4] = 0.20$ M, I = 0.5 ($NaClO_4$), 25°C. For (a), $[Co(ox)_3^{3-}] = 4.00 \cdot 10^{-3}$ M. For (b) [ascorbic acid] = 0.25 M.

$$Fe^{2+} + Co(ox)_3^{3-} \xrightarrow{H^+} Fe^{3+} + Co^{2+} + 3H_2ox$$

$$H_2A^{\cdot} + Co(ox)_3^{3-} \xrightarrow{H^+} Co^{2+} + 3H_2ox + H_2A_o$$

$$Fe^{3+} + H_2A^{\cdot} \longrightarrow Fe^{2+} + H_2A_o$$

where H_2A_o represents the oxidized form of neutral ascorbic acid.

Effect of diverse ions. The effect of diverse ions on the determination of iron(III) was investigated. The presence of 50 μg ml^{-1} of magnesium(II), calcium(II), chromium(III), manganese(II), zinc(II), cadmium(II), tungsten(VI), and lead(II) did not interfere. The interferences of 50 μg ml^{-1} of copper(II), cobalt(II), nickel(II), vanadium(IV), and molybdenum(VI) were pronounced, but 5 μg ml^{-1} of these metal ions did not interfere.

REFERENCES

1 R. A. Greinke and H. B. Mark, Jr., Anal. Chem., 44 (1972) 295.
2 Y. Kurimura, K. Ohashi, T. Otsuki and K. Yamamoto, Bull. Chem. Soc. Jpn., 44 (1971) 1293.
3 K. Ohashi, Bull. Chem. Soc. Jpn., 45 (1973) 3093.
4 K. Ohashi, K. Yamamoto, K. Yokouchi and Y. Kurimura, Nippon Kagaku Kaishi, (1972) 740.
5 L. Sommer, Collect. Czech. Chem. Commun., 28 (1963) 449.
6 S. P. L. Sörensen, Z. Anorg. Chem., 11 (1896) 2.

Analytica Chimica Acta, 92 (1977) 213—216

Short Communication

CORRELATION OF THE E.M.I.T. DIPHENYLHYDANTOIN ASSAY IN BLOOD PLASMA WITH A G.L.C. AND A SPECTROPHOTOMETRIC METHOD

S. STAVCHANSKY*, T. LUDDEN, J. P. ALLEN and P. WU

Drug Dynamics Institute, College of Pharmacy, University of Texas, Austin, Texas 78712 (U.S.A.)

(Received 3rd January 1977)

The growing number of publications from clinical investigations of diphenylhydantoin (DPH) [1—13] clearly demonstrates the usefulness of monitoring DPH plasma levels in patients who develop symptoms and signs of intoxication, show unexpected sensitivity, or fail to respond to therapeutic doses of the drug. General techniques for arriving at optimum, individual DPH dosage regimens based on plasma levels have been published recently [5, 6]. To obtain reliable pharmacokinetic data for the optimization of DPH therapy it is imperative to develop a sensitive, selective and practical assay. Numerous assay procedures for DPH in blood, urine and in the presence of other drugs have been devised [7—16]. In a recent report [17] the variability of results reported by 112 clinical laboratories, when three pooled plasma samples containing 11.3—23.9 $\mu g\ ml^{-1}$ of DPH as well as other anticonvulsants were assayed, was disturbing. The coefficients of variation were 41—57% for the clinical laboratories and 16—20% for the five reference laboratories involved.

The objective of the present investigation was to determine the reliability of the DPH plasma concentration reported by a clinical laboratory routinely performing the assay and evaluating the "Enzyme Multiplied Immunoassay Technique" (e.m.i.t.) system for anticonvulsant drug analysis.

The data presented show that the spectrophotometric method for the determination of diphenylhydantoin is unacceptable for clinical use. In addition, the practicality, specificity and precision of the e.m.i.t. system is confirmed. Finally, data were obtained showing no statistically significant difference between the clinical laboratories and reference laboratories, indicating that the radioimmunoassay (r.i.a.), e.m.i.t., and gas—liquid chromatographic (g.l.c.) procedures are useful, clinically interchangeable methods.

Experimental

Forty-two plasma samples were obtained from patients for whom 200—650 mg of diphenylhydantoin (sodium salt) daily had been prescribed. All plasma samples were obtained as a routine part of the procedure for epileptics visiting a clinic. After a sufficient amount of each sample had been dispatched to the Bexar County Clinical Laboratory, Texas, for determination of DPH levels, the remaining plasma was sent to the Drug Dynamics Institute, Austin, to be assayed by two reference techniques. The clinical laboratory was unaware that its performance was being monitored: their samples were assayed by one of two techniques; 25 samples were assayed by the commercial ^{125}I r.i.a. procedure (Clinical Assays Inc., Cambridge, Mass.), and the remaining 17 samples by the spectrophotometric method of Wallace et al. [18]. The reference laboratory assayed all 42 samples by the g.l.c. procedure of McGee [19] and also by a novel e.m.i.t. system for DPH analysis (Syva Corporation, Palo Alto, California). In addition, human plasma was spiked with diphenylhydantoin. The plasma concentration ranged from 0—50 $\mu g\ ml^{-1}$. These samples were analyzed by the g.l.c. and e.m.i.t. assays.

Results and discussion

Good correlation was obtained between the results of the two reference techniques (e.m.i.t. and g.l.c.) when human plasma spiked with diphenylhydantoin was studied. The results are presented in Table 1; the correlation coefficient was 0.995 with a standard error of 1.596. In addition, the relative standard deviation for the g.l.c. and e.m.i.t. assays is small. Linear regression analysis of all the correlations is presented in Table 2. The slope of the line resulting from the plot of DPH levels of the spiked plasma obtained by g.l.c. versus those obtained by the e.m.i.t. system serve as the standard for the statistical comparison of the slopes of the lines obtained when plasmas from patients were analyzed by the reference and clinical laboratory techniques.

TABLE 1

Correlation of diphenylhydantoin levels in spiked human plasma determined by e.m.i.t. and g.l.c. assays

DPH added ($\mu g\ ml^{-1}$)	G.l.c.					E.m.i.t.				
	DPH ($\mu g\ ml^{-1}$)		Mean	s[a]	s_r[a]	DPH ($\mu g\ ml^{-1}$)		Mean	s	s_r
2.5	2.3	2.5	2.4	0.09	4	2.2	2.2	2.2	0.26	12
5.0	5.1	4.8	5.0	0.18	4	5.2	5.7	5.5	0.34	6
10.0	9.6	9.9	9.8	0.18	2	12.1	10.7	11.4	0.83	7
20.0	19.0	19.3	19.2	0.18	1	22.5	19.8	21.3	1.89	9
30.0	28.5	29.3	28.9	0.62	2	32.3	28.6	30.4	3.24	11
40.0	39.0	39.5	39.3	0.35	1	40.7	35.3	38.0	4.24	11
50.0	54.8	48.4	50.1	2.4	5	48.2	42.7	45.4	3.95	9

[a] s = standard deviation. s_r = relative standard deviation.

TABLE 2

Linear regression analysis of all correlations

Correlation	Slope	Intercept	Correlation coefficient	Standard error	Standard deviation of slope
G.l.c. vs. e.m.i.t. Spiked plasma	0.911	1.886	0.995	1.596	0.043
G.l.c. vs. e.m.i.t. Patients' plasma	0.867	0.783	0.928	3.565	0.067
G.l.c. vs. Spectrophotometric Patients' plasma	0.677	2.740	0.833	3.804	0.125
G.l.c. vs. r.i.a. Patients' plasma	0.936	0.047	0.957	2.887	0.063

Good correlation was also obtained between the results of the two reference techniques when the plasma from patients was analyzed (Table 2). The correlation coefficient was 0.928 with a standard error of 3.565. Similarly, there was good correlation between the results of the reference g.l.c. assay and the radioimmunoassay clinical laboratory technique. Three samples assayed by the clinical laboratory by the r.i.a. technique were reported as $< 2.0\ \mu g\ ml^{-1}$. Two of these samples contained no measurable DPH when assayed by both reference techniques. The other sample was found to contain $1.3—1.7\ \mu g\ ml^{-1}$ by the reference techniques.

The correlation between the results of the g.l.c. reference technique and the spectrophotometric clinical laboratory technique was not quite as good as the other correlations (Table 2). Two samples reported by the clinical laboratory to contain less than $2.0\ \mu g\ ml^{-1}$ were found to contain 0.7—0.9 and $2.2—2.5\ \mu g\ ml^{-1}$ by the two reference techniques.

Statistical comparisons to determine the significance between the slopes of the lines obtained by the different methods, as shown in Table 2, were performed by means of a paired *t*-test. There was no statistically significant difference between the reference and laboratory techniques at $p < 0.05$. However, at $p < 0.1$, the spectrophotometric assay was significantly different from the g.l.c., e.m.i.t., and r.i.a. techniques. The statistical comparisons at $p < 0.05$ also indicated that there was no significant difference between the results reported from the clinical laboratories and the results obtained in the reference laboratory.

In conclusion, the e.m.i.t. system has several advantages over the current methodology for the determination of diphenylhydantoin in human plasma. The e.m.i.t. system provides simplicity, speed, accuracy and specificity, and requires about 50 μl of plasma. This makes it highly desirable for pediatric use; the e.m.i.t. system provides a rapid method for monitoring closely patients undergoing diphenylhydantoin therapy.

It is hoped that this communication will prompt others to evaluate the results of clinical laboratories and, if necessary, to implement improved

methods, such as the e.m.i.t. system, rather than to cease to use DPH levels as an adjunct to rational anticonvulsant therapy.

REFERENCES

1 F. Buchthal and O. Svensmark, Epilepsia, 1 (1959/60) 373; F. Buchthal; O. Svensmark and P. J. Schiller, Arch. Neurol. (Chicago), 2 (1960) 624; F. Buchthal, O. Svensmark and H. Simonsen, Arch. Neurol. (Chicago), 19 (1968) 567.
2 H. Kutt, W. Winters and F. McDowell, Fed. Proc. Fed. Am. Soc. Exp. Biol., 23 (1964) 492; Neurology, 16 (1966) 594; H. Kutt, W. Winters, R. Kokenge and F. McDowell, Arch. Neurol. (Chicago), 11 (1964) 642; H. Kutt, W. Winters, R. Scherman and F. McDowell, Arch. Neurol. (Chicago), 11 (1964) 649; H. Kutt, J. Haynes and F. McDowell, Arch. Neurol. (Chicago), 14 (1966) 489; H. Kutt and F. McDowell, J. Am. Med. Assoc., 203 (1968) 969.
3 M. Lund, R. S. Jorgensen and V. Kuhl, Epilepsia, 5 (1964) 51.
4 E. W. Loeser, Jr., Neurology, 11 (1961) 424.
5 G. E. Maner, P. W. Mullen, M. Rodgers, A. J. Robins and S. B. Lucas, Br. J. Clin. Pharm., 1 (1974) 163.
6 A. Richens, Epilepsia, 16 (1975) 627.
7 G. L. Plaa and C. H. Hine, J. Lab. Clin. Med., 47 (1956) 649.
8 O. V. Elesen, Acta Pharmacol. Toxicol. (Kbh), 23 (1965) 41.
9 O. Svensmark, P. J. Schiller and F. Buchthal, Acta Pharmacol. Toxicol., 16 (1960) 331; O. Svensmark and P. Kristensen, J. Lab. Clin. Med., 61 (1963) 501.
10 D. H. Sandberg, J. L. Resnick and C. Z. Bacallao, Anal. Chem., 40 (1968) 736.
11 T. Chang and A. Glazko, J. Lab. Clin. Med., 75 (1970) 145.
12 H. J. Kupferberg, Clin. Chim. Acta, 29 (1970) 283.
13 J. Wallace, Clin. Chem., 15 (1969) 323; Anal. Chem., 40 (1968) 978.
14 W. A. Dill, A. Kazenko, L. M. Wolf and A. J. Glazko, J. Pharmacol. Exp. Ther., 11 (1970) 846; W. A. Dill and A. Glazko, Clin. Chem., 18 (1972) 675.
15 J. Wallace, J. Biggs and E. V. Dahl, Anal. Chem., 37 (1965) 410.
16 I. L. Soo and N. H. Bass, Neurology, 20 (1970) 115.
17 E. C. Pippenger, J. K. Penry, B. G. White, D. D. Daly and R. Buddington, Arch. Neurol. (Chicago), 33 (1976) 351.
18 J. E. Wallace, J. K. Farqhar, H. E. Hamilton and B. A. Everhart, Clin. Chem., 20 (1974) 515.
19 J. McGee, Anal. Chem., 42 (1970) 421.

Analytica Chimica Acta, 92 (1977) 217—221

Short Communication

THE ANATOMICAL AND LONGITUDINAL VARIATION OF TRACE ELEMENT CONCENTRATION IN HUMAN HAIR

J. F. ALDER, A. J. SAMUEL* and T. S. WEST**

Chemistry Department, Imperial College of Science and Technology, South Kensington, London SW7 2AY (England)

(Received 6th May 1976)

Analysis for trace elements in hair has been used in toxicology [1], physiology [2] and pollution control [3], as well as for forensic purposes. Previously, the multi-element analysis of hair, applied only to whole hairs or long sections of hair [4, 5], has been of limited use for identification purposes [6]. This more detailed analysis of nine elements in short sections (1 cm) of hair was undertaken to discover the longitudinal variation in hair.

The detailed studies by Renshaw et al. [7] and Obrusnik et al. [8] have shown certain notable features in the trace metal profiles. For the several elements investigated by Obrusnik et al. [8], and both those investigated by Renshaw et al. [7], the concentration increased in the distal parts of the hair, and the distribution of trace element concentration in hair was not usually normal but often positively skewed; Renshaw et al. showed it to be log-normal.

Although many data exist for trace metals in human scalp hair, few data are available for hair from other anatomical sites. Lima et al. [9] reported the variation of six trace elements down one pubic hair found by neutron activation analysis; the data were normalized against the concentrations in scalp hair. Perkons et al. [10] also found that pubic hair generally contained higher trace metal concentrations than scalp hair.

Experimental

The multi-element atomic absorption spectrometer used has been described [11]. The samples, weighed on an Oertling QO1 quartz fibre microbalance, were introduced into the carbon furnace by an injector consisting of a borosilicate capillary with platinum wire plunger. The ashing and atomization conditions, wavelengths, ranges of linearity, detection limits, and precisions have been given in Tables 2 and 6 of a previous paper [11].

Present addresses:
*Shell Research Ltd., Sittingbourne Research Centre, Sittingbourne, Kent, England ME9 8AG.
**The Macaulay Institute for Soil Research, Craigiebuckler, Aberdeen, Scotland AB9 2QJ.

Sampling and washing. It is not known whether the hairs obtained were in the anagen or telogen phases; Kerr [12] and Obrusnik et al. [8] found no gross differences in trace metal concentration between these two states. The hairs used were pulled out by the subjects themselves; hair samples obtained from the scalp, axilla, pubes, chest, arm, leg, beard, eyelash and eyebrows of four volunteers were available.

The hair samples were treated for 2 h with diethyl ether in a Soxhlet extraction apparatus [11]. The scalp hairs were analysed in 1-cm lengths, and the pubic, axillary and chest hairs in 0.5-cm lengths; those from the other anatomical locations were either taken whole, or in 1-cm sections.

Results and discussion

The results were calculated by interpolation from calibration curves constructed for aqueous solution samples as described previously [13].

Trichograms for the nine elements are given in Fig. 1 for the samples from a male subject (aged 23 years). For scalp hair, and for most elements, the elemental concentration near the distal end is greater than near the root. The root sections contain very much lower concentrations than the rest of the hair, except for nickel and copper. The results for many other samples from different individuals showed that, except for copper, the concentration of most elements is very much lower close to the root end than in the rest of the hair. The silver concentrations (Fig. 1) for the two scalp hairs differ greatly. In general, there is considerable variation down the length of scalp hairs and this does not appear to follow any given pattern. The body hairs often show a wider range of concentrations than scalp hairs and many, e.g. from arm, leg and axilla, show large variation within an individual hair.

No apparent difference was found in the composition of male and female hair. The comments regarding the longitudinal variation of trace elements in scalp hair are not applicable in every case. In one exceptional subject (male 2, aged 22 years) there was a large increase in Si, Al and Fe (Fig. 2) near the root of the hair; although the manganese concentrations (Fig. 2) for two hairs differed by a factor of 3, the concentration profiles for Ni, Cu, Ag and Cr for this subject showed no exceptional features.

The reason for the changes in concentration along the length of scalp hair has been the subject of some discussion. The work of Renshaw et al. [7, 8] showed a relatively uniform increase towards the distal end of the hair but the features found in this study have been less specific. In many cases the root sections of scalp hair contain smaller amounts than the distal parts; the increased amounts must arise from external sources if hair is dead after it emerges from the scalp. Indeed, considering the ion-exchange nature of hair and the continuous but variable contamination to which it is exposed, it is not surprising that the trace metal content of hair does vary longitudinally.

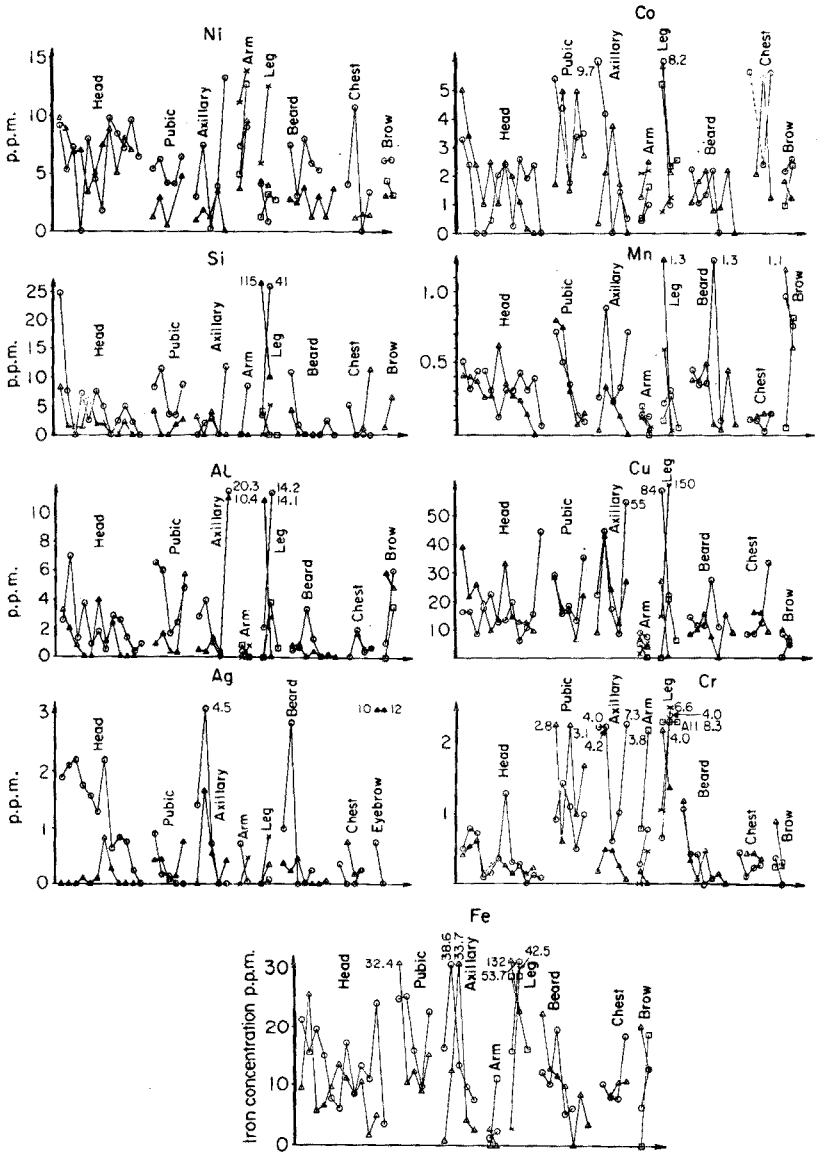

Fig. 1. Distribution of trace metals.

Conclusions

The complex nature of the variation of trace metals in human hair has been demonstrated in this study. Although there are many cases where the trace metal content is higher at the distal end than at the root, this is not found in all samples. The level of trace metal content is not constant even for Mn, Cu, Fe, Ni, Co and Cr, which are essential elements. There appears to be no

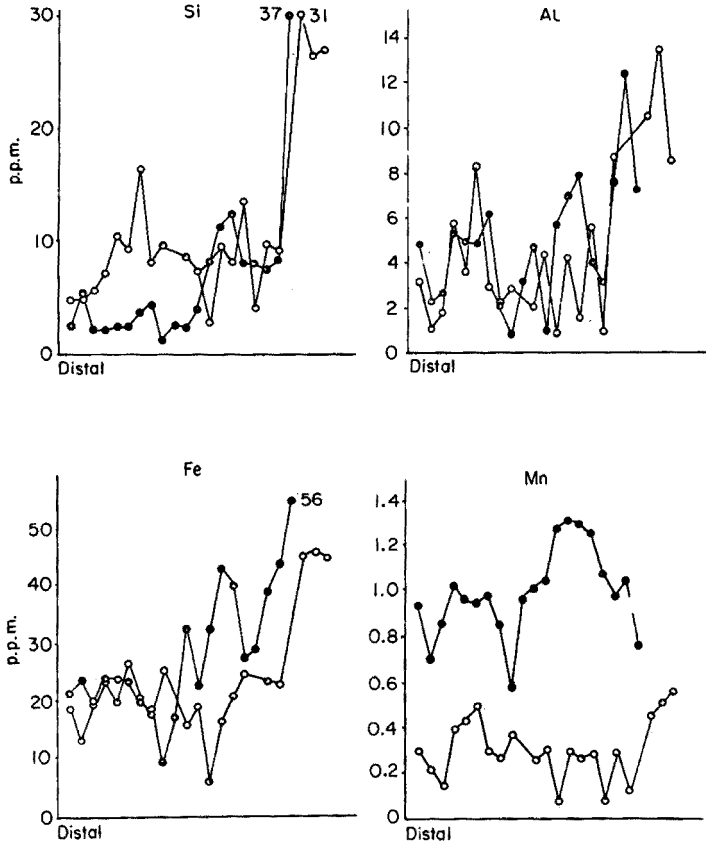

Fig. 2. Distribution of trace metals in the scalp hair of Male 2. The hairs were sampled every 10 mm starting at the distal end.

systematic difference in the average trace metal concentrations in hair from different anatomical sites. There is some evidence that trace element correlations exist within one individual's hair. Also, similar longitudinal trace element profiles (for the same element and at the same site) can be found within an individual. The detailed trace element composition of hair appears to have individual characteristics; these may be of interest in attempts to identify individuals by the analysis of their hair.

Other analytical data, too numerous for presentation here, are available from the authors.

The authors are indebted to the Home Office for financial support (to J. F. A. and A. J. S.) and for lending the equipment used.

REFERENCES

1 P. R. V. D. R. Copeman and J. C. Bodenstein, J. For. Med., 2 (1955) 196.
2 W. H. Strain, L. T. Steadman, C. A. Lankau, W. P. Berliner and W. J. Poris, J. Lab. Clin. Med., 68 (1966) 244.

3 D. I. Hammer, J. F. Finklea, R. H. Hendricks, C. M. Shy and R. J. M. Horton, Am. J. Epidemiol., 93 (1971) 84.
4 D. E. Bryan, V. P. Guinn and D. M. Settle, General Atomic Report no. 6152 (chemistry) USA Energy Comm. (1965).
5 R. F. Coleman, F. H. Cripps, A. Stimson and H. D. Scott, Atomic Weapons Research Establishment Report No. 0-86/66 (1966).
6 R. Cornelis, J. Radioanal. Chem., 15 (1973) 305.
7 G. D. Renshaw, C. A. Pounds and E. F. Pearson, J. For. Sci., 18 (1973) 143; Nature, 238 (1972) 162.
8 I. Obrusnik, J. Gislason, D. K. McMillan, J. D'Auria and B. D. Pate, J. For. Sci., 17 (1972) 426; J. Radioanal. Chem., 15 (1972) 115.
9 F. W. Lima, H. Shibota and L. T. Atalla, Proc. Int. Atom. Energy Agency, 1 (1965) 119.
10 A. K. Perkons, P. A. Vlossak, N. Erickson and R. F. Jervis, Proc. Can. Soc. For. Sci., 3 (1964) 40.
11 J. F. Alder, D. Alger, A. J. Samuel and T. S. West, Anal. Chim. Acta, 87 (1976) 301.
12 M. F. Kerr, Proc. Can. Soc. For. Sci., 2 (1962) 143.
13 J. F. Alder, A. J. Samuel and T. S. West, Anal. Chim. Acta, 87 (1976) 313.

Analytica Chimica Acta, 92 (1977) 223—225

Short Communication

THE DETERMINATION OF NITRITE IN SEA WATER — A REVISION CONCERNING STANDARDIZATION*

OLIVER C. ZAFIRIOU and MARY B. TRUE

Chemistry Department, Woods Hole Oceanographic Institution, Woods Hole, Massachusetts 02543 (U.S.A.)

(Received 24th November 1976)

Low sensitivities and high variability found in this laboratory while standardizing the low-level nitrite method of Wada and Hattori [1] have been traced to erratic instability of the stock solution employed to make standards. Both the stock and standards in this method are dissolved in "nitrite-free water" made by boiling for 30 min deionized water acidified with 11 M HCl (1 ml l^{-1}). This water has a pH of ca. 2 and may be 0—100% saturated with air, depending on handling after boiling. The standards are used immediately but the stability of the stock is not indicated by Wada and Hattori [1].

Nitrous acid is unstable in solution. Some pertinent reactions [2, 3] are: (1) $2HNO_{2(aq)} = N_2O_3 + H_2O$; (2) $N_2O_{3(aq)} = NO_{(aq)} + NO_{2(aq)}$; (3) $(NO, NO_2, N_2O_3)_{(aq)} = (NO, NO_2, N_2O_3)_{(g)}$; (4) $NO_{(aq)\,or\,(g)} + \frac{1}{2}\,O_{2(aq)\,or\,(g)} = NO_{2(aq)\,or\,(g)}$; (5) $2NO_2 + H_2O = HNO_{2(aq)} + HNO_{3(aq)}$. Sequence (1)-(2)-(3) leads to loss of N by evaporation. In the presence of oxygen, sequence (1)-(2)-(4)-(5) leads to oxidation of nitrous to nitric acid.

Experimental

At 10 mM nominal concentration, the stock solution is ideally suited to determination of nitrous acid directly by ultraviolet absorption spectrometry [4]; to determine the extent to which dissolved oxides are present, solutions were made basic, and the nitrite and nitrate concentrations were determined at 366 and 305 nm, respectively, nitrate requiring a small correction for nitrite absorption. This method was used to analyze the stock solution after various preparation and storage conditions.

Results and discussion

As shown in Table 1, losses of 1—26% occurred in preparation, with decomposition at ca. 10% h^{-1} following immediately thereafter under optimal conditions. Clearly, the technique used in preparation is crucial to

*Woods Hole Oceanographic Institution Contribution Number 3706.

TABLE 1

Stability of stock nitrite solutions[a] of $10.0 \cdot 10^{-3}$ M nominal concentration

Treatment	Time	Molarity found[b] ($\cdot 10^{-3}$ M)			HNO_2 or NO_2^- loss (%)
		Acid solution total HNO_2	After neutralization		
			(NO_2^-)	(NO_3^-)	
A[c]	0	—	7.4		26
B[d]					
1. Determined immediately	0	—	10.1; 9.9; 9.8; 9.9	—	1
2. Shaken vigorously for 30 s, then left in dark	60 min	9.1; 8.8	—	—	10
3. Shaken once, then left in a closed brown polypropylene bottle and subsampled at:	2 min	9.8	—	—	2
	4 min	9.7	—	—	3
	1 day	5.0	—	—	50
4. Shaken once a day in a closed brown polypropylene bottle	10 days	—	1.5	8.2	85
5. Magnetically stirred in an open container and subsampled at:	5 min	8.8	—	—	12
	20 min	6.9	—	—	31
	60 min	4.3	3.5	6.6	~60

[a]Made as recommended by Wada and Hattori [1].
[b]Determined as described in text. The spectrophotometric error in determinations is about ±1% for HNO_2 and NO_2^-, ±5% for NO_3^-.
[c]Treatment A: wash $NaNO_2$ into volumetric flask with air-saturated "nitrite-free water" shake 30 s to dissolve; dilute to mark with base to "kill" reactions.
[d]Treatment B: dilute solid $NaNO_2$ quickly to the mark with unshaken "nitrite-free water".

the yield. Atmospheric oxidation yielding nitrate is apparently the major reaction. The rate of this reaction is expected to be limited by reaction (1), with kinetics described by Hine [3]: rate = k $[HNO_2]^2$. Considerable loss results when the sodium nitrite is dissolved in only a small amount of "nitrite-free water" before dilution to the mark (Table 1A), as might be expected from the kinetics and the high nitrous acid concentrations generated in the presence of air by this procedure. Even if the solutions are prepared so that they have nearly the nominal concentration, significant decomposition occurs within 30 min. This decomposition is more marked if the solution is further agitated, e.g. during sampling.

Since ordinary distilled or deionized water should be less than 10^{-6} M in nitrite, there is no need to use "nitrite-free water" in making the stock solution, which is nominally 10^{-2} M. The chloroform-stabilized $5 \cdot 10^{-3}$ M standard as described by Strickland and Parsons [5] is recommended here as the stock solution for both the high and low-level methods. This solution is stable for 30 days.

Although the stock solution need not be made with "nitrite-free water", the standards made by dilution must be, and thus the stability of these dilute solutions is crucial. If the rate-limiting step stated above applies, then these very dilute solutions of nitrous acid may be acceptably stable for immediate use. When $0.1 \cdot 10^{-6}$ M standard solutions — the highest concentration in the Wada and Hattori method — made with "nitrite-free water" were analyzed in triplicate at 0, 5, 20, 40, 120, and 240 min after preparation by the method of Strickland and Parsons [5], no significant change was found. At this level, the relative standard deviation was about 2.5%. Therefore, standards made by diluting the neutral stock solution with "nitrite-free water" and used immediately should give acceptable results.

[Dr. Wada (personal communication, 1976) states that his group has abandoned "nitrite-free water" for making stock solutions and standards, using instead freshly deionized water. This procedure was used to obtain most of their oceanic data [6], which are therefore not affected by the calibration difficulties reported here.]

REFERENCES

1 E. Wada and A. Hattori, Anal. Chim. Acta, 56 (1971) 233.
2 F. A. Cotton and G. Wilkinson, Advanced Inorganic Chemistry, Interscience-Wiley, New York, 1972, p. 360.
3 J. Hine, Physical Organic Chemistry, McGraw-Hill, New York, 1962, p. 385.
4 D. M. Waldorf and A. L. Babb, J. Chem. Phys., 40 (1964) 1476.
5 J. D. H. Strickland and T. R. Parsons, A manual of sea-water analysis, Bull. Fish. Res. Bd. Canada, 167 (1972) 77.
6 E. Wada and A. Hattori, Limnol. Oceanogr., 16 (1971) 766.

Analytica Chimica Acta, 92 (1977) 227—232

Book Reviews

E. Pretsch, T. Clerc, J. Seibl and W. Simon, *Tabellen zur Strukturaufklärung organischer Verbindungen mit spektroskopischen Methoden*, Springer-Verlag, Berlin, 1976, price D.M. 28.00, U.S. $11.50.

This book contains a compilation of spectral data as an aid to the structural identification of organic compounds. Comprehensive tabulated data are presented for the most important and widespread techniques, viz. proton n.m.r., carbon-13 n.m.r., infrared, and ultraviolet—visible spectroscopy, and for mass spectrometry. A useful feature of the book is that the data are arranged in two ways. Thus, a section titled "combined tables" summarizes all the above types of spectral data under headings for the various classes of organic compound. Subsequent sections provide more detailed tables under the various spectroscopic techniques. Another useful aspect of this publication is that reference spectra are given in each section for common organic solvents that could contaminate the sample. Quite detailed information is given in the tables, for example in the n.m.r. sections some coupling constants to "other nuclei" are listed and in the m.s. section isotopic abundances and accurate masses are provided.

The tabulated information is very clearly presented and the detailed compound and subject index should enable the appropriate data to be quickly located. Although there are many other compilations of spectral data available, most of these are devoted to only one or two techniques. This publication is attractive in that it provides adequate information on the most important techniques in one conveniently sized package. The inclusion of detailed ^{13}C n.m.r. data is particularly noteworthy as this technique has recently become established as a very powerful one for the structural identification of organic compounds.

In summary, this is an excellent publication marketed at an amazingly low price. Accordingly it should make an extremely worthwhile purchase for organic and analytical chemists who use spectroscopic methods. The authors deserve credit for their considerable efforts, and the publishers ought to be congratulated for keeping the price low in times of outrageously high specialist book prices.

W. B. Jennings

Charles K. Mann, Thomas J. Vickers and Wilson M. Gulick, *Instrumental Analysis*, Harper and Row, New York, 1974, xiv + 766 pp., price £15.00.

There are several books which give a comprehensive, up-to-date account of modern instrumental analysis for student instruction at the undergraduate

level. The present text compares very favourably with these in many respects and, in general, is one of the best books of its kind available. The first third of the book deals with basic electronics in a manner suitable for those who are not strongly mathematically inclined. It includes description of basic electrical concepts, filters, amplifiers, feedback, signal processing and analog and digital instrumentation. These sections are not written in isolation but are related to specific analytical instrumentation described later in the book. The next 390 pages are concerned with spectrometry (atomic absorption, emission and fluorescence, u.v.—visible absorption in solution, molecular luminescence, infra red, raman, microwave, n.m.r., e.s.r. and mass spectrometry). Generally, the chapters have a discussion of the fundamental processes, instrumentation and application. Finally, there are descriptions of chromatography (29 pp.) and electrochemical methods (72 pp.), appendices and an index.

The sections on electronics and spectroscopy (ca. 85% of the book) are very impressive. They are written and printed with clarity and with numerous illustrations. Each chapter concludes with a section on problems to be solved. The treatment is comprehensive and up-to-date, with little to criticize in the selection of topics, other, perhaps, than the omission of plasmas and carbon furnace devices from the atomic spectroscopy section. The chromatography and electrochemistry sections are much less detailed, especially the former. The authors might well consider omitting them from a second edition, in favour of producing a second volume containing a more comprehensive treatment of these aspects, together with those topics which are not included in the present text. The most important of these would be x-ray fluorescence and related subjects, radiochemical techniques and automated analysis. Yet even as it stands, the book is highly recommended for undergraduate and post-graduate teaching, and will not be without value to practicing analysts who feel they need to up-date their knowledge of instrumental analysis.

A. Townshend.

G. J. Dickes and P. V. Nicholas, *Gas Chromatography in Food Analysis*, Butterworths, London, 1976, pp. x + 393, price £16.00.

This book, written by members of the staff of Avon County Council's Scientific Advisers' Department, will be an excellent acquisition for laboratories involved in the analysis of foods and beverages of all types. The book is sub-divided into five main parts. Part I gives a sound, useful general introduction to all practical aspects of gas chromatography; if there remains anyone not yet conversant with the practical side of g.l.c., then they need search no further for a useful introductory text — the material would also be valuable for first- or second-year students. Part II gives recommended methods and stationary phases. Part III contains 8 chapters, devoted to the analysis of

dairy products; fats and oils; meat, fish and eggs; essential oils; fruits, vegetables and non-alcoholic beverages; alcoholic beverages and vinegar; sugar products and syrups; cereals and their products. Part IV deals with food additives, and Part V with food contaminants. There is a good subject index, and three useful appendices.

This is the type of book that industrial and public health analysts require. It is written by analysts with a wealth of experience. Each chapter contains an extensive bibliography — and here, perhaps, the sole grounds for criticism of this book arise; although there are some references to material published in 1972—1974, the great majority are to work that was published in the sixties and is beginning to look a bit long in the tooth. The approach is clearly pre-h.p.l.c. in vintage, but this book remains essential for those whose bread and butter comes from analysing putative bread and butter.

D. M. W. Anderson

E. F. Mooney (Ed.), *Annual Reports on NMR Spectroscopy, Vol. 6B*, Academic Press, London, 1976, vii + 239 pp., price £9.40.

Volume 6B of Annual Reports contains two reviews. The first, by W. A. Thomas, is relatively short (40 pages) and is entitled: "N.m.r. and Conformations of Amino Acids, Peptides, and Proteins". Applications of proton, carbon-13, and nitrogen-15 n.m.r. spectroscopy in this area are reviewed up to December 1971. However, in a 6-page addendum the author has attempted to summarize the main developments through to 1975. The rest of this volume is devoted to an annual report on fluorine-19 n.m.r. for the year 1971. This chapter (by L. Cavalli) is very comprehensive and presents a large amount of tabulated shift and coupling constant data for organic, inorganic, organometallic, and organometalloid fluorine compounds.

Both reviews are well presented, though it was very easy to confuse reference and compound numbers as both are printed in the same typeface. The use of boldface for compound numbers and/or superscripts for reference numbers would have been preferable. More seriously, it is questionable whether reviews of the 1971 literature are relevant in 1976, particularly as n.m.r. has been a rapidly developing subject. The first author has made a creditable attempt to salvage the situation by providing an addendum, but the result is obviously less satisfactory than a unified up-to-date review. One can sympathize with authors whose very considerable efforts have been dissipated by a long delay in publication. In this connection it is interesting to note that Volume 4 in this series, which was published in 1971, contained literature coverage for 1969. Recent trends need to be reversed if this series is to continue to be useful to n.m.r. spectroscopists.

In short, this volume would have been a worthwhile purchase had it been available a few years ago.

W. B. Jennings

Zbigniew Galus, *Fundamentals of Electrochemical Analysis*, Ellis Horwood, Chichester, 1976, xviii + 520 pp., price £23.50.

This book is rather more restricted in scope than suggested by the title. By deliberate choice of the author it is confined to the voltammetric techniques of polarography, chronopotentiometry, stationary electrode voltammetry and rotating disc voltammetry.

Although the approach is not particularly analytical in the conventional chemical sense, a few pertinent references to such analytical scope are made in the essentially theoretical twenty-chapter discussion. Two chapters have analytical titles, namely "Equations of Electroanalytical Methods" (Chapter 7) and "Electroanalytical Investigations of Complexes" (Chapter 14). Each suggests interesting pauses for digression in this review.

The chapters leading up to Chapter 7 take up two fifths of the book and are mainly concerned with relations between limiting currents and concentration, taking in such matters as the structure of the electrode double layer and the general nature of electrode processes including diffusion effects and charge transfer. General characterization of the various voltammetric techniques discussed form the basis of Chapter 2 and this might be taken as a brief background introduction to many chapters including, what might from the main chapter heading have been an analytical Chapter 7. However, the subsidiary title, namely "Determination of Kinetic Parameters of Electrode Processes" is a better guide to what Chapter 7 and indeed much of the whole book is really about.

The section incorporating Chapters 8—13 is shorter and occupies about one fifth of the book. In this section, there is a move away from those electrode processes in which the depolariser in the solution reacts with the electrode to give a product, to considerations of electrode processes preceded or followed by the charge transfer.

In Chapter 14 homage is paid to the important part played by polarography in investigations of the composition and stability of complexes and of the mechanisms of complex formation. A truly interesting chapter, followed by Chapter 15, entitled "ECE Processes". What do these letters mean? They apparently refer to three-stage mechanisms, consisting of two electrochemical stages with an intervening chemical stage (ECE), a process that can be undertaken by the reduction of *o*-nitrophenol.

The rest of the book is directed to a discussion of topics such as the influence of adsorption on electrode processes, cyclic methods, deviations from normal depolarizer transport and new developments in polarography.

The complete work represents a painstaking systematic approach with the discussion of each theme being taken through the techniques in order. However, although this is an interesting work for which it is easy to develop a liking, it must be confessed that the book is more suited for the person who is likely to become a devoted student of electroanalytical or general electrochemistry rather than the analytical practitioner of wider interests.

J. D. R. Thomas

V. Šedivec and J. Flek, *Handbook of Analysis of Organic Solvents*, Ellis Horwood, Chichester, 1976, 455 pp., price U.S. $34.20, £18.00.

This book contains a great deal of information; 1012 references are given to a wide range of work published between 1874 and 1972. The treatment falls into three parts. Part I gives basic information dealing with sampling and treatment of samples, the determination of basic physical properties, and procedures for the analysis of unknown compounds and of two and three component mixtures. Part II comprises 16 chapters, each dealing with a functional group or solvent class, and giving information on methods of detection, preparation of characteristic derivatives, methods of determination, and data for important members of the group or class. Lastly, there are 3 Appendices, covering some 80 pages, giving tables of physical constants.

This will be a useful reference book for those dealing with a wide range of organic solvents: the analytical methods used are largely classical, with some use of gas chromatography, but little attention is given to any of the spectroscopic methods. There is some duplication of references — for example, references 240 and 324 are identical, 454 and 508 are identical, 903 and 916 are identical. In general, however, the authors, the translator and the translation editor have worked carefully and conscientiously to create a useful book for the reference shelf.

Yoshiro Masada, *Analysis of Essential Oils by Gas Chromatography and Mass Spectrometry*, Halsted Press, Chichester (a Division of J. Wiley), 1976, ix + 334 pp., price U.S. $49.70, £28.90.

This is a reference book for the essential oils specialist in the fields of perfumery, spices and flavours. It consists largely of 64 short chapters, each devoted to an essential oil; the botanical and geographical origins of the oil are quoted, followed by its physico-chemical constants, a gas chromatogram and a mass spectrum in which at least the major chemical components are identified. Each chapter also quotes a number of references: these are very largely drawn from the 1965—1972 period, but there are a few references to data published in 1974.

This should be regarded as the English edition of a revised version of the book first published in 1968 by the author, who is Professor of Pharmaceutical Chemistry at Kyoto College of Pharmacy, Japan. The author has not received a great deal of help with the translation and proof-reading: there is an interesting selection of quaint phrases and mis-spellings e.g. Califolnia, furfulyl, Turky, dereived, biennal, "to formery reported compounds". "with reminds of lemon odor". Each chapter contains what appears to be a summary, in Japanese characters, of the main text, and Part II of the book — admittedly only 34 pages — is entirely in Japanese. As the latter part appears to give a brief introduction to the chemistry of essential oils and terpenes, followed

by a description of the analytical methods and the operating conditions used for gas chromatography and mass spectroscopy, English-speaking readers may find this book rather frustrating. It is difficult to understand why the author — and such a reputable publishing house — did not exercise a little patience and wait until a really complete English translation of the original Japanese text was available. The price is almost unbelievable — clearly anticipating relatively few sales for a very specialised subject.

(continued from page 4 of cover)

PRINTED IN THE NETHERLANDS

VOL. 92 No. 1 ANALYTICA CHIMICA ACTA AUGUST 1977

CONTENTS

(continued on inside page of the cover)